ISBN: 978-9940-46-034-1

ENGINEERING AND ARCHITECTURE SCIENCES

IVPE 2020

ENGINEERING AND ARCHITECTURE SCIENCES

Theory, Current Researches and New Trends

Dr. Öğretim Üyesi Can Çivi
Dr. Öğretim Üyesi Tuncay Yılmaz

IVPE 2020

ENGINEERING AND ARCHITECTURE SCIENCES

Theory, Current Researches and New Trends

Editors
Asst. Prof. Dr. Can ÇİVİ
Asst. Prof. Dr. Tuncay YILMAZ

Editors
Asst. Prof. Dr. Can ÇİVİ
Asst. Prof. Dr. Tuncay YILMAZ

First Edition •© October 2020 /Cetinje-Montenegro

ISBN • 978-9940-46-034-1

web: www.ivpe.me

Tel. +382 41 234 709

e-mail: office@ivpe.me

Cetinje, Montenegro

PREFACE

Engineering and architecture disciplines have scientists who work on similar research topics with different perspectives or with similar perspectives on different subjects. In addition, the number of scientists working on interdisciplinary research is increasing day by day, thus providing valuable solutions to very important engineering / architectural problems. An important technology or perspective in a field can make a significant contribution to the solution of problems existing in other areas. For this reason, recognizing each other's work in different fields and encouraging the synthesis of these studies will create different perspectives and contribute to the solution of problems that have not been solved until today through interdisciplinary studies.

In this book, the main goal is to bring scientists from different disciplines together, to open the horizons of scientists and to create new ideas for future joint interdisciplinary research. In line with this goal, this book contains studies from different disciplines in the fields of engineering and architecture. We would like to thank the authors who contributed to the creation of the book and the referees who contributed to the evaluation of the studies for their great efforts and wish the researchers success in their future work.s

Editors
Asst Prof. Dr. Can Çivi
Asst Prof. Dr. Tuncay Yılmaz

CONTENTS

REFEREES

Prof. Dr. Ayhan İstanbullu, Balıkesir University, Turkey

Prof. Dr. Elif Ebru ŞİŞMAN, Namık Kemal University, Turkey

Prof. Dr. T. Ennil Bektaş, Çanakkale Onsekiz Mat University, Turkey

Assoc. Prof. Dr. Hatice Umut Tuğlu Karslı, İtanbul University, Turkey

Asst. Prof. Dr. Can Çivi, Manisa Celal Bayar University, Turkey

Asst. Prof. Dr. Feran Aşur, Van Yüzüncü Yıl University, Turkey

Asst. Prof. Dr. Mehmet Söylemez, Adıyaman University, Turkey

Asst. Prof. Dr. Seyfullah Keyf, Yıldız Technical University, Turkey

Asst. Prof. Dr. Tuncay Yılmaz, Manisa Celal Bayar University, Turkey

Inst. Dr. Hande Sezgin, Istanbul Technical University, Turkey

Dr. Onur Pekcan, Middle East Technical University, Turkey

CHAPTER I

VISUALIZING THOUGHT: INVESTIGATIONS OF THE THIRD DIMENSION IN LANDSCAPE DESIGN STUDIO EXAMPLE

Assoc. Prof. Dr. Arzu KALIN*

*Karadeniz Technical University, Trabzon, Turkey
e-mail: arzuk@ktu.edu.tr, Orchid ID: 0000-0003-2988-1916

1. Introduction

Recently, digital drawing and modeling techniques provide numerous possibilities for perceiving, constructing, and manipulating the third dimension of design. Moreover, that contemporary landscape architecture education, like similar ones, extends these possibilities to every stage of training process is inevitable.

2. Material and methods

In this respect, in the landscape design studio of senior students, we argued that starting a design with a three dimensional line was the first step of this process. We considered the project area among the skyscrapers as a volume. Thus, every student prepared their proposals in a changing frame from traditional drawing to digital three-dimensional modeling techniques.

Designing the third dimension of line in landscape design is always a problematic process, like in every design training process which is started with a line and resulted in a product. In our design studio, which was conducted by five instructors with student groups of seven and implemented in the Department of Landscape Architecture in the Karadeniz Technical University, we investigated the third dimension of design process. The students were presented two different mass housing area and we asked them to determine an original concept and to create an environmental design. In the following step, I directed my students to design the area among the residences as a three-dimensional volume while determining their concepts, from the beginning. In the consequent step, there was an intense concept research. First of all, contemporary buildings, architects, environments, which applied 3D in a successful manner and relevant movements, were analyzed deeply. On this stage, every student tried to determine their own original concepts.

During the analysis process, what we searched for was actually how to get the “three-dimensional line”. Although we started on a plan, every student described their lines by considering the elements, which could be perceived as a construction system in which the lines could be increased by putting them successively, so which had a vertical depth. When lines crossed successively, every student used different modeling techniques

considering the design process. The only student who prepared her design with a model was Esma İşler. She applied her origami-based construction on the whole field by covering the whole of topography, the activity areas, and hard floor. Esma, whose project was one of the projects, describing the third dimension strongly, applied "The High Line" paving design sample to her field successfully [1]. In her design with the fashion concept, Elif Kıycı emphasized the third dimension by means of the coloring in shades in a computer program, CorelDraw. Two students who applied coloring technique in Photoshop were Harun Ünal and Harun Yetgin. They built up their designs by using the 3D modeling techniques while designing the activity areas and spaces. Moreover, Aybike Demirel started her design with an ecology concept. While defining and designing the details of all activity areas, she also used 3D modeling and determined decisions on the plan. Azer Özgür and Mine Dilikoğlu searched for the third-dimension by trying to transforming the intersections of lines, which were increased successively into the activity areas.

3. Results

In the landscape design studio where the third dimension in design was investigated, all designs were constructed in 5 stages.

1. Concept development and creating design thinking lines
2. Overlapping design thinking lines in the plan and model
3. Development of overlapping lines in the third dimension
4. Spatial layering analysis
5. Activity-space and detail solutions

3.1 Concept development and creating design thinking lines

It is foreseen that a certain design concept will be selected during the concept development phase and that it will be developed as a design idea. At this stage, Elif, who determined the concept of Fashion as the starting point of her design idea by using the curves and texture of the fabric material (Figure 1). She abstracted the fabric folds (shrinking) and texture and used these lines in her design (Figure 2).

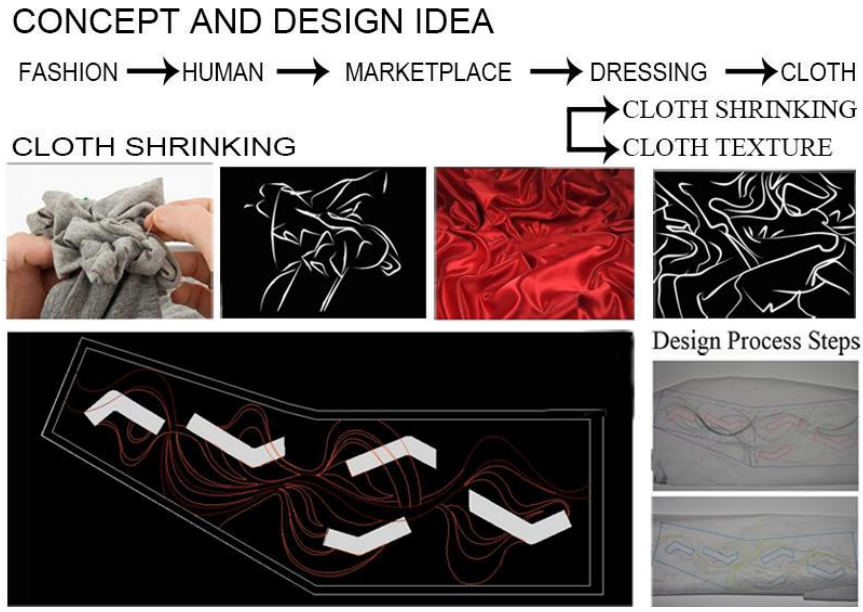

Fig. 1 Fashion as a concept and design idea.

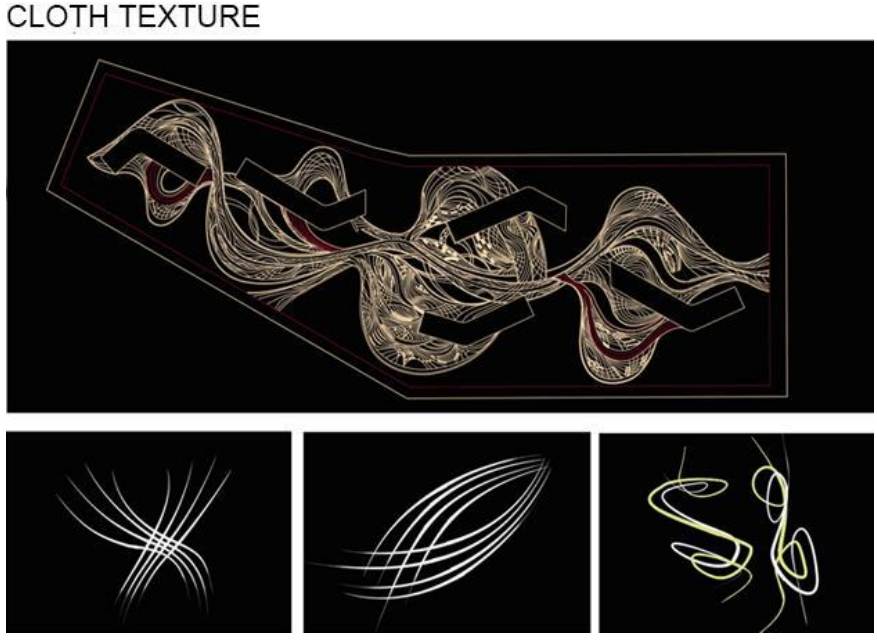

Fig. 2 Cloth shrinking and texture abstracts as design elements.

*"**EK:** The concept which I considered to design the volume among the residences was FASHION since in my opinion, fashion was the desire of the masses, and also it was one of the most efficient ways to reveal quality, comfort, inequality and an elite aesthetic perception. Furthermore, puckering, curling, and waving possibilities of fabric seemed inspiring for design. For this reason, I decided to use dress metaphor for my design. In this metaphor, main axe and residences symbolized the wave of dress fabric; and more detailed paving and furniture were constructing the linear analogy of cloth texture. Thus, linear construct of my design presented the main axe as a long and slight band which was puckered on some points while the activity areas were the layers above and below these smocking."*

Fig. 3 Final design project by Elif Kıycı.

3.2 Overlapping design thinking lines in the plan and model

At this stage, the students overlapped the linear elements they created from the concepts they determined, as different layers, in the plan and then on the model. Azer created her design by overlapping the curvilinear form, which she used as "Zero form", both in the plan and on the model (Figures 4 and 5).

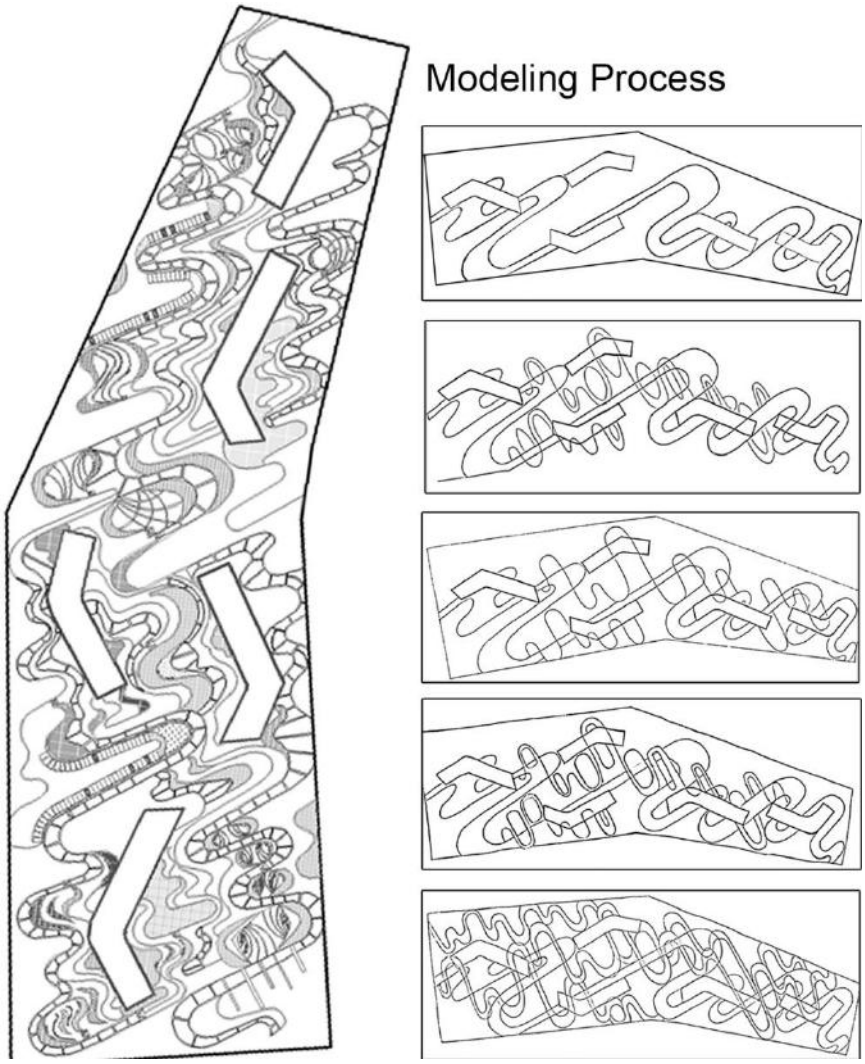

Fig. 4 Layering process of design idea in a plan drawing.

*"**AÖ:** I was searching Suprematism movement for concept of my design; and I thought that art actually could not be shaped with the inspiration of the concept "Zero of Form" and Malevich's quotation "In a desperate attempt to rid art of the ballast of objectivity, I took refuge in the form of the square"[2]. The idea to use the "Zero of Form" as my concept came about at this point.*

Fig. 5 Layering process of design idea on a model and the final model by Azer Özgür.

When reconsider it, art was such an abstract concept that it could not be shaped. Therefore, formal concept of design would not be shaped in a specific form since my concept was the "Zero of Form". For this reason, I avoided taking refuge in a specific form such as square, circle, and triangle; and in my project, I aimed to catch this "shapeless" form within organic lines. Thus, my goal was to depict suprematist thoughts on that greed for worldly goods was worthless whereas humanity and brotherhood were perpetual which was related to my concept."

In the project, which is the second example of the same phase, Mine cut the lines she produced in the plan from the colorful papers and used them in the model and developed her project (Figures 6 and 7).

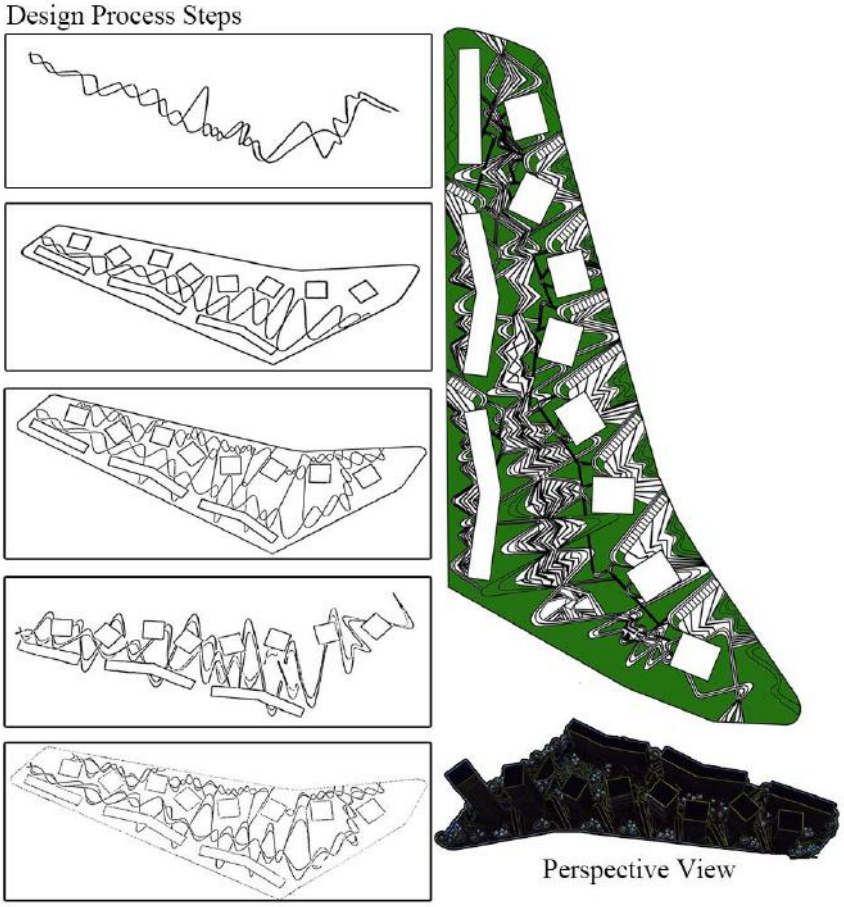

Fig. 6 Layering process of design idea in a plan drawing and final project and model by Mine Dilikoğlu.

*"**MD:** I supposed an artificial shore line passing through at the middle of the area among the skyscrapers, and sent waves from two opposite directions to this line. Therefore, I revealed a movement on the visual analogy of continuous movement of two crossed waves on my main axe. The lines gathered successively by these waves and intersections of these lines not only increased the visual effect of my design, but also provided possibilities to describe the activity areas in which the inhabitants gathered their memoirs, experiences, shares, interaction, and socialization."*

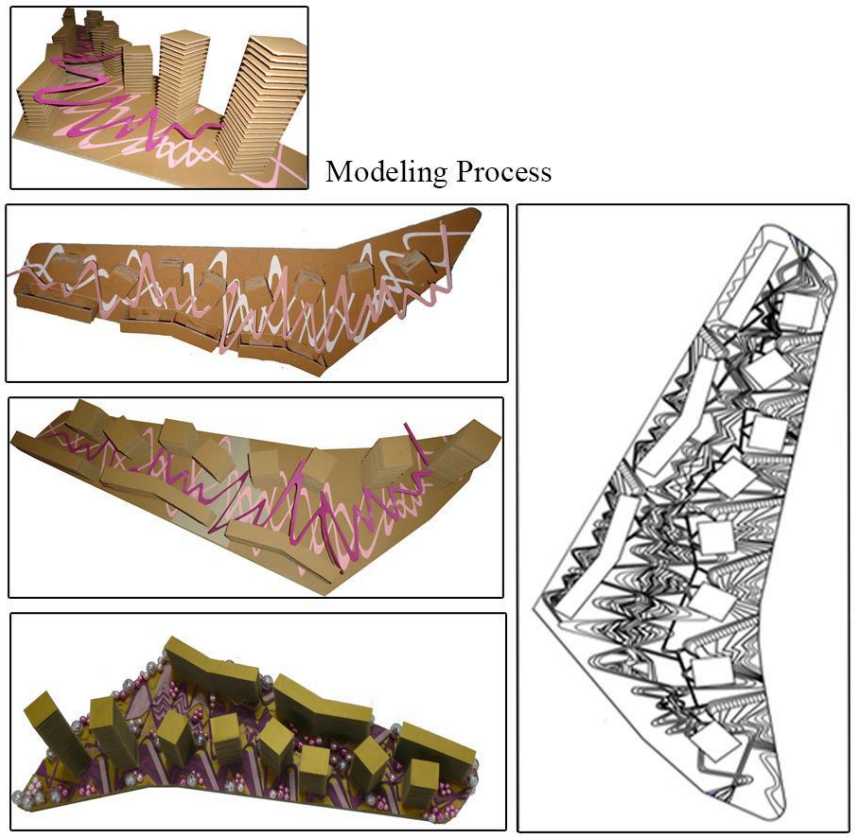

Fig. 7 Layering process of design idea on a model and the final project by Mine Dilikoğlu.

In her project, which is the last example of this group, Esma designed the linear elements directly on the model using origami and developed her project (Figure 8).

*"**EI:** The reason of my choosing origami as the main concept of my design was to describe continuity on the ground and the third dimension. For this reason, first of all, I modeled the field in long, slight, and rectangular bands. Modeling hills by folding and lifting each band around the activity areas was facilitating to describe the topography in 3D, on one hand; and on the other hand, it was restrictive. Even so, in order to describe the third dimension more strongly, I placed a construction system, which I created by using origami techniques, on the main axe. I tried to eliminate the uniformity of the linear movement on the whole ground by using linear green spaces in different size and shapes and by making the construction on the middle axe transparent on some points."*

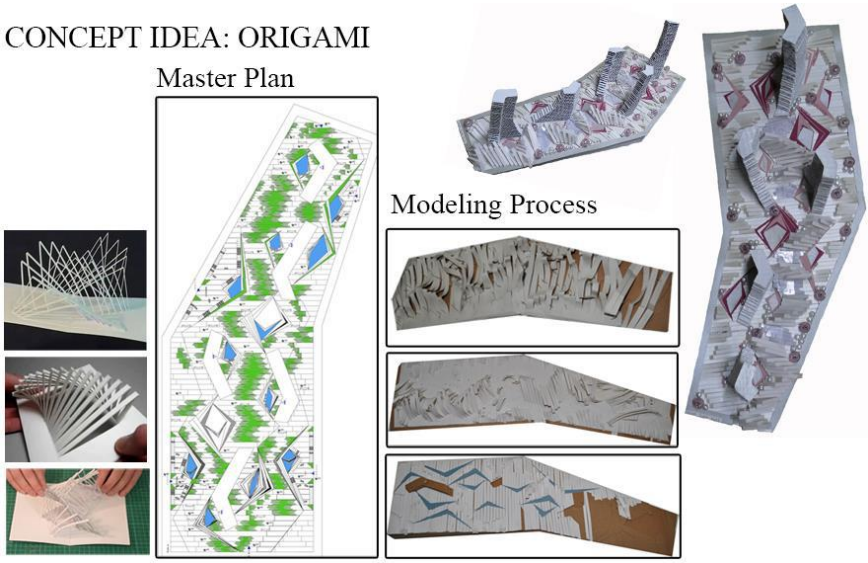

Fig. 8 Layering process by using origami and final project and model by Esma İşler.

3.2 Development of overlapping lines in the third dimension

At this stage, the space between the masses in the design area has been considered as a volume and how it will be designed is planned. In the first project to be given as an example of this stage, Harun Ünal has defined the purple colored main axes that will form the third dimension here (Figure 9). In the second project, Harun Yetgin determined the main axis of the designed volume as a broken line and developed his design accordingly (Figure 10).

*"**HÜ:** I decided to search for the concept of "dragonfly while making my investigation how to reflect the area among residences as a volume, on animals and their living quarters. It had an amazing wing system which had a capacity of moving through opposite directions simultaneously. Moreover, this wing system even became the source of inspiration in improving of a model of Skorsky's helicopter [3]. Therefore, I was inspired by the wing movements of dragonfly on air which was designed by drawings on computer and crossed positions of these wings to develop the main axe. I designed the visual analogy of two wings of dragonfly with the help of two broken lines, crossed each other, on the main axe, and I designed one couple wings of dragonfly by means of the other broken lines, stuck in the main axe."*

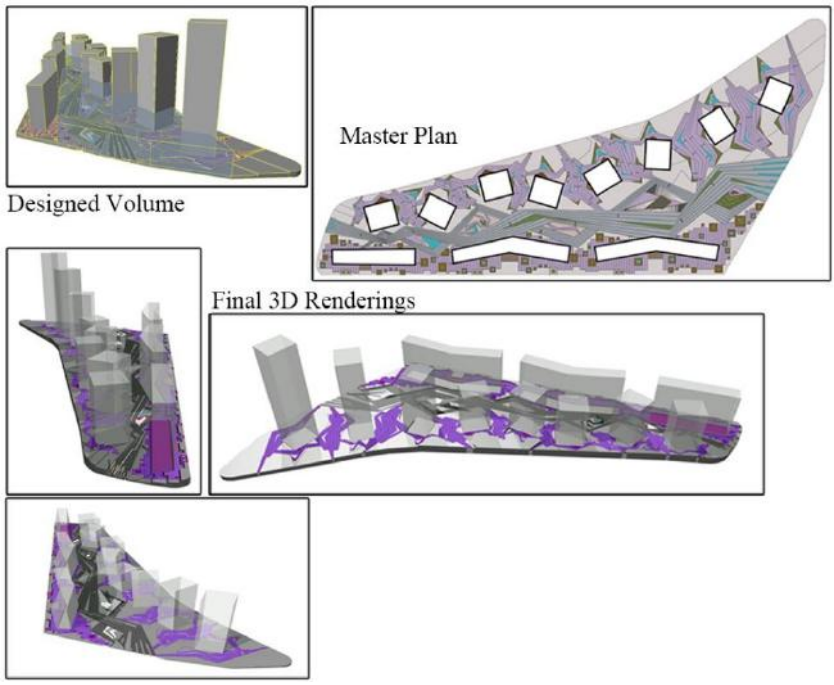

Fig. 9 Main axe investigations in designed volume and final project by Harun Ünal.

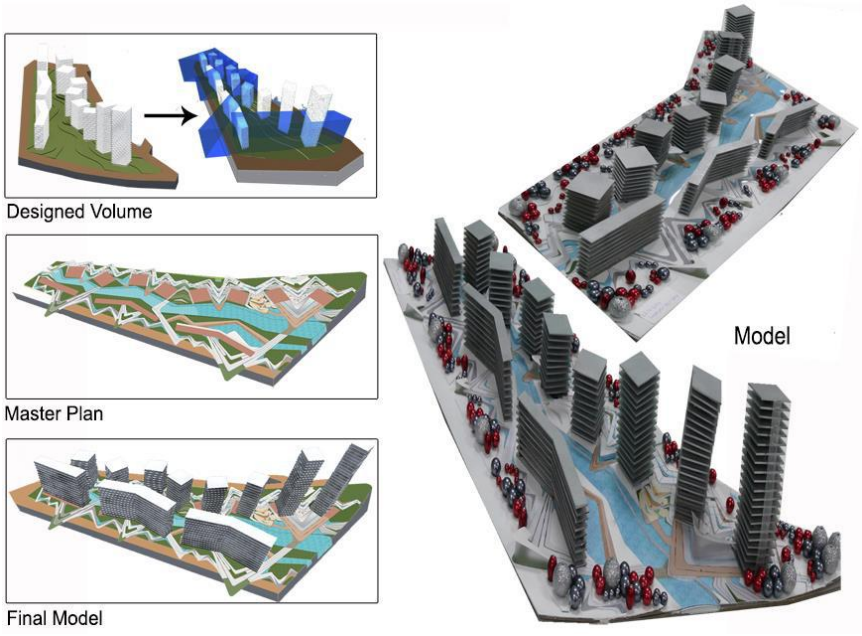

Fig. 10 Main axe investigations in designed volume and final model by Harun Yetgin

3.2. Spatial layering analysis

At this stage, the relationships between the different layers of the design are visualized. In the project, which is the first example at this stage, Harun Yetgin arranged a water-weighted main axis. The circulation axes, green areas and water areas accompanying the main axis have been determined as different spatial layers (Figure 11). In the second project, Harun Ünal determined the circulation axis system, wooden surfaces, greens in the pavement and water areas as spatial layers (Figure 12).

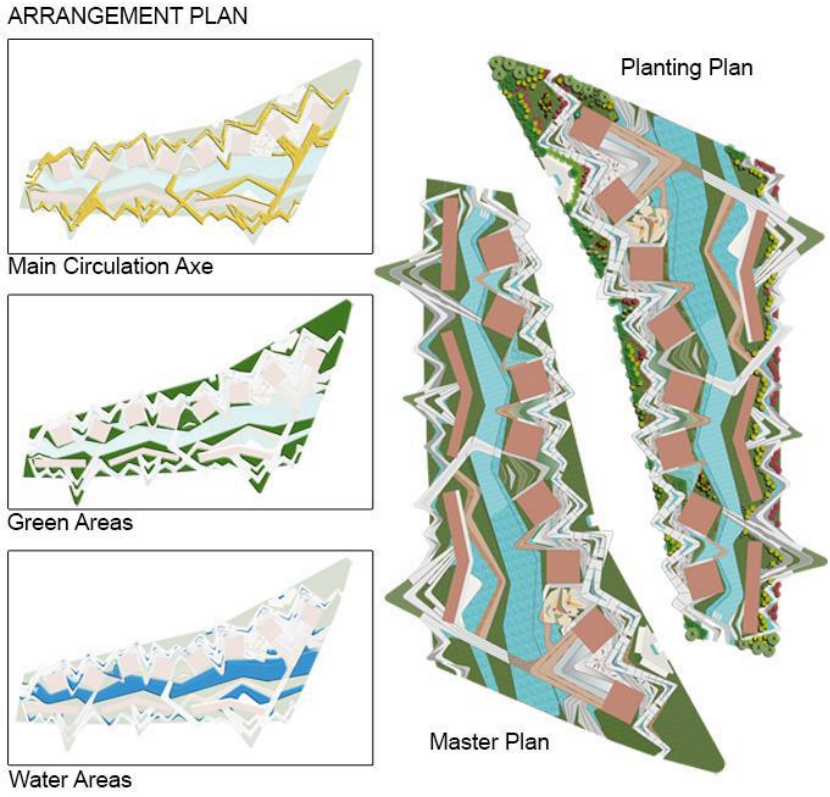

Fig. 11 Space layering analysis and final project by Harun Yetgin

*"**HY:** I constructed the theme of my design on transparency and permeability. The valley among residences suggested to me that I could create the third dimension by deepening the floor and filling the middle axe with water. Therefore, I decided to use water as the concept of my design. Every inhabitant of my design could make any activity on water which they desired. Thus, I created the main lines of my design by intersections of liner axes rising form the contours of the buildings.*

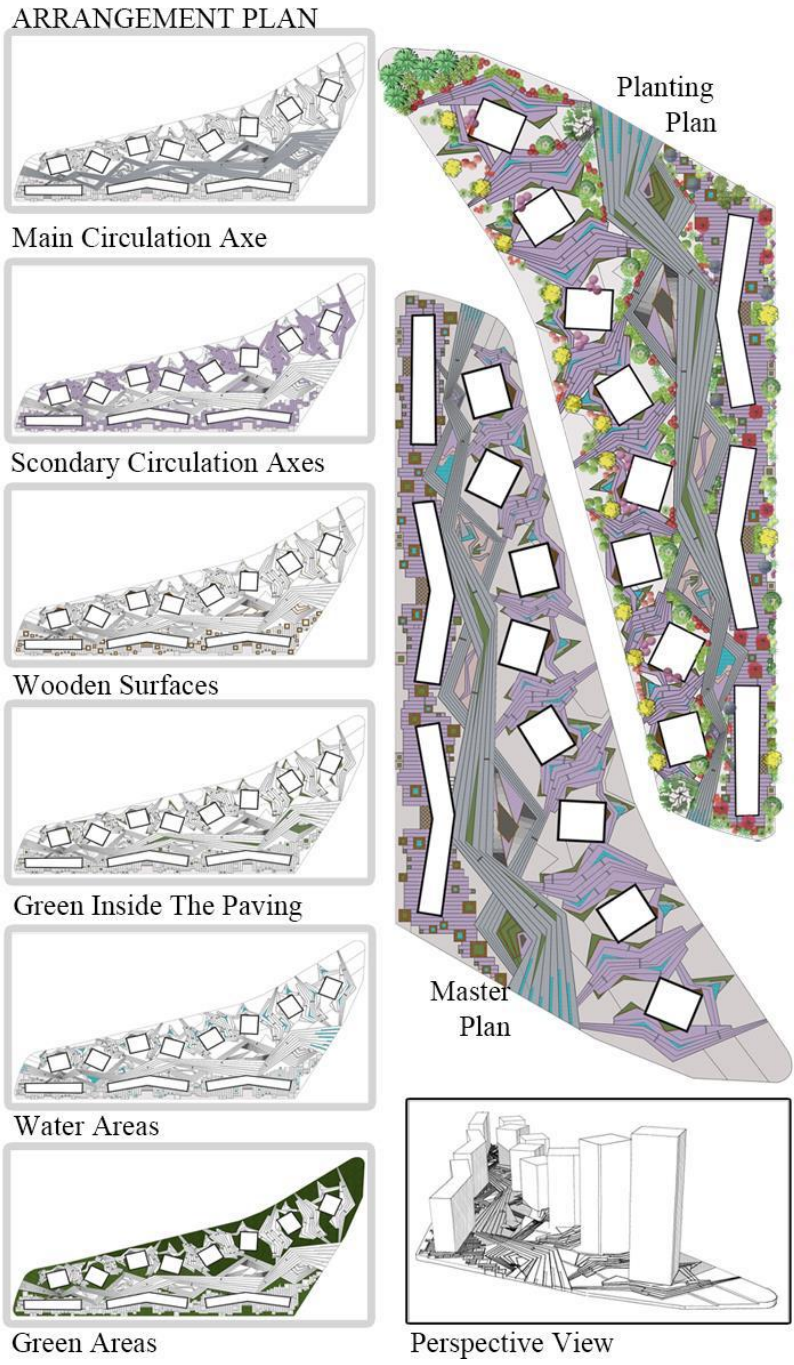

Fig. 12 Space layering analysis and final project by Harun Ünal

In the following steps, I deepened the floor of the valley to minus elevations for water field. Finally, I had an opportunity to use the vertical elevation on the valley side of the skyscrapers and this described to me the 3D vertical movement."

3.3. Activity-space and detail solutions

At this stage, there are activity and space solutions regarding the formal approach in design. The three-dimensional details of the designed activities were created and the activity-space relations were visualized. In the first project of this stage, Harun Yetgin modeled the activity areas at two points on the main axis (Figure 13).

Fig 13 3D renderings of activity, space and details.

In the second sample project, Aybike gives three-dimensional renderings of original and creative areas such as the perfume garden and the eating area (Figure 14).

"AD: I started shaping my project and activity areas by choosing the concept of ecology. My goal to choose this concept was to meet my inhabitant's desire for natural green in some respect. For this reason, the inspiration source of main design would be "plant" which had a whole structure from its roots to leaves. Therefore, I tried to meet this green desire of these inhabitants in skyscrapers by creating activity areas and close residential environment, reached by means of an axe system, resembling the roots of a tree. In this respect, entrance to the area was

very important for me since tiredness should start wiping out when the inhabitants arrived to the entrance; and they should feel that this tiredness disappeared in residences."

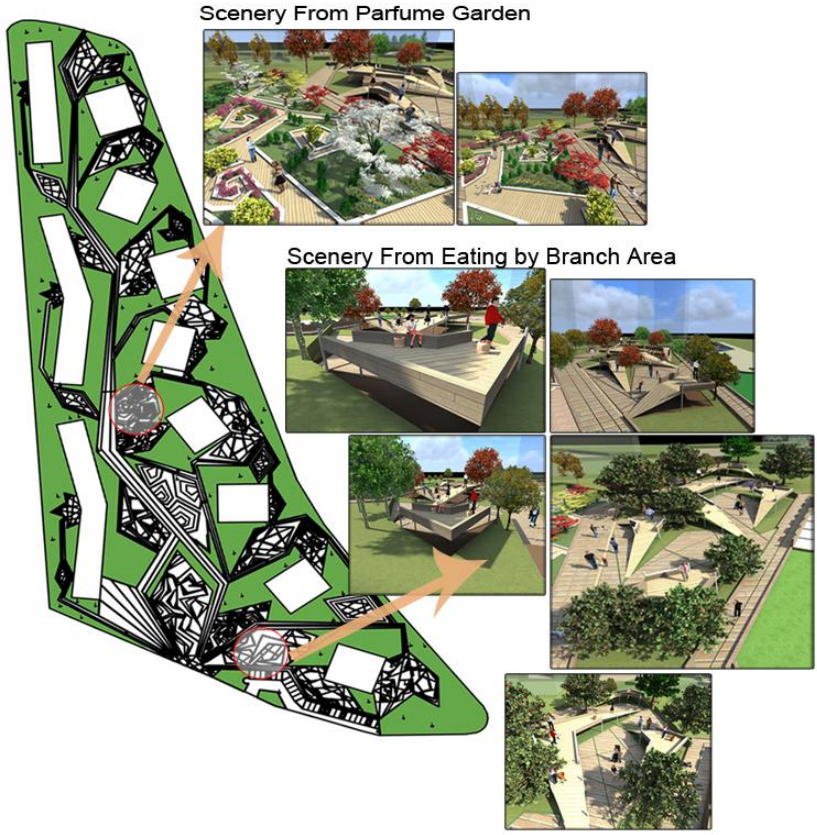

Fig. 14 3D renderings of creative activity spaces and final project by Aybike Demirel.

3. Conclusion

Three-dimensional thinking has always been a challenge in the design process, which should be handled as a complex system from the determination of the concept to the final design. Feedback and the interaction of the different stages in the design process are extremely important to cope with this challenge. As defined by the project process exemplified in the study, determining the next step of each step will make an extremely positive contribution to the success of any design project.

Acknowledgements

I would like to express my ongoing appreciation to other instructors of Environmental Design Studio VI: Ali Özbilen the head of Landscape

Architecture Department, Cengiz Acar, Mustafa Var and Sema Mumcu for their positive inspirations on our creative design studio process.

I also thank to you Aybike Demirel, Azer Özgür, Elif Kıycı, Esma İşler, Harun Ünal, Harun Yetgin and Mine Dilikoğlu, especially for your interminable patience, courage to try new ways and valuable support for our team spirit. Working with you was a great and amazing challenge in which all of us discovered various things in each following step.

References

[1] James Corner Field Operations, Diler Scofidio, Renfo, The High Line, *DLLE 1002 Urban Hybrids-Evoluation in Regeneration Spain, Landscape*, [2010]: pp. 22-47.

[2] http://www.kazimirmalevich.org/quotes/ Last Accessed: 01.09.2020.

[3] http://en.wikipedia.org/wiki/Westland_Dragonfly Last Accessed: 01.09.2020

CHAPTER II

FLORISTIC COMPOSITION OF CONIFEROUS FOREST BIOTOPES, THE CASE OF KURUCASILE (BARTIN/ TURKEY)[1]

Asst. Prof. Dr. Burçin EKICI* & Prof. Dr. Metin SARIBAŞ**

*Tekirdag Namık Kemal University, Faculty of Fine Arts Design and Architecture 59030 Tekirdag/ Turkey
e-mail: bekici@nku.edu.tr, Orcid ID: 0000-0002-2553-5656

**Retired member of Bartın University, e-mail: metinsar@hotmail.com

1. Introduction

Environmental pressure groups are increasing in the developing world. Therefore, the importance of habitat protection is increasing and potential ways to support environmental protection efforts in the world are explored (Chokor, 1992). Vegetation and ecological classification are required for a broad assessment of ecosystem health and the continuity of endangered habitats and wildlife (Jensen et al., 2000). The field planning made based on ecological data determines the interaction between existing land uses in the landscape and the ecological criteria for land use accordingly.

When making spatial planning, the changes that the land use alteration may cause on the biotope structure must be taken into account in order to ensure the continuity of flora and fauna as well as the functionality of ecosystems. This is because the biotope level is the first element to reveal the changes caused by field use. Besides, biotopes are areas, the borders of which can be drawn and which can be represented in cartography and they can easily be handled in planning. As one of the modern nature protection components, biotope mapping is very important for the protection of endangered, rare and valuable biotopes.

The physical properties of the environment are closely related to the existing vegetation potential. Physiologically similar areas are classified by biotope mapping and an analytical approach is taken for wildlife protection planning. This enables evaluating the potential of the area and it also sets ground for the long- term protection planning and rehabilitation projects (Imanishi et al., 2005). Biotope maps can reveal the geographic distribution of vegetation types and explain the relationship between this distribution and one or more features of the environment (Küchler, 1984). The former landscaping studies can be explained with the help of existing

[1] This study was produced from the PhD thesis named “Mapping of the Biotopes in the Kurucasile (Bartin) Coastline and its Surrounding Areas”.

plants in the area and information about the ecology of the area in the past and present can be provided (Clare & Bunce, 2004). Thus, the factors that the biotope is exposed to and their severity can be revealed to determine the threats.

When previous researches on biotope mapping are examined, it is observed that these maps are the basis of landscape planning and nature protection. In this research, analytical methods have been developed for wildlife habitat protection planning by classifying physiologically similar areas. Thus, threats against the natural environment are shown and changes in nature are revealed (Zohary, 1947; Küchler, 1984; Chokor, 1992; Mellink, 1993; Blab et al., 1995; Bastian, 1996; Hadjibiros, 1996; Jensen et al., 2000; Clare & Bunce, 2004; Imanishi et al., 2005; Müller et al., 2003).

In this research, coniferous biotopes of Kurucaşile (Bartın) and its vicinity are mapped. Thus, the changes caused in the biotope structure due to land use during spatial planning have been revealed in order to ensure the continuity of flora and fauna and the functionality of ecosystems. It is aimed to integrate the content of biodiversity with spatial planning and to reveal the effects of changes in land use on biodiversity. In addition, the natural potential of the area has been revealed by researching biotopes. When research results are used by planning authorities, economic and ecological benefits will be provided in terms of resource use, which may contribute to reduction or prevention of environmental pressures.

2. Materials and methods

Kurucaşile is established on an area of 1 546 km² on the Western Black Sea coast. The surface area is 159 km² (Çilsüleymanoğlu, 1996). The district is surrounded by the Black Sea, Bartin, Cide and Amasra on the north, south, east and west respectively. There are Cenozoic and Mesozoic sedimentary rocks in the research area. Çakraz formation, Himmetpasa and Gökcetepe formation and Cretaceous aged Kazpinari formation cover a large space in the area (Haner & Türk, 2000). The most common soil group in the district is gray brown podzolic soils. Alluvial soils, which occupy a very small amount, are usually located in the subsoil of the valley. These soils with sand, clay and miles form the most fertile areas. The area dominated by the temperate Black Sea climate, which can receive rainfall in all seasons, is in the "humid climate" group according to the water balance sheet prepared in line with Thornthwaite method. While the *Euxine* section of the *Euro- Siberian* floristic region prevails on the northern slopes of the area facing the Black Sea due to the warm and humid sea climate, Pseudo maquis elements are also seen from place to place. Kurucasile forests are predominantly composed of broad- leaved species and

coniferous taxa. The material of the study consists of coniferous forest biotopes in Kurucaşile district. Coniferous forest biotopes consist of *Pinus brutia*, *Pinus nigra* subsp. *pallasiana* and *Pinus sylvestris*.

The study was carried out in three phases; analysis of the existing data of the area and the research subject, field studies and evaluation of the data obtained from field studies. In the first phase, information about vegetation and climate, soil, geological, geomorphological and hydrological data were collected to characterize the growth medium. In the second phase, floristic researches were started. In this context, field studies were carried out in the sample areas and a plant was collected for diagnostic purposes and a "Field study form" was completed for each sample area. With this form, data were obtained about cover value of herbaceous vegetation, amount, combination and dominance of species, cover ratio of woody vegetation, length of layers and the size, coordinates, growth medium characteristics and habitat value of the sample area. Species composition of vegetation cover and frequency of species in sample areas were determined by means of this field study form. Accordingly, the characteristic species representing the biotope type were determined. As vegetation is an indicator in floristic studies, Braun-Blanquet (1964) method was used to show the ecological structure. With this method, the amount of existing plants in an area covered with vegetation is determined by observation and coverage values are expressed as % of the total area (Braun- Blanquet, 1964).

In the identification of the plants collected from the field and made into herbarium material, the herbarium of Hacettepe University Faculty of Science was used. In addition to herbarium facilities, especially, the works of Davis (1965- 1985), Davis et al. (1988) and Güner et al. (2000), as well as Symonds & Chelminsky (1958), Symonds & Merwin (1963), Tutin et al. (1964), Tutin et al. (1968- 1980), Hora (1981), Fitter et al. (1986), Yaltırık (1988), Schönfelder & Schönfelder (1990), Gibbons (1993), Yılmaz (1993), Baytop (1997), Uluocak (1994), Schönfelder & Schönfelder (1995), Seçmen et al. (1995), Yaltırık & Efe (1996), Kremer (1998), Erik et al. (1998), Zeydanlı et al. (1999), Altan (2000), Ekim et al. (2000), Durmuşkahya (2006), Akman et al. (2007), Namıkoğlu (2007) and Özhatay et al. (2010) were used.

3. Results

Coniferous forest biotopes detected in the research area are *Pinus sylvestris* L., *Pinus nigra* Arnold. ssp. *pallasiana* (Lamb.) Holmboe and *Pinus brutia* Ten. *Pinus brutia* communities which grown at a high temperature, are seen in the coastal areas and southern slopes. *Pinus nigra* subsp. *pallasiana* and *Pinus sylvestris* forest biotopes which are resistant

to drought, are dominate in the holes between valleys and on the southern view.

Coniferous forest biotopes are mainly dominated by *Pinus sylvestris*; *Pinus sylvestris* is a species requesting low temperature and water and not affected by spring frosts. As it is resistant to frost and drought, it is the dominant tree of forests on the northern slopes of the Black Sea mountains and on the narrow valley bases. (Figure 1). It has been observed that it is mostly located on northern view in very sloping areas.

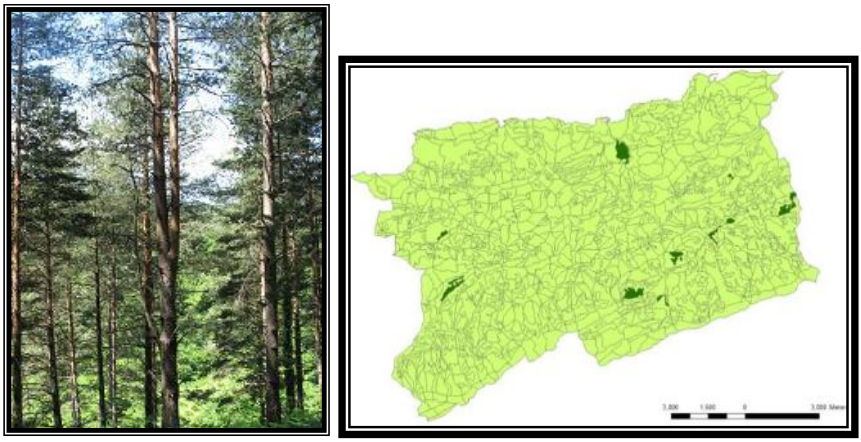

Figure 1. *Pinus sylvestris* societies and map of these biotopes in the research area (Ekici, 2012)

Pinus sylvestris biotopes are mixed with *Pinus nigra* ssp. *pallasiana* on the southern hillside. *Abies nordmanniana* subsp. *bornmuelleriana* is also included in this mixture at low altidudes. *Pinus sylvestris*, accompanied by *Carpinus betulus*, *Fagus orientalis*, and *Populus tremula* species, form small groups in the vicinity of Buyukcubuk, Kiran Hill and Kayaliksuyu, which receive cooler and damp winds from the north and dominated by medium depth soils. It is mostly spread through the gray brown podzolic soils dominated by red sandstone, claystone bedrock. This biotope is accompanied by woody plants such as; *Arbutus unedo*, *Cornus sanguinea*, *Corylus avellana* var. *avellana*, *Rhododendron ponticum* subsp. *ponticum*, *Rosa canina*, *Rubus caesius*, *Buxus sempervirens*, *Cistus creticus*, *Cornus mas*, *Crataegus microphylla*, *Erica arborea*, *Juniperus communis* subsp. *nana*, *Smilax excelsa* and *Vaccinium arctostaphylos*. The most common herbaceous vegetation cover in research areas consist of; *Anagallis arvensis* var. *arvensis*, *Crepis foetida* subsp. *rhoeadifolia*, *Euphorbia amygdaloides* var. *amygdaloides*, *Hypericum perforatum*, *Petasites hybridus*, *Rumex conglomeratus*, *Rubia peregrina*, *Sambucus ebulus* and *Torilis arvensis* subsp. *arvensis* and dominant taxa is *Dryopteris filix- mas* (Table 1).

Table 1. Vegetation analysis of forest biotopes dominated by *Pinus sylvestris* (Abbreviations: Rss: Red sandstone- claystone, Ldl: Limestone-dolomitic limestone, Gbp: Gray brown podzolic, Ryp: Red yellow podzolic)

Research area number	**1**	**2**	**3**	**4**	**5**	**6**	**Availa-bility**
View	N	S	NE	N	S	N	
Slope (%)	55	50	50	30	60	45	
Dimensions of the area (m^2)	400	400	400	400	400	400	
Geological structure	Rss	Rss	Ldl	Rss	Ldl	Ldl	
Soil structure	Gbp	Gbp	Gbp	Ryp	Gbp	Gbp	
Tree species	**Vegetation cover**						
Pinus sylvestris	2	2	1	3	2	1	6
Carpinus betulus	+			+	+		3
Castana sativa	1	1	+		1		3
Abies nordmanniana subsp. *bornmuelleriana*		1				1	2
Fagus orientalis				1		+	2
Pinus nigra		1				+	2
Populus tremula	+			1			2
Quercus cercis var. *cercis*		1				+	2
Quercus infectoria subsp. *infectoria*			+			+	2
Shrub species							
Juniperus communis subsp. *nana*	1	2	+	2		1	5
Cornus mas			+		+	1	3
Rhododendron ponticum subsp. *ponticum*	1	2				1	3
Rosa canina			1		1	2	3
Herbaceous species							
Dryopteris filix- mas	2	2	2	1	1	2	6

Euphorbia amygdaloides var. *amygdaloides*	+	+	1		+	1	5
Hypericum perforatum	+	1		1	+	1	5
Rumex conglomeratus	+		+	+	+	1	5
Anagallis arvensis var. *arvensis*			+	+	+	1	4
Crepis foetida subsp. *rhoeadifolia*	1	1			+	1	4
Petasites hybridus	1		1		1	+	4
Rubia peregrina	1	+			+	+	4
Sambucus ebulus	1	1	1			1	4
Torilis arvensis subsp. *arvensis*	+			+	+	1	4
Agrostis capillaris	1	1		1			3
Anacamptis pyramidalis		+	r		+		3
Asplenium trichomanes	1		1			+	3
Barbarea vulgaris	1	+		+			3
Briza maxima	+	+			+		3
Dorycnium graecum	1	2		2			3
Galium palustre	1		+		+		3
Hedera helix				+	+	1	3
Hordeum murinum subsp. *leporinum* var. *leporinum*	+	1	+				3
Primula vulgaris subsp. *vulgaris*		1	+			+	3
Ranunculus constantinopolitanus	1	1	1				3
Sophora jaubertii			2	1	1		3
Trifolium campestre			1		+		3
Trifolium ochroleucum	1	1	1				3
Dominant species	*Dryopteris filix- mas*						

Research areas: Buyukcubuk (1; X: 4624200 Y: 466325), Meryemler (2; X: 4625225 Y: 474650), Kayaliksuyu (3; X: 4627100 Y: 466925), Kiran Hill (4; X:

4624124 Y: 473750), Geyliksuyu (5; X: 4631950 Y: 478925), Kapisuyu (6; X: 4631075 Y: 479275), **Area 1:** *Cistus creticus* (+), *Anthemis cretica* subsp. *pontica* (+), *Centaurium erythraea* subsp. *erythraea* (r), *Cirsium hypoleucum* (+), *Holcus lanatus* (1), *Mentha aquatica* (+), *Plantago lanceolata* (+), *Prunella vulgaris* (+), **Area 2:** *Corylus avellana* var. *avellana* (+), *Centaurium erythraea* subsp. *erythraea* (+), *Dactylis glomerata* subsp. *hispanica* (1), *Dryopteris abbreviata* (1), *Ophyris oestrifera* subsp. *oestrifera* (+), *Plantago lanceolata* (+), *Plantago major* subsp. *major* (+), *Potentilla reptans* (+), *Rumex crispus* (+), **Area 3:** *Buxus sempervirens* (r), *Crataegus microphylla* (+), *Rubus caesius* (1), *Bellis perennis* (+), *Convolvulus arvensis* (+), *Foeniculum vulgare* (r), *Fragaria vesca* (+), *Geranium dissectum* (r), *Ophyris oestrifera* subsp. *oestrifera* (+), *Potentilla reptans* (+), *Prunella vulgaris* (+), **Area 4:** *Cornus sanguinea* (+), *Erica arborea* (+), *Smilax excelsa* (1), *Cynosurus echinatus* (1), *Lamium purpureum* var. *purpureum* (1), *Lolium perene* (+), **Area 5:** *Dryopteris abbreviata* (1), *Foeniculum vulgare* (+), *Rumex crispus* (+), **Area 6:** *Anthemis triumfettii* (+), *Bellis perennis* (+), *Coronilla varia* subsp. *varia* (1), *Geranium dissectum* (+), *Salvia forskahlei* (1).

Coniferous forest biotopes are mainly dominated by *Pinus nigra* ssp. *pallasiana*; *Pinus nigra* ssp. *pallasiana* biotopes, which is resistant to winter cold and drought, are mostly located in the inner parts. These biotopes spread mostly around Doganci and Kanatli and the southern slopes of Yukari and Yanik hill, at approximately 400- 700 m (Figure 2). These biotopes are mixed with *Pinus pinaster* and leafy trees in this areas. *Pinus nigra* ssp. *pallasiana* communities are mixed with *Quercus infectoria* subsp. *infectoria* and *Castanea sativa* in Dogancı and Kanatli where marl, clayey limestone and sandstone bedrock dominates.

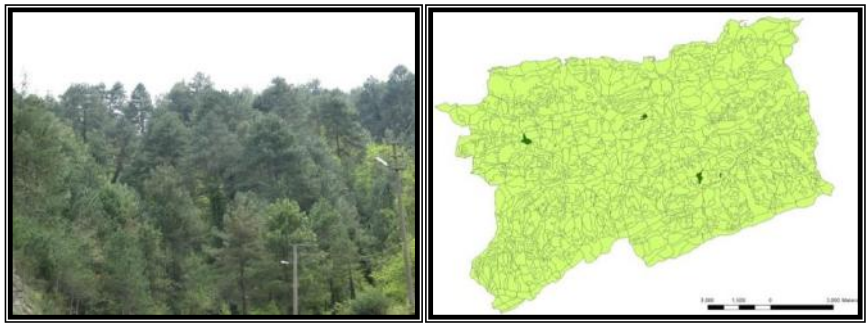

Figure 2. *Pinus nigra* ssp. *pallasiana* societies and map of these biotopes in the research area (Ekici, 2012)

Some pseudo maquis elements like *Pistacia terebinthus* subsp. *terebinthus*, *Cistus creticus*, *Cistus salviifolius*, *Erica arborea* and *Juniperus oxycedrus* subsp. *oxycedrus* where destroyed the *Pinus nigra* ssp. *pallasiana* forests, are seen in the research area. Other woody species identified in these localities; *Ostrya carpinifolia*, *Populus tremula*, *Prunus spinosa* subsp. *dasyphylla*, *Rosa canina*, *Rubus caesius* and *Rubus hirtus*.

Having limited occupancy as well as the openings in the forest and the forest edges allow for the development and diversification of herbaceous vegetation. The dominant herbaceous species of the biotope are; *Anthemis cretica* subsp. *pontica*, *Briza media*, *Dorycnium graecum*, *Dryopteris filix-mas*, *Hedera helix*, *Salvia forskahlei*, *Sambucus ebulus*, *Sophora jaubertii*, *Tanacetum corymbosum* subsp. *cinereum* and *Trifolium campestre* (Table 2).

Table 2. Vegetation analysis of forest biotopes dominated by *Pinus nigra* subsp. *pallasiana* (Abbreviations: Rss: Red sandstone- claystone, Mcl: Marl-clayey limestone, Mcst: Marl- claystone- sandstone- tuff, Esct: Exfoliation sandstone- claystone- tuff, Ryp: Red yellow podzolic Gbp: Gray brown podzolic)

Research area number	**7**	**8**	**9**	**10**	**Availab il-ity**
View	N	N	N	N	
Slope (%)	65	65	60	50	
Dimensions of the area (m²)	400	400	400	400	
Geological structure	Rss	Mcl	Mcst	Esct	
Soil structure	Ryp	Gbp	Gbp	Gbp	
Tree species	**Vegetation cover**				
Pinus nigra subsp. *pallasiana*	2	2	2	2	4
Carpinus betulus	1			1	2
Castanea sativa		1	1		2
Ostrya carpinifolia		+	+		2
Populus tremula	+		+		2
Prunus avium			1	+	2
Quercus cerris var. *cerris*	+			+	2
Quercus infectoria subsp. *infectoria*	1		+		2
Shrub species					
Cistus creticus		+	+		2
Cornus mas	+			1	2
Corylus avellana var. *avellana*	1			1	2
Erica arborea		+	+		2

Juniperus oxycedrus subsp. *oxycedrus*		+	+		2
Pyracantha coccinea	+			+	2
Rosa canina		+	+		2
Rubus hirtus		+	+		2
Vaccinium arctostaphylos	+			r	2
Herbaceous species					
Dryopteris filix- mas	2	1	1	2	4
Briza media	1	+	+	1	4
Dorycnium graecum	2	+	+	2	4
Anthemis cretica subsp. *pontica*	1	+	+		3
Hedera helix	2	1		1	3
Salvia forskahlei	2	2		1	3
Sambucus ebulus	1	1		1	3
Sophora jaubertii	1	2	+	2	3
Tanacetum corymbosum subsp. *cinereum*	+	+		+	3
Trifolium campestre	1	+	1		3
Avena barbata subsp. *barbata*	1			1	2
Briza maxima	+			1	2
Cerastium glomeratum		1	2		2
Chamaecytisus hirsutus			+	+	2
Cirsium vulgare	1	+			2
Crepis foetida subsp. *rhoeadifolia*	1			1	2
Cynosurus echinatus	+	+			2
Dactylis glomerata subsp. *hispanica*	1			1	2
Euphorbia amygdaloides var. *amygdaloides*	1			+	2
Juncus effusus	+	+			2
Primula vulgaris subsp. *vulgaris*		r		+	2
Ranunculus constantinopolitanus	+			1	2

Rumex conglomeratus	+			+	2
Dominant species	*Dryopteris filix- mas*				

Research areas: Yukaritasca (7; X: 4627425 Y: 466850), Doganci (8; X: 4631325 Y: 474575), Kanatli (9; X: 4629350 Y: 466300), Yanik Hill (10; X: 4627900 Y: 466450), **Area 7:** *Carduus nutans* (+), *Lysimachia verticillaris* (r), **Area 8:** *Pistacia terebinthus* subsp. *terebinthus* (r), *Cistus salviifolius* (+), *Rubus caesius* (+), **Area 9:** *Prunus spinosa* subsp. *dasyphylla* (r), *Euphorbia cyparissias* (+), **Area 10:** *Pinus pinaster* (1), *Convolvulus arvensis* (+), *Hieracium pannosum* (+), *Plantago lanceolata* (+), *Trifolium lappaceum* (+).

Coniferous forest biotopes are mainly dominated by *Pinus brutia* Ten.; *Pinus brutia* biotopes, which spreads mostly in coastal areas in the research area, are locally located on the slopes facing the shore. These biotopes which form forests as the dominant trees at low altitudes, are seen on the narrow coastal strip between 100 and 200 m. *Pinus brutia* biotopes seen Aydogmus, Alapinar and Obruk which along the coastal zone and along the valleys the sea effect (Figure 3).

Figure 3. *Pinus brutia* societies and map of these biotopes in the research area (Ekici, 2012)

Pinus brutia, which is not selective in soil requirements, grows in moderately deep, moist- arid and acid- alkaline soils up to 200 m from the shore in the research area. It was determined that the taxon spread around Aydogmus and Obruk, especially in calcareous and sandy soils. Sandstone and limestone bedrock dominate these areas. *Pinus brutia*, which is an opinionated species, can live in different ecological conditions in the area. However, there are significant differences in the number of species and participation rates of the accompanying plant species. Pseudo maquis elements are found up to a height of about 200 m on the coastline. It has been observed that in some parts of the *Pinus brutia* biotopes seen along the coastal zone and along the valleys with the sea effect. In the areas where the forests are destroyed, the composition is accompanied by maquis species like *Arbutus unedo*, *Cistus creticus*, *Cotinus coggyria*, *Juniperus oxycedrus* subsp. *oxycedrus*, *Laurus nobilis*, *Paliurus spina- christi*,

Phillyrea latifolia, *Pistacia terebinthus* subsp. *terebinthus*, *Quercus coccifera*, *Quercus petraea* subsp. *iberica*, *Rhus coriaria* and *Spartium junceum*. Anthropogenic effects have been observed in some part of biotopes and ruderal vegetation has been determined in these areas which increase the diversity of herbaceous species. *Centaurea calcitrapa* var. *calcitrapa*, *Datura stramonium*, *Euphorbia amygdaloides* var. *amygdaloides*, *Malva alcea*, *Plantago lanceolata*, *Rumex conglomeratus* ve *Scabiosa atropurpurea* subsp. *maritima* Centaurea taxa constitute a large space in these areas (Table 3).

Table 3. Vegetation analysis of forest biotopes dominated by *Pinus brutia* (Abbreviations: Rss: Red sandstone- claystone, Mcl: Marl-clayey limestone, Ldl: Limestone- dolomitic limestone, Ryp: Red yellow podzolic Gbp: Gray brown podzolic)

Research area number	**11**	**12**	**13**	**Availability**
View	N	N	S	
Slope (%)	60	50	60	
Dimensions of the area (m²)	400	400	400	
Geological structure	Rss	Mcl	Ldl	
Soil structure	Ryp	Gbp	Ryp	
Tree species	**Vegetation cover**			
Pinus brutia	1	1	+	3
Laurus nobilis	+	+		2
Quercus petraea subsp. *iberica*	+	+		2
Shrub species				
Cistus creticus	+	+		2
Juniperus oxycedrus subsp. *oxycedrus*	+	+		2
Rhus coriaria	+	+		2
Herbaceous species				
Hedera helix	2	+	1	3
Rumex conglomeratus	1	1	+	3
Salvia tomentosa	2	1	2	3
Anagallis arvensis var. *arvensis*	1		1	3
Avena barbata subsp. *barbata*		+	1	3

Blackstonia perfoliata subsp. *serotina*		+	+	2
Calamintha nepeta subsp. *glandulosa*	+	1		2
Centaurea calcitrapa var. *calcitrapa*		1	+	2
Clematis vitalba	1		+	2
Coronilla varia subsp. *varia*	2		+	2
Crepis foetida subsp. *rhoeadifolia*	1		1	2
Euphorbia amygdaloides var. *amyg.*	1		+	2
Geranium robertianum	1		+	2
Iris germanica	+	+		2
Plantago lanceolata		1	+	2
Rubia peregrina	1	1		2
Sambucus ebulus		1	1	2
Dominant species	*Hedera helix*			

Research areas: Aydogmus (11; X: 4627250 Y: 472250), Alapinar (12; X: 4631725 Y: 474225), Obruk (13; X: 4625175 Y: 478525), **Area 11:** *Pistacia terebinthus* subsp. *terebinthus* (r), *Quercus coccifera* (+), *Arbutus unedo* (+), *Phillyrea latifolia* (+), *Rubus caesius* (1), *Arum maculatum* (1), *Convolvulus arvensis* (1), *Euphorbia seguieriana* subsp. *seguieriana* (+), *Helleborus orientalis* (+),*Lamium purpureum* var. *purpureum* (1), *Onopordum tauricum* (r), *Senecio aquaticus* subsp. *erraticus* (+), *Torilis japonica* (+), *Hordeum murinum* subsp. *leporinum* var. *leporinum* (+), *Orobanche minor* (r), **Area 12:** *Cotinus coggyria* (r), *Paliurus spina- christi* (+), *Spartium junceum* (+), *Calystegia sepium* ssp. *sepium* (+), *Campanula rapunculoides* subsp. *rapunculoides* (1), *Centaurium pulchellum* (r), *Datura stramonium* (+), *Galium verum* subsp. *verum* (+), *Genista tinctoria* (1), *Malva alcea* (r), *Origanum vulgare* ssp. *vulgare* (2), *Osyris alba* (+), *Pallenis spinosa* (+), *Prunella vulgaris* (1), *Scabiosa atropurpurea* subsp. *maritima* (1), *Scolymus hispanicus* (+), *Torilis arvensis* subsp. *arvensis* (+), *Trifolium pratense* var. *pratense* (1), **Area 13:** *Carpinus betulus* (+), *Castanea sativa* (+), *Quercus infectoria* subsp. *infectoria* (+), *Ligustrum vulgare* (+), *Rhododendron ponticum* subsp. *ponticum* (1), *Rosa canina* (1), *Smilax excelsa* (+), *Hypericum bithynicum* (1).

4. Discussion

The ecological planning approach forms the basis of efficient and balanced use of natural resources. However, today, it is observed that critical environmental problems occur due to the plans made without considering the ecological and functional integrity of natural systems. Ecological information should be integrated in management decisions and planning to ensure the continuation of biodiversity. Damaged habitats should be planned by planners and designers in such a way that the

negative impact is minimized and the habitat value is increased. Biotope mapping is crucial for nature protection and for making land use decisions.

Within the scope of this study, in which the coniferous forest biotopes that spread around Kurucasile (Bartin) coastline and its vicinity are mapped, detailed data about the flora and its habitats were collected. With the acquisition of biotope inventory, it will be possible to determine the natural resources of the region, to protect and use, to minimize the environmental effects threatening its immediate environment and to transfer natural values to future generations in a healthy way.

When the degeneration amount of existing biotopes in the research area is observed, it is very likely to see that the amount of distortion increases as you approach the settlement. Field observations confirm this increase, especially from the interior areas to the coastal areas. In order for the damaged areas to renew themselves, first of all, degeneration caused by the use of forest products and land uses should be taken under control.

Coniferous forest biotopes dominated by *Pinus sylvestris*, *Pinus nigra* ssp. *pallasiana* ve *Pinus brutia*, which spread in the research area, covers an area of 910 ha. When the spatial distribution of these biotopes is examined, it is seen that the forests dominated by *Pinus sylvestris* distinguish, which is followed by *Pinus nigra* ssp. *pallasiana* forests. The forest biotopes dominated by *Pinus brutia* is the least observed.

Pinus sylvestris societies, which occupy the most area among the coniferous forest biotopes with 407 ha, establish forests as dominant trees on the north- facing slopes and narrow valley bases of the mountains. Biotopes are generally seen in northern parts. On the other hand, ecological sensitivity caused by drought occurs in the southern slopes. *Carpinus betulus*, *Fagus orientalis* and *Populus tremula* species accompanying *Pinus sylvestris* offer unique views with its altering colors in autumn. Considering the visual effects of these forests and their contribution to recreation, it is recommended to evaluate them in terms of nature tourism by taking necessary protection measures. Due to the wood of *Quercus* sp., which is mixed in these biotopes, it is exposed to illegal cuts and the intense intervention of the local people collecting *Castanea sativa* fruit. Therefore, these areas are open to social pressure. However, these biotopes host endemic *Abies nordmanniana* subsp. *bornmuelleriana* and *Anacamptis pyramidalis* geophytes. For this reason, it is an area that should be protected in terms of the importance of highly natural areas and the value of plant species conservation.

Pinus nigra ssp. *pallasiana* is the second largest biotope among the coniferous fores biotopes with its 307 ha area. The drought- tolerant species is generally seen in small amounts in pits between the valleys and

on southern parts. *Pinus nigra* ssp. *pallasiana* societies mix with *Ostrya carpinifolia*, *Quercus cerris* var. *cerris*, *Quercus infectoria* subsp. *infectoria* and *Castanea sativa* on the lower slopes of Doganci, Kanatli and Yanik Hill with a sea climate. Local people make extensive use of these trees. Therefore, these biotopes are open to human intervention. In the study, *Euphorbia cyparissias* taxon, which is a new record for the area, was detected (Figure 4). These areas, which are very rich in plant variety, are sensitive biotopes that require urgent protection. For this reason, it is necessary to take the necessary protection measures in degenerated areas.

Figure 4. *Euphorbia cyparissias* taxon detected for the first time in the research area (Ekici, 2012)

In *Pinus nigra* ssp. *pallasiana* forest biotopes, *Castanea sativa*, *Prunus avium*, *Prunus spinosa* subsp. *dasyphylla* fruit trees and fruit bushes such as *Cornus mas*, *Corylus avellana* var. *avellana*, *Rosa canina*, *Rubus caesius* and *Rubus hirtus* occupy a large space. In afforestation and rejuvenation studies in biotopes, it is recommended to secure the presence of these taxa. Thus, the continuity of ecological life will be ensured and the ethnobotanical use of the forests by people will be increased.

In the research area, small sets of coniferous forest biotopes dominated by *Pinus brutia* requiring high temperature are seen in the coastal region and along the valleys where sea effect penetrates. These biotopes, where Mediterranean vegetation elements are seen extensively, cover an area of approximately 196 ha.

It has been observed that in some parts of biotopes, social pressure increases and environmental pollution occurs due to construction and household wastes. In these areas where anthropogenic effects are frequently observed, pseudomaceous elements such as *Cistus creticus*, *Rhus coriaria* and *Spartium junceum* have been observed to gradually cover the points of destruction. Anthropogenic effect on these biotopes should be prevented and necessary sanctions should be applied immediately. They need to be protected ecologically due to their natural scenery effect as well as their vegetative potential.

References

Akman, Y., Ketenoğlu, O., Kurt, L., Güney, K., Hamzaoğlu, E. & Tuğ, N., (2007), *Angiospermae*, Palme Publishing, ISBN: 9944- 341- 21- 5.

Altan, T., (2000), *Natural Vegetation*, Cukurova University Press No: 2353, Adana.

Bastian, O. (1996): "Biotope mapping and evaluation as a base of nature conservation and landscape planning", *Ekologia*, 15 (1).

Baytop, T., (1997), *Turkish Plant Names Dictionary*, Turkish Language Association Publications: 578, Ankara.

Blab, J., Riecken, U. and Ssymank, A., (1995), "Proposal on a criteria system for a National Red Data Book of Biotopes", *Landscape Ecology*, 10 (1).

Braun- Blanquet, J., (1964), *Pflanzensoziologie*, New York.

Clare, T. and Bunce, R.G.H., (2004), "The potential for using trees to help define historic landscape zones: A case study in the English Lake District", *Landscape and Urban Planning*, 74 (1): 34- 45.

Chokor, B.A., (1992), "Environmental pressure groups and habitat protection in the developing world: The case of Nigeria", *The Environmentalist*, 12 (3).

Çilsüleymanoğlu, S., (1996), *Bartın Folk Culture*, Turkish History Association Press, Ankara.

Davis, P.H., (1965- 1985), *Flora of Turkey and The East Aegean Islands*, Edinburgh University Press (Volume 1- 2- 3- 4- 5- 6- 7- 8- 9).

Davis, P.H., Mill, R.R. and Tan, K., (1988), *Flora of Turkey and The East Aegean Islands*, Edinburgh University Press (Volume 10).

Durmuşkahya, C., (2006), *Trees and Shrubs in the Aegean Region*, Ministry of Environment and Forestry General Directorate of Nature Conservation and National Parks Press, ISBN: 975- 8273- 86- 8, Ankara.

Ekici, B., (2012), *Mapping of The Biotopes in The Kurucaşile (Bartın) Coastline and Its Surrounding Areas*, Bartın University Institute of Science PhD Thesis, Bartın.

Ekim, T., Koyuncu, M., Vural, M., Duman, H., Aytaç, Z. and Adıgüzel, N., (2000), *Turkey Red Book of Plants*, Publication of Nature Protection Society of Turkey, Ankara.

Erik, S., Akaydin, G. and Göktaş, A., (1998), *Natural Plants in Capital City*, Ankara Governorship Environmental Protection Directorate, Ankara.

Fitter, R., Fitter, A. and Blamey, M., (1986), *Pareys Blumenbuch*, Wild Pflanzen Deutschlands und Nordwesteuropas Press, London.

Gibbons, B. and Brough, P., (1993), *Blüten- Pflanzen*, Franckh- Kosmos Verlags- GmbH & Co., ISBN: 3- 440- 07504- 4, Stuttgart.

Güner, A., Özhatay, N., Ekim, T. and Başer, K.H.C., (2000), *Flora of Turkey and The East Aegean Islands*, Edinburgh University Press (Volume 11).

Hadjibiros, K., (1996), "Sustainable development in a country with extensive presence of valuable biotopes", *Environmentalist* 16 (1).

Haner, B. and Türk, Y., (2000), "Mineral Resources Potential of The Western Black Sea Basin", *Turkey 12th Coal Congress Proceedings*, Zonguldak.

Hora, B., (1981), *The Oxford Encyclopedia of Trees of The World*, Oxford University Press.

Imanishi, J., Shimabayashi, Y. and Morimoto, Y., (2005), "A new analytical method for wildlife habitat conservation planning on a city scale using the classification of physiologically homogeneous areas", *Landscape Ecology Engeneering*, 1: 157- 168.

Jensen, M.E., Redmond, R.L., Dibenedetto, J.P., Bourgeron, P.S. and Goodman, I.A., (2000), "Application of ecological classification and predictive vegetation modeling to broad- level assessment of ecosystem health", *Environmental Monitoring and Assessment*, 64 (1).

Kremer, B.P., (1998), *Die bäume Mitteleuropas*, Stuttgart: Kosmos, ISBN: 3- 440- 07604- 0.

Küchler, A.W., (1984), "Ecological vegetation maps", *Vegetatio*, 55: 3- 10.

Mellink, E., (1993), "Biological conservation of Isla de Cedros, Baja California, Mexico: assessing multiple threats", *Biodiversity & Conservation*, 2 (1).

Müller, R., Nowicki, C., Barthlott, W. and Ibisch, P.L., (2003), "Biodiversity and endemism mapping as a tool for regional conservation planning; case study of Pleurothallidinae (Orchidaceae) of the Andean rain forest in Bolivia", *Biodiversity and Conservation*, 12: 2005- 2024.

Namıkoğlu, N.G., (2007), *Trees and Shrubs in Turkey*, NTV Press, ISBN: 978- 975- 6690- 80- 2, İstanbul.

Özhatay, N., Özhatay, E. and Erdem, A.Ö., (2010), *Natural Plants in Sile*, Işık University Press, ISBN: 978- 975- 6494- 02- 8, l, İstanbul.

Schönfelder, P. and Schönfelder, I., (1990), *Was Blüht am Mittelmeer*, Franckh- Kosmos Verlags- GmbH & Co., ISBN: 3- 440- 05790- 9, Stuttgart.

Schönfelder, P. and Schönfelder, I., (1995), *Der Kosmos-Heilpflanzenführer*, Franckh- Kosmos Verlags- GmbH & Co., ISBN: 3- 440- 06954- 0, Stuttgart.

Seçmen, Ö., Gemici, Y., Görk, G., Bekat, L. and Leblebici, E., (1995), *Seed Plants Systematics*, Ege University Press No: 116, İzmir.

Symonds, W.D. and Chelimsky, S.V., (1958), *The Tree Identification Book*, William Morrow and Company, New York.

Symonds, W.D. and Merwin, A.W., (1963), *The Shrub Identification Book*, William Morrow and Company, New York.

Tutin, T.G., Burges, N.A., Chater, A.O., Edmondson, J.R., Heywood, V.H., Moore, D.M., Valentine, D.H., Walters, S.M. and Webb, D.A., (1964), *Flora Europeae*, Cambridge University Press (Volume 1).

Tutin, T.G., Burges, N.A., Heywood, V.H., Moore, D.M., Valentine, D.H., Walters, S.M. and Webb, D.A., (1968- 1980), *Flora Europeae*, Cambridge University Press, (Volume 2- 3- 4- 5).

Uluocak, N., (1994), *Groundcover Plants Textbook*, İstanbul University Press No: 3874, İstanbul.

Yaltırık, F., (1988), *Dendrology II Angiospermae*, İstanbul University Press No: 3509, İstanbul.

Yaltırık, F. and Efe, A., (1996), *Herbaceous Plants Systematics*, İstanbul University Press No: 3940, İstanbul.

Yılmaz, O., (1993), *Scrub Plants*, Ankara University Agricultural Faculty Press No: 1326, Ankara.

Zeydanli, U., Erdoğan, M.K. and Gemici, Y., (1999), *Wildflowers Guide In METU Campus*, Middle East Technical University Press, Ankara.

Zohary, M., (1947), "A vegetation map of Western Palestine", *Journal of Ecology*, (34) 1.

CHAPTER III

PARTICIPATORY APPROACH ON CAMPUS VEGETATIVE LANDSCAPE DESIGN: A CASE STUDY IN VAN, TURKEY

Hande ÖZVAN* & Dr. Pınar BOSTAN**

*Van Yuzuncu Yil University, Van, Turkey
e-mail:handeozvan1@gmail.com, Orcid ID: 0000-0002-3738-6272

**Van Yuzuncu Yil University, Van, Turkey
e-mail:pinaraslantas@yyu.edu.tr, Orcid ID: 0000-0002-8947-1938

1. Introduction

University campuses are one of the green and open urban spaces that include both structural and vegetative elements. With its large green space potential, a-well designed campus landscape contributes to the social and cultural life of students by enabling outdoor activities and promotes the natural ecosystem of the environment. Most of the students and academics are unaware of how much the campus landscape in which they spend a significant amount of time can affect them. However, natural landscapes in a well-designed campus have many positive physical and spiritual effects on people (Zhou, 2017; Seitz et al., 2014; Lau et al., 2014; Lau and Yang, 2009). Spending time physically on campus is not the only option to feel this effect. Even if the windows of the office, laboratory, or classroom have a natural green view, the positive effect of the green spaces can be felt. According to a study performed by Tennessen and Cimprich (1995), students who had a view of green spaces from their dormitory windows performed significantly better on the attentional tasks than students that have less natural green views from their dormitory windows. It has been proven by various studies that the natural environment improves attention on tasks of people and significantly reduces stress (Mennis et. al., 2018; Chang and Bae, 2017; Lambert et al., 2015; Seitz et al., 2014; Kaltenborn and Bjerke, 2001; Tennessen and Cimprich, 1995; Ulrich et al., 1991; Kaplan and Kaplan, 1989). Besides, stress recovery is faster and complete when ones are exposed to natural settings rather than the non-natural urban environments (Ulrich et al., 1991). Natural environments on campus don't mean just aesthetic appeal value. There should be a peaceful and stress-free green space for students and staff (Griffith, 1994). Scientific studies have proven that university students prefer open green spaces when they are stressful, upset or depressed due to reasons such as being under the pressure of study hard, economic problems, personal or family problems (Seitz et al., 2014; Lau et al., 2014). Open green areas with natural environments on campuses provide ones to cope with stress (Lau et al.,

2014), physiologically and physically well-being (Speake et al., 2013), and feeling calm and peace by being in nature. Furthermore, students' awareness of nature is supported by green areas in the campus landscape.

Another important factor is that the quality and quantity of green areas on campuses are important for people as well as for natural life. With a well-designed campus landscape, it is provided a positive contribution to the urban by employing increased plant diversity and green areas. With its large green space potential and natural environment, campus areas add value to the lives of habitats thereby preserving biodiversity (Rakhshandehroo et al., 2017).

According to Hanan (2013), when it comes to "campus design", studies usually focused on the architectural structure rather than the students' needs and expectations. Most of the studies have handled the vegetative design of campus as an ordinary landscape design and ignored students' views during the design process of campus (Lin and Dong, 2018; Hajrasouliha and Ewing, 2016; Banning and Kaiser, 1974). As Johnson and Castleden (2011) stated there are very few campus design studies conducted by seeking students' opinions apart from senior managers, donors, designers, and planners. The study performed by Peker and Ataöv (2019), examined how open space design affects students' learning process through exploratory inquiry. They concluded that the physical environment as a powerful component has a positive effect on students' learning process.

Today, unlike traditional design approaches, modern design approaches, in which users are indirectly and\or directly involved in the design process, are in demand. It differs from other design methods in terms of ensuring user participation. If people living in the region are included in the design and planning process by paying attention to opinions of them, the outputs are expected to satisfy them (Atwa et al., 2019), which should be one of the top priorities of designers. Ozdemir (2019), emphasized the importance of participatory approach while designing playgrounds that contribute to the psychological, social, and physical development of children. In another study, Xu et al., (2020) used participatory approach as a mapping method to identify suitable areas for the Silk Road cultural landscape corridor planning in Zhangye, China. These kinds of researches focus on the participatory approach by incorporate the users and acquire feedbacks, which will help designers within the long-term decision-making process so on optimize designs and meet users' needs. Some studies show that the use of common design alternatives arising from user-designer relationships should be encouraged in areas such as landscape management and landscape planning (Murgue et al., 2015). According to Mahayudin et al. (2015), the campus landscape

design should consider user needs and should be attractive and interesting with its appearance at every season for ones who lives in.

This study focused on the campus landscape design with a participatory approach by incorporating users and designers with an environmentalist and socio-cultural perspectives. The main purpose of the study was to propose a vegetative landscape design on a suitable land within the Van Yuzuncu Yil University (Van YYU) campus according to the students' demands and gaps that were identified with the survey. The design was evaluated by the 30 students who studying at the Faculty of Architecture and Design at the Van YYU through a 3D video presentation. Second aim of the study is to increase the level of awareness of students towards the environment they live in.

2. Materials and methodology

2.1. Material of study

Van YYU is a higher educational institution established on the edge of Lake Van. The university is located in the eastern part of Turkey, and 15 km away from the city center (Fig. 1). Van YYU Zeve campus is located on 720 hectare area on the shore of Lake Van. The university was established on July 20, 1982. The university provides education with 15 faculties, 5 institutes, 13 graduate schools, and 14 research centers. The university continues its education and training activities at the four different campuses, these are Zeve, Gevas, Ercis, and Ozalp campuses. The university has an Erasmus Exchange Program agreement with 21 universities from eight countries in Europe. Approximately, 30.000 students including associate, undergraduate, graduate, doctorate, and foreign students receive education at the Van YYU. Opinions of 300 students studying in any department and evaluation of 30 students of Faculty of Architecture and Design about the campus vegetative landscape design of Van YYU were the basic materials of the study.

The Van YYU Zeve campus site plan, where this study was carried out, was presented in Figure 2 to cover main buildings, main road networks, gates, and open green areas.

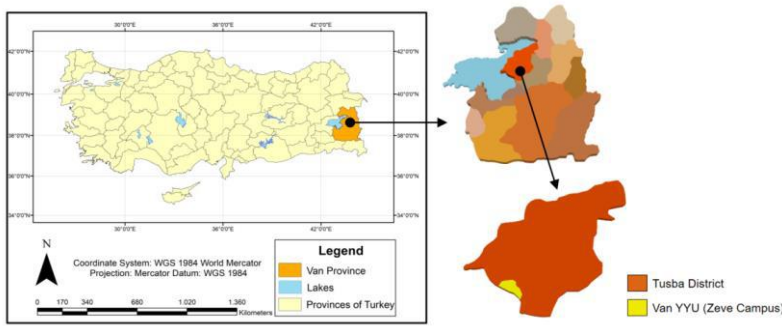

Fig. 1 Location of the Van YYU Zeve Campus over Turkey, Van province, and Tusba District.

Fig. 2 The Van YYU Zeve Campus site plan with main buildings, main road networks, gates and open green areas.

2.2. Methodology

The first step of the study was to reveal the deficiencies of campus vegetative landscape design according to the students' point of view through a participatory approach. To discover users' perception of the Van YYU campus vegetative landscape, a survey with eleven questions was asked to 300 students. The survey was conducted with face-to-face interviews for three weeks in June 2019. The survey was designed to reveal students' expectations from the campus open green spaces in terms of vegetative compositions, elements they deem insufficient, and the functions they need. In the second step, a landscape design proposal was made by considering these expectations in the appropriate area within the Van YYU campus. AutoCAD was used for drawing the 2D plan; SketchUp and Realtime Landscaping Architect programs were used for 3D modeling. In the third step, the video presentation of the design was presented to the

student group of 30 people. Since this student group consists of undergraduate and graduate students studying at the Faculty of Architecture and Design, we have defined this group as an expert. In the last step, we commented on the feedback we received from the students. The flowchart of the study is given in Figure 3.

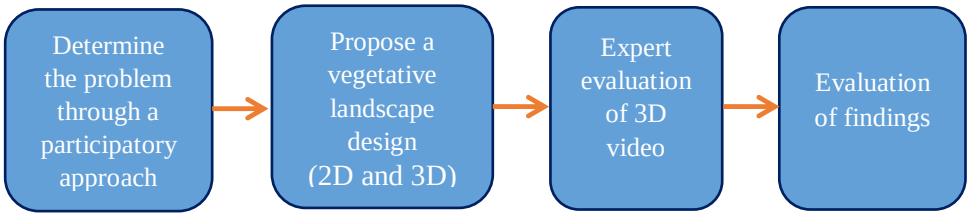

Fig. 3 Flowchart of methodology

2.2.1. Participatory approach

A participatory design approach has its own methodological orientation, methods, and techniques (Spinuzzi, 2005). Desk-based research, surveys, observations, interviews, and interactive polling are some of the participation methods. In participatory design, involving the user information as a resource that will contribute to the design process forms the basis of participation. Xu et al., (2020) stated that direct or indirect data collection ideas or approaches might be used to take the ideas of residents while making design, planning, or management decisions. While direct methods involve one-to-one communication with individuals or groups, indirect methods include involving people in any evaluation process. The participatory approach provides sustainable and fine quality outputs, also it contributes to individual achievements. Since people would like to express themselves and participate directly in the design process (Sanders, 2002), people's sensitivity to the environment they live in is supported with the participatory approach. Another benefit of this method is that, the designer is assisted in creating areas where users will enjoy being in it (Spinuzzi, 2005).

3. Results and discussion

3.1. Students' characteristics

The 300 respondents comprised 156 (52%) females and 144 (48%) males, 214 (71.3%) of whom are undergraduate and 86 (28.7%) are postgraduate students. Respondents' ages were ranged from 18 to 27. The numbers of undergraduate, graduate and doctoral students for female and male students participating in the survey were shown in Table 1.

Table 1 Number of undergraduate, graduate and doctoral students for female and male students participating in the survey.

	Number of students		
	Undergraduate	Graduate	Doctoral
Female	110	35	11
Male	104	28	12

3.2. Students' perception on Van YYU campus landscape

Survey questions and rates were represented as tables in Appendix A. In this section, we evaluated the students' perceptions of the Van YYU campus landscape based on their answers to the questionnaire.

According to the evaluation of the survey, we saw that most of the participants were not pleased with the Van YYU campus landscape. When it was requested to score the campus vegetative design on the five-scale Likert (Likert, 1932), the majority of the participants gave scores: 2 (not very good) and 1 (not at all). The insufficient open green space and plant diversity, the dominance of structural elements, and untidy planting were defined as disturbing elements in campus design. Generally, students agreed on the lack of utilizations, shade trees, vegetative diversity, and urban furniture that allow them to spend time in the outdoors at the campus. Most of the students thought that trees, shrubs, lawns, and seating units like gazebo, bench, and pergola were inadequate on the campus. Additionally, they stated that firm ground covering and structural elements such as parking lots take up a lot of space on the campus. Due to insufficient vegetative elements and urban furniture in Van YYU campus, students generally had to spend their free time in canteens or indoors. According to the answers given, whereas half of the students spent their free time at the university coastline, 41.7% of the students' preferred faculty gardens for their free time. Compared to other parts of the campus, the university coastline was a relatively better-designed area with more plant diversity and urban furniture. Therefore, this area was a place where many of the students went to the coastline to have a good time and relax.

Participants were asked which kind of plants they usually want to see on campus? The students mostly replied to this question as lawns and deciduous trees. Complementary to each other, deciduous trees and large grass areas were preferred by students for sitting, resting, and recreational activities on the campus. In addition to this, the students were using open green spaces for reading/relaxation purposes at a high rate. In another question, preferences about several utilizations were asked to students for outdoor activities at open spaces of campus. Students preferred mostly amphitheatre, fragrance garden, flower exhibition area, observation terrace, and orchard utilizations. Concerning vegetative composition

preference, most of the students wanted to see trees, shrubs, and grass fields at the campus. Instead of uniform vegetative design, the students preferred different sizes and types of plant compositions at open green spaces of campus. When asked which properties of plants affect students mostly on campus landscape, the great majority of students chose the flower/leaf/fruit color and fragrance. Following this view, according to the students' opinion, these plants should be visually aesthetic and provide shade. In this case, the vegetative design proposal to be made should address the students' visual and olfactory perceptions.

One of the aims of this study was to increase environmental awareness. To contribute to this, we considered placing a descriptive sheet in front of the plants at the campus. We asked that if students wanted to have information about plants through the descriptive sheets. The positive response given by 88% of the participants was satisfactory as it showed the environmental awareness of the students.

According to the survey results, the students need an exciting environment with colorful and fragrant trees, flowers, and a variety of uses where they could socialize, as well as relax, and calm down over large green areas at the campus.

3.3. Landscape vegetative design proposal on Van YYU campus

According to findings obtained from the participatory approach, the most suitable area was decided as the Faculty of Agriculture garden at the campus for proposing landscape vegetation design (Fig. 4). The factors that were effective in choosing this area were as follows: the number of students studying at this faculty was high so that student circulation in that region was intense; the selected area was close to many uses such as shuttle area, open-air stadium, ATMs, stationery, and market; the area was located on the main axis of the campus, thus more students would be able to benefit from the designed area. Besides, the area had fairly wide free space (represented with red color in Figs. 4 and 5) thus; it was suitable for landscape design in terms of students' usage and location.

Fig. 4 Google Earth image* (left) and photograph (right) of the study area
* red line describes the border of Faculty of Agriculture garden.

Fig. 5 Concept diagram of landscape vegetative design on of Faculty of Agriculture garden. The five main utilizations and their covering area are expressed in different colors on the map.

Similar utilizations in terms of functionality were covered under five main utilizations. These utilizations were lawns, nursery-greenhouse, fragrance gardens, orchards, and rock gardens (Fig. 5). These usages were selected, as students in the study area mostly preferred them. The lawn included an amphitheater, observation terraces, open green spaces, and ornamental pool; nursery-greenhouse utilization included flower exhibition areas, botanical garden, and greenhouse. The planned project was represented in Figure 6.

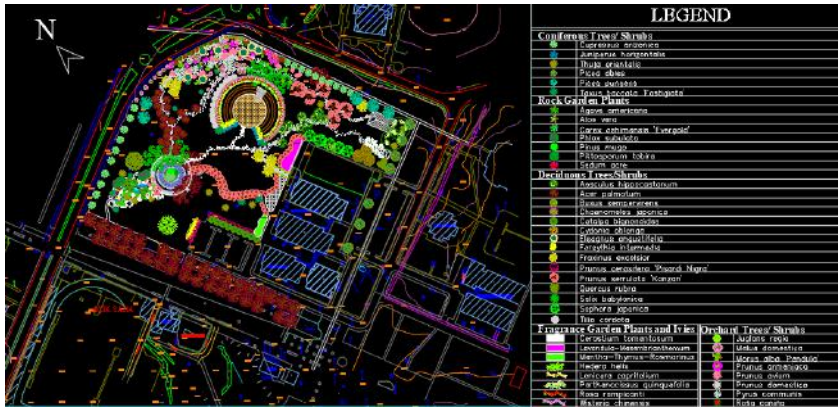

Fig. 6 Plan view of vegetative design of Faculty of Agriculture garden. Plants are listed in the legend according to type and where they are used.

Leaf, fruit and flower color and fragrance of the plants were defined as the most impressive plant features. The plants used in the design were selected according to these features (Fig. 6). Coniferous trees were used to provide privacy in certain areas. Coniferous trees used were *Cupressus arizonica, Juniperus horizontalis, Thuja orientalis, Picea abies, Picea pungens,* and *Taxus baccata* 'Fastigiata'. Deciduous trees that have different colours and calligraphic structures in every season were used for their shade feature and aesthetic values. Deciduous trees used were *Aesculus hippocastanum, Acer palmatum, Buxus sempervirens, Chaenomeles japonica, Catalpa bignonoides, Cydonia oblonga, Eleagnus angustifolia, Forsythia intermedia, Fraxinus excelsior, Prunus cerasifera 'Pisardii Nigra', Prunus serrulata* 'Kanzan', *Quercus robur, Salix babylonica, Sophora japonica*, and *Tilia cordota*.

In the south of the area, broad-leaved trees were preferred for parking lot planting. The uses of conifers and fruit trees were avoided to prevent damage and any pollution to the vehicles (Fig. 6). The main axis was defined by alley afforestation in the west part of the area where student circulation was intense. In the northeast and northwest parts of the area, coniferous trees and shrubs were predominantly used (Fig. 6). Natural crushed stones provided the circulation in the garden.

Participants preferred mostly lawns and deciduous trees among all vegetative design elements. A proposed design consisted of leafy trees and grass areas where students could be intertwined with nature in their leisure activities. The existing greenhouse was expanded and a nursery garden was placed according to the students' requests as represented in Figure 7. The various deciduous trees, shrubs, and lawns were designed around the nursery. Another highly rated utilization was a botanical garden. For this

reason, a botanical garden in the nursery was proposed. A building was added to the adjacent parcel for plant production and cultivation.

(a) (b)

Fig. 7 3D view of the nursery design from different angles. (a) Top view; (b) Front view.

By considering the requirements of students, an orchard with edible fruits, trees with colorful leaves and flowers were designed in the north and northeast directions of the area (Fig. 8). It was appropriate to use fruit trees for the benefit of students as well as natural life. The shade function and aesthetic value of leafy trees were taken into consideration in the design. The coniferous shrubs were used as the limiting elements to separate the study area with neighbouring parcels (Fig. 8). The orchard plants used in the design were *Juglans regia, Malus domestica, Morus alba* 'Pendula', *Prunus armeniaca, Prunus avium, Prunus domestica, Pyrus communis*, and *Rosa canina*.

(a) (b)

Fig. 8 3D view of the orchard design from different angles. (a) Top view; (b) View from different angle.

With 12.6% of all choices, the most desirable utilization was the amphitheater on the campus. For this purpose, an amphitheater was designed to provide a place for concerts, public presentations, and graduation ceremonies of students' (Fig. 9). The amphitheater was designed using wood cladding and had five stairs. The height of a stair riser was 45 cm, and the tread dimension was 120 cm. The red rubber flooring material was used on the top floor of the amphitheater. Orchards surrounded the amphitheater from its north and west parts. At the top stage of the amphitheater, pergolas and vines wrapped around them, and benches

beneath the pergolas allowed students to sit and relax. The ivy types used were *Hedera helix, Lonicera caprifolium, Parthenocissus quinquefolia, Rosa rampicanti,* and *Wisteria chinensis*. The amphitheater was surrounded by trees, plenty of shrubs, border plants, and an orchard to ensure its harmony with the environment. The amphitheater was suitable for users to experience the landscape of a garden from a high viewing terrace. In this respect, the amphitheatre also performed as an observation terrace, which was one of the high rated utilization.

(a) (b)

Fig. 9 3D view of the amphitheatre design from different angles. (a) Top view; (b) Front view.

We wanted to leave some free space between buildings and garden, therefore we did not place big trees in front of the faculty buildings. The fragrance garden located in front of the buildings was composed of different aromatic annual, biennial, and perennial plant composites. Fragrance garden could be also served as a flower exhibition area with different-colored flowers. Fragrance garden plants were *Cerastium tomentosum, Lavandula, Mesembryanthemum* (pink carpet), *Mentha, Thymus,* and *Rosmarinus*. At the right next to the fragrance garden, pruned *Cupressus macrocarpa* evergreen shrub was used to highlight building entrance. The pruned *Buxus sempervirens* evergreen shrub was used on the roadside from the buildings to the garden (Fig. 10).

(a) (b)

Fig. 10 3D View of the fragrance garden design from different angles. (a) Top view; (b) Front view.

Considering the slope of the area and the angle of the sun's rays, a rock garden was located at the northwest side of the study area. As can be seen

from the 2D plans and 3D views (Figs. 6 and 11); xeric, annual, biennial and coniferous plants, and uniform rocks were used together. The Rock garden plants used were *Agave americana, Aloe vera, Carex oshimensis* 'Evergold', *Phlox subulata, Pinus mugo, Pittosporum tobira, Sedum acre,* and *Sedum spectabile* 'Autumn Joy'.

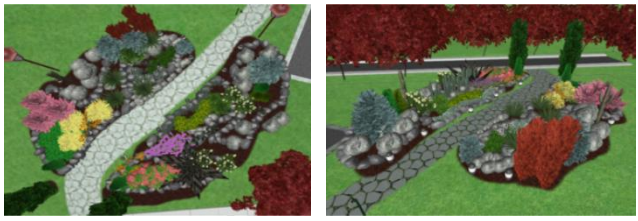

(a) (b)

Fig. 11 3D view of the rock garden design from different angles. (a) Top view; (b) Views from different angle

The ornamental pool was relatively less preferred by the students (7.7% of all choices). However, to complete the vegetative composition and to use the rehabilitation effect of water, the 12 m^2 ornamental pool with a wooden plant casing was designed to serve sitting and relaxing (Fig. 12). Besides, there was a wooden flower parterre with a diameter of eight m^2 in the middle of the ornamental pool. The *Gazania* (treasure flower) and *Mesembryanthemum* (pink carpet) were planted in this flower parterre. The ornamental pool, designed with the flower parterre and the natural elements around it, was proposed as a healing element for stressful students and academic-administrative staff. As shown in Figure 12, the ornamental pool was surrounded by stone steps. Circulations of these steps help coincidental meetings and pedestrian flows at the garden.

(a) (b)

Fig. 12 3D View of the ornamental pool design from different angles. (a) Top view; (b) Front view.

The most significant shortcoming in the vegetative design of the campus according to the students participating in the survey was the lack of functional open green spaces. A large grass field was proposed for this

purpose, which allowed students to lie down on grasses and perform free activities (Fig. 13). Moreover, a broad-leaved *Quercus robur* (English oak) was designed over the grass field. This large, cold-tolerant deciduous tree was used as a focal point in the study area. Acorns are an important nutritional source of animals such as birds, squirrels, and rabbits, from this aspect oak tree would contribute to natural life of the campus. The 45 cm high wooden seating unit was designed around the *Quercus robur*. The seating unit was considered as a place to allow students to read, relax, and chat in the garden.

The vegetative design could be easily perceived from the plan, but it was difficult to perceive on a human scale as the study area was fairly flat. To break the monotony and create contrast in the area, an artificial grass hill was built over an open green area. In this way, we increased the difference in contour in the garden. Hence students could better perceive the garden within the field of view (Fig. 13).

(a) (b)

Fig. 13 3D View of the Quercus robur and an artificial grass hills design. (a) Top view with a certain angle; (b) Front view.

According to the survey, most of the students stated that they would like to have information about plants in the garden through description sheets belong to each of them. These identification sheets were helpful to improve the environmental awareness of students. Therefore, it was recommended to use plant description sheets as represented in Figure 14.

(a) (b)

Fig. 14 Sample plant description sheet and sitting unit around the Quercus robur. (a) Top view with a certain angle; (b) Front view.

3.4 Evaluation of 3D video presentation

In this part of the study, an expert group of 30 student watched the video presentation of the proposed design. In the evaluation part, we asked five questions about the video presentation that they could answer as "yes" or "no". In question 1, we asked if there was enough space for social activities in the designed garden. The proportion of experts saying "yes" was 86.7%. In second question, we asked if the vegetable diversity and harmony in the area were satisfactory. 90% of students answered this question as "yes". In third question, we asked if they think the aesthetic and functional properties of the plants used were satisfactory. Likewise, a large majority (86.7%) answered "yes" to this question. In fourth question we asked if they found that the designed garden was relaxing and attractive. The rate of experts who say “yes” to this question was 76.7%. The positive answers to this question were relatively low compared to other questions. This might be because, although the experts liked the area in terms of vegetative diversity and harmony, they might have perceived many activities as a negative feature relatively in a small area. In fifth question, we asked if experts would like to spend time in this designed area. Experts stated that they would be happy to be in this garden with a rate of 86.7%. The expert group evaluated the area, which was designed in line with the opinions of user group, almost positively. This showed that, with the proposed design, an exemplary vegetative landscape design has been developed in which deficiencies were eliminated and needs were met.

4. Conclusions

This study emphasized the necessity of involving users in the landscape design process of university campuses, which was one of the open green spaces. The proposed participatory approach integrated user views and landscape design. The major data source of the study consisted of student views. The main purposes were to reveal student expectations and needs in outdoor spaces of campuses and represented a vegetative design proposal in line with their opinions. With the survey and video presentation, the aim was to increase the awareness of the students on the campus open green areas where they spent a significant part of their time. This study, which emphasized the importance of the participatory approach, was thought to guide future studies on campus landscape design. The studies that measure how students' motivation and academic achievement are affected by the student-centered participatory approach in campus landscape design, should be considered in future research.

Acknowledgments: The authors thank sincerely to volunteer students of Van Yuzuncu Yil University for taking time for our questionnaire and video presentation and sharing their opinions with us.

Appendix A

Questions: 1., 4., 5. and 6. are multiple choice questions.

Table A.1 Which properties of plants affect you most on campus landscape?

	Frequency	Percent (%)
Flower / Leaf / Fruit colour	194	36.1
Fragrance	158	29.4
Size	71	13.2
Shape	70	13
Texture	45	8.4
Total	538	100

Table A.2 Which types of plant do you like most?

	Frequency	Percent (%)
Lawn	76	25.3
Deciduous	71	23.7
Parterre/bordure flowers	50	16.7
Ivy	39	13
Coniferous	36	12
Groundcover plant	28	9.3
Total	300	100

Table A.3 Which vegetative compositions you want to see in the campus green areas?

	Frequency	Percent (%)
Large grass areas	35	11.7
Trees, shrubs, grass	149	49.7
Only trees	57	19
Only flower beds	59	19.6
Total	300	100

Table A.4 Which functions the trees should have on campus?

	Frequency	Percent (%)
Shadow	191	18.7
Privacy	105	10.3

	Frequency	Percent (%)
Wind, dust and noise preventive	109	10.6
Air cleanser	124	12.1
Preventing bad view	90	8.8
Aesthetic	198	19.3
Edible fruits	100	9.8
Provide spatial continuity	107	10.4
Total	1024	100

Table A.5 Please tick the utilizations you like to see in campus.

	Frequency	Percent (%)
Rock gardens	126	7.7
Fragrance gardens	167	10.3
Orchards	153	9.4
Amphitheatre	206	12.6
Flower exhibition areas	154	9.5
Observation terraces	154	9.5
Vertical gardens	117	7.2
Nursery-Greenhouses	125	7.7
Ornamental pool	125	7.7
Open green spaces	153	9.4
Botanical gardens	149	9.1
Total	1629	100

Table A.6 For which purposes do you use open green areas in campus?

	Frequency	Percent (%)
Recreational Activities	96	16.3
Sportive Activities	139	23.6
Reading/ Relieving	237	40.2
Eating	118	20
Total	590	100

Table A.7 Where do you spend your free time in campus?

	Frequency	Percent (%)
University coastline	150	50
Faculty garden	125	41.7
Library	9	3
Cafeteria	16	5.3
Total	300	100

Table A.8 Do you pleased with vegetative design of campus?

	Frequency	Percent (%)
Yes	27	9
No	273	91
Total	300	100

Table A.9 What are the deficiencies in campus vegetative design?

	Frequency	Percent (%)
Insufficient open green space	163	54.3
Insufficient plant diversity	84	28
Surplus of structural elements/wide firm ground	31	10.3
Neglected / Untidy planting	22	7.3
Total	300	100

Table A10. Would you like to see a descriptive sheet placed in front of plants?

	Frequency	Percent (%)
Yes	264	88
No	36	12
Total	300	100

Table A11 Please rate the campus vegetative design from 1 to 5?

	Frequency	Percent (%)
Not good at all	92	30.7
Not very good	106	35.3
Neither good nor bad	75	25
Good	18	6
Very good	9	3
Total	300	100

References

1. Atwa, S.M.H., Ibrahim, M.G., Saleh, A.M., Murata, R. (2019). Development of sustainable landscape design guidelines for a green business park using virtual reality. Sustainable Cities and Society,48, 1-13.
2. Banning, J.H., Kaiser, L. (1974). An ecological perspective and model for campus design. The Personnel and Guidance Journal, 52 (6), 370–375.

3. Chang, P.J., Bae, S.Y. (2017). Positive emotional effects of leisure in green spaces in alleviating work-family spillover in working mothers. International Journal of Environmental Research and Public Health, 14, 757.
4. Griffith, J.C. (1994). Open space preservation: an imperative for quality campus environments. Journal of Higher Education, 65(6), 645–669.
5. Hajrasouliha, A.H., Ewing, R. (2016). Campus does matter: The relationship of student retention and degree attainment to campus design. Planning for Higher Education Journal, 44(3), 30-45.
6. Hanan, H. (2013). Open space as meaningful place for students in ITB campus. Procedia Social and Behavioral Sciences, 85 (20), 308–317.
7. Johnson, L., Castleden, H. (2011). Greening the campus without grass: using visual methods to understand and integrate student perspectives in campus landscape development and water sustainability planning. Area, 43(3), 353–361.
8. Kaltenborn, B.P., Bjerke, T. (2001). Associations between environmental value orientations and landscape preferences. Landscape and Urban Planning, 59, 1-11.
9. Kaplan, R., Kaplan, S. (1989). The experience of nature: A psychological perspective. New York: Cambridge University Press.
10. Lambert, K.G., Nelson, R.J., Jovanovic, T., Cerdá, M. (2015). Brains in the city: Neurobiological effects of urbanization. Neuroscience and Biobehavioral Reviews, 58, 107-122.
11. Lau, S.S.Y., Yang, F. (2009). Introducing healing gardens into a compact university campus: design natural space to create healthy and sustainable campuses. Landscape Research, 34(1), 55-81.
12. Lau, S.S.Y., Gou, Z., Liu, Y. (2014). Healthy campus by open space design: Approaches and guidelines. Frontiers of Architectural Research, 3, 452-467.
13. Likert, R. (1932). A technique for the measurement of attitudes. Archives of Psychology, 22 (140), 55.
14. Lin, L., Dong, Y. (2018). A study on the campus landscape design of the national university of Singapore. IOP Conference Series: Materials Science and Engineering.
15. Mahayudin, M.R., Yunos, M.Y.M., Mydin, A.O., Tahir, O.M. (2015). Developing sustainable campus landscape criteria: An evaluation Universiti Pendidikan Sultan Idris as a green campus. Advances in Environmental Biology, 9(4), 201-204.

16. Mennis, J.P., Mason, M., Ambrusa, A. (2018). Urban greenspace is associated with reduced psychological stress among adolescents: A Geographic Ecological Momentary Assessment (GEMA) Analysis of activity space. Landscape and Urban Planning, 174, 1-9.

17. Murgue, C., Therond, O., Leenhardt, D. (2015). Toward integrated water and agricultural land management: Participatory design of agricultural landscapes. Land Use Policy,45,52-63.

18. Ozdemir, A. (2019). An approach on children's experiences of participatory planning, Cities,93,206-214.

19. Peker, E., Ataöv, A. (2019). Exploring the ways in which campus open space design influences students' learning experiences. Landscape Research, 44(7), 1-17.

20. Rakhshandehroo, M., Yusof, M.J.M., Arabi, R., Parva, M., Nochian, A. (2017). The environmental benefits of urban open green spaces. Alam Cipta, 10 (1), 10-16.

21. Sanders, E.B.N. (2002). Design and the social sciences, Publisher: Taylor & Francis, Editors: Frascara, Jorge, pp.1-7. Chapter From user-centered to participatory design approaches.

22. Seitz, C.M., Reese, R.F., Strack, R.W., Frantz, S., West, B. (2014). Identifying and improving green spaces on a college campus: A photovoice study. Ecopsychology, 6(2), 98-108.

23. Speake, J., Edmondson, S., Nawaz, H. (2013). Everyday encounters with nature: students' perceptions and use of university campus green spaces. Human Geographies – Journal of Studies and Research in Human Geography, 7(1), 21-31.

24. Spinuzzi, C. (2005). The methodology of participatory design. Technical Communication, 52(2),163-174.

25. Tennessen, C.M., Cimprich, B. (1995). Views to nature: effects on attention. Journal of Environmental Psychology, 15, 1, 77-85.

26. Ulrich, R.S., Simons, R.F., Losito, B.D., Fiorito, E., Miles, M.A., Zelson, M. (1991). Stress Recovery during exposure to natural and urban environments. Journal of Environmental Psychology, 11, 201-230.

27. Xu, H., Zhao, G., Fagerholm, N., Primdahl, J., Plieninger, T. (2020). Participatory mapping of cultural ecosystem services for landscape corridor planning: A case study of the Silk Roads corridor in Zhangye, China. Journal of Environmental Management, 264,1-10.

28. Zhou, R. (2017). Discussion on campus landscape construction. ADESS 2017. International conference on arts and design, education and social sciences (pp. 989-994). Yinchuan, China.

CHAPTER IV

DIFFERENT TECHNIQUES USING FOR THE SURFACE ACID-BASE CHARACTERIZATION OF SOLIDS

Assoc. Prof. Dr. Ceyda BİLGİÇ

Eskişehir Osmangazi University, Eskişehir, Turkey
e-mail: cbilgic@ogu.edu.tr, Orcid ID: 0000-0002-9572-3863

1. Introduction

Excluding Coulombic forces and metallic bonding, which are less commonly encountered, the intermolecular interactions can be classified into two categories: The Lifshitz–van der Waals (LW) interactions and the acid-base (AB) interactions. The LW interactions include the London (dispersion) forces, Debye (dipole/ induced dipole) forces and Keesom (dipole/ dipole) forces. London forces result from the natural oscillations of the electron clouds of the molecules inducing synchronous oscillations in the neighboring molecules. They are always present regardless of the polarity of the substances. Molecules possessing permanent dipoles are capable of exhibiting Debye and Keesom interactions with other molecules. Since Debye forces seldom amount to more than a few percent of the London forces, they are usually neglected or rolled together with the dispersion forces in a single term. Keesom forces can be comparable in magnitude to the London forces. However, the interactions among multiple permanent dipoles cancel out in bulk condensed phases due to their vector nature. These dipoles thus have very little effect on the thermodynamic properties of the condensed phases. For example, in water vapor, 76% of the cohesive energy comes from dipole interactions, whereas in liquid water only 2.4% (Van Oss et al., 1986:378). The LW interactions of condensed phases are therefore primarily dispersed interactions, although small contributions resulting from the presence of permanent dipoles may also be accounted for in this term. Unlike LW interactions, AB interactions between molecules in bulk phases or across interfaces are not always present but can arise when proton or electron donating/sharing occurs between neighboring molecules or functional groups, leading to complexation or adduct formation. Two acid-base theories, Brønsted theory (Brønsted, 1923:718) and Lewis theory (Jensen, 1980:135), are frequently used to describe the AB interactions. The former defines acids and bases as proton donors and acceptors, whereas the latter defines acids and bases as electron (density) acceptors and donors. The Brønsted definition is convenient for describing reactions in aqueous solutions, but it covers a narrower range of interactions than the Lewis definition because the presence of proton is required. All Brønsted acids are Lewis acid-base adducts with the acid component being H^+, and

all Brønsted bases are also Lewis bases. In the present work, all acids and bases are referred to the Lewis definition if not otherwise specified. Three types of AB reactants can be identified: those which act exclusively as acids, those which act exclusively as bases, and those which can act as both acids and bases. The first two types are termed by van Oss et al. (Van Oss et al., 1988:884) as *monopolar* acids and bases, respectively, and the third category of *bipolar* materials. To complete the notation, inert materials incapable of neither acid nor base interactions are termed *apolar*. This nomenclature is misleading because AB interactions have little to do with the polarity of the reactants, but the terminology *monofunctional*, *bifunctional*, and *inert* shall nonetheless be used to distinguish between the above categories of materials.

Virtually all AB characterization methods require the usage of some type of 'probes'. In most cases, they are molecular probes with their own chemistry. Ideal probes should be mono-functional so that what results from the measurements are the 'absolute' acidity or basicity of the substance of interest. However, since most molecules are bi-functional to some extent, the best choices are using those which are predominantly acidic or basic. What one obtains thus is some 'combined' acidity or basicity.

Gutmann and co-workers introduced the Donor Number *DN* (Gutmann, 1978) and Acceptor Number *AN* (Mayer, 1975:1235) to describe the AB properties of Lewis acids and bases. *DN* is defined in terms of the molar exothermic heat of mixing of the candidate solvent with a reference acid, antimony pentachloride, in a dilute (10^{-3} M) solution in dichloromethane.

Many other experimental techniques have been developed for solid surface AB characterization, such as electrokinetic titration in both aqueous and non-aqueous media, X-ray photoelectron spectroscopy (XPS), indicator dye adsorption/titration, calorimetry, and inverse gas chromatography (IGC). Fowkes (Fowkes, 1990:669), Berg (Berg, 1993:75), Chehimi et al. (Chehimi et al., 1992:137), and Contescu and Schwarz (Contescu and Schwarz, 1999) have given reviews of some of these techniques. Since each technique has its own AB scale, it is difficult to rank the AB properties of two materials if data from different techniques are given. In some cases, different techniques may yield opposite predictions when AB properties of two materials are compared.

Solid catalysts, including solid acid, solid base, and supported metal catalysts, are important from both academic and industrial viewpoints (Hocking, 1998; Olah and Molnar, 2003; Weissermel and Arpe 1997; Wittcoff and Reuben 1996). Catalytic properties of many heterogeneous catalysts depend strongly on their acid/base properties (Che et al.,

2004:281; Tanabe, 1989; Fraissard and Petrakis, 1994; Corma, 1995:559; Busca, 2007:5336). To design new catalysts, a convenient index for acid/base properties of a wide range of solids is needed. Physical parameters such as electronegativity have been used as a conventional index, but a chemical index is more preferable. The titration of acidic and basic sites using indicators in aprotic solvents such as benzene or hexane is a classical method to obtain a chemical index of acid/base properties of solids (Nakamoto, 1986:108; Karge, 2008:1096), but this method has at least three problems. First, the titration cannot be conducted in aqueous suspension, because this would eliminate the differences in acid strength of the various sites. Second, bulky indicator molecules are hindered from diffusing into the interior of the solids, which may cause the miss judgment because visual observation of the indicator molecules and their change upon protonation by acid sites is restricted to the surface. Third, generally used indicators are not selective for either Brønsted or Lewis acid sites. Temperature-programmed desorption (TPD) has been used for the analysis of acid/base properties of solids (Deeba and Hall, 1985:85; Tsuji et al., 2003:8793). Other techniques, including the measurements of adsorption isotherms and isobars and calorimetric measurements, have also being used for the characterization of the acid/base properties of solids (Deeba and Hall, 1985:85; Auroux, 1997:71; Solinas and Ferino, 1998:179). However, these methods cannot be used for discrimination of the type (Brønsted or Lewis type) of acid sites except for a method by Matsuhashi et al. (Matsuhashi, et al., 2004:554; Matsuhashi, et al., 2006:1): comparison of adsorption hearts of N_2 and Ar.

A traditional method of the Hammett indicator was widely used for measuring the acid strengths of solid acids or superacids and ionic liquids (Tanabe, et al., 1989:142; Yurdakoç et al., 1999:319; Wang and Wang, 2006:325). The amount of acid sites on a solid surface can be measured by amine titration immediately after the determination of acid strength. In the amine titration method, indicators are used and the color of suitable indicators adsorbed on the surface will give the measure of its acid strength. The method consists of titrating a solid acid, suspended in petroleum ether, with *n*-butylamine using an indicator (Benesi, 1957:970). This method gives the total amounts of both Brønsted and Lewis acids and is rarely applied to colored or dark samples where the usual color change is difficult to observe (Aucejo, et al., 1986:187).

IGC has frequently been applied for surface characterization of solids, in particular, for their thermodynamic behavior and their Lewis acidic–basic character (Balard, 2000; Sun, and Berg, 2003:151; Mohammadi-Jam and Waters, 2014:21; Kumar, et al., 2014:9). Lewis acid-base parameters and specific interaction parameters have been determined by evaluating the retention volume data obtained by IGC with the adsorption

of some nonpolar and some polar adsorbates on solids. The adsorption specific free energy (ΔG^{sp}), specific enthalpy (ΔH^{sp}), and specific entropy (ΔS^{sp}) of polar probes on solids were determined. By correlating ΔG^{sp} with donor and acceptor numbers of the probes, the acidic (K_A) and the basic (K_D) parameters of the solids were calculated.

Infrared is the most powerful technique for the study of solid's acidity. Pyridine is a widely used probe for the acidity of solid oxides, zeolites, and zeolite-like materials (Costa, 2000:193; Shirazi, 2008:1300; Covarrubias, 2009:118). IR spectroscopy of pyridine attached to Brønsted acid sites (acidic hydroxyls), Lewis centers (e.g. Al-containing entities) and cations (such as alkaline metal, alkaline earth, rare earth or transition metal ions) is very popular because of the rather sharp bands which can be observed in the deformation region. The positions of the bands are typical of the respective adsorption sites. A band at 1450 cm^{-1} is assigned to the vibration mode of pyridine adsorbed onto Lewis acid sites or to that of pyridine coordinately bonded to cations. This band provides information about Lewis acid sites. A band at 1540 cm^{-1} is due to pyridinium ions formed at the expense of Brønsted acid sites. Finally, a band at 1490 cm^{-1} is attributed to both Lewis and Brønsted acid sites. Therefore, using the integrated intensities of the bands at 1540 and 1450 cm^{-1} as a measure of the amount of pyridine adsorbed on Brønsted and Lewis acid sites, valuable information can be obtained about the relative concentrations of these two kinds of acid sites (Pizzio, 2005:994).

Compared to characterizing the surface acid/base properties (type, strength, number) of solid by various techniques. The acid, or basic properties of solid surfaces, are important and interesting aspects of the surface structure of solids. The surface characteristics of the solids need to be known for their effective use especially, as ion exchangers, catalysts, and adsorbents. Acid/base catalyzed reactions belong to the technologically most important classes of heterogeneous catalytic conversions. Acid/base properties seem to be important in many organic reactions. A variety of techniques have been developed for the characterization of type, strength, and numbers of acid sites on solids.

The use of various techniques for solid surface acid-base (AB) characterization are required. Many techniques as wetting measurements, X-ray photoelectron spectroscopy, microcalorimetry, titration, Fourier transform infrared spectroscopy (FTIR) and inverse gas chromatography (IGC) has been used to obtain detailed information on solid surfaces. One of the oldest techniques for measuring acidity is based on a proposal by Hammett for ordering strengths of solid acids on the basis of amine titrations. Other techniques used to characterize surface acidity and

basicity include the adsorption of acidic and basic gas-phase probe molecules combined with spectroscopic measurements (IR) and calorimetric, gravimetric, or thermal desorption measurements. Infrared is also a very powerful technique for understanding the acidity of solids. IGC has frequently been applied for surface characterization of solids, in particular, for their thermodynamic behavior and their Lewis acidic–basic character.

In the present work, different techniques using for surface acid-base characterization of solids are compared. The surface acidity of solids was investigated with IGC, FTIR, and Hammett acidity functions, that is, the *n*-butylamine titration method. Lewis acid-base parameters and specific interaction parameters have been determined by evaluating the retention volume data obtained by IGC with the adsorption of some nonpolar and some polar adsorbates on solids. On the other hand, the nature of Brønsted and Lewis acidic sites in solids were investigated using FTIR spectrums of adsorbed pyridine. Additionally, the amount of acid sites on a solid surface can be measured by amine titration immediately after the determination of acid strength. This method gives the total amounts of both Brønsted and Lewis acids and is rarely applied to colored or dark samples where the usual color change is difficult to observe.

2. Methods

Various techniques for solid surface acid-base (AB) characterization are used. Different techniques employ different scales to rank acid-base properties. Based on the results from literature and the authors' own investigations for mineral oxides, these scales are compared. The comparison shows that Isoelectric Point (IEP), the most commonly used AB scale, is not a description of the absolute basicity or acidity of a surface, but a description of their relative strength. That is, a high IEP surface shows more basic functionality comparing with its acidic functionality, whereas a low IEP surface shows less basic functionality comparing with its acidic functionality. The choice of technique and scale for AB characterization depends on the specific application. For the cases in which the overall AB property is of interest, IEP (by electrokinetic titration) and $H_{0,max}$ (by indicator dye adsorption) are appropriate. For the cases in which the absolute AB property is of interest such as in the study of adhesion, the heat of adsorption of probe gases (by calorimetry or IGC) and in situ IR spectroscopy coupled with probing molecules, including pyridine, acetonitrile, CO_2, and chloroform.

2.1. Indicator dye adsorption

The indicator dye adsorption method is frequently used in the study of oxide catalysts and clay materials (Tanabe; 1989). A basic indicator is

defined as a non-ionized or neutral substance capable of adding one proton per molecule

$$B + H^+ \leftrightarrow BH^+, \quad (1)$$

and changing its color depending on the extent of the reaction (Hammett, 1935:67). The strength of such an indicator is expressed by

$$pK_{BH^+} = - \log (a_{H^+} + a_B) / a_{BH^+} \quad (2)$$

where *a* stands for activity. The higher pK_{BH^+} is, the more basic the indicator is.

In practice, the solid sample (usually in powder form) of interest is dispersed in a neutral solvent such as benzene, and then different organic indicators are added. The acidic strength of a solid is defined as its ability to convert an adsorbed natural base indicator into its conjugate acid form, which is indicated by the color change of the indicator. It is expressed by the Hammett acidity function H_0 (Hammett, 1935:67), which is:

$$H_o = pK_{BH^+} + \log [B] / [BH^+], \quad (3)$$

where [B] and $[BH^+]$ are the concentrations of the base indicator and its conjugate acid respectively. The smaller H_0 is, the stronger acidity is. Similarly, the basic strength is defined as the ability of the surface to convert an adsorbed acid into its conjugate base form, and expressed by H_0 of the conjugate acidic site of the basic surface site. Thus, both acidity and basicity are expressed with the same scale and no acid indicators are necessary. Theoretically, a solid with a certain H_0 value can change all indicators whose $pK_{BH^+} > H_0$ into their acid forms and keep those whose $pK_{BH^+} < H_0$ in their base forms. In reality, because of the surface heterogeneity, there is always a distribution of acidic and basic sites of different strength existing on the surface. The number of reactive sites within a given strength range is then determined by amine titration for acidic sites (Tanabe, 1970), and trichloroacetic acid titration for basic sites (Yamanaka and Tanabe, 1975:2409). It is found that the highest H_0 value of the acid sites and that of the base sites always coincide at a value termed $H_{0,max}$, which is used as the overall measure of the solid acid-base properties. A solid with a large positive $H_{0,max}$ has strong basic sites and weak acidic sites. Again, this method measures the proton affinity of the solid surface, and as one may expect, there exists a qualitative correlation between $H_{0,max}$ and Isoelectric Point (IEP). The apparent limitation of the dye indicator method is that it can only be applied to Brønsted acids and bases. Another problem is that pK_{BH^+} values of the indicators are measured in aqueous media, while the titration is carried out in nonaqueous media such as benzene. Corrections for pK_{BH^+} due to the

change of medium may be necessary.

2.1.2 The method of titration using Hammett Indicator

2.1.1. Indicators

Acid strength measurements and acid amount determination were made according to the adapted method of antititration, inserting method, and using an ultrasonic oscillator (Benesi, 1957:970; Wang, et al., 2006:325). The Hammett Indicators were used for the acid strength from $H_0 \leq +7.2$ to $H_0 \leq -8.2$. The limits of the H_0 of samples were established by observing the color of the adsorbed form of suitable indicators. Neutral red (pKa: 6.8), methyl red (pKa: 4.8), *p*-dimethylaminoazobenzene (pKa: 3.3), thymol blue (pKa: 2.8) indicators were used according to those color observations. Their acid colors are red and basic colors are yellow. The indicators were resolved in dry benzene solution overnight and its concentration was 0.1% (g/L) which are the same as those used by Benesi.

2.1.2. Titration procedure

In the titration procedure, the sample was weighed (*ca* 0.02–0.04 g) and transferred to ten vials. Petroleum ether (1.5 ml) was injected to the vials using a pipette. The desired amount of standard *n*-butylamine in petroleum ether (*ca* 0.5 mol l^{-1}) was calculated according to the degree of titration. The degrees of bentonite titration were 0.1, 0.2, 0.3, 0.4, 0.5, 0.6, 0.7, 0.8, 0.9 and 1.0 mmol *n*-butylamine per gram catalyst (mmol g^{-1}). The calculated amount of standard *n*-butylamine solution was added to each vial. The ten vials were fixed and were oscillated in the ultrasonic oscillator for 50 min. The determined indicators were added to each group. After a few minutes for diffusion and reaction of the indicator, the color of indicators in the vials of some groups changed from acid color to basic color and some of them did not. The total acid amount of solid surface is equal to the sum of mmol g^{-1} values of the changed vials.

2.2. Inverse gas chromatography (IGC)

Inverse gas chromatography is a powerful technique for investigating the characteristics of solid surfaces in powder form. The experiments are conducted in the same manner as conventional gas chromatography, except that it is the stationary phase in the column rather than the gas phase, which is of interest. The versatility of IGC in material characterization is described in detail by Sun and Berg (Sun and Berg, 2003). The extent and nature of the interactions between the injected probe gas and the solid are manifested in the shape and relative elution time of the chromatogram. When IGC is used to study the solid surface energetics and acid-base properties, it is usually operated in the infinite dilution regime, which corresponds to very low surface coverage, by the

adsorbates. Many papers regarding surface characterization by IGC at infinite dilution have been published (Harding, et al., 1998:841; Sun and Berg, 2002:59; Keller and Luner, 2000:401; Asten et al., 2000:175; Mukhopadhyay and Schreiber, 1995:47).

At infinite dilution, the net retention volume, V_N, which is the amount of carrier gas required to elute the injected probe gas from the column, is related to the surface energetics and acid-base properties of the solid of interest by the following equation:

$$RTLnV_N = 2N.(\gamma_S^d)^{1/2}.a.(\gamma_L^d)^{1/2} + (-\Delta G^{SP}) + C \qquad (4)$$

where V_N is the net retention volume of the n-alkane probe, R is the gas constant, T is the absolute column temperature (K), a is the molecular surface area coated with a kind of adsorbed alkane, N is Avogadro's number, and C is the constant. In this equation, γ_S^d is the dispersive component of the surface free energy of the solid phase, and γ_L^d is the dispersive component of the surface free energy of the probe. The plot of $\left(RT\ln V_N\right)$ versus $a.\left(\gamma_L^d\right)^{1/2}$ can be useful. Such a plot is linear and the slope of the lines gives dispersive free energy of the solid phase. The values of $a.\left(\gamma_L^d\right)^{1/2}$ are necessary for the calculations and can be easily found in the literature. The specific component-free energy of adsorption (ΔG^{sp}) is related to the solid phase's ability to act as an acceptor or donor of electrons. For alkane probes, because there are no polar interactions, ΔG^{sp} is equal to zero (Das and Steward, 2012:1337):

$$\Delta G^{SP} = \Delta H^{SP} - T.\,\Delta S^{SP} \qquad (5)$$

To evaluate the ΔG^{sp}, $RT\ln(V_N)$ for each probe (including the alkanes) is plotted against $a.\left(\gamma_L^d\right)^{1/2}$. This plot gives a straight line for the alkane series which is used as the reference line. The vertical distance between the n-alkane line and the point where the polar probe is gives the $-\Delta G^{sp}$ value of that polar probe (Gamble et al., 2013:39, Kumar et al., 2014:9). According to the following equation, specific components of the adsorption enthalpy (ΔH^{sp}) and entropy (ΔS^{sp}) can be determined from ΔG^{sp}'s relationship with the temperature:

$$\frac{\Delta G^{sp}}{T} = \frac{\Delta H^{sp}}{T} - \Delta S^{sp} \qquad (6)$$

A plot of $\Delta G^{sp}/T$ versus 1/T should yield a straight line with slope ΔH^{sp} and intercept ΔS^{sp}. The acidic–basic parameters can be obtained from the calculated ΔH^{sp} values using the following equation (Lazarevic et al., 2009:41).

$$-\frac{\Delta H^{sp}}{AN^{*}} = K_A \frac{DN}{AN^{*}} + K_D \qquad (7)$$

where K_A and K_D parameters define the analyses surface's acid and base constants respectively, AN^{*} is the modified acceptor number of the adsorbed probe while DN is the donor number. The K_A and K_D values can be calculated with the aid of probes that have acidic, basic, and amphoteric properties. According to the above equation, representing the $-\Delta H^{sp}/AN^{*}$ versus DN/AN^{*}, one gets K_A as the slope and K_D as the intercept. Finally, a general definition of the nature of a solid surface can be obtained through the determination of the S_C parameters known as K_D/K_A. According to the values obtained from these parameters, it is accepted that $S_C \leq 0.9$ means the surface is acidic, $S_C \geq 1.1$ means basic, and if it is between 0.9 and 1.1, the surface is amphoteric (Ho and Heng, 2013:164, Kumar et al., 2014:9).

2.3. Spectroscopic investigation

IR spectroscopy is a powerful tool for identifying the nature (type and strength) of acid/base sites (Busca, 2007:5366; Kondo, 2010:11576; Lavalley, 1996:377; Knözinger, 2007:1135; Busca, 2010:2217; Datka, 1992:186; Emeis, 1993:347; Selli and Forni, 1999:129; Onfroy, 2005:99). It can easily distinguish between Brønsted and Lewis acids by using probe molecules such as ammonia or pyridine (Lavalley, 1996:377; Knözinger, 2007:1135; Busca, 2010:2217). Acid and base strength of solids can be estimated from peak shift values of adsorbed probe molecules (Shimizu, 2008:89; Haffad, 1998:227; Travert, 2004:16499) or the profile of absorbance versus desorption temperature (Shimizu, 2008:89). Experimental determination of the integrated molar extinction coefficient enables us to estimate the number of acid and basic sites (Lavalley, 1996:377; Datka, 1992:186; Emeis, 1993:347; Selli and Forni, 1999:129; Onfroy, 2005:99). For example, Niwa and co-workers reported that IR combined with NH_3-TPD method simultaneously gave the information about acid-type (Brønsted and Lewis) and strength and number of acid sites of zeolites and sulfated ZrO_2 (Suzuki, 2007:151; Suzuki, 2007:5980; Katada, 2008:76). However, in the case of solids

such as SiO_2, the main fingerprint band of Lewis acid sites overlaps with the absorption of SiO_2, indicating that NH_3 cannot be widely applied. Although other basic probes (pyridine and CD_3CN) and acidic probes (CO_2, $CHCl_3$, and benzaldehyde) have been applied to characterize acid/base properties of a specific solid, there are few IR studies on a wide range of solids under the same condition in order to establish a database for acid/base properties of the solids. In this paper, we studied the acid/base properties of a wide range of solids by IR with various probe molecules. To provide a database for acid/base properties and a simple method to determine acid/base indexes by IR, the following research strategies are adopted. We apply several probes to a wide range of solids and select the convenient probe in terms of the spectral shape. The peak shift values are used to estimate the acid or base strength and the peak area combined with the molar extinction coefficient of the adsorbed species are used to estimate the number of Brønsted and Lewis acid sites and basic sites.

2.3.1. FTIR-pyridine adsorption and desorption methods

The FTIR spectra of solids were recorded on a Perkin Elmer 100 FTIR spectrometer in the 4000 to 400 cm^{-1} wavenumber range using DRIFT (Diffuse Reflectance Infrared Fourier Transform) technique. A spectrum of the bentonite was obtained using KBr dilution, and finely powdered KBr was used as a reference. For acidity determinations by FTIR, the sample was heat-treated at 400 °C overnight, followed by evacuation at *ca* 10^{-5} Torr for 2 h at the same temperature. Pyridine adsorption was performed at room temperature until saturation (60 min). The sample was then evacuated for 10 min at 100 °C and cooled to room temperature before recording the spectrum. The desorption of the probe molecule was successively monitored stepwise by evacuating the sample for 10 min at 100, 150, 200, 300, and 400 °C and cooling to room temperature between each step, to record the spectrum (Yurdakoç et al., 1999:319; Seddigi, 2001:63).

2.3.1.1. Pyridine

Infrared is also a very powerful technique for understanding the acidity of solids. The positions of the bands are typical of the respective adsorption sites. Pyridinium ion (PyH^+) produced by the reaction of pyridine with Brønsted acid sites shows bands around 1545 (ν19b) and 1638 cm^{-1} (ν8a). Coordinatively bound pyridine on Lewis acid sites shows bands around 1445 (ν19b) and 1610 cm^{-1} (ν8a). Physisorbed or hydrogen-bonded pyridine shows bands around 1440 (ν19b) and 1597 cm^{-1} (ν8a). The band around 1490 cm^{-1} is common to vibrations due to PyH^+ and coordinatively bound pyridine.

A band at 1450 cm^{-1} is assigned to the vibration mode of pyridine adsorbed onto Lewis acid sites or to that of pyridine coordinately bonded to cations. This band provides information about Lewis acid sites. A band at 1540 cm^{-1} is due to pyridinium ions formed at the expense of Brønsted acid sites. Finally, a band at 1490 cm^{-1} is attributed to both Lewis and Brønsted acid sites. Therefore, using the integrated intensities of the bands at 1540 and 1450 cm^{-1} as a measure of the amount of pyridine adsorbed on Brønsted and Lewis acid sites, valuable information can be obtained about the relative concentrations of these two kinds of acid sites (Masukawa, 1997:10).

A generally recognized tendency (Knöuzinger, 1976:184) that, compared to ammonia, the bands for the adsorbed pyridines are relatively sharp and well resolved and do not overlap the absorption of SiO_2 and zeolites. This implies that pyridine is a more suitable probe molecule for the assignment of acid types (Lewis or Brønsted) of various oxides. As discussed later, these properties will allow determining the number of each acid site by measuring the integrated molar extinction coefficients of adsorbed pyridine for Lewis and Brønsted acid sites.

2.3.1.2. Acid properties

In the literature (Knöuzinger, 2007:1135; Busca, 2007:5366), acid properties (type, strength, and number) of various solids have been studied by IR spectroscopy with various probe molecules such as ammonia, pyridine, substituted pyridines, nitriles, aliphatic amine, ethers, ketones, aldehydes, aromatics, alkenes, carbon monoxide, alkanes, N_2 and H_2. Each report adopts different measurement conditions, and a study of a wide range of solids under the same condition is lacking. Measuring various solids by IR with a series of common probe molecules, which is ammonia, pyridine, and CD_3CN, and explored the method to measure the acid properties of a wide range of solids.

2.3.1.3. Basic properties

Basic properties of solids have been studied by IR with acidic probe molecules such as CO_2, SO_2, methane, acetylene, pyrrole, chloroform, alcohols, and thiols (Lavalley, 1996:377; Busca, 2010:2217). However, compared to the acidity characterization, IR characterization of basic solids has been less investigated. Hence, the general probe molecules for a wide range of solids should be explored. Generally, basic solids are ionic and, consequently, they have Lewis acid site (the exposed metal cation) adjacent to the basic site (surface oxygen). In their catalytic application, acid-base pair sites rather than purely basic sites play an important role in the catalysis by basic solids. Therefore, molecules that can interact with the acid-base pair site of solids are suitable as probe

molecules for the characterization of basic solids. For example, benzaldehyde has been used as a probe molecule for the acid-base pair site of solids (Niwa, 1985:2550; Niwa, 1991:297). Nitrobenzene also interacts with the acid-base pair site of solids (Shimizu, 2009:17803).

3. Conclusion

In the present work, various techniques for solid surface acid-base characterization are compared. It was shown that the isoelectric point, IEP, is not a description of absolute basicity or acidity of a surface, but a description of their relative strength. That is, a high IEP surface shows more basic functionality comparing with its acidic functionality, whereas a low IEP surface shows more acidic functionality comparing with its basic functionality. The choice of technique and scale for AB characterization depends on the specific application. For the cases in which the overall AB property is of interest, IEP (by electrokinetic titration) and $H_{0,max}$ (by indicator dye adsorption) are appropriate. For the cases in which the absolute AB property is of interest such as in the study of adhesion, the heat of adsorption of probe gases (by calorimetry or IGC) and in situ IR spectroscopy coupled with probing molecules, including pyridine, acetonitrile, CO_2, and chloroform.

The Amine titration method provides another valuable knowledge about the total acid amount of solid surface. The total acid amount determined by indicator dye adsorption which is the summation of acid sites. IGC is an extremely sensitive and convenient way to evaluate the Lewis acid-base parameters by adsorption of some nonpolar and polar adsorbates. The overall acid-base character of solids can be evaluated from K_D/K_A ratio; namely, the surface is considered to be basic for $K_D/K_A > 1$, and the surface is considered to be acidic for $K_D/K_A < 1$.

The acid/base properties (type, strength, number) of a wide range of solids were studied by IR with various probe molecules: ammonia, pyridine, CD_3CN, CO_2, $CHCl_3$, benzaldehyde, and nitrobenzene. For acidity characterization, CD_3CN is a suitable probe molecule for the strength of acid sites and pyridine for the type and number of acid sites. For basicity characterization, $CHCl_3$ is a suitable probe molecule for the strength of basic sites and nitrobenzene for the number of basic sites. The application of nitrobenzene adsorption to the quantification of the surface basic site is verified. The comprehensive IR results in this study will give a convenient chemical index for acid/base properties of a wide range of solids and will be available to characterize Lewis/Brønsted acid sites and basic sites on solids by a simple IR experiment, providing a powerful tool for designing new catalysts.

References

Asten, A. V., Veenendaal, N.V., Koster, S. (2000), Surface characterization of industrial fibers with inverse gas chromatography, *Journal of Chromatography A*, 888(1-2), 175-196.

Aucejo, A., Burguet, M.C., Corma, A.A., Fornes, V. (1986), Beckman rearrangement of cyclohexanone-oxime on HNaY zeolites: kinetic and spectroscopic studies, *Applied Catalysis*, 22(2), 187-200.

Auroux, A. (1997), Acidity characterization by microcalorimetry and relationship with reactivity, *Topics in Catalysis*, 4, 71–89.

Balard, H., Brendle, E., Papirer, E. (2000), *in Acid-Base Interactions: Relevance to Adhesion Science and Technology* (Ed: K. Mittal), VSP: Utrecht, The Netherlands, pp 1- 299.

Benesi, H.A. (1957), Acidity of catalyst surfaces: II. Amine titration using Hammett indicators, *The Journal of Physical Chemistry*, 61, 970-973.

Berg, J.C. (1993) *Role of Acid-Base Interactions in Wetting and Related Phenomena*, in: JC. Berg (Ed.), Wettability, Marcel Dekker, New York, 1993, 75-148.

Brønsted, J.N. (1923), Einige Bemerkungen über den Begriff der Sauren und Basen. *Recueil des Travaux Chimiques des Pays-Bas,* 42, 718-728.

Busca, G. (2010), Bases and Basic Materials in Chemical and Environmental Processes, Liquid versus Solid Basicity, *Chemical Reviews*, 110(4), 2217–2249.

Busca, G., (2007) Acid catalysts in industrial hydrocarbon chemistry, *Chemical Reviews*, 107(11), 5366-5410.

Che, S., Liu, Z., Ohsuna, T., Sakamoto, K., Terasaki, O., Tatsumi, T. (2004), Synthesis and characterization of chiral mesoporous silica, *Nature*, 429 (6989), 281–284.

Chehimi, M.M., Pigois-Landureau, E., Delamar, M., Watts, J.F., Jenkins, S.N., Gibson, E.M. (1992), The use of X-ray photoelectron spectroscopy, Fourier transform infrared spectroscopy and inverse gas chromatography in the study of acid-base interactions of polymers, solvents and metal oxides, *Bulletin de la Societe chimique de France*, 129, 137-144.

Contescu, C.I., Schwarz, J.A. (1999) *Acid-Base behavior of surfaces of porous materials*, in: Schwarz, J.A., Contescu C.I. (Eds.), Surfaces of Nanoparticles and Porous Materials, Marcle Dekker, New York, 51-102.

Corma, A. (1995) Inorganic solid acids and their use in acid-catalyzed hydrocarbon reactions, *Chemical Reviews*, 95, 559-614.

Costa, C., Dzikh, I.P., Lopes, J.M., Lemos, F., Ribeiro, F.R. (2000), Activity–acidity relationship in zeolite ZSM-5, Application of Brönsted-type equations, *Journal of Molecular Catalysis A: Chemical*, 154(1-2), 193-201.

Covarrubias, C.; Quijada, R.; Rojas, R. (2009) Synthesis of nanosized ZSM-2 zeolite with potential acid catalytic properties, *Microporous and Mesoporous Materials*, 117, 118-125.

Datka, J., Tutek, A.M., Jehng, J.H., Wachs, I.E. (1992), Acidic properties of supported niobium oxide catalysts: an infrared spectroscopy investigation, *Journal of Catalysis*, 135, 186–199.

Das S.C., Stewart P.J. (2012), Characterising surface energy of pharmaceutical powders by inverse gas chromatography. *Journal of Pharmacy* and *Pharmacology.* 64(9):1337-1348.

Deeba, M., Hall, W.K. (1985) The Measurement of Catalyst Acidity II: Chemisorption Studies, *Zeitschrift für Physikalische Chemie,* 144 (144), 85–103.

Emeis, C.A. (1993), Determination of integrated molar extinction coefficients for infrared absorption bands of pyridine adsorbed on solid acid catalysts, *Journal of Catalysis*, 141, 347–354.

Fowkes, F.M. (1990), Quantitative characterization of the acid-base properties of solvents, polymers, and inorganic surfaces, *Journal of Adhesion Science and Technology*, 4(1), 669-691.

Fraissard, J., Petrakis, L. (1994), *Acidity and Basicity of Solids: Theory, Assessment and Utility*, NATO ASI Series, Kluwer Academic, Dordrecht, 1994, pp. 1–513.

Gamble, J.F., Dave, R.N., Kiang, S., Leane, M.M., Tobyn, M., Wang, S.S.Y., (2013), Investigating the applicability of inverse gas chromatography to binary powdered systems: an application of surface heterogeneity profiles to understanding preferential probe-surface interactions, *International Journal of Pharmaceutics*, 445, 39–46.

Gutmann, V. (1978) *The Donor-Acceptor Approach to Molecular Interactions*, Plenum Press, New York.

Haffad, D., Chambellan, A., Lavalley, J.C. (1998), Characterisation of acid-treated bentonite. Reactivity, FTIR study and ^{27}Al MAS NMR, *Catalysis Letters*, 54, 227-233.

Hammett, L.P. (1935), Reaction rates and indicator acidities, *Chemical Reviews*, 16, 67-79.

Harding, P. H. , Berg, J. C. , Panjabi, G. (1998), Identification of a Surface Phase Transition in Synthetic Hydroxyapatite using Inverse Gas Chromatography, *Journal of Materials Science Letter*, 17 (10), 841-843.

Ho R., Heng J.Y.Y., (2013), A Review of inverse gas chromatography and its development as a tool to characterize anisotropic surface properties of pharmaceutical solids, *KONA Powder Part Journal*, 30, 164–180.

Hocking, M.B. (1998), *Handbook of Chemical Technology and Pollution Control*, Academic Press, San Diego, California, pp. 1–830.

Jensen, W.B. (1980) *The Lewis Acid-Base Concepts*, An Overview, John Wiley and Sons, New York, 4, 135-142.

Karge, H.G. (2008), *Concepts and Analysis of Surface Acidity and Basicity: Handbook of Heterogeneous Catalysis*, Wiley, New York, pp. 1096–1122.

Katada, N., Tsubaki, T., Niwa, M. (2008), Measurements of number and strength distribution of Brønsted and Lewis acid sites on sulfated zirconia by ammonia IRMS–TPD method, *Applied Catalysis A: General*, 340, 76–86.

Keller, D. S., Luner, P. (2000), Surface energetics of calcium carbonates using inverse gas chromatography, *Colloids and Surfaces A*, 161(3), 401-415.

Knöuzinger, H. (1976), Specific poisoning and characterization of catalytically active oxide surfaces, *Advances in Catalysis*, 25, 184-271.

Knöuzinger, H. (2007), *Handbook of Heterogeneous Catalysis*, 2nd ed., Willey, NewYork, pp. 1135-1163.

Kondo, J.N., Nishitani, R., Yoda, E., Yokoi, T., Tatsumi, T., Domen, K. (2010), A comparative IR characterization of acidic sites on HY zeolite by pyridine and CO probes with silica-alumina and γ-alumina references, *Physical Chemistry Chemical Physics*, 12, 11576-11586.

Kumar, B.P., Reddy, T.M., Reddy, K.S. (2014), Surface Characterization of 2-Hydroxypyrimidine Sulphate by Inverse Gas Chromatography. *Journal of Pharmaceutical Investigation*, 44, 9−14.

Lavalley, J.C. (1996), Infrared spectrometric studies of the surface basicity of metal oxides and zeolites using adsorbed probe molecules, *Catalysis Today*, 27, 377-401.

Lazarevic S., Radovanovic Z., Veljovic Dj, Onjia A., Janackovic Dj, Petrovic R. (2009), Characterization of sepiolite by inverse gas chromatography at infinite and finite surface coverage. *Applied Clay Science*, 43(1), 41–48.

Matsuhashi, H., Yamagata, K., Arata, K. (2004), Distinction of Acid-type on Solid Acid Surface by Comparison of Adsorption Heats of Nitrogen and Argon, *Chemistry Letters*, 33(5), 554-555.

Matsuhashi, H., Arata, K. (2006), Adsorption and desorption of small molecules for the characterization of solid acids, *Catalysis Surveys from Asia*, 10, 1-7.

Masukawa, T., Komatsu, T., Yashima, T. (1997), Strong acid sites generated in aluminosilicate region of SAPO-5, *Zeolites*, 18(1), 10-17.

Mayer, U., Gutmann, V., Gerger, W. (1975), The acceptor number–a quantitative empirical parameter for the electrophilic properties of solvents, *Monatshefte für Chemie*, 106, 1235-1257.

Mohammadi-Jam, S., Waters, K.E., (2014), Inverse gas chromatography applications: a review, *Advanced Colloid Interface*, 212, 21–44.

Mukhopadhyay, P., Schreiber, H. (1995), Aspects of acid-base interactions and use of inverse gas chromatography, *Colloids and Surfaces A, Physicochemical and Engineering Aspects*, 100, 47-71.

Nakamoto, K. (1986), *Infrared and Raman Spectra of Inorganic and Coordination Compounds*, 4th ed., Wiley, New York, pp. 108–115.

Niwa, M., Inagaki, S., Murakami, Y. (1985), Alumina: Sites and Mechanism for Benzaldehyde and Ammonia Reaction, *Journal of Physical Chemistry*, 89(12), 2550–2555.

Niwa, M., Suzuki, K., Kishida, M., Murakai, Y. (1991), Benzaldehyde-ammonia titration method for discrimination between surfaces of metal oxide catalysts, *Applied Catalysis*, 67(1), 297-305.

Olah, G.A., Molnar, A. (2003), *Hydrocarbon Chemistry*, 2nd ed., Wiley, New York, pp. 1–871.

Onfroy, T., Clet, G., Houalla, M. (2005) Quantitative IR characterization of the acidity of various oxide catalysts, *Microporous and Mesoporous Materials*, 82, 99–104.

Pizzio, L.R. (2005), Mesoporous titania: effect of thermal treatment on the texture and acidic properties, *Materials Letters.*, 59, 994-997.

Seddigi, Z.S. (2001), Nature of the FTIR Band in Acidic Zeolites, *Reaction Kinetics and Catalysis Letters*, 73(1), 63-70.

Selli, E., Forni, L. (1999), Comparison between the surface acidity of solid catalysts determined by TPD and FTIR analysis of pre-adsorbed pyridine, *Microporous and Mesoporous Materials*, 31, 129–140.

Shimizu, K.I., Higuchi, T., Takasugi, E., Hatamachi, T., Kodama, T., Satsuma, A. (2008), Characterization of Lewis acidity of cation-exchanged montmorillonite K-10 clay as effective heterogeneous catalyst for acetylation of alcohol, *Journal of Molecular Catalysis A*: *Chemical*, 284, 89–96.

Shimizu, K.I., Miyamoto, Y., Kawasaki, T., Tanji, T., Tai, Y., Satsuma, A. (2009), Chemoselective hydrogenation of nitroaromatics by supported gold catalysts: mechanistic reasons of size-and support-dependent activity and selectivity, *Journal of Physical Chemistry C*., 113, 17803-17810.

Shirazi, L.; Jamshidi, E.; Ghasemi, M.R. (2008), The effect of Si/Al ratio of ZSM-5 zeolite on its morphology, acidity and crystal size, *Crystal Research and Technology,* 43(12), 1300-1306.

Solinas, V., Ferino, I. (1998), Microcalorimetric characterization of acid–basic catalysts, *Catalysis Today*, 41, 179–189.

Sun, C., Berg, J. C. (2002), Effect of moisture on the surface free energy and acid-base properties of mineral oxides, *Journal of Chromatography A*, 969, 59-72.

Sun, C., Berg, J.C. (2003), A review of the different techniques for solid surface acid-base characterization, *Advances in Colloid Interface Science,* 105(1-3), 151-175.

Suzuki, K., Noda, T., Katada, N., Niwa, M. (2007) IRMS-TPD of ammonia: Direct and individual measurement of Brønsted acidity in zeolites and its relationship with the catalytic cracking activity, *Journal of Catalysis*, 250, 151–160.

Suzuki, K., Sastre, G., Katada, N., Niwa, M. (2007), Ammonia IRMS-TPD measurements and DFT calculation on acidic hydroxyl groups in CHA-type zeolites, *Physical Chemistry Chemical Physics*, 9, 5980–5987.

Tanabe, K. (1970), *Solid Acids and Bases, Their Catalytic Properties*, Kodensa, Tokyo, Acedemic Pres, New York, pp 1-58.

Tanabe, K., Misono, M.; Ono, Y.; Hattori, H. (1989), New Solid Acids and Bases, Their Catalytic Properties, *Studies in Surface Science and Catalysis*, vol.51, Kodansha, Tokyo, Elsevier, Amsterdam, pp. 1-364.

Travert, A., Vimont, A., Lavalley, J.C., Montouillout, V., Delgdo, M.R., Pascual, J.J.C., Areán, C.O (2004), Evidence for Discrepancy between the Surface Lewis Acid Site Strength and Infrared Spectra of

Adsorbed Molecules: The Case of Boria-Silica, *Journal of Physical Chemistry B,* 108, 16499–16507.

Tsuji, H., Okamura-Yoshida, A., Shishido, T., Hattori, H. (2003), Dynamic behavior of carbonate species on metal oxide surface: oxygen scrambling between adsorbed carbon dioxide and oxide surface, *Langmuir*, 19, 8793–8800.

Van Oss C.J., Good R.J., Chaudhury M.K. (1986), The role of van der Waals forces and hydrogen bonds in "hydrophobic interactions" between biopolymers and low energy surfaces. *Journal of Colloid Interface Science*, 111, 378-390.

Van Oss CJ, Chaudhury MK and Good RJ (1988), Interfacial Lifshitz–van der Waals and polar interactions in macroscopic systems, *Chemical Reviews*, 88(6): 927–941.

Van Oss C.J., Good R.J., Chaudhury M.K. (1988), Additive and nonadditive surface-tension components and the interpretation of contact angles, *Langmuir,* 4(4), 884–891.

Wang, K., Wang, X., Li, G. (2006), Quantitatively study acid strength distribution on nanoscale ZSM-5, *Microporous and Mesoporous Materials*, 94, 325-329.

Weissermel, K., Arpe, H.J. (1997), *Industrial Organic Chemistry*, 3rd ed., VCH, Weinheim, 1997, pp. 1–482.

Wittcoff, H.A., Reuben, B.G. (1996), *Industrial Organic Chemistry*, Wiley, New York, 1996, pp. 1–560.

Yamanaka T., Tanabe K. (1975), New determination of acid-base strength distribution of a common scale on solid surfaces, *The Journal of Physical Chemistry*, 79 (22), 2409-2441.

Yurdakoç, M., Akçay, M., Tonbul, Y., Yurdakoç, K. (1999), Acidity of Silica Alumina Catalysts By Amine Titration Using Hammett Indicators and FT-IR Study of Pyridine Adsorption, *Turkish Journal of Chemistry*, 23, 319-327.

CHAPTER V

COD REMOVAL FROM CARPET WASHING WASTE WATER USING DK MEMBRANE[1]

Prof. Dr. Duygu KAVAK

Eskişehir Osmangazi University, Eskisehir, Turkey
e-mail: dbayar@ogu.edu.tr, Orcid ID: 0000-0002-1189-3110

1.Introduction

Most of the waste water in the carpet washing industry originates from dyeing processes. For this reason, there are dyes that are not fixed to the yarns and auxiliary chemicals, most of which are in the surfactant class, in carpet washing waste water. This situation causes high content of color and organic matter in waste water. pH values are generally not neutral and complex waste water results are obtained. In case of insufficient treatment, the dyes in the waste water cause color and toxic substances in the receiving environment. Although color poses an aesthetic problem at first, it prevents photosynthesis by decreasing the light transmittance in natural waters when it reaches high levels (Çapar, 2004).

Also they have high value of chemical oxygen demand (COD) that is one of the important parameters that express the amount of organic pollution in wastewater. This expression refers to the amount of oxygen to be added to carbon dioxide in organic matter in the water (Tan, 2006; Zheng, et al., 2013).

Membrane technology, which is known to be environmental friendly, has ease of construction and control, low consumption of energy, no requirement of chemical substances to be added and is feasible for recovery of valuable metals (Licínio et al., 2015). Chemical oxygen demand (COD) is one of the most important parameters used in determining the pollution degree of industrial waste-water. The membrane processes provided the highest COD removal from waste water (Madaeni and Mansourpanah, 2006).

There are four various pressure-driven membrane methods: microfiltration (MF), ultrafiltration (UF), nanofiltration (NF) and reverse osmosis (RO) (Piedra et al. 2015). Among these membrane methods, nanofiltration uses membranes with very small pores (<1 nm) and

[1] In this study, devices and tools bought by Eskişehir Osmangazi University Research Foundation were used (Project Number: 201215031).

requires operating pressures in the 10-50 bars range (Gherasim and Mikulášek 2014). There are two ways to operate nanofiltration process. While in dead-end filtration, all of the solution is directed towards the membrane area under applied pressure, in cross-flow filtration entire solution is directed parallel to the membrane surface (Tsibranska and Tylkowski 2013, Kavak 2017b).

In this study, it was aimed to remove COD from carpet washing waste water with the nanofiltration method. For this purpose, the effects of membrane pressure (10, 15, 20 bar) and feeding temperature (25, 35 °C) parameters on the COD removal efficiency of carpet washing wastewater with DK polymeric membrane were investigated.

2.Material and Methods

In the experimental study, the wastewater of the carpet washing company in Eskişehir was used. The values of raw wastewater, COD, pH, max. absorbance and conductivity are shown in Table 1.

Table 1: Properties of raw carpet washing waste water

Parameter	**Value**
COD, mg/L	576
Max. Absorbance, nm	324
pH	7.76
Conductivity, µS/cm	254

Commercial Poliamid TFC DK nanofiltration membrane used in this study was provided by GE Osmonics. The properties of the used membrane are given in the Table 2 (https://www.sterlitech.com).

Table 2: Properties of DK Membrane

Properties	**DK membrane**
Feed	Industrial/Food
Type	High Rejection
pH Range	2-10
$MgSO_4$ Rejection	96.0%
Pore Size/MWCO	150-300 Da
Flux (GFD)/psi	22/100
Polymer	Polyamide-TFC

COD test kits were used to determine the amount of COD in carpet washing wastewater and treated wastewater. Test kits were opened and a 2 ml waste water sample as added. The kits placed on the Hach LT 200 branded thermoreactor were stored at 148ºC for 2 hours. After 2 hours the

kits were removed from the thermoreactor and allowed to cool to room temperature. Sample test kits arriving at room temperature were placed in a Hach Lange DR 3900 spectrophotometer and the results read in mg/L.

Membrane experiments were conducted in a cross-flow test system (SEPA CE Sterlitech) as shown in Fig. 1.

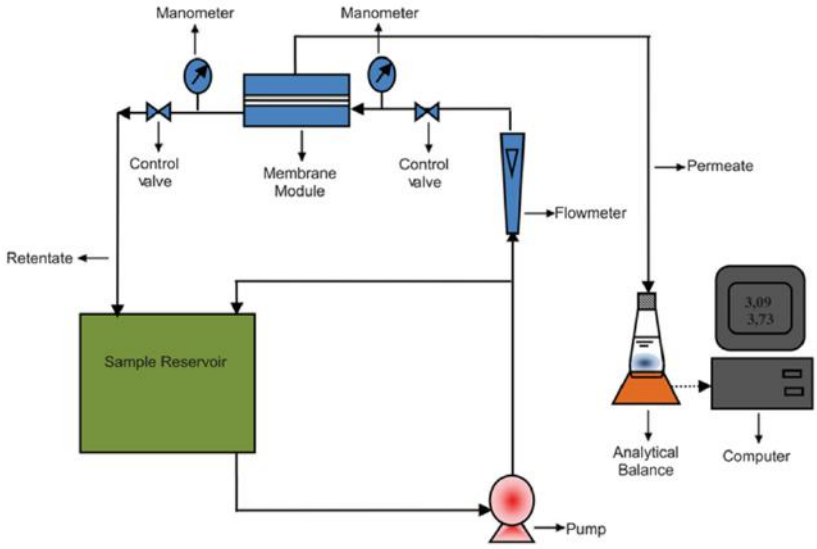

Figure 1: Schematic diagram of the cross-flow NF experimental set-up.

This system is formed by a membrane module, a hydraulic hand pump, a feed tank, a high pressure pump, an analytical balance for the measurement of flux, a computer, a thermostat, a flowmeter and other necessary fittings. The stainless steel cross-flow filtration system had a total volume of 5 L and contained an effective membrane area of 0.015 m^2. Synthetic wastewater taken from feed tank by centrifugal pump was transmitted to the membrane cell. Amount of permeate was measured by an analytical balance which was connected to the computer (Kavak 2017a, Kavak 2017b).

COD removal efficiency (E_F, %) was calculated as Eq. (1) based on the COD concentrations of a determined species in the permeate (C_P, mg/L) and in the feeding (C_F, mg/L).

$$E_F = \frac{C_F - C_P}{C_F} \times 100 \quad (1)$$

3. Results and Discussion

The COD removal performance of the DK membrane is shown in Fig.2.

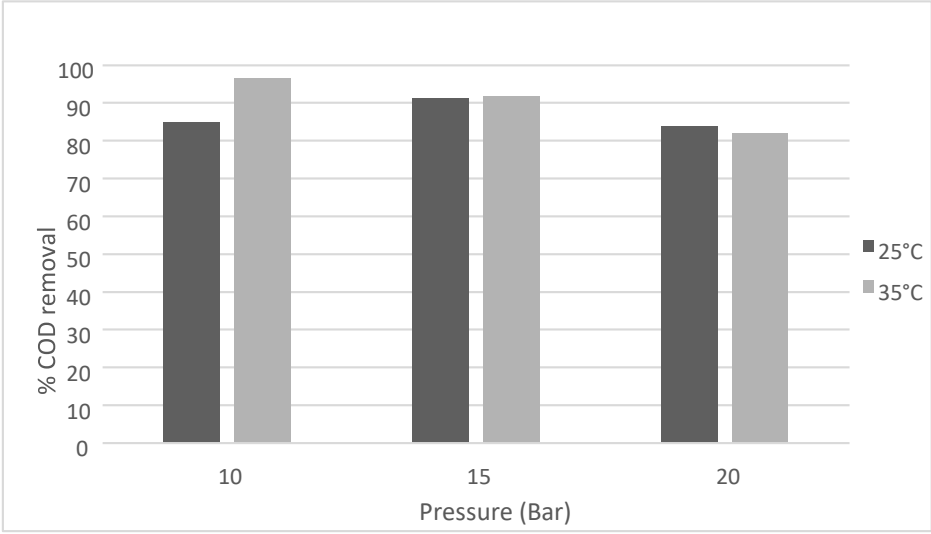

Figure 2: COD removal of waste water (feed temperature: 25ºC and 35 ºC, membrane pressure: 10, 15 and 20 bar).

COD removal percentages at the end of 60 minutes were obtained as 85.1%, 91.2% and 83.8% for 10, 15 and 20 bar pressures at 25ºC temperature, respectively (Figure 2).

According to Figure 2, COD removal percentages at the end of 60 minutes were obtained as 96.4%, 91.8% and 81.9% for 10, 15 and 20 bar pressures at 35ºC temperature, respectively. At 35ºC, COD removal decreases as membrane pressure increases. It was observed that COD removal did not change significantly with the temperature increase, except for 10 bar. The maximum COD removal was obtained as 96.4% at 35ºC and 10 bar.

COD discharge limit value for carpet waste water of Water Pollution Control Regulation is 200-300 mg/L (https://www.mevzuat.gov.tr). As a result of the analysis, it was seen that the COD values were in the range of 50-100 mg/L. Since the COD concentrations obtained for all conditions in this study are below the discharge limits, the DK membrane can be used for the treatment of carpet washing waste water.

4. Conclusions

In this study, COD removal from carpet washing waste water by cross-flow nanofiltration method using DK membrane was investigated. The maximum COD removal was obtained as 96.4% at 35ºC and 10 bar. After the experiments, COD concentrations remaining in permate are found to be lower than the discharge values defined for industrial wastewater by Water Pollution and Control Regulation in Turkey. According to the experimental results, DK membrane is efficient for COD removal from carpet washing waste water.

5. References

Çapar, G., Yetiş, Ü. ve Yılmaz, L., Halı boyama atıksularının membran prosesleri ile arıtımı. Sosyal Siyaset Konferansları Dergisi, 14(2) (2004), 9-15.

Gherasim, C-V. and Mikulášek, P. Influence of operating variables on the removal of heavy metal ions from aqueous solutions by nanofiltration. Desalination 343, (2014), 67-74.

https://www.mevzuat.gov.tr (Erişim tarihi:07.09.2020)

https://www.sterlitech.com (Erişim tarihi:06.09.2020)

Kavak D. Treatment of dye solutions by DL nanofiltration membrane, Desalination and Water Treatment 69(1) (2017a), 116-122.

Kavak D. Removal of Iron, Copper and Zinc Mixtures from Aqueous Solutions by Cross Flow nanofiltration, Fresenius Environmental Bulletin, 26(1a) (2017b), 1101-1107.

Licínio M. Gando-Ferreira Joana C. Marques and Margarida J. Quina, Integration of ion-exchange and nanofiltration processes for recovering Cr(III) salts from synthetic tannery wastewater, Environmental Technology 36(18) (2015), 2340–2348.

Madaeni, S. And Mansourpanah, Y. Screening membranes for COD removal from dilute wastewater. Desalination(197), (2006), 23-32.

Piedra, E. Á1varez and J.R. Luque, S. Hexavalent chromium removal from chromium plating rinsing water with membrane technology. Desalination and Water Treatment 53, (2015), 1431-1439.

Tan, A. Atık Sularda Bazı Kirlilik Parametrelerinin İncelenmesi, (Yayımlanmamış Yüksek Lisans Tezi), Trakya Üniversitesi Fen Bilimleri Enstitüsü, (2006), 85 s.

Tsibranska, I.H. and Tylkowski, B. Concentration of ethanolic extracts from Sideritis SSP. L. by nanofiltration: Comparison of dead-end and

cross-flow modes. Food and Bioproducts Processing 91, (2013), 169-174.

Zheng, Y., Yu, S., Shuai, S., Zhou, Q., Cheng, Q., Liu, M. and Gao, C., Color removal and COD reduction of biologically treated textile effluent through submerged filtration using hollow fiber nanofiltration membrane. Desalination 314, (2013), 89-95.

CHAPTER VI

COLOR REMOVAL FROM DAIRY INDUSTRY WASTE WATER USING UB70 MEMBRANE[1]

Prof. Dr. Duygu KAVAK

Eskişehir Osmangazi University, Eskisehir, Turkey
e-mail: dbayar@ogu.edu.tr, Orcid ID: 0000-0002-1189-3110

1.Introduction

Dairy Industry very important in the food industry with 15% production value is a sub-sector. Modern dairy processing plants in Turkey have increased in recent years. Especially in the last decade, many advanced technology investments have been made in the dairy processing industry (Gönenç and Tanrivermiş, 2008). Waste water is used in the production cycles of different products. In the dairy industry, water has been an important processing medium. Water is used in at all stages of the dairy industry including cleaning, sanitation, heating, cooling and floor washing normally the water requirement is very large. Dairy waste water contains proteins, carbohydrates, lipids, organic matter such as BOD and COD, suspended material such as solid matter and oil.

There are many applications of membrane separation technology in dairy industry. Some applications in milk concentration are protein and lactose component seperation, filtration, and bacteria reduction (Chen et al., 2018). The possibility of generating good-quality reuse water to minimize consumption and reduce the generation of effluents resulted in an interest for membrane separation processes in the dairy industry. (Galvão, 2018).

Membrane technology, is very attractive for wastewater treatment due to its effectiveness in removing organic and multivalent metals. It can operate at relatively low pressures and provide good permeability flow rates. Furthermore, the separation is carried out without phase change and without the use of chemical or thermal energy, so the process becomes energy efficient (Licínio et al., 2015). Pressure-driven membrane processes are called microfiltration (MF), ultrafiltration (UF), nanofiltration (NF) and reverse osmos (RO) (Sert et al., 2016).

[1] In this study, devices and tools bought by Eskişehir Osmangazi University Research Foundation were used (Project Number: 201215031).

Ultrafiltration uses a finely porous membrane to separate water and microsolutes from macromolecules and colloids. The average pore diameter of the UF membrane is in the 10–1000 Å range (Baker, 2012).

In this study, color removal from dairy industry wastewater were investigated by ultrafiltration method. In order to determine the effect of filtration pressure (4 and 8 bars) and feed temperature (25ºC and 35ºC) on color removal, dairy waste water was passed through UB70 membrane.

2.Material and Methods

Waste water used in this study was provided from the dairy industry in Eskişehir. The waste water obtained from the factory was taken the day before the experimental work was started and stored in the refrigerator in the laboratory to ensure that the properties of the waste water did not change. The values of raw wastewater, COD, pH, max. absorbance and conductivity before the treatments are shown in Table 1.

Table 1: Properties of raw dairy industry waste water

Parameter	**Value**
COD, mg/L	3039
Max. Absorbance, nm	365
pH	12
Conductivity, µS/cm	3003

Feed tank and membrane filtration system has been cleaned before starting the experiment in order to reduce the contamination inside. Membrane system cleaning was carried out in three stages; membrane system was first cleaned with pure water, then cleaned with 0.1-0.2% acidic solution and as the final stage membrane system was again cleaned with pure water.

Color was analyzed using the Hach Lange DR 3900 UV-vis spectrophotometer at the λmax value of 365 nm. UB70 commercial UF membrane used in the experiments was obtained from TriSep™. Table 2 shows the specific properties of the UB70 membrane (https://www.sterlitech.com)

Table 2: Specific properties of the UB70 membrane

Properties	**UB70**
Type	Industrial Wastewater
pH	2-11
Flux (GFD)/psi	48/3
Pore size/MWCO	0.03 µm
Polymer	Polyvinylidene Fluoride

Sterlitech-SEPA CF cross flow membrane system was used in the experimental study. A schematic representation of the system is given in Figure 1.

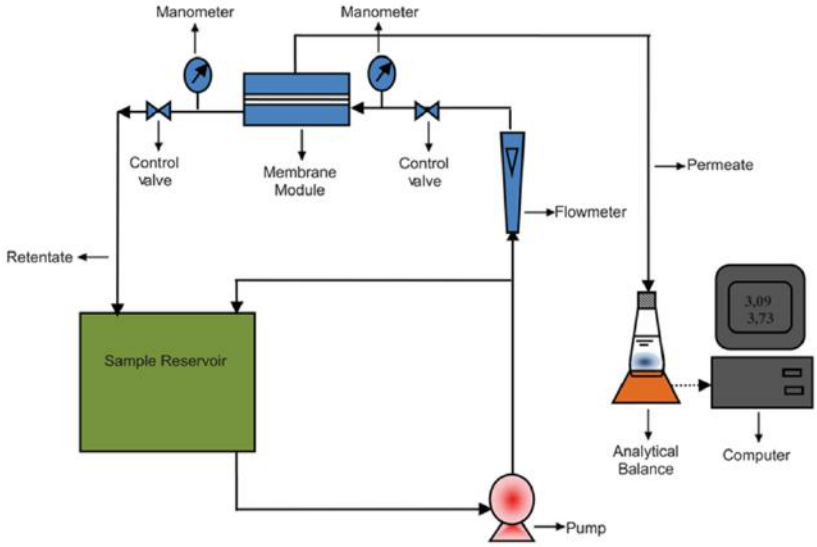

Figure 1: Schematic diagram of the cross-flow UF experimental set-up.

This system consists of a membrane module, feed tank, pressure pump, scales, flowmeter, computer, thermostat and necessary fasteners. The effective area of the membrane in the system is 150 cm^2 (Kavak, 2017a, Kavak, 2017b). Temperature control is provided by WiseCircu heater in the system. This heater is used to keep the waste water in the supply tank at the desired temperature levels. During the filtration time, the retained and permeate streams returned to the feeding volume for maintaining the homogeneity of samples.

Color removal efficiency (E_F, %) was calculated as Eq. (1) based on the concentrations of a determined species in the permeate (C_P, mg/L) and in the feeding (C_F, mg/L).

$$E_F = \frac{C_F - C_P}{C_F} \times 100 \quad (1)$$

3. Results and Discussion

The color removal performance of the UB70 membrane is shown in Fig.2 and Fig.3. Very high percentage of color rejections were observed at all pressure and temperature values. At the end of 120 minutes color

removal percentages were obtained as 88.87% and 99.70% for 4 and 8 bar pressures and 25ºC temperature, respectively (Figure 2).

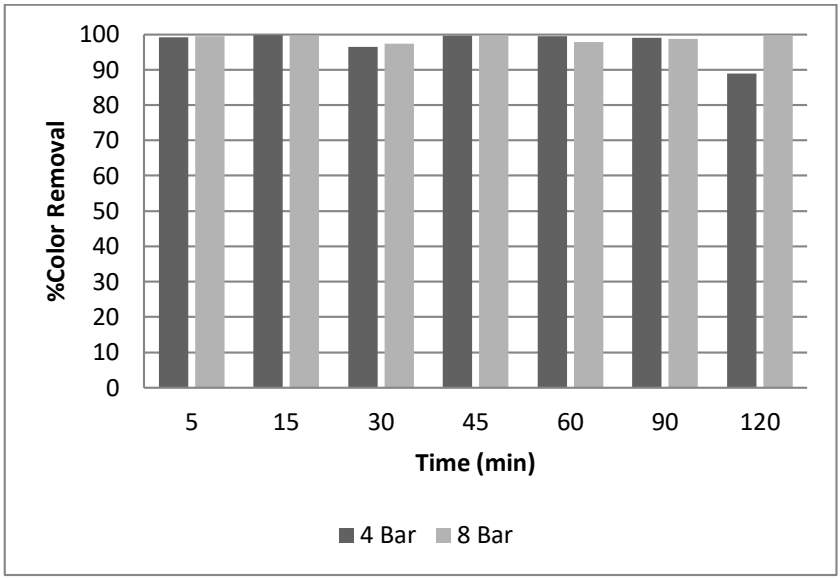

Figure 2: Effect of pressure on the color removal of dairy industry wastewater (feed temperature: 25ºC, filtration pressure: 4, 8 bar).

As can be seen from Fig. 2, color removal increases with an increase in membrane pressure at the end of 120 minutes. The maximum color removal was obtained as 99.7% at 25 ºC and 8 bars.

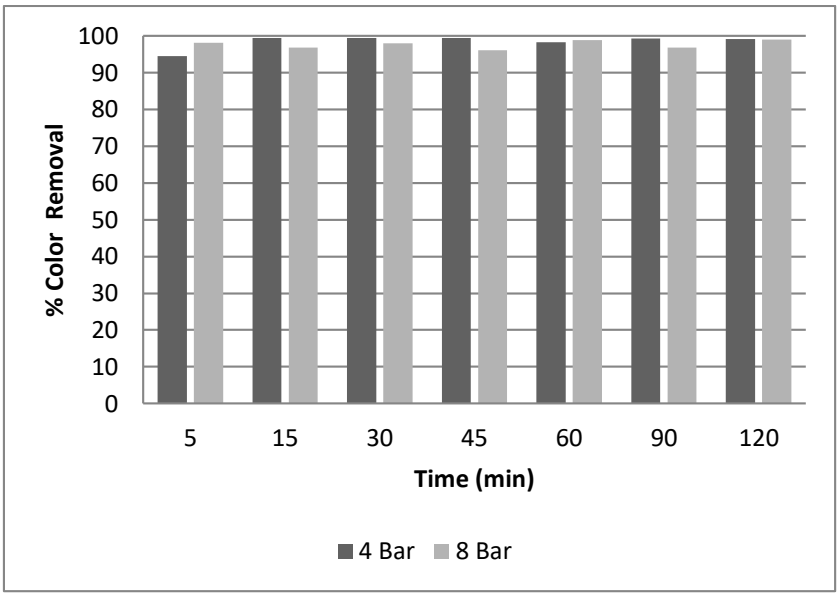

Figure 3: Effect of pressure on the color removal of dairy industry wastewater (feed temperature: 35ºC, filtration pressure: 4, 8 bar).

According to Figure 3, color removal percentages were obtained as 99.16% and 99.03 for 4 and 8 bar pressures and 35ºC temperature, respectively.

At 4 bar; as the feed temperature was increased from 25 ºC to 35ºC at the end of 120 minutes, the color removal increased from 88.87% to 99.16%, respectively. At 8 bar; with the increase of temperature, the color removal of UB70 membrane increased slightly. As can be seen from Fig. 3, increasing pressure does not affect color rejection significantly.

The maximum color removal was obtained as 99.7% at 25ºC and 8 bar.

4. Conclusions

In this study, performance of a UB70 membrane has been studied to treatment of dairy industry wastewater by cross-flow UF at different operating conditions. Effects of different factors including operating pressure and feed temperature were investigated. The maximum color removal was obtained as 99.7% at 25 ºC and 8 bar after 120 min of UF. According to the experimental results, UF membrane system is efficient for color removal dairy industry wastewater.

5. References

Baker, R. W., Membrane technology and applications, John Wiley&Sons, 2nd edition, (2012), 538.

Chen, Q., Zhao, L., Yao, L., Chen, Q., Ahmad, W., Li Y., and Qin, Z., The application of membrane separation technology in the dairy industry, Technological Approaches for Novel Applications in Dairy Processing, (2018), 23-43.

Galvão, D.F., Membrane technology and water reuse in a dairy industry, Technological Approaches for Novel Applications in Dairy Processing, (2018), 163-173.

Gönenç, S. and Tanrivermiş, H., An overview of the Turkish dairy sector, International Journal of Dairy Technology, 61, 1, (2008), 3–10.

https://www.sterlitech.com (erişim tarihi: 04.09.2020).

Kavak D., Treatment of dye solutions by DL nanofiltration membrane, Desalination and Water Treatment 69(1) (2017a), 116-122.

Kavak D., Removal of Iron, Copper and Zinc Mixtures from Aqueous Solutions by Cross Flow nanofiltration, Fresenius Environmental Bulletin, 26(1a) (2017b), 1101-1107.

Licínio M. Gando-Ferreira Joana C. Marques and Margarida J. Quina, Integration of ion-exchange and nanofiltration processes for recovering Cr(III) salts from synthetic tannery wastewater, Environmental Technology 36(18) (2015), 2340–2348.

Sert G. Bunani S. Kabay N. Egemen Ö. Arda M. Pek T.Ö. and Yüksel M., Investigation of mini pilot scale MBR-NF and MBR-RO integratedsystems performance—Preliminary field tests Journal of Water Process Engineering 12 (2016), 72–77.

CHAPTER VII

CURRENT RESEARCHES IN BIOGAS PRODUCTION

PhD Student Koray GÜNAY* & Asst. Prof. Dr. Zehra Gülten YALÇIN**& Research Assistant Dr. Mustafa DAĞ***

* Çankırı Karatekin University, Çankırı, Turkey
e-mail: koray.gunay37@gmail.com, Orcid No: 0000-0002-4329-2037

** Çankırı Karatekin University, Çankırı, Turkey
e-mail: zaltin@karatekin.edu.tr, Orcid No: 0000-0001-5460-289X

*** Çankırı Karatekin University, Çankırı, Turkey
e-mail: mudag@karatekin.edu.tr, Orcid No: 0000-0001-9540-3475

1. Introduction

Discovery of alternative energy sources is related to some reasons such as the abrupt end of nonrenewable energy sources (fossil fuels), global climate changing, instability of oil prices and independence of energy [1]. Nonrenewable energy sources (fossil fuels) have been running out very quickly in densely populated areas where people do not have access to alternative modern energy sources [2]. In the nature trees, plants, fertilizers, waterfalls, geothermal sources, sun, come and go events, wind and wave energy, human and animal muscle strength all these are renewable energy sources. Still, global priorities, some factors such as politic issues, economic cost and environmental anxieties are admittedly forced to select the way gaining energy [3]. At the near future renewable energy is thought as one of the most innovative technologies to put an end to the addiction of the nonrenewable energy sources. The development of renewable energy is one of the most important strategies for ensuring energy safety in every single country on Earth. Due to the huge urbanization amount of solid wastes are being produced so that eliminating this huge amount of solid wastes is a big issue to keep cities clean and safe. On the other hand, these wastes have enormous biogas potential owing to their organic content. Although cattle manure is a basic source of biogas production in rural areas and urban life offers a large amount of biomass to produce biogas, these cannot be effectively utilized. In contrast, rural and urban wastes can be used to produce biogas as a raw material source [4]. Composing a resource for renewable energy by eliminating these raw materials with environmentally friendly technologies (such as anaerobic digestion reactors) has become a primary goal in the energy policies of nations. This goal is going to provide a significant contribution to national energy safety accompany with reducing the environmental pollution [4].

2. Wastes and the importance of waste management

Waste was first defined in Turkey in the Environmental Law No. 2872 dated 1983 as "Harmful substances that are thrown into the environment or released as a result of any activity" [5]. Wastes have different types depending on various factors such as consumption or post-production, packaging wastes. Depending on chemical or physical properties, that wastes consist of solid, liquid and gas forms. Solid wastes refer to substances in the solid phase that must be eliminated regularly for human and environmental health. Regardless of the origin, such as domestic, commercial or industrial, waste is defined as the loss of economic value of raw material, fuel or water after use [6]. According to the United Nations Environment Program (UNEP), solid waste is stated as "substances that the owner does not want, does not need, does not use and it needs to be treated and removed" [7]. The most important topic of today's world is to find a solution for environmental pollution and productive waste management in developing economies. Increasing in energy-demanding has caused to use of excessive fossil fuels, and this situation has reached a result in global warming that affects the whole world. These urgent problems are awaiting for solutions which have pushed researchers to find innovative approaches about preventing stubble burning, balancing fossil fuel demand and producing substances such as bioenergy, biomaterials and biochemicals from organic wastes [8], [9].

Current solid waste management presents the simple form of the processing process. Therefore it has been compulsory to find a productive and effective way for conversion process from solid wastes to energy. For example, in the cities of India there is an amount of urban solid waste production 0,3-0,5 kg per person. It has been seen that anaerobic digestion is the best way to utilize this enormous amount of waste to produce renewable energy, keeping cities clean and safe. Anaerobic digestion is also known as biomethanization that is widely used for waste management. Owing to anaerobic digestion wastes are degraded in the absence of O_2 to produce biogas and which are eliminated in the most productive and safest way. The options other than anaerobic digestion include laborious, costly and non environmentally friendly applications. Biomethanization applications have recently been developed to process a wide range of wastewater, slurries and solid wastes that are presented [10]. This technology has widely been used for over 100 years, but it is still open to technological development [11]. It is possible to produce bioenergy from a wide variety of wastes. It has been given some potential organic wastes (defined as biomass) below to produce biogas:

Sewage Slurry/Water: Sewage and sewage water have negative effects on both the environment and human health, but the cost of processing

sewage water is also an undeniable fact. On the other hand, it is a subject that takes intense attention to think organizationally, technically and economically about reducing sewage water amount and preventing wastewater. Anaerobic digestion is widely used to produce biogas from sewage water and keep sewage water in a balance. In treating wastewater or at any other related areas, it is done biogas production as a renewable energy source [12].

Household/Food Wastes: This kind of waste is one of the most important components of urban solid wastes that include restaurant waste, canteen waste, food-processing waste and domestic food waste. Storage of household/food waste has started to be a big problem globally [13]. The amount of household/food waste is estimated to happen a sharp increasing from 2.78 Billion ton to 4.16 Billion ton in countries of Asia [14]. Owing to the development in industry and urbanization of China, it is expected to be 10% percentage increasing in household/food waste rate [15]. Therefore, the processing and eliminating of household/food waste properly [16], [17], [18], preventing odor consisting and insects are the top priority for urban life in global perspective [19], [20]. Household/food wastes have very rich organic content so that as raw material, they are so suitable to produce various products with high added value [21], [22]. Although household/food waste is an abundant and easy source for biomethane production, the pH lowered by organic acids they have at high organic loading rate can significantly inhibit anaerobic bacteria. Recent studies have made it clear that; the co-digestion of household/food waste and sewage sludge enormously improves energy recovery, resulting in an economical and feasible approach [23], [24], [25], and [26]. In different regions of the world, the composition of household/food waste shows different physicochemical properties depend on where they were grown up. Some household/food wastes are rich about carbohydrates such as rice, pasta and vegetables, while some household/food wastes such as meat, fish and eggs are rich about protein and lipids. In addition, household/food wastes have some general properties such as 74-90% moisture content, 85 ± 5% high volatile solids fraction and 5.1 ± 0.7 average acidic pH values which can be estimated all around the world [27], [28]. Typical household/food wastes consist of biodegradable components such as carbohydrates (%41-62), proteins (%15-25) and lipids (%13-30). In general, household/food wastes have been proven to have different proportions of nutrients, micro components and heavy metals; but the variety was found to be very high [29]. Household/food wastes have relatively less C / N ratio than the C / N ratio (between 13.2-24.5) that have been accepted efficient [28], [30], and [31]. In fact, an excessive C / N ratio causes an increase in acid production, which inhibits methane formation; low C / N ratio also leads to conversion to ammonium, suppressing methanogenesis. The optimum

C / N ratio for biodegradable substrates is between 20 and 25. In addition, the optimum C / N ratio for some biomass that durable is against biodegradable could be up to 40. Owing to their structural characteristics, with their wide availability and high biodegradability organic fractions, food wastes are potential sources which offer high energy and they greatly influence the performance of anaerobic digestion (AD) [29], [32].

Lignocellulosic Wastes: On Earth, it is one of the most abundant biomass sources with approximately 200-Billion-ton production [33]. Owing to the development in the agricultural industry by the increase in agricultural production, the amount of lignocellulosic waste has shown a great accumulation in every area of these sectors. Forestry wastes, woody wastes and urban wastes also contribute to this huge waste pool. An average urban waste consists of approximately 60% lignocellulosic wastes [34].

Vegetable and fruit Wastes: In both developed and developing countries, fruit and vegetables are significant natural sources that provide vitamins, minerals and dietary fiber. The production of fruit and vegetables has continuously increased in Asia, South America and many developed countries all around the world. Asia, as the world's largest vegetable source, is responsible for 61% of global vegetable production. China, India and Brasilia meet 30% of the world fruit supply market [35]. Potato (81 Mt), tomato (36 Mt), citrus (29 Mt), banana (25 Mt), apple (17 Mt), grape (17Mt) and specific crops processing industry produce large quantities of fruit-vegetable wastes and by-products worldwide.

The United States Food and Agriculture Organization (FAO) statistics for 2013 indicated that global fruit production increased by approximately 3% annually in the decade that passed 804.4 million tons in 2012 [36]. FAO also states that approximately 36-56% of all produced fruits has eventually been waste [37]. The way that causes fruits to waste includes a wide period (such as harvesting, mechanic-processing damages, storage, illness and transportation). There are two types of fruit wastes consisting while it is being processed: solid wastes are shells, seeds, and membranes while liquid wastes are wash water and fruit juice [38]. The average volatile solid (VS) composition of fruit wastes is 78.3% carbohydrates, 8.5% protein and 6% fat [39] and the theoretical methane yield is 0.43 Nm^3 CH4 / kg volatile solid or 0.04 Nm^3 CH4 / kg fruit waste.

Due to flavor components, methane yield from fruit wastes is much less than expected to be obtained [40]. These flavor components are classified as esters, alcohols, aldehydes, ketones, lactones and terpenoids. Compounds of the terpenes family such as geraniol, thymol and carvacrol are known as cytotoxins [41]. In research was conducted by Wikandari et

al. (2013) [40], it was reported that terpenotes, aldehydes and alcohols, which are found 0.5% ratio in fruit waste, can decrease methane production by 99% ratio. Limonen, which is a terpenoid and an important component of peel oil from citrus, causes failure in continuous mesophilic AD process at a concentration of 400 μL / L [42]. It also causes failure in continuous thermophilic AD process at a concentration of 450 μL / L [43]. Due to the flavor components, it is essential to treat fruit wastes (as pre-treatment) before using them to produce biogas.

Animal Production Wastes: Production and classification of animal manure vary depending on the animal type, climate, diet, age and health conditions of the animal [44]. Animal manure and slurry cause a continues environmental pollution if it does not be appropriately managed. Animal manure and slurry cause continuous environmental pollution if it does not be managed appropriately [45]. In many recycling strategies, bioenergy from animal manure can provide many benefits such as preventing environmental pollution, reducing greenhouse gas emissions and obtaining valuable energy as by-products. The USA has scheduled to produce bioenergy from 60 Million Ton animal manure up to 2030 [46]. With processing 5995 Mt animal wastes in 27 countries of the EU, bioenergy from animal wastes has become more common [47]. The composition of lignocellulosic materials in animal manure varies depending on some factors such as the type of animal, diet, digestion and also type of production. In comparison with vegetable and fruit wastes, animal manure has higher lignocellulosic content. While cattle manure has the highest ratio (more than half) of lignocellulosic content in its dry matter, pork and poultry manure has less than 40% lignocellulosic content in a dry matter [48]. Storage/disposal of cattle manure in open areas emits unpleasant odors, has air pollutant and harmful substances with a greenhouse effect; it may also threaten human health with ammonia, volatile organic compounds, hydrogen sulfide and solid particles [49]. In addition to air pollution, it also causes pollution in soil and groundwater [50]. On the other hand, manure emits two important greenhouse gases; methane (CH_4) and nitrite oxide (NO_2) [51].

2.1 Anaerobic digestion in waste management

Anaerobic Digestion (AD) is a biological process conducted by various microorganisms under oxygen-free conditions to produce biogas. During the AD process, organic substances are degraded by various microorganisms to biogas (approximately 50-75% CH_4 and 25-50% CO_2) [52]. Organic substances are degraded in four stages in the anaerobic digestion process. The first stage is hydrolysis, that is accepted as a speed-limiting stage due to the degradation of complex polymers to monomers. This stage is crucial for biogas production and enhancing yield. Because the more it gets monomers from polymers by hydrolysis,

the more it gets substrates to provide to microorganisms for next stages [53]. In addition, during the hydrolysis stage, it may appear some unwanted long-chain fatty acids and toxic by-products (complex heterocyclic components) which can interrupt the whole stages and stop producing biogas [54]. The second stage is named as acidogenesis that monomers are degraded to long-chain fatty acid, lactic acid, pyruvic acid, acetic acid and formic acid. The third stage is acetogenesis. In this stage, some organic acids such as lactic acid, pyruvic acid are degraded to H_2 and acetic acid [55]. The fourth stage is methanogenesis, where methane production takes place under strict anaerobic conditions [55]. All these 4 stages may be summarized in Figure.1 [56].

By anaerobic digestion, it can be eliminated organic wastes to prevent environmental pollution and converted to valuable products. These are i) wastewater and organic wastes are processed by anaerobic digestion to prevent environmental pollution and converted to valuable products such as biogas. ii) It may be prevented by greenhouse gas emission by effective waste management [57]. The anaerobic fermentation of organic wastes to produce biogas is an important application for the waste management strategy [58]. In the European Union (EU) the number of biogas plants has been increasing year by year. It has widely been used to eliminate some organic wastes such as manure, harvest wastes, industrial food wastes, and to produce biogas [59].

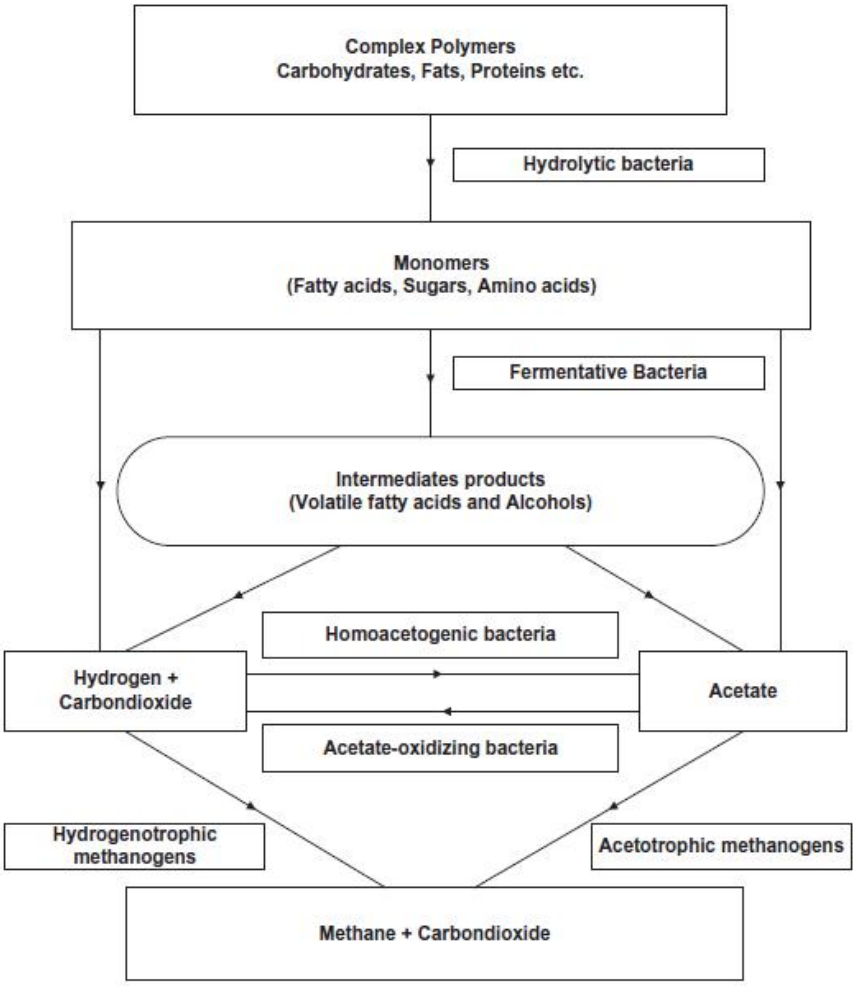

Figure 1: Biochemistry of the anaerobic digestion process (modified from Mkoma and Mabiki (2011)).

3. Factors affecting the anaerobic digestion process

There are some parameters which affect anaerobic digestion stability of the process. These parameters are temperature range, pH, hydraulic retention time (HRT), the configuration of digestion, mixing, long-chain fatty acid, presence of inhibitors, etc. [60].

Temperature; It significantly affects the microbial metabolic activity of communities, the solubility of various compounds and hydrolysis kinetics in the reactor. The microorganisms which take a mission in anaerobic digestion can stay alive in a wide range of temperature, but they are very sensitive to temperature fluctuation. Thermophilic methanogens and their some types require the optimum temperature to

overcome a higher organic loading rate. It was reported that the accumulation of biogas at the given temperatures: psychrophilic (at 0-20 ° C), mesophilic (at 25-40 ° C) and thermophilic (at 50-65 ° C) conditions [61].

pH; Many studies stated that pH is the most important parameter that affects anaerobic co-digestion [62], [63], [64]. Methanogens can stay alive at a wide range of pH, but at neutral pH (6.8-7.3) they show maximum activity. It is understood from studies that the performance of the reactor highly depends on the buffering capacity. In the same way, sewage slurry and food waste have rich content, some minerals that can buffer the system against the decreasing of pH [63], [64].

Organic Loading Rate (OLR); Reactor performance is reported to support biogas production efficiency during anaerobic co-digestion up to a certain OLR increase. OLR also affects key parameters such as total solids (TS), volatile solids (VS), pH, oxidation-reducing potential, conductivity, ammonium-N^+. While it can be processed effectively up to 2-3 kg VS / m^3 / day organic loading rate in mesophilic conditions; it can be processed in 4-5 kg VS / m^3 / day thermophilic conditions [65], [66], [67].

Hydraulic Retention Time (HRT); Hydraulic retention time affects the methane yield such as other parameters. HRT has a close relation to OLR; the higher HRT is, the higher OLR is [68], [69] and [70]. Therefore, HRT significantly affects digestion rate, microbial flux and C / N ratio [71], [72]. The optimized HRT supports better anaerobic digestion in the name of biogas yield. Many studies showed that the optimum methane yield (316 mL CH_4/g) is observed at 25 days HRT. At 12 days/month and 20 days/month, it was seen that the highest volatile fatty acid (VFA) accumulation [66], [71].

Volatile Fatty Acids (VFA); VFA are intermediate products which are produced at the hydrolysis stage of the anaerobic digestion. If the feedstock has a low buffering capacity, and the organic loading rate is high, the accumulation of volatile fatty acids can cause in a pH drop that would inhibit methane production [73]. It was reported that the AD process is generally vulnerable at 3500 mg / L UYA concentration and above [74], [75].

Long-Chain Fatty Acids (LCFA); LCFA are known to be inhibitors for methanogens and acidogenic groups at micro / macro concentrations [60]. Although the high organic loading rate of food waste leads to the accumulation of LCFA, which is an inhibitor for methanogens, there is no report on the inhibitory concentration of LCFAs for anaerobic co-digestion [76], [76]. Oleic acid can inhibit methane production at even 3

and 300 mg/L concentration [78], [79]. The inhibitor concentration for anaerobic co-digestion varies from 130 mg/L to 1000 mg/L).

Minerals; High concentration of dissolved salt (such as calcium, magnesium, potassium and sodium) in organic waste such as food waste and sewage sludge could inhibit microbial development, negatively affect anaerobic co-digestion or cause lower methane yield [80], [81], [82]. Recent studies have stated that concentrations of 2-15 g / L limit microbial metabolism; but it appears to improve the solubility of carbohydrates and proteins [31], [83]. Sodium concentrations in the range of 0.1-0.23 g / L are favorable for the development of acetoclastic methanogens and mesophilic anaerobes [31].

Nitrogen Based Compounds; The degradable of food wastes such as meat and dairy products release nitrogen ions to the media. It offers the basic food source and buffering capacity to the system for the development of microorganisms at a concentration of 500 mg / L. It has a moderate inhibitory effect on methane production at concentrations of ≥1500 mg / L. Ammonium ions pass through the cell wall and weaken the metabolic activity of methanogens, disrupting methane production; In addition, increasing the ammonium ion concentration allows specific types of methanogens to dominate within the microbial community in the reactor [84], [85].

Microbial Communities and Their Role; AD process requires different microbial communities and their full activity. In the first stage, the hydrolytic bacteria belonging to Bacteroidetes and Firmicutes are dominant. These species of bacteria are more durable against environmental conditions and have the ability to short AD process two times. At the second stage of AD process acidogenic bacteria belonging to *Bacteroidetes*, *Chloroflexi*, *Firmicutes*, ve *Proteobacteria* species degrade simple sugars to volatile fatty acids, CO_2 and H_2. Acidogenic bacteria include Bacteroidetes, Chloroflexi, Firmicutes, Proteobacteria. At the third stage, acetogenic bacteria include Pelotomaculum, Smithllela, Syntrophobacterhe, Syntrophus and Syntrophomonas that take the critic role in the AD process. Acetogens are responsible for the transformation of propionates, which can inhibit the metabolic activity and development of methanogens at low concentrations (200 ± 50 mg / L) [74]. At the final stage, the methanogenic arc (the group of microorganisms with different molecular structure) is responsible for the production of methane; it belongs to the groups of acetoclastic, hydrogenotrophic and methylotrophic bacteria [86].

4. Biogas

Biogas is said that “For millions of years in naturally formed marshes, microorganisms produce a mixture of gases containing methane, carbon

dioxide and trace amounts of hydrogen, nitrogen and hydrogen sulfide, using organic and inorganic substances for their metabolic activities in an oxygen-free or limited oxygen environment. This gas produced that is named as swamp gas, manure gas or biogas" [87]. As a simple definition biogas, in an oxygen-free environment, organic substances are degraded to a gas mixture that contains various gases (CH_4, CO_2, H_2S, etc.). Biogas is produced from various organic wastes, and that offers a renewable energy source. Among renewable energy sources, biogas (CH_4) offers an alternative to fossil fuels [88]. Typical biogas composes of 60-70% methane, 30-35% carbon dioxide, 1-2% hydrogen sulfide and 0,3-3% nitrogen [89], [90]. Biogas is produced from vegetable, animal, urban and industrial wastes which have high organic matter content. Agricultural wastes are an important resource among vegetable wastes; unused parts of grains such as stalks, straw, rice, corn stalks, oil plants (canola, rapeseed) and wastes of forest products. In addition, animal wastes include especially cattle, sheep and poultry waste, slaughterhouse wastes; sewage and food industry wastes among urban and industrial wastes are rich resources for biogas production [91].

4.1 Physical properties of biogas

Biogas produced by anaerobic digestion that composes of various gases such as (CH_4-%60), carbon dioxide (CO_2-%40) and a trace amount of hydrogen sulfide (H_2S), hydrogen (H_2), nitrogen (N_2), carbon monoxide (CO), oxygen (O_2), water vapor (H_2O), other gases and volatile organic compounds [92]. The density of biogas is 1.3 kg/m^3, and the ignition temperature is 650-750 ºC. If the volume of biogas is >%45, it will be flammable [93]. The calorie value of methane offers between 21-24 MJ / m^3 or about 6 kWh / m^3 of heat or 2 kW / m^3 of electrical energy. This supplied energy can be used many purposes such as heating, cooking, lighting or producing electric energy [94]. The energy content of 1.0 m^3 pure biogas is equal to 1.1 lt gasoline, 1.7 lt bioethanol or 0.97 m^3 natural gas [95]. The heating value (55.5 MJ / kg) of 1 kg of methane depends on the composition of the biogas and corresponds to 1.2 kg of diesel or 3.7 kg of tree wood [96].

4.2. Biogas production

Biogas is produced by anaerobic digestion from many organic wastes such as agricultural wastes, animal wastes and urban wastes. Anaerobic digestion is defined that organic substances are degraded to methane and carbon dioxide in an oxygen-free environment [97]. As it was mentioned before that biogas production is composed of four stages: hydrolysis, acidogenesis, acetogenesis and methanogenesis. In order to all these stages are processing well, two different wastes should be used together. This is anaerobic co-digestion that offers more biogas production and

yields. In anaerobic co-digestion, some factors that may be affecting anaerobic digestion process such as C/N ratio, pH, OLR (organic loading rate) could be kept under control when compared with single anaerobic digestion [98]. Nutrition balance (carbon, nitrogen, phosphorus and sulphur, etc.) is very important for microorganism to get activity. Optimum C/N ratio is between 15 and 45, and anaerobic co-digestion can ensure the suitable ratio against acidic or ammonium inhibition [95], [99]. Anaerobic co-digestion, the intended anaerobic digestion of a mixture of two or more substrates that improves nutrient balance (C / N ratio) and optimizes bacterial growth by providing a more balanced composition content and feedstock. As a result, a significant increase in biogas production and efficiency is achieved [95].

4.3 Pre-treatments applying to biomass in the production of biogas

Pre-treatment is a key factor leading microorganisms to substrates easily and improving the bioconversion of organic substances into methane effectively. In order to increase biogas production and yield, pre-treatment methods applying to biomass which are divided into 4 sections. It may be stated these pre-treatments methods as physical, chemical, biological, and combination of these methods. It was reported that physical/mechanic among these methods is effective to break biomass into small parts for the next sections [100], [101], [102]. Thermal and microwave pre-treatments are among the most common and most effective pre-treatment types, which are widely used in continuous reactor types. Pretreatment methods vary significantly depending on the type and nature of waste [103], [104], [105], [106]. Kneading, crushing and chopping, which are among the mechanical pre-treatment methods, increase the surface area of the biomass and provide the substrate release for the anaerobic digestive microbial flora [107]. Owing to the low cost of biologic pre-treatment and not using chemicals are positive sites of this method [108]. Mechanical pre-treatment methods such as kneading, crushing and chopping have high energy demand. In addition, it requires the use of chemicals that have harmful and corrosive effects on the environment. For these reasons, a composition of these pre-treatment methods should be used to process biomass effectively and productively [109], [110]. Even though the high temperatures (180 °C – 210 °C) are widely used as a pre-treatment, high temperature is not suitable for biogas production. Lower temperatures (< 120 °C) are suitable for biogas production, and they may be utilized as a thermal pre-treatment. In addition to this, thermal pre-treatment offers several potential advantages that can be provided, such as avoiding chemicals, low-pressure requirement and low energy input [111], [112]. Common pre-treatment types may be stated as thermal, microwave, ultrasonic, chemical and

biological pre-treatment. Which one is suitable that is depending on the properties of the substrate.

5. Conclusion

To produce biogas from organic wastes, some important factors such as C/N ratio, pH, OLR (organic loading rate) etc. are expected to be effective to biogas production process accordance with the current researches and knowledge. Also mixing speed, hydraulic retention time and temperature could be effective over biogas production and yield. Every single factor needs to be taken attention to optimizing the whole production process for next researches.

Pre-treatment is another important subject that we have to mention. There are some pre-treatment methods (such as microwave, thermal, alkaline, acidic, ultrasonic, and biological pre-treatment) being used in biogas production. However, in choosing which method is suitable, there are other matters such as energy-saving, labor, applicability, environmental-friendly and sustainability have been carrying significance.

As it is known that it obtains organic manure after anaerobic digestion process of organic wastes. It is needed to research more about fermentative manure for using it in agricultural application. As renewable energy sources usage of organic wastes is to provide sustainable economic energy, cheaper, and healthier agricultural production. It is also important to protect our planet against global warming and environmental pollution by eliminating organic wastes.

References

[1] Al Mamun M.R. and Torii S. 2015. Removal of H_2S and H_2O by chemical treatment to upgrade methane of biogas generated from anaerobic Co-digestion of organic biomass waste, IPASJ 3 (12) (December 2015).

[2] Tuccho G. T., Henri C. Moll, Anton J.M. 2016. School Uiterkamp, Sanderine Nonhebel, Problems with biogas implementation in developing countries from the perspective of labor requirements, Energies 9 (9) (2016) 750, http://dx.doi.org/10.3390/en9090750.

[3] Our Common Future, Chapter 7: Energy: Choices for Environment and Development, UN Documents, Gathering a Body of Global Agreements.

[4] Tasnim F., Iqbal A.S., and Chowdhury A.R. 2017. Department of Chemical Engineering and Polymer Science, Shahjalal University of Science and Technology, Sylhet, 3114, Bangladesh. Renewable Energy 109 (2017) 434-439.

[5] Çevre Kanunu, RG. 11.08.1983 tarih ve 18132 Sayı.

[6] Read, A. D. (1999). A Weekly Doorstep Recycling Collection, I had no Idea We Could Overcoming the Local Barriers to Participation. Resources, Conservation and Recycling, 26, 217-249.

[7] Öztürk, İ. (2010). Katı Atık Yönetim ve AB Uygulamaları. İSTAÇ A.Ş. Teknik Kitaplar Serisi 2, İstanbul.

[8] Hagos, K., Zong, J., Li, D., Liu, C., Lu, X., 2017. Anaerobic co-digestion process for biogas production: Progress, challenges and perspectives. Renew. Sustain. Energy Rev. 76, 1485–1496.

[9] Karthikeyan, O.P., Mehariya, S., Wong, J.W.C., 2017a. Bio-refining of food waste for fuel and value products.Energy Procedia 136,14–21.

[10] Angelidaki, I., Karakashev D., Batstone D.J., Plugge C.M., Stams, A. J. M. Biomethanation and Its Potential. Methods in Enzymology, Volume 494. ISSN 0076-6879, DOI: 10.1016/B978-0-12-385112-3.00016-0. 2011.

[11] EPA, 2008. Anaerobic Digestion of Food Waste, Funding Opportunity No. EPA-R9-WST-06-004, U.S. Environmental Protection Agency Region 9, 2008, Prepared by: East Bay Municipal Utility District.

[12] Wim Rulkens*, Sewage sludge as a biomass resource for the production of energy: overview and assessment of the various optionsy, Energy & Fuels 22 (2008) 9-15.

[13] Capson-Tojo, G., Trably, E., Rouez, M., Crest, M., Steyer, J., Delgenès, J., Escudié, R., 2017. Dry anaerobic digestion of food waste and cardboard at different substrate loads, solid contents and co-digestion proportions. Bioresour. Technol. 233, 166–175.

[14] Melikoglu, M., Lin, C., Webb, C., 2013. Analyzing global food waste problem: pinpointing the facts and estimating the energy content. Open Eng. 3.

[15] Zhang, J., Lv, C., Tong, J., Liu, J., Liu, J., Yu, D., Wang, Y., Chen, M., Wei, Y., 2016. Optimization and microbial community analysis of anaerobic co-digestion of food waste and sewage sludge based on microwave pre-treatment. Bioresour. Technol. 200, 253–261.

[16] Gudo, A.J., 2014. Global biomethanation potential from food waste – a review. Agric.Eng. Int. CIGR J. 16, 178–193.

[17] Lin, C.S.K., Pfaltzgraff, L.A., Herrero-Davila, L., Mubofu, E.B., Abderrahim, S., Clark, J.H., Koutinas, A.A., Kopsahelis, N., Stamatelatou, K., Dickson, F., 2013. Food waste as a valuable

resource for the production of chemicals, materials and fuels.Current situation and global perspective. Energy Environ. Sci. 6, 426–464.

[18] Ma, Y., Yin, Y., Liu, Y., 2016. A holistic approach for food waste management towards zero-solid disposal and energy/resource recovery. Bioresour. Technol.

[19] Chen, E., Gu, X.Y., 2012. Advance in disposal and resource technology of food waste. Environ. Stud. Monit. 3, 57–61.

[20] Zhang, C., Su, H., Baeyens, J., Tan, T., 2014. Reviewing the anaerobic digestion of food waste for biogas production. Renew. Sustain. Energy Rev. 38, 383–392.

[21] Girotto, F., Alibardi, L., Cossu, R., 2015. Food waste generation and industrial uses: a review. Waste Manage. 45, 32–41.

[22] Kiran, E.U., Trzcinski, A.P., Ng, W.J., Liu, Y., 2014. Bioconversion of food waste to energy: a review. Fuel 134, 389–399.

[23] Koch, K., Plabst, M., Schmidt, A., Helmreich, B., Drewes, J.E., 2016. Co-digestion of food waste in a municipal wastewater treatment plant: comparison of batch tests and full-scale experiences. Waste Manage. 47, 28–33.

[24] Ratanatamskul, C., Wattanayommanaporn, O., Yamamoto, K., 2015. An on-site prototype two-stage anaerobic digester for co-digestion of food waste and sewage sludge for biogas production from high-rise building. Int. Biodeterior. Biodegradation 102, 143–148.

[25] Tuyet, N.T., Dan, N.P., Vu, N.C., Trung, N.L.H., Thanh, B.X., De Wever, H., Goemans, M., Diels, L., 2016. Laboratory-scale membrane up-concentration and co-anaerobic digestion for energy recovery from sewage and kitchen waste. Water Sci. Technol. 73, 597–606.

[26] Yin, Y., Liu, Y., Meng, S., Kiran, E.U., Liu, Y., 2016. Enzymatic pre-treatment of activated sludge, food waste and their mixture for enhanced bioenergy recovery and waste volume reduction via anaerobic digestion. Appl. Energy 179, 1131–1137.

[27] Fisgativa, H., Tremier, A., Dabert, P., 2016. Characterizing the variability of food waste quality: a need for efficient valorization through anaerobic digestion. Waste Manage. 50, 264–274.

[28] Zhang, R., El-Mashad, H.M., Hartman, K., Wang, F., Liu, G., Choate, C., Gamble, P., 2007. Characterization of food waste as feedstock for anaerobic digestion. Bioresour. Technol. 98, 929–935.

[29] Fisgativa, H., Tremier, A., Dabert, P., 2016. Characterizing the variability of food waste quality: a need for efficient valorization through anaerobic digestion. Waste Manage. 50, 264–274.

[30] Capson-Tojo, G., Rouez, M., Crest, M., Steyer, J.-P., Delgenès, J.-P., Escudié, R., 2016. Food waste valorization via anaerobic processes: a review. Rev. Environ. Sci. Bio/Technol. 15 (3), 499–547.

[31] Chen, Y., Cheng, J.J., Creamer, K.S., 2008. Inhibition of anaerobic digestion process: a review. Bioresour. Technol. 99, 4044–4064.

[32] Zhang, C., Su, H., Tan, T., 2013a. Batch and semi-continuous anaerobic digestion of food waste in a dual solid–liquid system. Bioresour. Technol. 145, 10-16.

[33] Zhang, Y.H.P., 2008. Reviving the carbohydrate economy via multi-product lignocellulose biorefineries. J. Ind. Microbiol. Biotech. 35 (5), 367–375.

[34] Holtzapple,M.T.,Lundeen,J.E.,Sturgis,R.,Lewis,J.E.,Dale,B.E.,1992. Pre-treatment of lignocellulosic municipal solid waste by ammonia fiber explosion (AFEX).Appl.Biochem.Biotechnol.34(1), 5–21.

[35] Barbosa-Cánovas, G.V., Fernández-Molina, J.J., Alzamora, S.M., Tapia, M.S., López-Malo, A., Chanes, J.W., 2003. Handling and Preservation of Fruit and Vegetables by Combined Methods for Rural Areas. Technical Manual FAO Agricultural Services Bulletin 149. Food and Agriculture Organization of the United Nations, Rome ftp:// ftp.fao.org/docrep/fao/005/y4358E/y4358E00.pdf.

[36] Food and Drug Administration, 2013. FAO Statistical Yearbook 2013,World Food and Agriculture http:// www.fao.org/docrep/018/i3107e/i3107e.PDF Accessed 2016/09/15.

[37] FAO-Food and Drug Administration, 2011. Global food losses and food waste – Extent, causes and prevention http://www.fao.org/docrep/014/mb060e/mb060e.pdf Accessed 2016/09/20.

[38] Gustavsson, J., Cederberg, C., Sonesson, U., Van Otterdijk, R., Meybeck, A., 2011. Global Food Losses and Food Waste. Food and Agriculture Organization of the United Nations, Rom.

[39] Schnürer, A., Jarvis, A. 2010. Microbiological Handbook for Biogas Plants. Swedish Waste Management U2009:03.

[40] Wikandari, R., Gudipudi, S., Pandiyan, I., Millati, R., Taherzadeh, M.J., 2013. Inhibitory effects of fruit flavors on methane production during anaerobic digestion. Bioresour. Technol. 145, 188–192.

[41] Rosato, A., Vitali, C., De Laurentis, N., Armenise, D., Milillo, M.A., 2007. Antibacterial effect of some essential oils administered alone or in combination with Norfloxacin. Phytomedicine 14 (11), 727–732.

[42] Mizuki, E., Akao, T., Saruwatari, T., 1990. Inhibitory effect of Citrus unshu peel on anaerobic digestion. Biol. Wastes 33 (3), 161–168.

[43] Forgács, G., 2012. Biogas production from citrus wastes and chicken feather: pre-treatment and co-digestion. Chalmers University of Technology.

[44] United States Department of Agriculture Natural Resources Conservation Service (USDANRCS), 1995. Animal Manure Management, RCA Issue Briefs No.Available from:https://www.nrcs.usda.gov/wps/portal/nrcs/detail/null/?cid=nrcs143_014211.

[45] Holm-Nielsen, J.B., Al Seadi, T., Oleskowicz-Popiel, P., 2009. The future of anaerobic digestion and biogas utilization. Bioresour. Technol. 100, 5478–5484.

[46] Union of Concerned Scientists (UCS), 2012. The Promise of Biomass: Clean Power and Fuel–If Handled Right. Cambridge, MA. Availablefrom:http://www.ucsusa.org/assets/documents/clean_vehicles/Biomass-Resource-Assessment.pdf.

[47] Holm-Nielsen, J.B., Al Seadi, T., Oleskowicz-Popiel, P., 2009. The future of anaerobic digestion and biogas utilization. Bioresour. Technol. 100, 5478–5484.

[48] Chen, S., Wei, L., Liu, C., Wen, Z., Kincaid, R.L., Harrison, J.H., Elliott, D.C., Brown, M.D., 2003. Fig. 1. Role of pre-treatment in multi-fuel biorefinery using agricultural biomass as feedstock. S. R. Paudel et al. Bioresource Technology 245 (2017) 1194–12051203.

[49] National Research Council, Ad Hoc Committee on Air Emissions from Animal Feeding, O Air Emissions from Animal Feeding Operations: Current Knowledge, Future Needs Vol Xxi, National Academies Press, Washington, DC, 2003, p. 263.

[50] Doorn, M.R.J., D.F. Natschke, P.C. Meeuwissen, Review of Emission Factors and Methodologies to Estimate Ammonia Emissions from Animal Waste Handling US Environmental Protection Agency, 2002.

[51] National Research Council, Ad Hoc Committee on Air Emissions from Animal Feeding, O Air Emissions from Animal Feeding Operations: Current Knowledge, Future Needs Vol Xxi, National Academies Press, Washington, DC, 2003, p. 263.

[52] Frigon, J.C., Guiot S.R. Biomethane production from starch and lignocellulosic crops: a comparative review. Biofuel Bioprod Bior 2010;4:447-58.

[53] Fernandes, T.V., Klaasse Bos, G.J., Zeeman, G., Sanders, J.P.M., van Lier, J.B., 2009. Effects of thermo-chemical pre-treatment on anaerobic biodegradability and hydrolysis of lignocellulosic biomass. Bioresour. Technol. 100 (9), 2575–2579.

[54] Yuan, H., Zhu, N.,2016. Progress in inhibition mechanisms and process control of intermediates and by-products in sewage sludge anaerobic digestion. Renewable Sustainable Energy Rev.58, 429–438.

[55] Deublein, D., Steinhauser, A., 2011. Biogas from Waste and Renewable Resources. Wiley-VCH.

[56] Mkoma, S.L., Mabiki, F.P., 2011. Theoretical and practical evaluation of jatropha as energy source biofuel in Tanzania. In: Bernardes, M.A.D.S. (Ed.), Economic Effect of Biofuel Production. InTech, pp. 181–200.

[57] Garfí, M. Martí-Herrero, J. Garwood A., Ferrer I. Household anaerobic digesters for biogas production in Latin America: A review. Renewable and Sustainable Energy Reviews 60 (2016) 599–614.

[58] Brandli, R.C., Bucheli, T.D., 2007. Organic pollutants in compost and digestate. Part 1. Polychlorinated biphenyls, polycyclic aromatic hydrocarbons and molecular markers. J. Environ. Monit. JEM 9, 456-464. http://dx.doi.org/10.1039/b617101j.

[59] Möller, K., Müller, T., 2012. Effects of anaerobic digestion on digestate nutrient availability and crop growth: a review. Eng. Life Sci. 12, 242-257. http://dx.doi.org/10.1002/elsc.201100085.

[60] Angelidaki, I. Ahring, BK. Effects of free long-chain fatty acids on thermophilic anaerobic digestion. Appl Microbiol Biotechnol 1992;37:808–12.

[61] Li, Q., Li, H., Wang, G., Wang, X., 2017a. Effects of loading rate and temperature on anaerobic co-digestion of food waste and waste activated sludge in a high frequency feeding system, looking in particular at stability and efficiency. Bioresour.Technol.237, 231–239.

[62] Lindner, J., Zielonka, S., Oechsner, H., Lemmer, A., 2015. Effect of different pH-values on process parameters in two-phase anaerobic digestion of high-solid substrates. Environ. Technol. 36, 198–207.

[63] Obulisamy, P.K., Chakraborty, D., Selvam, A., Wong, J.W.C., 2016. Anaerobic co-digestion of food waste and chemically enhanced primary-treated sludge under mesophilic and thermophilic conditions. Environ. Technol. 37, 3200–3207.

[64] Chakraborty, D., Karthikeyan, O.P., Selvam, A., Wong, J.W.C., 2017. Co-digestion of food waste and chemically enhanced primary

treated sludge in a continuous stirred tank reactor. Biomass Bioenergy. http://dx.doi.org/10.1016/j.biombioe.2017.06.002.

[65] Agyeman, F.O., Tao, W., 2014. Anaerobic co-digestion of food waste and dairy manure: effects of food waste particle size and organic loading rate. J. Environ. Manage. 133,268–274.

[66] Dhar, H., Kumar, P., Kumar, S., Mukherjee, S., Vaidya, A.N., 2016. Effect of organic loading rate during anaerobic digestion of municipal solid waste. Bioresour. Technol. 217, 56–61.

[67] Hagos, K., Zong, J., Li, D., Liu, C., Lu, X., 2017. Anaerobic co-digestion process for biogas production: Progress, challenges and perspectives. Renew. Sustain. Energy Rev. 76, 1485–1496.

[68] Rao, M.S., Singh, S.P., 2004. Bioenergy conversion studies of organic fraction of MSW:kinetic studies and gas yield-organic loading relationships for process optimization. Bioresour.Technol.95,173–185.

[69] Dareioti, M.A., Kornaros, M., 2014. Effect of hydraulic retention time (HRT) on the anaerobic co-digestion of agro-industrial wastes in a two-stage CSTR system. Bioresour. Technol. 167, 407–415.

[70] Liu, C., Wang, W., Anwar, N., Ma, Z., Liu, G., Zhang, R., 2017. Effect of organic loading rate on anaerobic digestion of food waste under mesophilic and thermophilic conditions. Energy Fuels 31, 2976–2984.

[71] Dareioti, M.A., Kornaros, M., 2014. Effect of hydraulic retention time (HRT) on the anaerobic co-digestion of agro-industrial wastes in a two-stage CSTR system. Bioresour. Technol. 167, 407–415.

[72] Chan, P.C., de Toledo, R.A., Shim, H., 2017. Anaerobic co-digestion of food waste and domestic wastewater-Effect of intermittent feeding on short and long chain fatty acids accumulation. Energy Renew 10.1016/j.renene.2017.07.029.

[73] Deublein, D., Steinhauser, A. Biogas from Waste and Renewable Resources. An Introduction. Wiley-VCH Verlag GmbH & Co. KGaA, 2008, ISBN: 9783527621705, DOI: 10.1002/9783527621705.

[74] Wang, Y., Zhang, Y., Wang, J., Meng, L., 2009. Effects of volatile fatty acid concentrations on methane yield and methanogenic bacteria. Biomass Bioenergy 33, 848–853.

[75] Schievano, A., D'Imporzano, G., Malagutti, L., Fragali, E., Ruboni, G., Adani, F., 2010. Evaluating inhibition conditions in high-solids anaerobic digestion of organic fraction of municipal solid waste. Bioresour. Technol. 101, 5728–5732.

[76] Salvador, A.F., Cavaleiro, A.J., Sousa, D.Z., Alves, M.M., Pereira, M.A., 2013. Endurance of methanogenic archaea in anaerobic bioreactors treating oleate-based wastewater. Appl. Microbiol. Biotechnol. 97, 2211–2218.

[77] Sousa, D.Z., Salvador, A.F., Ramos, J., Guedes, A.P., Barbosa, S., Stams, A.J., Alves, M.M., Pereira, M.A., 2013. Activity and viability of methanogens in anaerobic digestion of unsaturated and saturated long-chain fatty acids. Appl. Environ. Microbiol. 79,4239–4245.

[78] Appels, L., Lauwers, J., Degrève, J., Helsen, L., Lievens, B., Willems, K., Van Impe, J., Dewil, R., 2011. Anaerobic digestion in global bio-energy production: potential and research challenges. Renew. Sustain. Energy Rev. 15, 4295–4301.

[79] Dasa, K.T., Westman, S.Y., Millati, R., Cahyanto, M.N., Taherzadeh, M.J., Niklasson, C., 2016. Inhibitory effect of long-chain fatty acids on biogas production and the protective effect of membrane bioreactor. Biomed Res. Int. 1–9.

[80] Vallero, M.V.G., Hulshoff Pol, L.W., Lettinga, G., Lens, P.N.L., 2003. Effect of NaCl on thermophilic (55 °C) methanol degradation in sulfate reducing granular sludge reactors. Water Res. 37, 2269–2280.

[81] Wen-Hsing, C., Sun-Kee, H., Shihwu, S., 2013. Sodium inhibition of thermophilic methanogens. J. Environ. Eng. 129, 506–512.

[82] Fang, C., Boe, K., Angelidaki, I., 2011. Anaerobic co-digestion of desugared molasses with cow manure; focusing on sodium and potassium inhibition. Bioresour. Technol. 102, 1005–1011.

[83] Zhao, J., Liu, Y., Wang, D., Chen, F., Li, X., Zeng, G., Yang, Q., 2017a. Potential impact of salinity on methane production from food waste anaerobic digestion. Waste Manage. 67, 308–314.

[84] Fotidis, I.A., Wang, H., Fiedel, N.R., Luo, G., Karakashev, D.B., Angelidaki, I., 2014.Bioaugmentation as a solution to increase methane production from an ammonia-rich substrate. Environ. Sci. Technol. 48, 7669–7676.

[85] Wang, H., Fotidis, I.A., Angelidaki, I., 2015. Ammonia effect on hydrogenotrophic methanogens and syntrophic acetate-oxidizing bacteria. FEMS Microbiol. Ecol. 91, 11.

[86] Venkiteshwaran, K., Bocher, B., Maki, J., Zitomer, D., 2016. Relating anaerobic Digestion microbial community and process function. Microbiol. Insights 8, 37–43.

[87] Üçgül İbrahim, Gökçen Akgül. “Biyokütle Teknolojisi”, YEKARUM Dergi 1(1), 2010, 3-11.

[88] Subhaschandra Singha, T., Nath Verma, T., Nashinec P., Analysis of an Anaerobic Digester using Numerical and Experimental Method for Biogas Production. ICMPC 2017.Available online at www.sciencedirect.com. Science Direct Proceedings 5(2018)5202-5207.

[89] Anonymous, 2016. http://www.werf.org/.

[90] Rulkens, W. Sewage Sludge as a biomass resource for the Production of energy: overview and assessment of the various options. Energy & Fuels 2008;22:9-15.

[91] Koca, Ahmet. "Yenilenebilir bir Enerji Kaynağı: Biyogaz", Doğu Anadolu Böl. Arş. Dergisi, 5(3), 2007, 32-35.

[92] Surroop, D., Mohee, R. Comparative assessment of anaerobic digestion of municipal solid waste at mesophilic and thermophilic temperatures. Int J Environ Technol Manag. 14 (1/2/3/4), 238, 2011.

[93] Deublein, D., Steinhauser, A. Biogas from Waste and Renewable Resources. An Introduction. Wiley-VCH Verlag GmbH & Co. KGaA, 2008, ISBN: 9783527621705, DOI: 10.1002/9783527621705.

[94] He, P.J. Anaerobic digestion: an intriguing long history in China. Waste Management. 30 (4), 549, 2010.

[95] Rajendran, K., Aslanzadeh, S., Taherzadeh, M.J. Household Biogas Digesters. Energies. 5 (8), 2911, 2012.

[96] Fountoulakis, MS., Petousi, I., Manios, T. Co-digestion of sewage sludge with glycerol to boost biogas production. Waste Manage 2010;30:1849-53.

[97] Klass, D.L., 2004. Biomass for Renewable Energy and Fuels. Encyclopedia of Energy. Elsevier Inc., pp. 193–211.

[98] Noori, M., Saady, C., Massé, D.I. Impact of Organic Loading Rate on Psychrophilic Anaerobic Digestion of Solid Dairy Manure. Energies. 8, 1990, 2015.

[99] Gunnerson, C.G, Stuckey, DC. Integrated resource recovery: anaerobic digestion principles and practices for biogas systems World Bank Tech.Paper no.49;UNDP Project Management Report no.5; 1986.

[100] Passos, F., Hernandez-Marine, M., Garcia, J., Ferrer, I., 2014a. Long-term anaerobic digestion of microalgae grown in HRAP for wastewater treatment. Effect of microwave pre-treatment. Water Res. 49, 351–359.

[101] Passos, F., Uggetti, E., Carrere, H., Ferrer, I., 2014b. Pre-treatment of microalgae to improve biogas production: a review. Bioresour. Technol. 172, 403–412.

[102] Yukesh, Kannah R., Kavitha, S., Rajesh, Banu J., Yeom, I.T., 2017. Synergetic effect of combined pre-treatment for energy efficient biogas. Bioresour. Technol. 232,235–246.

[103] Schwede, S., Rehman, Z.-U., Gerber, M., Theiss, C., Span, R., 2013. Effects of thermal pre-treatment on anaerobic digestion of Nannocloropsis salina biomass. Bioresour. Technol. 143, 505–511.

[104] Uma, R., Adish, K.S., Kaliappan, S., Yeom, I.T., Rajesh, B.J., 2012. Low temperature thermo-chemical disintegration of dairy waste activated sludge for anaerobic digestion process. Bioresour. Technol. 103, 415–424.

[105] Eswari, P., A., Kavitha, S., Parthiba Karthikeyan, O., Yeom, I.T., 2017. H_2O_2 induced cost effective microwave disintegration of dairy waste activated sludge in acidic environment for efficient biomethane generation. Bioresour. Technol. 244,688–697.

[106] Kavitha, S., Rajesh Banu, J., Kumar, G., Kaliappan, S., Yeom, I.T., 2018. Profitable ultrasonic-assisted microwave disintegration of sludge biomass: modelling of biomethanation and energy parameter analysis. Bioresour. Technol. 254, 203–213.

[107] Tamilarasan, K., Kavitha, S., Banu, J.R., Arulazhagan, P., Yeom, I.T., 2017. Energy-efficient methane production from macroalgal biomass through chemo disperser liquefaction. Bioresour. Technol. 228, 156–163.

[108] Kavitha, S., Subbulakshmi, P., Rajesh Banu, J., Gobi, Muthukaruppan, Yeom, I.T., 2017. Enhancement of biogas production from microalgal biomass through cellulolytic bacterial pre-treatment. Bioresour. Technol. 233, 34–43.

[109] He, L., Huang, H., Lei, Z., Liu, C., Zhang, Z. Bioresour. Technol. 171 (2014) 145–151.

[110] López González, L.M. Pereda, R.I. Dewulf, J. et al., Bioresour. Technol.169 (2014) 284–290.

[111] Hu, F., and Ragauskas, A. Bioenerg. Res. 5 (2012) 1043–1066.

[112] Merali, Z. Collins, S.R.A., Elliston, A. et al., Biotechnol. Biofuels 131 (2015) 226– 234.

CHAPTER VIII

PRODUCTION OF LIGHTWEIGHT COMPOSITE BASED ON GYPSUM-PLASTER WITH BASALT FIBER

Kadir GÜÇLÜER* & Osman GÜNAYDIN**

*Adıyaman University, Adıyaman, Turkey
e-mail: kgucluer@adiyaman.edu.tr , Orcid ID: 0000-0001-7617-198X

**Adıyaman University, Adıyaman, Turkey
e-mail: gunaydin@adiyaman.edu.tr, Orcid ID: 0000-0001-7559-5684

1. Introduction

Composite materials are created by combining two or more different materials. In this case, it maintains its chemical and mechanical properties in the materials that come together. The most important advantages that distinguish composite materials from other materials are their lightness and strength values [1].

Gypsum is one of the building materials that have reached today from ancient times. Archaeological findings indicate that the gypsum applications date back to 7000 BC. Modern construction technology can use the gypsum products that appear in waste form as well as gypsum as raw materials [2].

Gypsum-based materials, which can be used in the form of wall panels and boards in residential or commercial buildings, are among the sustainable building materials due to their lightness, economicity and ease of application. When supported with appropriate additives, disadvantageous situations can be developed [3].

Considering today's structures and construction techniques, it has become necessary to develop and support gypsum-based binders, materials or products economically and technically. In addition to the fact that the gypsum material has a very good temperature behavior, has an insulating property, it has disadvantages such as being brittle, low resistance to water and high creep in wet condition [4].

Basalt is a natural raw material consisting of frozen lava with a melting temperature of 1300-1500 ^{0}C [5]. Due to the geological feature of the Anatolian geography, basalts, which have been used in many regions and used throughout history, continue to be used today [6].

Basalt fiber is the inorganic fiber obtained by melting the basalt. It is completely environmentally and friendly inorganic; has no harmful effects on humanity and ecology [7]. Other advantages include high heat resistance, high resistance to chemical attacks, high shear strength and easy commercial availability [8].

There are different studies in the literature in this direction. Pardo et al. [9] have determined that the rice husk has a positive effect on the mechanical properties of composite materials produced by combining rice husk and polystyrene materials with gypsum-plaster. Vasconceleos et al. [10] in their experimental study on gypsum-based composite material produced using textile fiber, they determined that the fiber additive had an effect on the fracture energy results. Carvalho et al. [11] stated that the natural fiber additive affects the water/gypsum ratio but has a positive effect on impact resistance as a result of the experimental study in which they examined the microstructures of natural fiber added gypsum-based composites. Abad-Farfan et al. [12] carried out experimental studies on the temperature behavior of gypsum-based composites produced using different filling materials. Amara et al. [13] found that palm tree fiber reduced thermal conductivity as a result of their experimental studies on gypsum-based composite material produced using palm tree fiber. For this purpose, in this study, different basalt fiber and gypsum/water ratio composites were produced and their physical and mechanical properties were investigated.

2. Materials and methods

2.1. Materials

Gypsum according to the TS EN 13279-1[14] was used in the experimental investigation. The properties of the gypsum were presented in Table 1. Particle size distribution analysis of gypsum is given in Fig. 1. All of the gypsum grains are under 1000μm.

Table 1 Properties of gypsum

Properties	Value
Compressive Strength (MPa)	2.5
Flexural Strength (MPa)	1.0
Dry density (kg/m^3)	600-1000
First setting (min)	>50
Final setting (min)	180

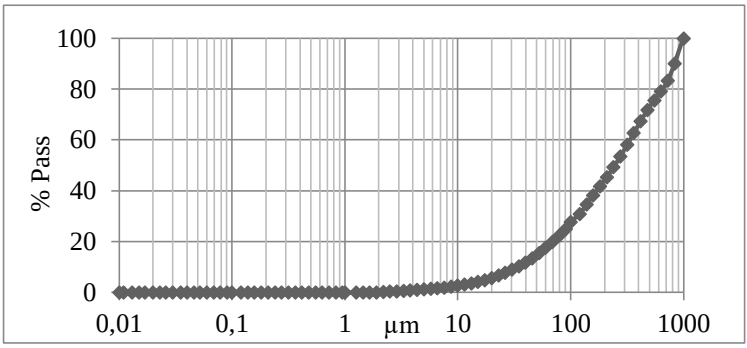

Fig. 1. Particle size distribution of gypsum

Basalt fiber (BF) with a length of 24 mm was used in the study and its technical properties are given in Table 2 (Fig.2).

Table 2 Properties of basalt fiber

Properties	**Tensile Strength (MPa)**	**Modul of Elasticity (GPa)**	**Fiber Diameter (µm)**	**Fiber Length (mm)**	**Specific Gravity (g/cm^3)**
Basalt Fiber	4850	86	10-22	24	2.64

Fig. 2. Basalt fiber

Three different water/gypsum ratios (0.60-0.65-0.70) were used in the preparation of the mixtures. In addition, 0.5% - 1% - 1.5% - 2% of the amount of gypsum-plaster in the mixture was added to basalt fiber. In order to increase the consistency of the mixture, a naphthalene sulfonate-based superplasticizer (SP) additive was used at the rate of 1% of the gypsum-plaster. Prismatic test molds with dimensions of 4x4x16 cm were used to shape the test samples. Mixing ratios for the production of test samples are given in the Table 3.

Table 3 Mixing ratios

W/G	0.60				0.65				0.70			
Series	Gypsum (g)	Water (g)	SP (%)	BF (%)	Gypsum (g)	Water (g)	SP (%)	BF (%)	Gypsum (g)	Water (g)	SP (%)	BF (%)
WT	1333.3	800	1	0	1230.8	800	1	0	1142.8	800	1	0
BF0.5	1333.3	800	1	0.5	1230.8	800	1	0.5	1142.8	800	1	0.5
BF1	1333.3	800	1	1	1230.8	800	1	1	1142.8	800	1	1
BF1.5	1333.3	800	1	1.5	1230.8	800	1	1.5	1142.8	800	1	1.5
BF2	1333.3	800	1	2	1230.8	800	1	2	1142.8	800	1	2

2.2. Methods

For the production of experiment samples, forced action mixer was used. Gypsum plaster and basalt fiber mixture was added to the water and mixed without agglomeration. The mortars that have a suitable consistency in the mixer are taken into prismatic molds of 4x4x16 cm and left to dry in natural weather conditions (Fig.3). The bulk density of the samples were made according to the constant weight method, in accordance with the TS EN 13279-2 [15] standard. Ultrasonic pulse velocity (UPV) measurements were carried out in accordance with ASTM C 597 [16]. Compressive and flexural strength tests were carried out in accordance with the TS EN13279-2 [15] standard.

Fig. 3. Produce of experimental samples

3. Results and discussion

3.1. Bulk density results

Bulk density results of the test samples are given in Fig. 4(a-c). Due to the increase in the W/G ratio in the mixing ratios, a decrease in bulk density values was detected.

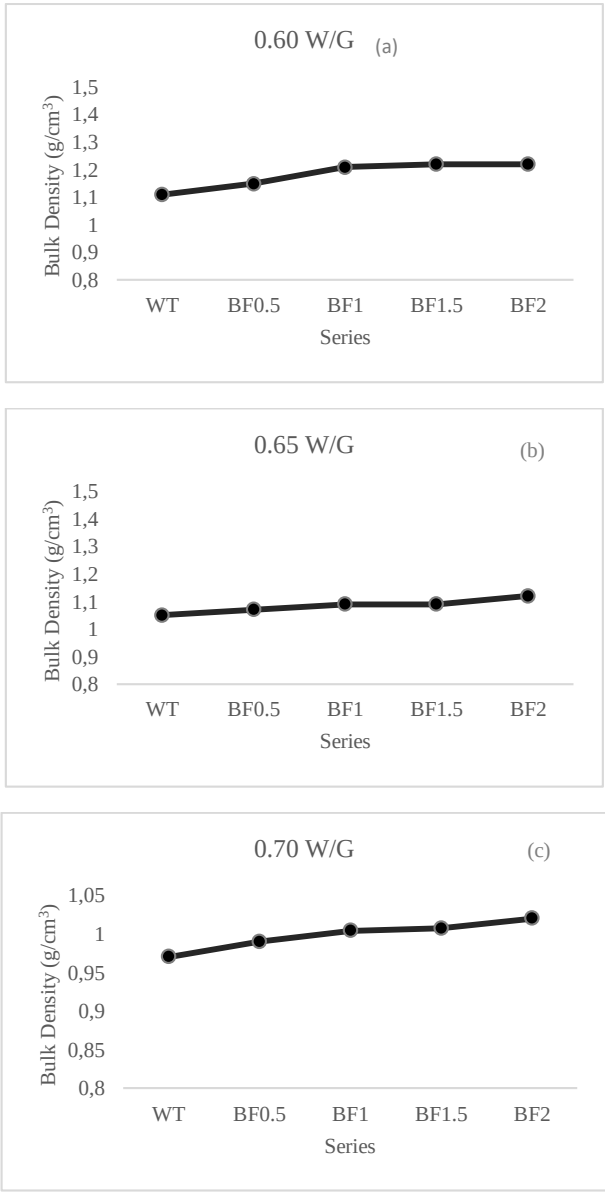

Fig. 4. Bulk density results; (a) 0.60 W/G, (b) 0.65 W/G, (c) 0.70 W/G

The highest bulk density values in all W/G ratios were determined in BF2 series. Bulk density values increased due to the increase in the amount of basalt fiber in the mixture. In mixtures with 0.60 W/G ratio, an increase of %9.90 in BF2 series bulk density was detected compared to the witness (WT) sample. This value was determined as %6.66 in mixtures with 0.65 W/G ratio and %5.15 in mixtures with 0.70 W/G ratio. With the increase of water in the mixture, an increase in void volume may occur and a

decrease in density values may be observed [17]. This information supports decreasing density values due to the increase in the amount of water in the mixture. In addition, the density of the Basalt fiber was higher than the gypsum-plaster, causing an increase in bulk density values in all series due to the increase of the amount of basalt fiber in the mixture.

3.2. Ultrasonic pulse velocity results

The ultrasonic pulse velocity is included in the non-destructive test methods. The use of non-destructive testing methods in building construction provides many advantages. These; economy, time saving and security. These tests can give information about the strength of the building materials, the gap structure, the cracks and deformation that exist in its structure [18]. Ultrasonic pulse velocity results of the experiment samples are given in Fig. 5(a-c).

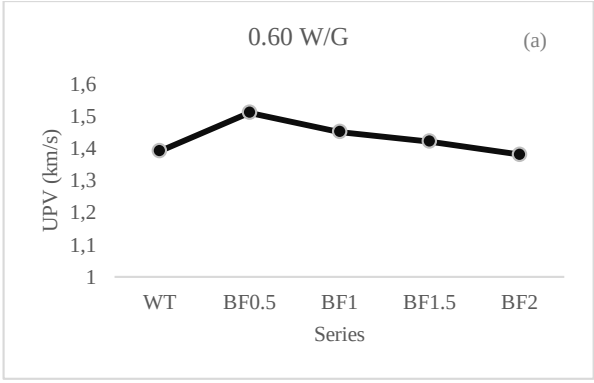

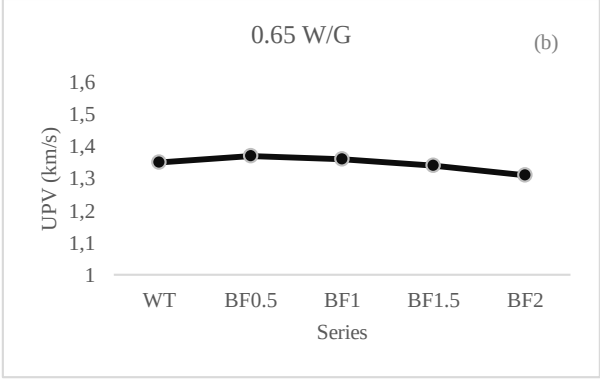

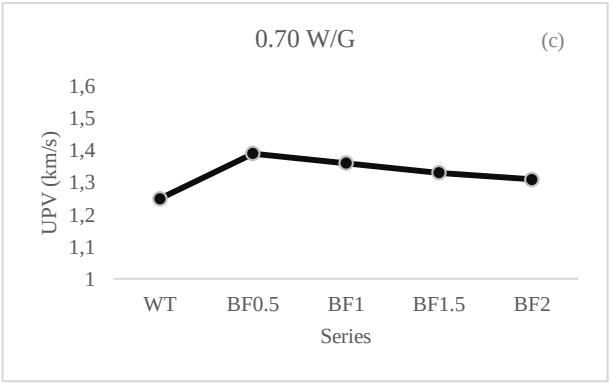

Fig. 5. UPV results; (a) 0.60 W/G, (b) 0.65 W/G, (c) 0.70 W/G

The highest UPV values were determined in the series of 0.60 W/G ratio. The lowest UPV values were observed in series with 0.70 W/G ratio. In all series, an increase in the ultrasonic pulse velocity values was determined depending on the increase in the amount of basalt fiber in the mixture. UPV values may vary depending on the density and void volume of the material [19]. Depending on the decrease in bulk density and the increase in void volume, sound waves will leave the material later and this will cause the UPV values to decrease [20]. Ultrasonic pulse velocity values, which decrease due to the increase in the amount of water in the mixing ratios, support this information. A decrease in ultrasonic pulse velocity values was observed in all series due to increase in the amount of basalt fiber. The homogeneity of the mixture can change with the addition of fibers [21]. The change in the consistency of the mixtures with the addition of basalt fiber may have affected homogeneity. It is thought that this situation may cause the decrease in UPV values due to the increase of basalt fiber ratio.

3.3. Compressive strength results

Compressive strength results of basalt fiber additive series with three different W/G ratios are given in the Fig. 6. As a result of the increase in the amount of water in the mixture; there was a decrease in compressive strength values of all series. The compressive strength is affected by the void volume in the material, and the compressive strength of the materials with high solid volume may be higher than the materials with high void volume [22]. In bulk density findings, a decrease was observed in the values due to the increase in the amount of water in the mixture ratio. Accordingly, the findings of compressive strength and bulk density findings support each other.

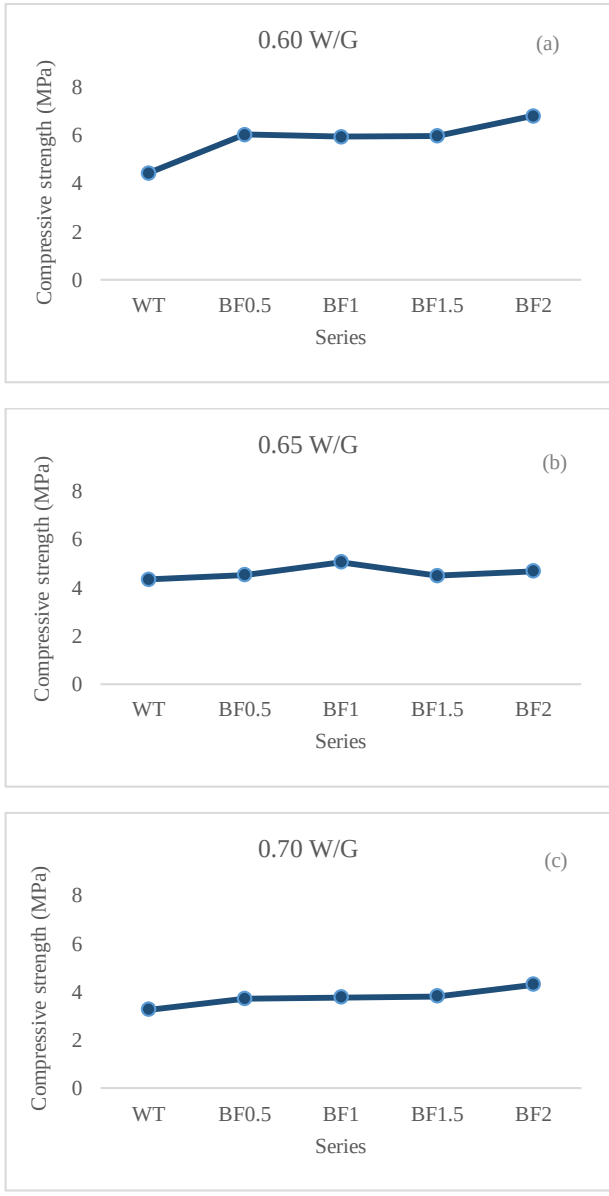

Fig. 6. Compressive strength results; (a) 0.60 W/G, (b) 0.65 W/G, (c) 0.70 W/G

Increase in the amount of basalt fiber in the mixture; it caused an increase in compressive strength values in all series. The lowest compressive strength value was determined as 4.29 MPa in BF2 series in mixtures with 0.70 W/G ratio. In series with 0.60 W/G ratio, the highest compressive strength value was determined as 6.81 MPa in BF2 series. In series with 0.65 W/G ratio, the highest compressive strength value was

determined as 5.06 MPa in BF1 series. In series with 0.70 W/G ratio, the highest compressive strength value was determined as 4.29 MPa in BF2 series. Basalt fiber, in the series with 0.60 W/G ratio, caused a %53.37 increase in compressive strength when the highest compressive strength value obtained was compared with the witness sample value. This situation was determined as %16.58 in the series with 0.65 W/G ratio. Likewise, in the series with 0.70 W/G ratio, it was determined as %31.59.

The compressive strength is mainly affected by the properties of component and mortar matrix [23]. The amorphousness in the crystal structure of basalt fiber can contribute to the development of compressive strength values. The more dense structure formed by the addition of basalt fiber may behave like aggregate [24]. This is thought to be the reason for increasing compressive strength values due to the increase in the amount of basalt fiber in all series.

3.4. Flexural strength results

Flexural strength test results of basalt fiber additive with three different W/G ratios and witness samples are given in Fig. 7. With the addition of basalt fiber in all series, flexural strength values increased compared witness samples.

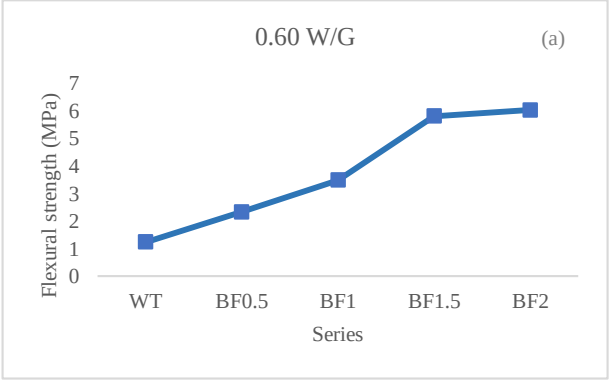

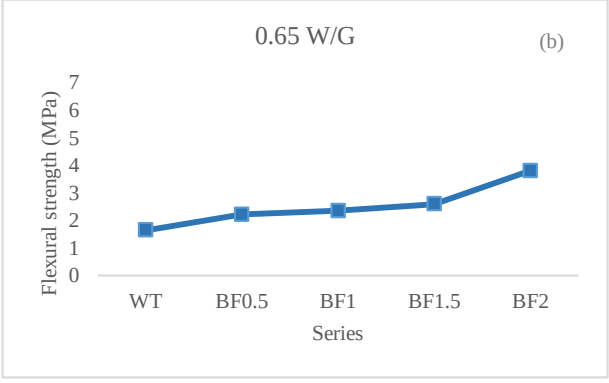

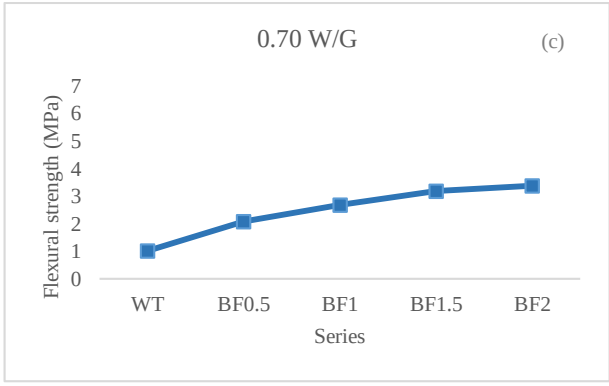

Fig. 7. Felxural strength results; (a) 0.60 W/G, (b) 0.65 W/G, (c) 0.70 W/G

The highest flexural strength values were determined as 6.02 MPa in BF2 series with 0.60 W/G ratio. The lowest flexural strength values were determined as 3.38 MPa in BF2 series with 0.70 W/G ratio. When the series with witness samples (WT) are compared among themselves, the highest flexural strength values were determined at the rate of 0.65 W/G. In the series with 0.60 W/G ratio, the increase in the flexural strength value of BF2 series with the highest flexural strength was determined as 4.78 MPa compared to the WT series. The same comparison value was determined as 2.16 MPa in the series with 0.65 W/G ratio and 2.36 MPa in the series with 0.70 W/G ratio.

4. Conclusion

As a result of the experimental study investigating the manufacturability of composite building material by using gypsum-plaster together with basalt fiber, the following results were achieved;

- The increase in the amount of water in the mixture decreased the bulk density values.
- The increase of basalt fiber additive in the mixture increased the compressive strength values.
- Increasing basalt fiber admixture in the mixture increased flexural strength values.
- The best mechanical property data were determined in series with 0.60 W/G ratio.

References

[1]. Campbell, F.C. (2010*). Introduction to composite materials, structural composite materials*. Chapter 1., ASM International.

[2]. Wimmrova, A., Keppert, M., Svoboda, L., Cerny, R. (2011). Lightweight gypsum composites: Design strategies for multi-functionality. *Cement and concrete composites*, 33: 84–89.

[3]. Dawood, E.T., Mezal, A.M. (2014). The properties of fiber reinforced gypsum plaster. *Journal of scientific research & reports*, 3(10): 1339-1347.

[4]. Kretova, V., Hezhev, T., Mataev, T., Hezhev, T., Vasily, A. (2015). Gypsum-cement-pozzolana composites with application volcanic ash. *Procedia engineering*, 117: 206 – 210.

[5]. Milikty, J., Kovacic, V., Rubnerova, V. (2002). Influence of thermal treatment on tensile failure of basalt fibers. *Engineering fracture mechanics*, 69:1025–1033.

[6]. Er, S., TuğRul, A. (2017). Doğal ve ergitilmiş bazaltların fiziko-mekanik özelliklerinin karşılaştırılması. Ulusal Mühendislik Jeolojisi ve Jeoteknik Sempozyumu, Adana, 316-323.

[7]. Borhan, M.T. (2012). Properties of glass concrete reinforced with short basalt fibre. *Materials and design*, 42:265–271.

[8]. Iang C.H., Mccarthy T.J., Chen D., Dong Q.Q. (2010). Influence of basalt fibre on performance of cement mortar. *Key engineering materials*, 93(6):426–427.

[9]. Pardo, J.D., Robayo, R.A., Trejos, L.A., Arjona, S.D. (2015). Lightweight composites based on gypsum with reinforcement of rice husk and polystyrene. *Informador técnico (colombia)*, 79(1) enero - junio: 26-32.

[10]. Vasconcelos, G., Camões, A., Fangueiro, R., Vila-Chã, N., Jesus, C., Cunha, F. (2013). Use of textile fibers in the reinforcement of a gypsum-cork based composite material. 1st Internatıonal Conference On Natural Fıbers, Guimarães/Portugal, 09-11 June.

[11]. Carvalhoa, M.A., Júniora, C.C., Juniorb, H.S., Tubinoc, R., Carvalhod, M.T. (2008). Microstructure and mechanical properties of gypsum composites reinforced with recycled cellulose pulp. *Materials research*, 11(4): 391-397.

[12]. Abad-Farfán, G., Muñoz-Cuenca, T.F., Torres-Jara, P.B., Efrén Vázquez-Silva, E. (2017). Obtaining a gypsum-cement blend, to be used as filling, with low hardening temperature. *Advances in materials*, 6(6): 115-121.

[13]. Amara, I., Mazioud, A., Boulaoued, I., Mhimid, A. (2017). Experimental study on thermal properties of bio-composite (gypsum

plaster reinforced with palm tree fibers) for building insulation. *International journal of heat and technology*, 35(3): 576-584.

[14]. TS EN 13279-1, (2009), Gypsum binders and gypsum plasters – Part 1: Definitions and requirements, Ankara.

[15]. TS EN 13279-2, (2014), Gypsum binders and gypsum plasters - Part 2: Test methods, Ankara.

[16]. ASTM C 597-97, (1998), Standard test method for pulse velocity through concrete. In: Annual Book of ASTM Standards. Easton (MD, USA): ASTM.

[17]. Kay, R. Estrada, J., Baker, C., Crandall, S., Hartin, J., Borovka, C., Kirsch, R., Sanchez, N., Koch, J., Dugas, J., Shipp, P., Master, R., Kankey, J., Link, B., Mcdougall, J. (2014). *The gypsum construction handbook*. Seventh Edition, Wiley, New Jersey.

[18]. Neville A.M. (2011). *Properties of concrete*. Pearson, London.

[19]. Shetty, M.S. (2005). *Concrete technology theory and practice*. S. Chand Company Limited, India, 2005, p 446-452.

[20]. Erdoğan T. (2015). *Beton*. METU Press, Ankara.

[21]. Ali, N., Canpolat, O., Aygörmez, Y., Mukhallad M. Al-Mashhadani, M.M. (2020). Evaluation of the 12-24mm basalt fibers and boron waste reinforced metakaolin-based geopolymer. *Construction and building materials*, 251:118976.

[22]. Iffat, S. (2015). Relation between density and compressive strength of hardened concrete. *Concrete research letter*, 6(4):182-189.

[23]. Demirel, B., Keles, T.O. (2010). Effect of elevated temperature on the mechanical properties of concrete produced with finelyground pumice and silica fume. *Fire safety journal*, 45(6)385-391.

[24]. Parveen, S., Pahm, T.M. (2020). Enhanced properties of high silica rice husk ash-based geopolymer paste by incorporating basalt fibers. *Construction and building materials*, 245:118422.

CHAPTER IX

COORDINATION OF COMBINED ACO AND ABC ALGORITHMS IN MULTI-AGENT PARALLEL PROCESSES ON THE CLOUD

Sasan HASHEMIPOUR

Islamic Azad University, Tabriz, Iran
e-mail: sasanhashemipour@hotmail.com, Orcid ID: 0000-0002-8948-9716

1. Introduction

The service composition is modular and coordinator of combined multi services—with multi-agent—to find a solution for NP-hard problems. It exposes a vast number of similar single services for different service providers in the cloud [9]. Multi-agent based is the best solution to use CMfg on cloud computing for flexibility and distributed resources network through using Qos for management in composition services [1]. Service providers and customers can dynamically publish, discover, and invoke services through it [5]. Service-based cloud computing is indeed a computing service—extends the research on combining distributed processing—and parallels processing to grid computing. Service life-cycle has consisted of service development, service registration, and service delivery. The three stages divided into offline and online—according to the service—and it is a correspondence to the quality of service [6]. Orchestration deployment of services in the cloud—from main functionality controlled in Fusion—finds the best service resolution for executable deployment components during the initial requests for the same services before than services' requests [2].

MQSC is based on multi-agent service composition for distributed algorithms in service tasks [3]. Multi-Agent system represents computing paradigm—based on multiple interacting agents—that are capable of intelligent reaction. The software agent uses some AI approach that is based on cooperation among several agents and solves a sizeable complex problem that keeps time execution at a lower level. The main focus of cloud computing is the efficient use of the infrastructure at a reduced cost. [8]. The basis of cloud computing is to create a set of virtual servers that are available for the clients. The code partitioning algorithm identifies the number of final partitions, based on the number of component web services in the composite web service [10-11]. Any web-assisted device can be used to access the resources through the main criteria of research. It gives a flexible environment to the client. Besides, because of the multi-agent process, it takes place conveniently. Moreover, the average time is also reduced at the time of service composition—because of agents [7].

2. Composition Algorithms

Composition technology has been comprehensively studied in service-oriented architecture (SOA) [16]. Combined services are the combination of one or more similar and straightforward services, and the implementation of hybrid services is done by agents that are similarly compatible and can work together. By combining the QOS combination to drive goals (speeding up and reducing time and cost), they can simultaneously have an optimized response.

2.1. ACO Algorithm

ACO is an evolution of the simulation algorithm proposed by Dorigo et al. [12]. It was inspired by the behavior of a real ant colony when programmers noticed similarities between the ants' food-hunting activities and the traveling salesman problem (TSP). Dorigo et al. [12] successfully solved the TSP problem by using the same principle that ants use to find the shortest route to a food source—which is fulfilled through communication and cooperation. ACO has been successfully applied to system fault detecting, job-shop scheduling, frequency assignment, network load balancing, graph coloring, robotics, and other combinational optimization problems [12]. In ACO, artificial ants travel in a graph to search for optimal paths according to pheromone and problem-specific local heuristics information. Pheromone information is assigned to the edges of the graph and is evaporated at a specific rate at each iteration. It is also updated according to the quality of the solutions containing this edge [13]. The ACO algorithm cannot respond to any request from services and coordinate composite service in cloud systems. Therefore, the developed algorithm enhances the satisfaction and responsiveness of web services and can serve as a convincing substitute for cloud systems.

2.1.1. ACO Algorithm Merit Function

To determine the satisfaction of this algorithm, all new elements, parameters, and variables should be used to improve this algorithm in order to increase the evaluation of the suitability of ant algorithm and to do so, two basic principles for calculating the algorithm must be considered;

- Ants' spent pheromones to reach the desired path;
- Ants' time to reach the shortest path through the pheromones is discussed.

In this relation $p_{ij}^{n}$the pheromone is the relation of merit that has two vector components; i, j. In this case, i is the vector x, and j is the vector y to n and τ_ (i1j1 and i2j2) pheromones of the pathways have α = 1, β = 1,

and γ = 1 values. α is the pheromone magnification coefficient, and β is a magnification coefficient of paths. Besides, $\eta_{i1j1,i2j2}$ and h_{i1j1} are cost and time over ants. The denominator of the sum of the paths taken with the assumption of service = s and cloud = c in the paths and l is the length of the paths i, j in computing the pheromone formula in the ant algorithm. The ACO pheromone calculation benefit function is as such;

$$ACO\_p_{ij}^{n} = \frac{[\tau_{i1j1}]^{\alpha}[\eta_{i1j1}]^{\beta}[h_{i1j1}]^{\gamma}}{\sum_{s=1,c=1}^{l_{i1j1,i2j2}}[\tau_{i1j1}]^{\alpha}[\eta_{i1j1}]^{\beta}}$$

2.1.2. Computing Time of Ant Algorithm

In computing the time of the ant algorithm, this algorithm is based on pheromones that pass by time to time, followed by other ants that are seeking to obtain pheromones along the path to calculate the shortest path. Pheromones are used to select the shortest route based on the paths taken and eventually expanding from the points of evaporated chemical pheromones. It is fulfilled based on the volatile time that becomes a state of traceable time; so that other ants can reach their unique target at an optimally reflective time. The so-called stand-alone algorithm in the combination of composite services is calculated from a distinct formula.

The Ant-based algorithm cost calculation is useful for calculating the cost formula of parameters such as d, i, and j, taking into account the initial cost that is equal to zero and the cost of the next route over the total distance cost. Based on this formula, the lowest cost can be selected from the available routes. Ant algorithm cost calculation formula is as follows;

$$ACO\_cost_{\mathrm{ij}d_s} = \frac{cost(t)_{ijd_s} + cost(t+1)_{ijd_s}}{\sum_{ijd_s}^{k} cost(t+1)_{ijd_s} + \Delta\tau_{ij_s}}$$

2.2. ABC Algorithm

The standard ABC performs well when dealing with single-objective optimization and achieves good solution quality and high convergence speed [14]. The exchange of information among bees is effective in the formation of collective knowledge and distinguish some parts in all hives. The most important part of the hive concerns exchanged information that is the dancing area—related to the quality of food sources among bees—which is called a waggle dance. Since information about all the current rich sources is available to an onlooker on the dance floor, it probably watches numerous dances and decides to employ itself at the most profitable source. There is a higher probability of onlookers who choose more profitable sources since more information is circulated about the more profitable sources. Hence, recruitment is proportional to the profitability of the food source [15].

2.2.1. The Bee Algorithm Fit Function

The basis of the bee algorithm's performance is based on the proper selection of the bee in the behavior of the bees to achieve more nectar. Since birth, more attention has been given to the specific goal of the bees by shortening the way for the bees to reach and feed the bees with emphasis on more nectars. In order to reduce the cost of wasting more data, two basic principles must be considered when calculating this algorithm that is as follows;

- The cost of the bee to reach the most nectar with the smallest flight;
- Bee time to reach the nectar with the least time wasted among the available nectar Computation of bee algorithm competence is like;

$$BCO\_p_{ij}^{n} = \frac{[N_{i1j1}]^{\alpha}[\zeta_{i1j1}]^{\beta}[h_{i1j1}]^{\gamma}}{\sum_{s=1,C=1}^{l_{i1j1,i2j2}}[N_{i1j1}]^{\alpha}[\zeta_{i1j1}]^{\beta}}$$

In the above relation, the pheromone p_{ij}^{n} is the competence relation that has two vector components i, j where i is the vector x, and j is the vector y to $N_{i1j1,i2j2}$. Nectar is the pollen that the bee seeks, with values of α = 1, 1 = 1, and 1 = 1. α is the nectar magnification coefficient, and the β is magnification coefficient of the paths ζ_{i1j1}. Moreover, h is the specified path edge, and the denominator of the fraction of total traveled paths—including service on the routes—for l times is more than the length of the paths, I and j. In calculating the total route traveled, the weight of service traveled depends on the route traveled in the bee algorithm.

2.2.2. Calculating the Time of the Bee Algorithm

The time calculation of the bee algorithm is based on how much the bees are interested in nectars. Accordingly, the amount of time it takes for the bees to find the optimal nectar and achieve its goal is calculated. The bees rotate gently to reach their target. Here is the time needed to find the nectar data needed to meet the needs of the bees interested in precisely searching for paths that would lead them to more nectars through hybrid services. Accordingly, in this study, it is necessary to obtain the juice. Therefore, at ζ_{ij_s}, i and j divide the service into d_{ij} to obtain the maximum juice in the service.

In the formula $\tau_{ij_sd}(t)$ the amount of juice in service is equal to the amount of route i, j. The total distance traveled by the service at i, j at node k at t. Circulation is the path to obtain the total pheromone circulation in the path i, j in the service. In the formula, with the original diameter of

nectar saliva matrix N in the bee, is calculated for the cost of nectar as follows:

$$BCO\_time_{ijd_s} = time_{ijd_s}(t) + \frac{\zeta_{ij_s} + N_{ij_sd}(t)}{\sum_{ijd_s}^{k}(1-\rho)_{ij_s}^{k} + \Delta N_{ijd_s}}$$

2.2.3. Calculate the Cost of the Bee Algorithm

It is useful to calculate the cost of the bee algorithm based on the formula calculation of the cost parameters such as d and i, j, that are taking into account the initial cost as equal as zero. The cost of the subsequent route over the total distance costs and based on this formula, the cost of the best route can be selected as follows:

$$BCO\_cost_{\mathrm{i}jd_s} = \frac{cost(t)_{ijd_s} + cost(t+1)_{ijd_s}}{\sum_{ijd_s}^{k} cost(t+1)_{ijd_s} + \Delta N_{ij_{cs}}}$$

3. Suggested Model

In this study, according to the general definition of the proposed method, the hybrid algorithm derived from the two ant algorithms (ACO) and the bee algorithm (ABC) used in the hybrid services is used as a descriptor of the general model scheme based on the needs of users. It reduces the search time that is embedded in them. It has two essential features in the following proposed algorithm model:

A. Using the Hybrid Algorithm, you can reduce execution time in services using the hybrid algorithm. You can effectively reduce time in services by using the combined algorithm SHACACS and reduce the run time in hybrid services.

B. Using the SHACACS hybrid algorithm derived from the combination of the Ant Algorithm (ACO) and the Bee Algorithm (ABC) can dramatically reduce the running cost of the hybrid services using the proposed SHACACS algorithm.

In this proposed algorithm, SHACACS can significantly address existing service needs in hybrid services by an efficient approach to hybrid services using the SHACACS hybrid algorithm derived from the combination of the two ant algorithms (ACO) and the bee algorithm (ABC). This has led to the creation of a hybrid algorithm for hybrid services that are fully described in the proposed model: The proposed method in parallel by implementing the mentioned algorithms in the form of an agent in the cloud service promotes positive performance and achieves the best performance in combined services. Based on the performance of the service in the agents, as well as the parallelization, we

have to design a new system to improve the performance in cases such as time and cost in order to use it to improve the combined services.

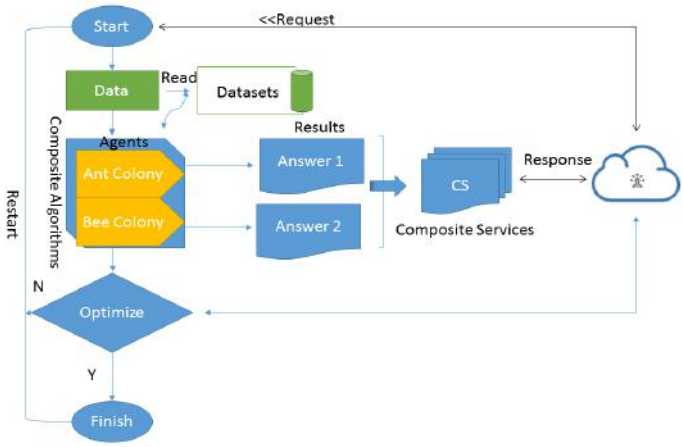

Figure1. SHACACS Model

By using this proposed method, which starts with Start, the x, y paths are selected as random by generating data. In this proposed method, we have two factors, x, and y, each of which is connected to an algorithm. x is related to the ACO (ant algorithm) factor and the connected (equipped) x-factor, which is designed and refurbished to improve combination services. y is also connected to ABC (bee algorithm), which is designed to serve combined services better. Each of these improved algorithms achieves the optimal answer separately. In summary, according to the proposed model of the SHACACS algorithm, each has access to two different responses—according to the specified function. After determining the specified answers, x goes to the agent controller to combine it in parallel in such a way that it can create the best answer for the users.

In the next step, x goes back to the recovery section, and in this step, it goes through the filtering of the results. It is made from a combination of bee and ant algorithms. As a result, the minimum cost and time, and the fitness function are again improved and coordinated, centralized, and sent to the cloud computing service whenever the answer is finalized. In this case, the combined service can use it, and the service will start working. The principle of the service used in this algorithm combines the ant and bee algorithm in a coordinated and parallel manner between the ant and bee algorithms to optimize time, cost, and functionality. If it is minimal, the answers will be sent in parallel to run the services in the cloud.

At this stage, to improve the desired algorithm, the SHACACS algorithm completes the answers to integrate the previous algorithms, and

previous results that are entered into action and minimally combines the desired answers by acknowledging the evolution of services and sends them to the output minimally. The SHACACS algorithm is a combination of ant and bee algorithms, using a combination of factors in the cloud to form a logical and complete answer for the combination of several algorithms. From this proposed SHACACS hybrid algorithm, it is possible to achieve the desired goals, such as reducing time and cost and increase the execution speed in hybrid services in order to combine services in hybrid services.

```
Begin
initialize  all pheromone levels to some constant>0
   initialize  all parameters necessary for algorithm stating
   agent and service composite is integrated with in agent
   create model for x,y path for ants-bees
   generic path create for ants
  prepared for movement  ants trust
   if conditions is trust for ultimate  opportunity to agents: Ants-bees
   repeat
      for every ant,bees do
         if all  things is trust
            do
                  tau0=Q/(nVar*mean(model.D(:))/8)/2;
               hau0=cs/(nVar*mean(model.D(:)));
               tau=tau0*ones(nVar,nVar);
               hau=hau0*ones(nVar,nVar);
               for i=1,...,ns  i scout[i]=Initialise_scout()
               flower_patch[i]=Initialise_flower_patch(scout[i])
               do until stopping_condition=TRUE i
               Recruitment()
               for i =1,...,nb
               flower_patch[i]=Local_search(flower_patch[i])
               flower_patch[i]=Site_abandonment(flower_patch[i])
               flower_patch[i]=Neighbourhood_shrinking(flower_patch[i])
               for i = nb,...,ns
               flower_patch[i]=Global_search(flower_patch[i])}
                while repeat
               receive to best answer
If not found
Create elite bees
Repeat
Do
for i =1,...,nb
               flower_patch[i]=Local_search(flower_patch[i])
               flower_patch[i]=Site_abandonment(flower_patch[i])
               flower_patch[i]=Neighbourhood_shrinking(flower_patch[i])
               for i = nb,...,ns
               flower_patch[i]=Global_search(flower_patch[i])}
Work to wtile to end
Receive to best answer
Combine  ants-bees
Best cost,time to recived to each appoint in
saved
Finish
```

Figure2. SHACACS Semicode

3.1. Compose Algorithms

This proposed SHACACS algorithm, using a combination of ant algorithm (ACO) and bee algorithm (ABC), can use a combination of algorithms according to Figure1. This proposed SHACACS algorithm can significantly lead to a more efficient and efficient method for combined services using the SHACACS hybrid algorithm in meeting the current needs of services in hybrid services. The combination of the two ant algorithms (ACO) and the bee algorithm (ABC) to better understand this proposed algorithm is to create a model of the proposed SHACACS algorithm in the form of a model in which all the different parts are displayed and can be used by using the algorithm. The ant (ACO) and the bee algorithm (ABC) lead to the creation of a hybrid algorithm for hybrid services.

The proposed method, by implementing the mentioned algorithms in the form of agents in services in clouds in parallel, promotes positive performance to achieve the best performance in combined services. Based on the performance of services in factors and parallelism, we have to design a new system to improve performance relationships such as time and cost for hybrid services. Due to the definitions of the mentioned algorithms, these algorithms cannot normally continue to work in convergence (parallel centralized) and meet the needs of users in hybrid services. Therefore, the use of SHACACS hybrid algorithm has many advantages compared to the mentioned algorithms, which are:

- Implement ant and bee algorithms in parallel;
- Execution of algorithms;
- Reduce execution time;
- Reduction in costs;
- Improve algorithms to service combined services;
- Improved search quality in hybrid services;
- The principles of the optimized algorithm are the use of ant and bee algorithms, which are based on finding the best competency function and parallelizing the algorithms for cloud services simultaneously to perform combined services in services.
- Combined Juice: Juice is a substance that is chemically removed from the saliva of a mixed insect. For the services available in the agents, the comparison of the ant and bee algorithm plays an essential role that it can perform better in the appropriate situation than the desired service in the combined services.

In this proposed method, the factors that use the two algorithms (ACO, ABC) in the combined services make able to act according to the needs of users to reduce search time and cost for services available on web services. The advantages of this algorithm can be mentioned as follows:

- Combined juice: In the combined algorithm, by using the combined juice in the agents, a better position and competence can be obtained than the desired service in the combined services.
- Integrated eye: In the combined algorithm based on the use of ACO and ABC algorithms, the integrated eye can play an essential role in better determining the combined services, to achieve the desired goal with high accuracy and better performance.
- Integrated wing: so that the combined algorithm can quickly get rid of obstacles and network traffic in the combined services and reach the desired goal faster.
- Integrated horns: Ants and bees use fused horns for a better sense of smell and optimal search of the path so that they can optimize the service request and provide the right combination for combined services.

4. Evaluation

This algorithm includes time function and cost function, according to ant and bee algorithms. This algorithm has double eyes (Eye fly exactly) for better vision than ant and bee algorithms. The ant algorithm uses the pheromone as a substitute for better vision due to its weak eyes. Bees have a more robust vision than ants. When combined, the eyes of these two insects become healthy eyes, which is not very efficient. In this way, two accurate double eyes are used to reduce traffic, two wings are used, which can fly against the obstacles in flight, away from the traffic of the route and the dead-end of the transfer route. In addition, the insect's sting increases the optimal search speed to reduce time loss during juice suction, leading to a so-called algorithm (SHACACS) that can increase the speed and reduce additional activity in combination services:

$$BestTimeHYB_{ACO,ABC} = BestTime_{ACO} + BestTime_{ABC} \times juice$$

4.1. SHACACS algorithm time calculation function

The combined time function of the SHACACS algorithm is the way that it first calculates the shortest time traveled by ants and then selects the best routes traveled by bees. The juice is the best way to find the service optimized for agents (ants and bees) to combine services in cloud systems.

$$BestCostHYB_{ACO,ABC} = juice \times BestCost_{ACO} + BestCost_{ABC} \times juice$$

4.2. The SHACACS algorithm cost calculation function

The combined cost function of the SHACACS algorithm is that it first measures the best path traversed by ants and then selects the best path traversed by bees. The juice is a combination of agents (ants and bees) to combine cloud services to increase the speed of finding the best-optimized service.

$$FitnessHYB_{ACO,ABC} = alpha \times (cs \times BestFitnessABC) \times \frac{beta(cs \times BestFitnessACO)}{Winged_{animal}} \times Qos$$

4.3. SHACACS hybrid algorithm competency function

$$Winged_{animal} = fly \times eye_{fly_{exactlt}} \times (ACO, ABC)$$

In this Winged-animal formula, which is to increase the efficiency of the SHACACS algorithm, the combined competency function (ACO, ABC agents) is found in parallel—first, the coefficients alpha = 1, beta = 1, QOS = 100 are considered. In addition, CS is the same combination service that is used with the best bee and ant function to use the $Winged_{animal}$ algorithm with the lowest cost and time and with increasing QOS efficiency. fly as wing and eye $eye_{fly_{exactlt}}(Ant_3ABC)$ as flat eye, measure, and hit the target with the least error to increase the efficiency of the cloud system with agents (Ant and ABC) in services.

5. Compression Algorithms

Due to the competence functions of the developed algorithms for the ant algorithm (ACO) and the bee algorithm (ABC) to achieve the proposed SHACACS algorithm—which is obtained by combining the two algorithms of ant and bee—from the table to show the values, minimize time and cost for ant and bee algorithms as well as improved SHACACS algorithm. A combination of algorithms is used, as shown below:

Algorithm	Fitness	Iteration
ACO	202.1185	200
ABC	4.5589	200
SHACACS	1.1518	200

Table 1: Comparison of algorithm competency functions with SHACACS

Through the definitions of ant and bee algorithms given in previous chapters, these algorithms cannot normally function as convergent (parallel-focused) and can meet user service needs in combination services.

Therefore, the use of SHACACS hybrid algorithm has many advantages, which are:

- Implement ant and bee algorithms in parallel
- Execution of algorithms
- Reduce execution time
- Reduction in costs
- Improve algorithms in how to service combined services
- Improved search quality in hybrid services

Algorithm	Time	Cost	Speed
ACO	$\sum_{i,cs}^{n} i \times path$	$\sum_{i,cs}^{n} i \times path$	$\sum_{i,cs}^{n} i \times path$
ABC	$\sum_{i,j,cs}^{n} path_{i,j,cs}^{n} nect$	$\sum_{i,j,cs}^{n} path_{i,j,cs}^{n} nect$	$\bigcup_{ij,cs}^{n} \sum_{i,j,cs}^{n} path_{i,j,cs}^{n} ne$
SHACACS	$min \sum_{i,cs}^{n} ipath, nec$	$min \sum_{i,cs}^{n} ipath, nec$	$\prod_{i,j,cs}^{n} \sum_{i,cs}^{n} ipath, necta$

Table1. Speed Convergence Algorithms (ACO-ABC-SHACACS)

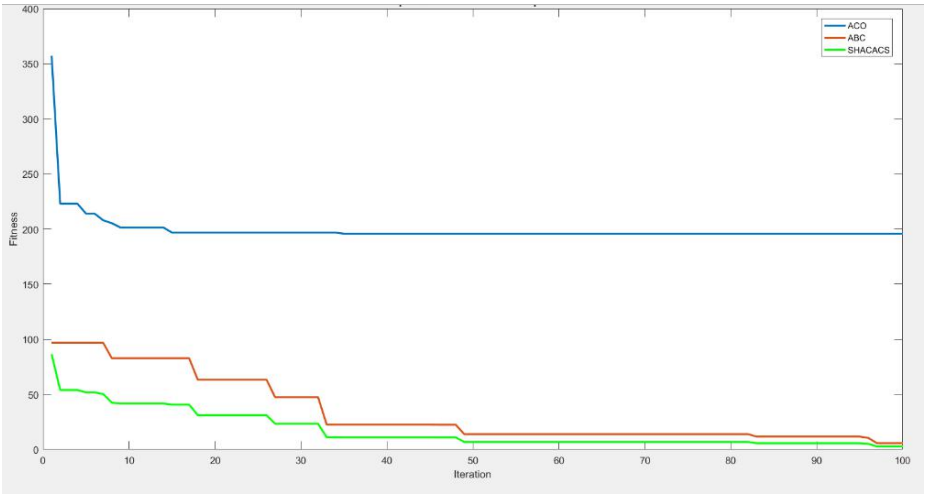

Figure3.Comparison Algorithms (ACO-ABC-SHACACS)

6. Conclusion

This study investigates all methods of creating and implementing algorithms by agents—resulting from the production of the hybrid algorithm of the Ant algorithm (ACO) and the Bee algorithm (ABC). On account of coordinating these Hybrid algorithms with ACO-ABC Colony Accessibility (SHACACS) and the proposed combined algorithms, the resulting algorithm runs composite services in parallel with cloud services. In this implementation and with the use of the Ant algorithm and the Bee algorithm, combined operating services simultaneously meet the different needs in various fields. Besides, the study clears out how respondents—regarding the composite services—are effective in reducing time and costs, administratively. The study is giving solutions in regards to using composite algorithms in composite service through genetics to improve the flexibility of multiple or straightforward services more efficiently in an agent. Every composite service by independent run enhances services efficiently; the computing cloud services can enhance time and speed through Ant and Bee algorithms.

References

[1] Zhang, L., Guo, H., Tao, F., Luo, Y. & Si, N. (2010). "Flexible management of resource service composition in cloud manufacturing", *Industrial Engineering and Engineering Management (IEEM)*, 2010 IEEE International Conference on, Macao, pp. 2278-2282.

[2] Simoens, P., Van Herzeele, L., Vandeputte, F. & Vermoesen, L. (2015). "Challenges for orchestration and instance selection of composite services in distributed edge clouds", *IEEE*, 2015 IFIP/IEEE International Symposium on Integrated Network Management (IM), Ottawa, pp. 1196-1201.

[3] Luo, J., Li, W., Liu, B., Zheng, X. & Dong, F. (2010). "Multi-Agent Coordination for Service Composition", *Springer London*, pp. 47-80.

[4] Yu, Q., Chen, L., & Li, B. (2015). "Ant colony optimization applied to web service compositions in cloud computing", *Computers & Electrical Engineering*, p. 41.

[5] Luo, J., Li, W., Liu, B., Zheng, X. & Dong, F. (2009). "Multi-Agent Coordination for Service Composition". *Agent-Based Service-Oriented Computing*, pp. 47-80. doi:10.1007/978-1-84996-041-0_3

[6] Zhenyu, L., Tiejiang, L., Tun, L. & Cai, L. (2010). "Agent-Based Online Quality Measurement Approach in Cloud Computing Environment", *IEEE, Web Intelligence and Intelligent Agent Technology (WI-IAT)*, 2010 IEEE/WIC/ACM International Conference on, Toronto, pp. 686-690.

[7] Virani, K., Virani, D. & Vaghasia, M. (2013). “Priority Based Service Composition Using Multi Agent in Cloud Environment”. *International Journal of computational Engineering Research*, 03(5), pp. 21-25.

[8] Talia, D. (2011). “Cloud Computing and Software Agents: Towards Cloud Intelligent Services”, *CEUR-WS*, Vol.741, pp. 2-6.

[9] Jula, A., Sundararajan, E. & Othman, Z. (2014). “Cloud computing service composition: A systematic literature review”. *Expert Systems with Applications*, 41(8), pp. 3809-3824.

[10] Chafle, G., Chandra, S., Mann, V. & Nanda, M. (2004). “Decentralized Orchestration of Composite Web Services”, *ACM*, Proceedings of the 13th international World Wide Web conference on Alternate track papers & posters: WWW Alt. 4, pp.134-14.

[11] Binder, W., Constantinescu, I., & Faltings, B. (2006). “Decentralized Orchestration of Composite Web Services”, *IEEE*, 2006 IEEE International Conference on Web Services (ICWS06), pp. 869-876

[12] Blum, C. (2009). “Ant colony optimization”. In: Proceedings of the 2009 genetic and evolutionary computation conference, Montreal, Canada; pp. 2835–51.

[13] Yu, Q., Chen, L., Li, B. (2015). “Ant colony optimization applied to web service compositions in cloud computing”, *Elsevier BV*, 41, pp. 18-27.

[14] Luo, J., Liu, Q., Yang, Y., Li, X., Chen, M. & Cao, W. (January 2017). “An artificial bee colony algorithm for multi-objective optimization”, *Elsevier*, 50, pp.235-251.

[15] Karaboga, D. et al. (2012). “A Comprehensive Survey: Artificial Bee Colony (ABC) Algorithm and Applications.” *Artificial Intelligence Review*, 42(1), pp. 21-57.

[16] Yuan, M., Zhou, Z., Cai, X., Sun, C. & Gu, W. (February 2020). “Service composition model and method in cloud manufacturing”, *Elsevier*, 61.

CHAPTER X

EARTHQUAKE FORECAST MODEL BASED ON SPATIALLY SMOOTHED SEISMICITY, TURKISH CASE

Dr. Hakan KARACA

Nigde Omer Halisdemir University, Turkey
e-mail: karaca26@hotmail.com, Orcid ID: 0000-0003-3291-5822

1. Introduction

The forecast studies based on spatially smoothed seismicity are based on the pioneering study of Kagan and Knophoff, 1977. Starting from late 90's the method have been receiving wide attention and sophisticated to a certain leve while the sensitivities of the proposed model is analyzed thoroughly. (Field et al., 2007, Helmstetter et al., 2006, 2007, 2012, Scholemmer et al., 2004,2007,2010 Zechar et al., 2010, Werner et al., 2010, Rhoades et al., 2011, Taroni et al., 2013, Scholemmer et al., 2018).

Especially Californian seismicity became a subject of several researchers in the field (Scholemmer et al., 2004, 2007, Kagan and Jackson, 2007, Helmstetter et al., 2007, Werner et al., 2011, Helmstetter and Werner, 2012 and 2014, Hiemer et al., 2013, Werner et al, 2018) due to its highly dense catalog. Japanese (Tsuruoka et al., 2012), Italian (Werner et al., 2010a, 2010b) and New Zealandian (Rhoades et al., 2011) catalogs have also been studied to test the proposed forecast models. In all these studies, the forecast models mostly are verified and the results offered crucial information in confirmation of the proposed models. Especially, as for the Californian case, which involved the ANSS catalog with 2.0 minimum magnitude of completeness, promising results encouraged further studies. However, as the minimum magnitude threshold increases or the period of completeness decreases with a small minimum magnitude of completeness the forecasting capacity is expected to decrease. Even the Poisson assumption is questioned in some cases and the non-Poissonian temporal distribution is pointed as the reason of failure (Werner et al., 2010a , Zechar et al., 2010, Rhoades et al., 2011).

At this point, it should also be automatically deduced that, for catalogs with large magnitude thresholds, the Poisson assumption might not be true. However, as the minimum magnitude threshold increases and the area of interest is limited, it is likely to have a non-Poissonian distribution. However, with larger minimum magnitude threshold and larger area of interest, the likelihood of having a stationary time series is higher, in alignment with the Poisson assumption. Henceforth, such an area and so

its seismic patterns might be experimented with the proposed forecasting method.

The performance of the forecast models developed by using spatially smoothed seismicity method is measured by a number of tests, which are based likelihood, and quantification of similarity in spatial, temporal and magnitude dimensions. The L-test (Likelihood) and N (Number)-test (Schorlemmer*et al.* 2007), the M-test, S-Test (Zechar et al., 2010) are proposed. If the spatial, temporal and magnitude distribution characteristics of seismicity can be successfully forecasted, these tests provide guidance in the development of a forecast model by offering information on the consistency of the developed model. In addition to the mentioned tests, R-test (Schorlemmer*et al.* 2007) and T-test (Rhoades et al., 2011), which are also introduced to measure the relative performance of a forecast with respect to a base model are developed to support the main tests.

In this study, the smoothed seismicity methods are exploited for forecast verification. The spatio-temporal variation, earthquake rate and magnitude distribution of seismic rate is investigated through spatially smoothed seismicity. Then the log-likelihood method is adapted and long-term spatio-temporal forecasting is implemented. The tests commonly employed in RELM experiments namely L-test (Likelihood) and N (Number)-test which measures the consistency of the proposed forecast are used to measure the degree of agreement between the model based on past seismicity and the observed seismicity which is forecasted as part of a back-testing scheme.

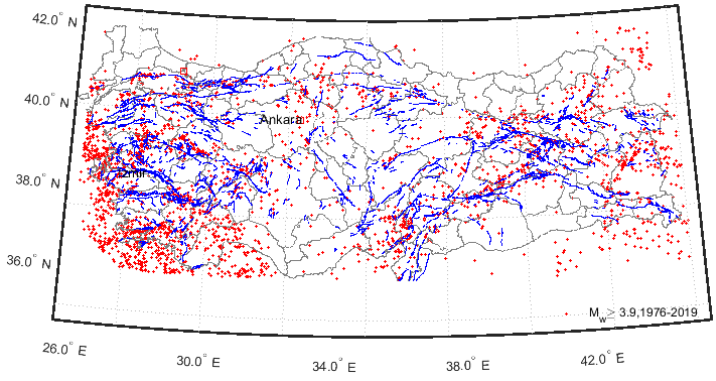

Figure 1. The Study Area Bounded by 26.0^0 E-32.0^0 E Longitudes and 36.0^0 N – 40.5^0 N Latitudes (MTA, 2018, KOERI, 2020)

In addition, the likelihood of the observed magnitude distribution and spatial patterns given the forecast models is tested for its consistency through M (Magnitude)-Tests and S (Space)-tests respectively. Though it is encouraging in the identification of seismically active areas producing events within a pattern, still there is more to overcome in order to improve the models.

2. Data and Methodology

The study area is bounded by 26^0 E to 45^0 E longitudes and 36^0 N to 42^0 N latitudes spanning entire Turkey. As can be seen in Figure 1, the earthquakes are generally clustered around the main Anatolian fault systems, North and East Anatolian Fault Zone and within the Aegean Region where the normal fault dominates.

For the purpose of the study, a catalog is created for the period between 1980 and 2019. The faults are gathered from General Directorate Of Mineral Research And Explorations (GDMRE, 2018) and the earthquakes are compiled by using Kandilli Observatory and Earthquake Research Institute (KOERI (http://www.koeri.boun.edu.tr/sismo/zeqdb/, Last Access Date: 11.05.2020). The compiled catalog is subjected to the homogenization for the purpose of unification of the magnitudes by using local magnitude conversion equations by Akkar et al., 2013 and it is declustered by using the time and space windows of Gardner and Knophoff (1974). The effect of declustering is quite visible in Figure 2, as the spikes indicating aftershock and foreshock sequences are largely removed. The maximum complete period is determined as the minimum magnitude of completeness is computed as 3.9 for the period starting at 1976 by using Cao and Gao (2001).

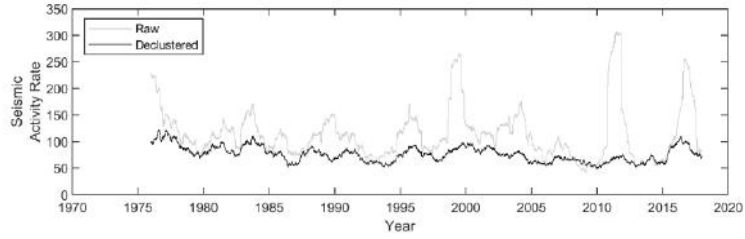

Figure 2. Yearly Seismic Activity Rate Computed for Sliding Window Technique (Left) and The Magnitude Distribution Characteristics of Earthquakes According to Robust Fitting Techniques (Right)

The single most important prerequisite in using this method is the assumption of stationarity of earthquake time series. Indeed, according to Poisson assumption, which is based on the constant earthquake rates in temporal dimension, any earthquake time series is supposed to be stationary. The earthquake time series in Figure 2 display irregular fluctuations around a stable mean. Actually, the left panel in Figure 3, clarifies these fluctuations in more detail. Most of the yearly earthquake rates fall between 95% confidence interval.

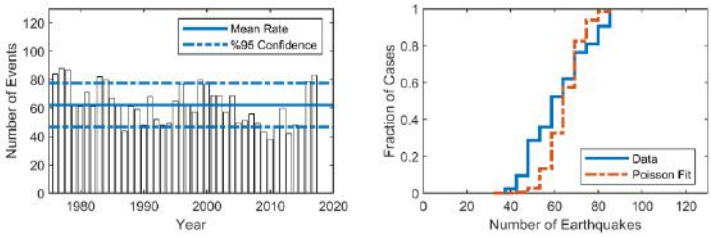

Figure 3. Observed Yearly Magnitude Distribution (Mw≥3.9, 1976 - 2019) for the Considered Period (Left) and the Cumulative Distribution Function of Yearly Earthquake Rates with Poisson Fit (Right)

The right panel in the same figure is much more explanative whether the data follow a stationary character. The distribution of number of earthquakes as represented by fraction of cases display a Poisson character closely. The variation between the Poisson model and the data is caused by the fluctuations. According to Poisson assumption, these fluctuations are expected to even out given sufficient time or relatively become insignificant as the data accumulates.

As an important input in forecast studies, the magnitude distribution of the sampled data is also derived. The variety of theories developed to model the magnitude distribution and amassed studies over the time, is the sign of importance of the subject and associated complexity (El Isa and references therein). Especially the large magnitude distribution and its relationship with the magnitude distribution characteristics of the rest, still draws researchers. In such a setting, the real solution to this problem seems like is awaiting accumulation of sufficient evidence. In this study, In order to reflect the magnitude distribution characteristics, among the characteristic, truncated and unbounded models, the unbounded Gutenberg-Richter (GR) relationship (See Figure 4) is preferred. Henceforth, the magnitude distribution is modeled through the robust fitting technique () as shown in equation 1,

$$p(m) = 10^{a-b(m-m_{\min})} / 10^{a-b(m(1)-m_{\min})} \quad (1)$$

where a and b are GR constants and m_{min} is the minimum magnitude of earthquakes involved in the computation.

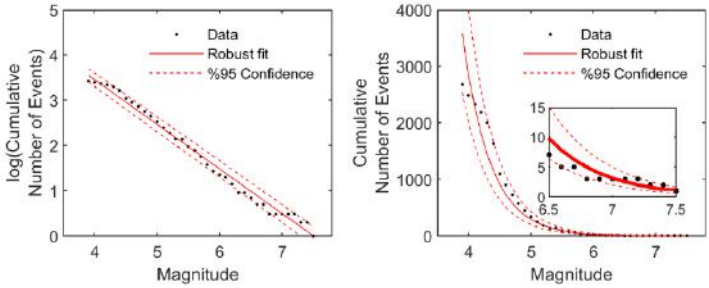

Figure 4. The Magnitude Distribution Characteristic of the Gathered Data (Mw≥3.9, 1976 - 2019)

The mainstream ideas lie beneath the forecasting algorithms as either precursory seismic activation or quiescence or both. All these forecasting algorithms have its roots in the basic idea that large earthquakes tend to occur close to the locations of smaller earthquake clusters (Werner et al., 2011). Hence, by using this assumption, the earthquake catalogs which are generally thought to be missing the large magnitude events due to the time gap between the long return periods of large magnitude events and the coverage period of the existing catalogs, can be exploited to predict the large magnitude events. In other words, there is a proportionality between the density of the seismic activity and the spatial distribution of larger magnitude earthquakes accordingly. Hence overall magnitude distribution is thought to be best modelled by unbounded Gutenberg-Richter relationship as shown in Figure 4.

As one of the crucial tests, whether the forecast is successful or not, the similarity of the spatial distribution of the studied model and the forecast model is compared. Therefore, after obtaining the magnitude distribution characteristics, the spatial distribution is examined. The employed method uses spatially adaptive smoothing kernel bandwidths based on the study of Kagan and Knopoff (1977) which later commonly applied in earthquake forecasting algorithms. The optimum kernel bandwidths are computed by letting the seismic events decide on the correlation distance based on the distances of the neighboring events. The spatial seismicity rates are smoothed by using the simple Gaussian isotropic kernel:

$$K_d(r) = c(D)\exp\left(-\frac{|r|^2}{2D^2}\right) \quad (2)$$

where D is the smoothing distance and $c(D)$ is the normalizing factor. The spatial binning is based on a grid system formed by 2.5x2.5 kms boxes. The 2.5 km distance approximately covers 0.0625^0 longitude and 0.05^0 latitude. The information gain per each model with respect to the reference model is measured by

$$G = \exp\left(\frac{\log(LL) - \log(LL_r)}{N_t}\right) \quad (3)$$

where LL is the log-likelihood of the candidate model and LL_r is the log-likelihood of the reference model, and N_t is the total number of earthquakes greater than the minimum magnitude of completeness in the candidate model. The log-likelihood of a model is determined by the product of probabilities in each spatio-temporal-magnitude bin of the each unit area as the event occurrence at each unit is assumed to be independent. As the joint likelihood of numerous number of units might be unfeasibly small, log-likelihood of the candidate model is computed through the summation of the log values of probabilities in each unit as shown in Equation 4.

$$\log(LL) = \log\left(\prod_i \prod_j p(\lambda^t(i,j), \omega^o(i,j))\right) = \sum_i \sum_j \log\left(p(\lambda^t(i,j), \omega^o(i,j))\right) =$$

$$\sum_i \sum_j \left[-\lambda^t(i,j) + \omega^o(i,j)\log(\lambda^t(i,j)) - \log(\omega^o(i,j)!)\right] \quad (4)$$

Where p is the occurrence probability, λ_i is the normalized spatial density in earthquakes per unit time in the training catalog, w_i is the number of observed events in the learning catalog for each cell i. Here one thing should be clarified: if the catalog is partitioned into two parts of varying sizes and periods to determine the optimum spatial kernel bandwidth, for every event added to the training catalog and removed from the learning catalog, the optimum bandwidth might vary. Therefore, partitioning of the catalog with uneven time periods would be beneficial if the training part is sufficiently large enough to allow detecting the seismic patterns.

The determination of optimum number of neighbors and so the optimum kernel bandwidths for each event, leads to the determination of the most likely spatial smoothing algorithm and so the spatial distribution of the activity rate densities.

$$\mu(\vec{r}) = \sum_{i=1}^{N_l} K_{d_i}\left(\vec{r} - \vec{r}_i\right) \tag{5}$$

where N_l is the total number of earthquakes above minimum magnitude of completeness in the training and learning catalogs. After that, in order to generate forecasts by using an inverse Poisson distribution, the obtained spatial activity rate densities are normalized by the following equation.

$$\mu^*(i,j) = \frac{\mu(i,j)}{\sum_i \sum_j \mu(i,j)} \tag{6}$$

The spatially normalized activity rate density is the spatial pattern of projection and when combined with the overall temporal rate for the entire region, is used for forecast. The expected number of events for each cell for a considered period of year, *T*,

$$\Lambda = \lambda(i,j), i,j \in S) = (Tn)\mu^*(i,j) \tag{7}$$

where *n* is the yearly rate of earthquakes for the entire region of interest computed by dividing total number of earthquakes, N_l, above the minimum magnitude of completeness by the total number of years covered by learning and training periods.

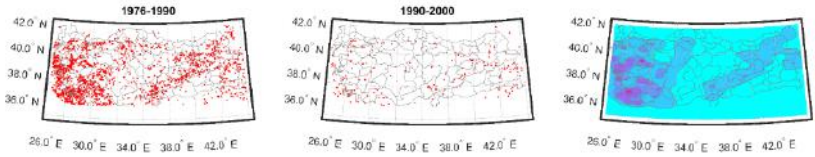

Figure 5. An Example to the Training Catalog (1976-1990), learning catalog (1990-2000) and Spatial Activity Density Map (1976-2000) Developed by Using the Training and Learning Catalogs,

The same equation could be modified to forecast earthquakes with certain magnitude ranges by using the magnitude distribution characteristics, *p(m)*, of the entire region formulated in equation 1.The expected number of earthquakes with magnitude m, is expressed by the following equation

$$\Lambda^m = \lambda(i,j,m) = (Tn)\mu^*(i,j)\,p(m) \tag{8}$$

The forecast is then compared with the observed data, Ω, and various tests are performed for its consistency. These tests are based on generation of synthetic catalogs, $\hat{\Omega}$,based on the forecast and determine the similarity

of the spatio-temporal, temporal, spatial and magnitude-wise distribution of the observed data with the generated catalogs based on forecast. The simulation is performed by using the spatial activity rate densities, μ, and then the simulated earthquakes are positioned through inverse poisson function.

$$n(i,j) = invpoisson\left(N_s \mu^*(i,j)\right) \tag{10}$$

where, n is the number of simulated earthquakes for each spatial and magnitude bins, N_s, is the total number of earthquakes simulated. The simulated number of earthquakes are computed as the mean rate of the earthquake time series displayed in Figure 2 and 3. This is where the stationarity comes into scene, which is essential for the forecast method presented in here.

After generation of synthetic catalogs, $\hat{\Omega}$, in order to determine the consistency of the forecast model, a number of consistency tests are used. Among these tests, the likelihood test, or the L-test is simply based on determining the likelihood of the observed data, Ω, given the forecast, Λ. Then, the likelihood of the observed data must be checked with the likelihood of the generated catalogs for the verification of the consistency of the proposed forecast. The likelihood of the observed data, Ω, with associated number of events for each spatial bin, $w(i,j)$, given mean occurrence rates obtained from spatial activity rate density maps with the number of events, $\mu(i,j)$ is the following

$$L(\Omega|\Lambda) = L(\mathrm{w}|\mu) = \log p(\mathrm{w}|\mu) = -\mu + \mathrm{w}\log(\mu) - \log(\mathrm{w!}) \tag{9}$$

Then, the simulated catalogs, $\hat{\Omega}$, are also processed for its likelihoods given the earthquake rates, μ, obtained from spatial activity rate density maps.

$$\hat{L}_i = L\left(\hat{\Omega}_i \middle| \Lambda\right) \tag{11}$$

Then, the joint likelihood of the observed data and the family of joint likelihoods of the simulated catalogs in equation 11 are then compared in order to determine the quantile score of the computed likelihood for the observed data. A quantile score is computed by using the following equation

$$\gamma = \frac{\hat{L}_i \middle| \hat{L}_i \le L}{\hat{L}} \tag{12}$$

By this equation, the fraction of simulated forecasts, $\hat{L}$, smaller or greater than likelihood of the observed data, L, is assessed. Indeed, the quantile score could be evaluated as the statistical significance of the joint likelihood of the observed catalog.

The number test, N-test, another crucial indicator in evaluating the proposed forecast model, simply requires the comparison of the observed number of events with the number of events for all the synthetic catalogs generated by the forecast. The test aims to verify the temporal sensitivity of the forecast model as it isolates the earthquake rates. The quantile score is computed in order to justify the number of observed earthquakes with the simulated number of earthquakes, which are probable with the existing model.

$$\delta = \frac{\hat{N}_i \left| \hat{N}_i \le N \right.}{\hat{N}} \tag{13}$$

The M-test, is based on the determination of the joint likelihood of the magnitude distribution of the observed events given the forecast and verification of the likelihood with the joint likelihoods of the simulated catalogs given the forecast model. Given the observation, Ω^m, and the forecast model, Λ^m, the likelihood of the observed data, M, is computed by using the following equation.

$$M = L\left(\Omega^m \middle| \Lambda^m\right) \tag{14}$$

Similarly, the likelihood of the magnitude distribution of the simulated catalog given the magnitude distribution of the forecast model is computed by using the following equation.

$$\hat{M} = L\left(\hat{\Omega}^m \middle| \Lambda^m\right) \tag{15}$$

Here one thing should be clarified; the earthquake rates as spatial activity rate densities obtained from the forecast model has to be normalized by using the ratio of observed events to the total number of events used to generate the forecast.

$$\begin{aligned} \Omega \sim w^m &= \sum w(i,j) \\ \Lambda \sim \lambda^m &= \frac{N_{obs}}{N_{forecast}} \sum \lambda(i,j) \end{aligned} \tag{16}$$

Indeed, the sum of all the spatial activity rate densities in each bin gives the total number of events used to generate the forecast. The reason for such an adjustment is to be able to isolate the magnitude distribution and avoid the influence of different number of events over the magnitude

distribution. The quantile score, κ, is developed to test the consistency of the observed magnitude distribution with the forecast.

$$\kappa = \frac{\hat{M}_i \left| \hat{M}_i \le M \right.}{\hat{M}} \tag{17}$$

The space test or S-test is developed to test the consistency of the likelihood of observed spatial pattern of earthquakes with the likelihood of simulated spatial patterns given the forecast model. The aim is to isolate the spatial pattern from the magnitude and temporal distributions and evaluate only the consistency of spatial patterns. Similar to L-test, N-test and M-tests, a quantile score is introduced for the quantification of consistency. The likelihood of the observed spatial pattern, Ω^s, given the forecast, Λ^s, is mathematically modeled by the following equation.

$$S = L\left(\Omega^s \middle| \Lambda^s\right) \tag{18}$$

Like the other tests, the likelihood of the simulated spatial pattern, $\hat{\Omega}^s$ given the forecast model, Λ^s, is computed by using,

$$\hat{S} = L\left(\hat{\Omega}^s \middle| \Lambda^s\right) \tag{19}$$

The quantile score is obtained by determining the fraction of likelihood of spatial patterns of simulated cases smaller or equal to the likelihood of the observed spatial distribution given the forecast model.

$$\varsigma = \frac{\hat{S}_i \left| \hat{S}_i \le S \right.}{\hat{S}} \tag{20}$$

The L-test, N-test, M-test and S-test are developed to validate the proposed forecast models in certain aspects. The consistency of the forecast model is checked with these tests, in other words any inconsistency or improbability of the forecast model is quickly identified through these tests.

The most crucial part in setting the forecast scheme and testing methodologies is the selection of the training, learning and forecast catalogs. If the training and learning catalogs were not long enough for the right identification of spatial, temporal and magnitude-wise seismic patterns, then it would not be surprising if the forecast model fails. Since there is not a method in determination of a sufficient length of a catalog, which allow the right identification of the seismic patterns, then subjective selection of the lengths of the training, learning and forecast methods is required. For that matter, a number of schemes shown in Table 1 are developed to monitor the performance of the proposed forecast method.

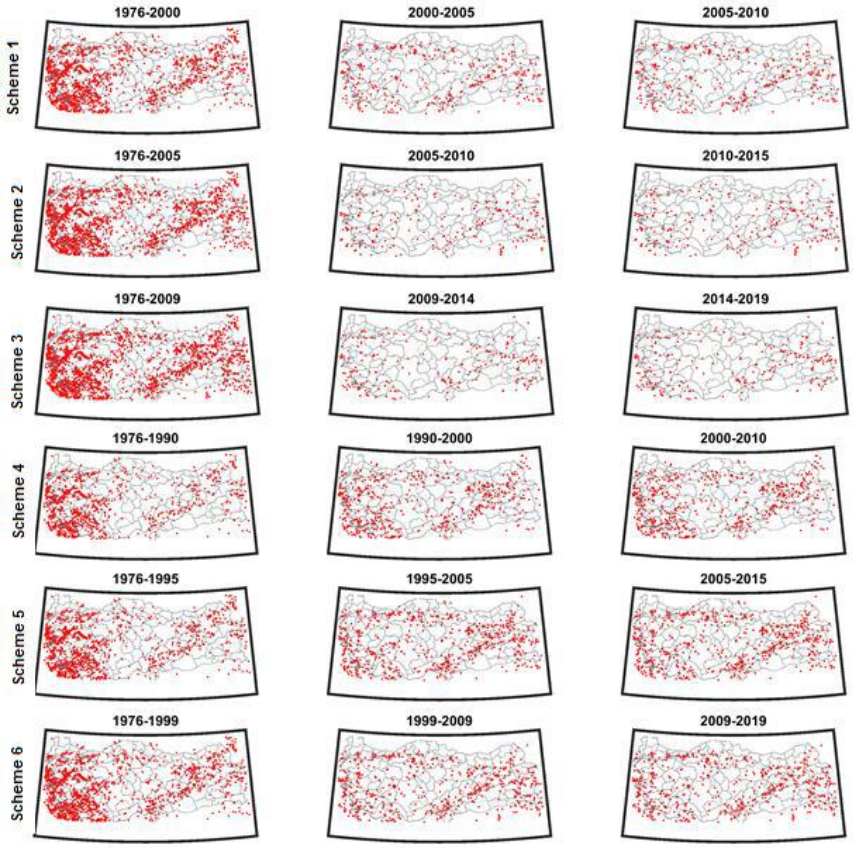

Figure 6. The Spatio-Temporal Distribution Patterns of Seismicity of Training, Learning and Observation Catalogs for All Schemes

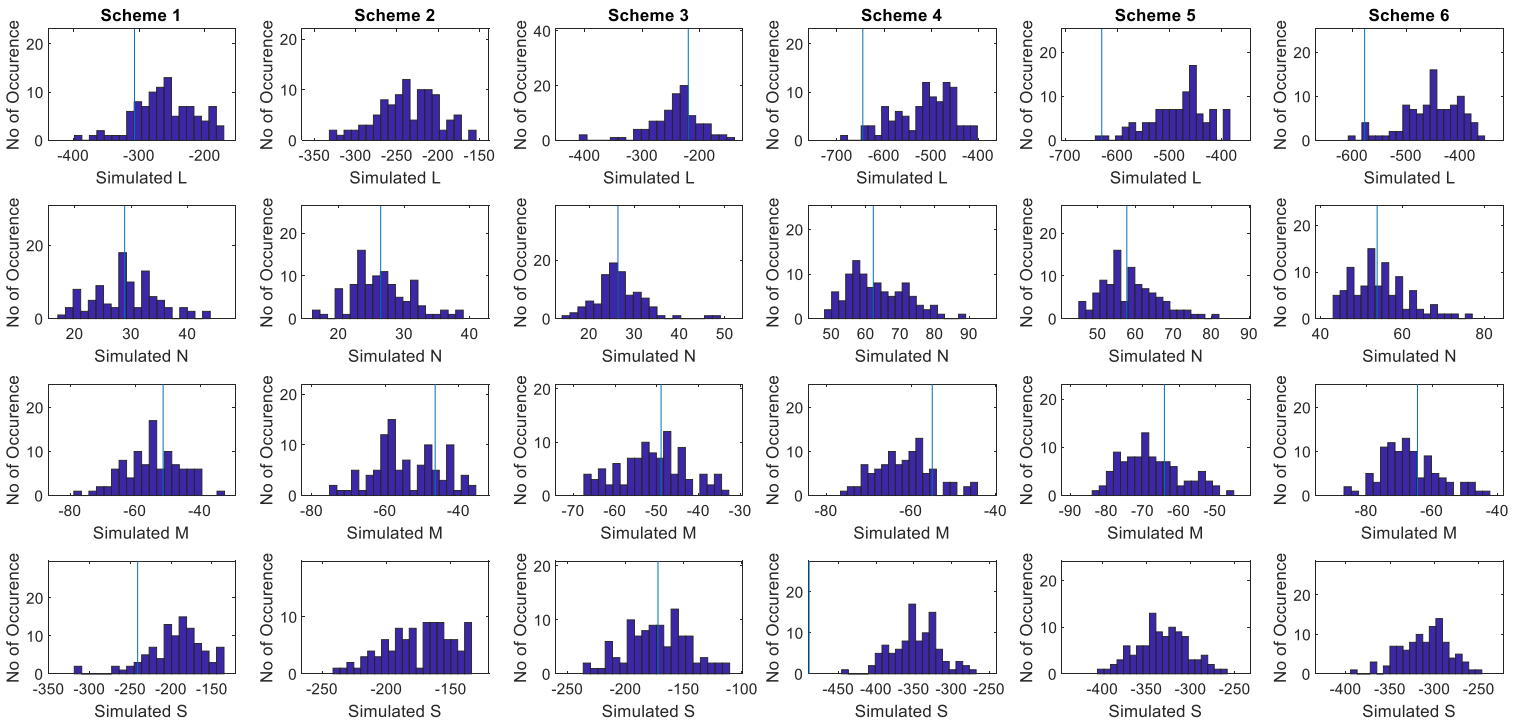

Figure 7. Histogram of the Likelihood Distribution of 100 Simulated Catalogs and the Likelihood of the Observed Catalog Given the Forecast Model (Vertical Lines)

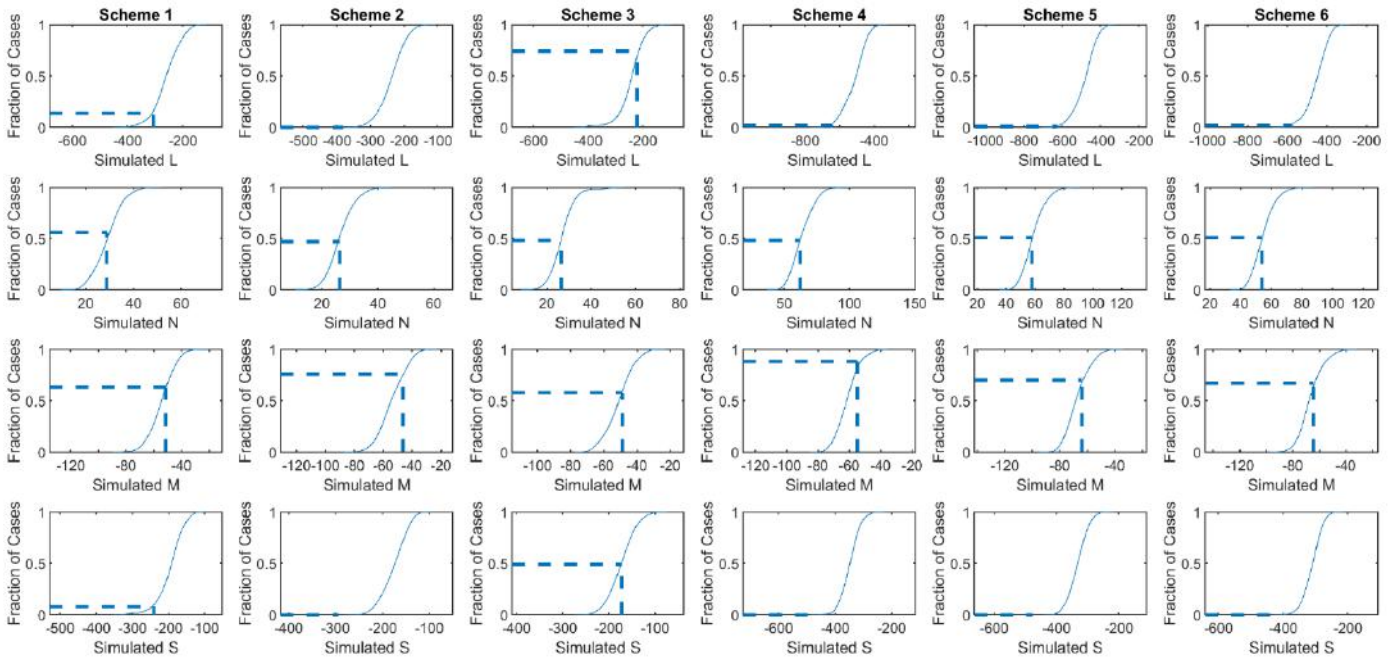

Figure 8. The Cumulative Distribution of Likelihood of Simulated Catalogs Given the Forecast and the Fraction of Cases the Likelihood of the Observed Catalog Greater than the Likelihood of Simulated Catalogs in terms of Likelihood, Number of Events, Magnitude and Spatial Distribution

Table 1. Forecast Schemes Developed for 5-year and 10-year Periods for Mw≥5.0

Scheme No	Forecast	Pattern Recognition		Pattern Projection
		Training Catalog	Learning Catalog	Verification Catalog
1	5-year	1976-2000	2000-2005	2005-2010
2		1976-2005	2005-2010	2010-2015
3		1976-2009	2009-2014	2014-2019
4	10-year	1976-1990	1990-2000	2000-2010
5		1976-1995	1995-2005	2005-2015
6		1976-1999	1999-2009	2009-2019

The training, learning and observation catalogs are displayed in Figure 6 for better visualization. All these maps at least clarify where seismically active areas and the areas with almost no seismic activity. Indeed, even with a simple visual examination, one can be convinced the existence of spatial and temporal patterns.

3. Results

The likelihood test identifies the consistency of the spatial distribution and earthquake rates of the observed catalog given the forecast model. For every spatial bin, by using the number of observed earthquakes and the expected earthquake rate in terms of spatial activity rate densities obtained from the forecast model, the Poisson probabilities are computed. For the entire are, if the individual probabilities are multiplied, the likelihood of the observed catalog given the forecast model is obtained.

Hence, this test can be considered as a requirement for the confirmation of the Poisson distribution of the earthquake occurrences. As can be followed from subplots in first row of Figures 7 and 8, the likelihood values fall within the boundaries of the likelihoods of the simulated catalogs. Given the precision of the grids and the spatial scale, the results cannot be discarded as failure at all. It can even be said that, except for Scheme 2, the observed catalog can be considered as one of the possibilities that could be occurred before it did.

The likelihood of earthquake rates of the observed catalog given the forecast model is very much consistent according to the N-tests. Hence, it can safely be concluded that the earthquake rates of the training and learning catalogs are very close to observed catalogs, which mean that the Poisson assumption holds true for each scheme.

Table 2. Comparison of Forecasted (Mw≥5.0) and Observed Number of Earthquakes (Mw≥5.0) for 5-year and 10-year Periods

Scheme No	N_{obs}	$\mu(N_f)$.	$\sigma(N_f)$.	Fraction of Cases
1	31	29,03	5,68	0,56
2	37	26,48	4,64	0,47
3	23	26,78	5,41	0,48
4	66	63,43	8,40	0,48
5	68	58,65	7,44	0,51
6	63	54,54	6,91	0,51

The number of observed earthquakes and the mean and standard deviation of number of earthquakes of the simulated catalogs given in Table 2 is sufficient to prove the existence of a continuous earthquake rates. However, it should also be mentioned that the deviation of the number of observed earthquakes and the mean earthquake rate obtained from simulated catalogs in schemes 4 to 6 implies that the proposed models capabilities are limited beyond a certain limit.

The fraction of cases greater than the likelihood of the observed catalog given the forecast is also an indicator in determination of the consistency of the forecast models. Given in the last column of Table 2, as the fraction of cases remain closer to 50%, the forecast model can be said to be one of the very probable models.

According to Figure 7 and 8, the likelihood of the magnitude distribution of the observed catalog given the forecast model is quite consistent as the likelihood values of the magnitude distribution of the 100 simulated catalogs given the forecast model envelops the likelihood. Scheme 3 differs in high consistency of the likelihood values relative to the other schemes, whereas the likelihood of the other schemes slightly deviates from the mean of the likelihood of the simulated catalogs in terms of its magnitude distribution.

The likelihood of the spatial distribution obtained by using the observed catalog is clearly not consistent as can be viewed from Figure 7 and 8. Only scheme 3 display satisfactory results while the likelihood values of other schemes are either at the lower tail of the cumulative likelihood distribution of the simulated catalogs or not within the boundaries of the cumulative distribution at all.

At this point, it should be emphasized that the high precision used in the analysis, in other words the sizing of the grids, and the subjectivity involved in selection of the training, learning and observation catalogs have a determinant influence over the results of this study. The spatial distribution, which is one of the most important element in forecast studies,

is very sensitive to the methods used in modeling. Unlike the magnitude distribution and the earthquake rates, which are not as sensitive due to overall handling of the data, the spatial distribution require a detailed modeling.

Among the schemes, the scheme 3 can be identified as the most consistent model with the observed catalog. This implies that, the division of the catalog into training, learning and observation catalogs seem to be quite successful in catching the embedded seismic patterns. Therefore, it can be concluded that, there is a pattern of seismicity that could be identified and successfully projected into the future, but since subjectivity involved in identification of this pattern, a lot of effort must be spent in identification.

4. Conclusion and Recommendation

The main difference of this study from most of the previous studies is that the minimum completeness magnitude threshold of the catalogs is 3.9 in moment magnitude. On the other hand, studies based on RELM techniques utilizes input catalogs with lesser minimum magnitudes to try to achieve forecast of the higher magnitude earthquakes. Clearly, as the higher magnitudes imply longer return periods, even longer than the covered period of the gathered catalogs, the lack of smaller magnitude earthquakes might cause either fluctuations or nonstationary behavior of the earthquake times series.

In such a setting, with higher minimum completeness magnitude threshold, this study aimed to investigate the existing seismic patterns, which the forecast models could capture. For that matter, the consistency tests indicate a continuity in magnitude distribution characteristics and earthquake rates regardless of the subjective partitioning of the catalog into training, learning and observation catalogs. Indeed, the magnitude distribution, which might give clues about the physical characteristics of the earthquake producing areas, is an indicative factor in seismic studies. On the other hand, the earthquake rate is important in revealing the nature of temporal distribution characteristics. A continuous earthquake rate, regardless of its interval, point to the Poisson nature of the data, which indeed is the basic assumption defining the earthquake occurrence pattern in temporal domain.

The likelihood and the spatial distribution patterns have both include the spatial spread of the earthquakes. Relatively lower performance of the L-tests and S-tests directly point to the high precision and the pattern mismatches due to the subjective partitioning of the catalogs. Indeed, the successful consistency tests in Scheme 3 imply that there is a pattern in magnitude, rate and spatial distribution of the investigated data, but it’s the partitioning that cause a mismatch between training, learning and

observation catalogs. Consequently, it could be concluded that one of the issues in using the investigated method with larger minimum magnitude of completeness is the subjective partitioning. The uncertainties that may arise due to limited amount of data and the inadequacy of the training, learning and observation parts in the determination of earthquake rates, spatial and magnitude distributions is one of the main cause of lower performance of the investigated forecast technique. At this point, it should also be mentioned the sensitivity, especially in spatial dimension, has a decisive influence over the performance of the investigated method as well. With lower sensitivity, in other words larger grids, a higher performance would be expected.

Another cause of lower performance could be identified as the irregularity of the earthquake time series. The fluctuations causing these irregularities sways the earthquake rates even beyond 95% confidence interval might be the cause of lower performance of some of the tests (Lombardi and Marzocchi, 2010). Indeed, if the earthquake time series is stationary, as the covered period for the training, learning and verification catalogs becomes longer, it is automatically expected that the irregular fluctuations in terms of swells and contractions would eventually even out. However, since the short and long-term forecasts mostly do not cover beyond 10 years, these irregularities of the earthquake time series would create a flaw in the forecast algorithm. The fact that these irregularities would eventually even out in longer terms would be trivial for the urgent expectations as materialized by the developed forecast schemes. The pattern of failure in some of the tests and explanations of the reasons of failure is quite informative about the issue of stationarity in earthquake forecasts based on spatially smoothed seismicity models. The susceptibility of the method to the slightest fluctuation or variation in temporal pattern leading to the failure of the method would bring the question about the degree of stationarity required sufficient for the method to perform within acceptable limits. A straight line, which means a constant number of earthquakes per unit time, would definitely yield the perfect results when the method is applied. However, with a perfect straight line, or a constant earthquake rates, one does not even need to perform an extrapolation let alone forecast which would be unnecessary.

In any case, whether the earthquake time series display uneven fluctuations or slight irregularities, the discrepancies in the forecast model cannot be avoided (Bray and Schoenberg, 2013). Hence, a further development of the method should be sought to account for all the irregularities and uneven fluctuations regardless of the fact that eventually all would be even out.

REFERENCES

Bray, A., Schoenberg F.P. (2013) Assessment of Point Process Models for Earthquake Forecasting, *Statistical Science*, 28(4), 510-520

Field, E. H. (2007). Overview of the working group for the development of Regional Earthquake Likelihood Models (RELM), *Seismological Research Lett*ers, 78(1), 7–16, doi: 10.1785/gssrl.78.1.7.

Helmstetter, A., Kagan, Y., Jackson D. (2006). Comparison of short-term and long-term earthquake forecast models for southern California. *Bulletin of the Seismological Society of America*, 96 (1), pp.90-106.

Helmstetter, A., Y. Y. Kagan, and D. D. Jackson (2007). High-resolution time-independent grid-based forecast for M ≥ 5 earthquakes in California, *Seismological Research Lett*ers 78, 78–86, doi: 10.1785/gssrl.78.1.78.

Helmstetter, A., & Werner, M. J. (2012). Adaptive Spatiotemporal Smoothing of Seismicity for Long-Term Earthquake Forecasts in California. *Bulletin of the Seismological Society of America*, 102(6), 2518-2529. doi: 10.1785/0120120062

Helmstetter, A., Werner, M. J. (2014). Adaptive Smoothing of Seismicity in Time, Space, and Magnitude for Time-Dependent Earthquake Forecasts for California, *Bulletin of the Seismological Society of America*, Vol. 104, No. 2, pp. 809–822

Hiemer S., Jackson D.D., Wang Q., Kagan Y.Y., Woessner J., Zechar J.D., Wiemer S. (2013) A Stochastic Forecast of California Earthquakes Based on Fault Slip and Smoothed Seismicity, *Bulletin of the Seismological Society of America* 103(2A):799-810, doi:10.1785/0120120168

Kagan, Y. and L. Knopoff (1977). Earthquake risk prediction as a stochastic process, *Physics of the Earth and Planetary Interiors*, 14, 97-108; doi: 10.1016/0031-9201(77)90147-9.

Kagan Y.Y., Jackson D., Rong Y. (2007) A Testable Five-Year Forecast of Moderate and Large Earthquakes in Southern California Based on Smoothed Seismicity, *Seismological Research Letters* (2007) 78 (1): 94–98. doi: 10.1785/gssrl.78.1.94

Lombardi, A. M., and W. Marzocchi (2010). The assumption of Poisson seismic-rate variability in CSEP/RELM experiments, *Bulletin of the Seismological Society of America*, 100, no. 5A, 2293–2300, doi: 10.1785/0120100012.

Rhoades D.A., Schorlemmer D., Gerstenberger M.C., Christophersen A., Zechar J.D., Imoto M. (2011) Efficient Testing of Earthquake Forecasting Models, *Acta Geophysica*, 59(4), 728-747

Schorlemmer, D. Gerstenberger M., Wiemer S., Jackson D. (2004) Earthquake Likelihood Model Testing, *Seismological Research Letters*, 78(1):17-29 doi: 10.1785/gssrl.78.1.17

Schorlemmer, D. and M.C. Gerstenberger (2007). RELM testing center, *Seismological Research Letters*, 78 (1), 30.

Schorlemmer, D., Zechar J.D., Werner M.J., Field E.H., Jackson D.D., Jordan T.H., and the RELM working group (2010) First Results of the Regional Earthquake Likelihood Models Experiment, *Pure and Applied Geophysics*, 167, 859-876

Shrolemmer D., Werner M.J. et al. (2018) The Collaboratory for the Study of Earthquake Predictability: Achievements and Priorities, *Seismological Research Letters*, 89(4), 1305-1313

Taroni, M., J. D. Zechar, and W. Marzocchi (2013). Assessing annual global M 6+ seismicity forecasts, *Geophysical Journal International*, 196(1),422–431, doi: 10.1093/gji/ggt369

Tsuruoka, H., Hirata, N., Schorlemmer, D. et al. (2012). CSEP Testing Center and the first results of the earthquake forecast testing experiment in Japan. *Earth Planet and Space*, 64, 661–671

Werner M.J., Zechar J.D:, Marzocchi W., Wiemer S. and the CSEP Italy Working Group (2010) Retrospective Evaluation of the Five-Year and Ten-Year 2 CSEP-Italy Earthquake Forecasts, *Annals of Geophysics*, 53(3), doi: 10.4401/ag-4840

Werner M.J., Helmstetter A., Jackson D.D., Kagan Y.Y. (2009) High Resolution Long- and Short-Term Earthquake Forecasts for California, *Bulletin of the Seismological Society of America* 101(4) doi: 10.1785/0120090340

Zechar J.D., Gerstenberger M.C., Rhoades D.A. (2010) Likelihood-Based Tests for Evaluating Space–Rate–Magnitude Earthquake Forecasts, *Bulletin of Seismological Society of America*, 100(3), 1184-1195

CHAPTER XI

ASSESSING THE VARIATIONS OF MAXIMUM AND MINIMUM TEMPERATURES OVER VAN LAKE BASIN, TURKEY[1]

Dr. Pınar BOSTAN

Van Yuzuncu Yil University, Van, Turkey, e-mail:pinaraslantas@yyu.edu.tr
Orcid ID: 0000-0002-8947-1938

1. Introduction

Climate change is a very important threat for our world. Discovering the variation of minimum and maximum temperature occurring in the long term is important for climate change studies. Especially minimum temperature trend is considered as an important indicator of climate change. The focus of this study is to reveal linear trends of annual minimum and maximum temperature in the long term over the Van Lake basin in Turkey. Meteorological observations measured from eight stations for 1975-2015 period over study area are used for trend analysis. Seven of these stations are inside the basin, while Baskale station is located outside the basin but close to the basin boundary. The reason for the Baskale station to be included in the study is that, it is aimed to measure the temporal trend in the maximum and minimum temperatures of a point located at a higher elevation than the other stations inside the basin.

Non-parametric Mann-Kendall trend test was used to reveal variation in the maximum and minimum temperatures. 90%, 95%, and 99% confidence intervals were used to detect trend. Results were associated with land cover status of basin. MODIS (Moderate Resolution Imaging Spectroradiometer) land cover datasets (MCD12Q1) belongs to 2001 and 2019 were used to evaluate land cover variation through time of Van Lake basin.

According to findings, increased minimum temperature trend is observed at six stations and increased maximum temperature trend is observed at seven stations. There is no observed trend for both variables in Ahlat station. In addition, minimum temperature trend is not observed at Gevas station. The amount of green areas in Ahlat and Gevas are higher and urbanization in these two areas are not as high as other locations. It can be said that, forest cover and urbanization have positive and negative effects on climate change, respectively. In Van, where urbanization is most intense, trend have been observed at maximum and minimum temperature

[1] The author acknowledge the General Directorate of Meteorology for providing monthly observational data.

according to 95% and 99% confidence intervals, respectively. Muradiye, Tatvan, and Baskale stations have maximum and minimum temperature trend at %99 confidence interval. The statistical values of Mann-Kendall test above four observed at minimum temperatures in Muradiye and Van are remarkable.

2. Materials and methodology

2.1. Material of study

The study area is Lake Van Basin that is located at the far east part of Turkey (Fig. 1). The area of basin is about 16.000 km^2. Lake Van basin has a high topography. The high mountains are located at the northern and southern parts of the basin. The mean elevation of basin is about 2200-2400 m., minimum elevation is about 1500 m. and maximum elevation is approximately 4000 m.

The primary data source was obtained from the General Directorate of Meteorology (MGM). The datasets consisted of monthly maximum and minimum temperature measured at eight meteorological stations between 1975 and 2015 over Lake Van basin of Turkey. Annual averages were calculated from monthly observations. Erroneous data (for example higher minimum temperature record than maximum temperature for the same month) and outliers were defined at the time series datasets and either validated or removed. Descriptive information of meteorological stations were given in Table 1.

In order to reveal land cover status and variation of basin, MCD12Q1 (land cover type) dataset was used in this study. The data provides global land cover types at yearly intervals (2001-present) with six different classification schemas. The Annual International Geosphere-Biosphere Programme (IGBP) classification type (land cover type-1) was used in this study. This data has 500 m spatial resolution and 17 class of land cover types. Each pixel on the map represents 250.000 m^2 (500 m x 500 m) that is 25 ha area. The datasets belong to 2001 and 2019 were downloaded from MODIS webpage.

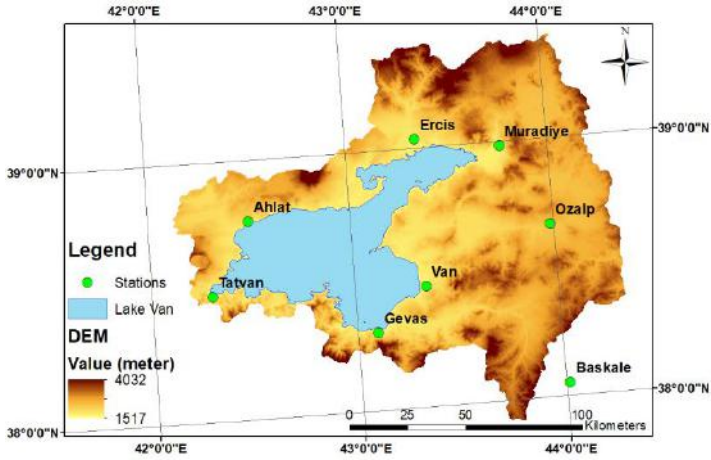

Fig. 1 Meteorological stations over Van Lake basin and the DEM (Digital Elevation Model obtained from 3 arc-seconds Shuttle Radar Topography Mission)

Table 1 Descriptive information of meteorological stations

Id	Station	Lat. (N)	Long. (E)	Elev. (m)
1	Muradiye	38.98	43.76	1706
2	Van	38.47	43.33	1671
3	Tatvan	38.50	42.28	1665
4	Ozalp	38.65	43.97	2100
5	Gevas	38.29	43.12	1694
6	Ercis	39.02	43.33	1678
7	Ahlat	38.74	42.47	1750
8	Baskale	38.04	44.01	2354

2.2 Methodology

2.2.1 Mann-Kendall test

Deviation of minimum and maximum temperature of eight meteorological stations for 1975-2015 were analysed with Mann-Kendall (MK) non-parametric test. The MK test is a rank-based non-parametric test to evaluate the trend existence and its significance. The MK test has been frequently used to detect trend in time series data (Bostan, 2020; Yue et al. 2002; Kendall 1970; Mann 1945). The MK test is based on the null hypothesis that the sampled data are independent and identically distributed, which means that there is neither trend nor serial correlation among the data points. The alternative hypothesis is that a trend exists in the data. A positive or negative value of Mann-Kendall test statistic *Z*

represents an upward or downward trend, respectively (Bostan, 2020; Cui et al. 2017; Bostan, 2013; Novotny and Stefan, 2007).

The first step in the MK method is to calculate a statistic definition by the variable *S*, which is the sum of the difference between the data points shown in the Equation (2.1) below:

$$S = \sum_{i=1}^{n-1} \sum_{j=i+1}^{n} Sgn(x_j - x_i) \tag{2.1}$$

where n is the number of values in the data, and x_j and x_i are the sequential data values.

When $n \geq 8$, the statistic S is approximately normally distributed with the mean and variance (corrected for ties) as follows in Equations (2.2 and 2.3):

$$E(S) = 0 \tag{2.2}$$

$$V(S) = \frac{n(n-1)(2n+5) - \sum_{m=1}^{n} t_m m(m-1)(2m+5)}{18} \tag{2.3}$$

where t_m is the number of ties of event m. Tie *(t)* represents the number of observation groups that have the same value. If there is one group of observations with three exact values in the dataset, then t equals *1 and m* equals *3* (Bostan, 2020; Bostan 2013). The normally distributed S statistic allows for the computation of the standardised test statistic Z of the MK test. The Z statistic is calculated as presented in Equation (2.4):

$$Z = \begin{cases} \dfrac{S-1}{\sqrt{V(S)}}, S > 0 \\ 0, S = 0 \\ \dfrac{S+1}{\sqrt{V(S)}}, S < 0 \end{cases} \tag{2.4}$$

3. Results and discussion

Mean annual minimum and maximum temperature values of meteorological stations were represented visually by Fig. 2 and 3,

respectively. To identify trends at the data, linear, quadratic and cubic trend lines were applied to observations of each station.

MK test results for all stations were represented in Table 2, and increasing and decreasing trends according to three confidence intervals were highlighted.

There was a tendency to increase in the annual average minimum temperature values at all stations except the Gevas (Fig. 2).

The increases in minimum temperatures were remarkable in Van, Muradiye, Tatvan, and Baskale stations. Among these settlements, the places where urbanization is growing rapidly are Van and Tatvan. Minimum temperatures increased more than 2 °C in the Van and Tatvan over the study period.

There was a subtle tendency to increase in minimum temperatures in Ahlat, Ercis, and Ozalp stations where urbanization are less.

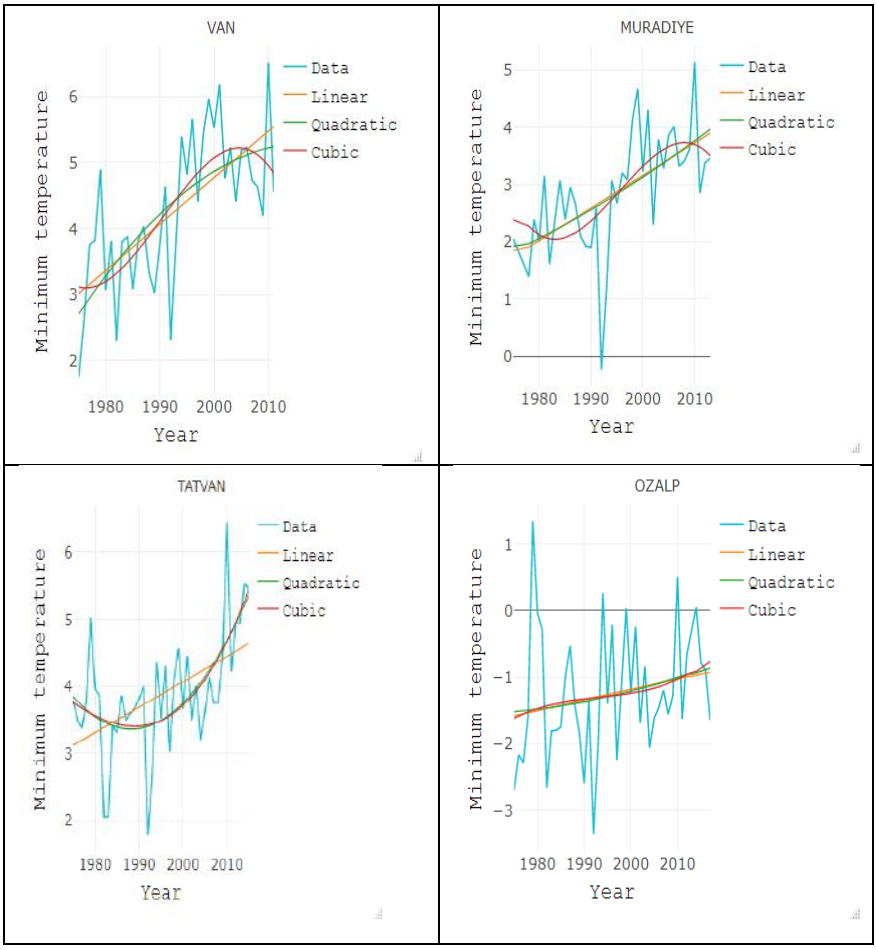

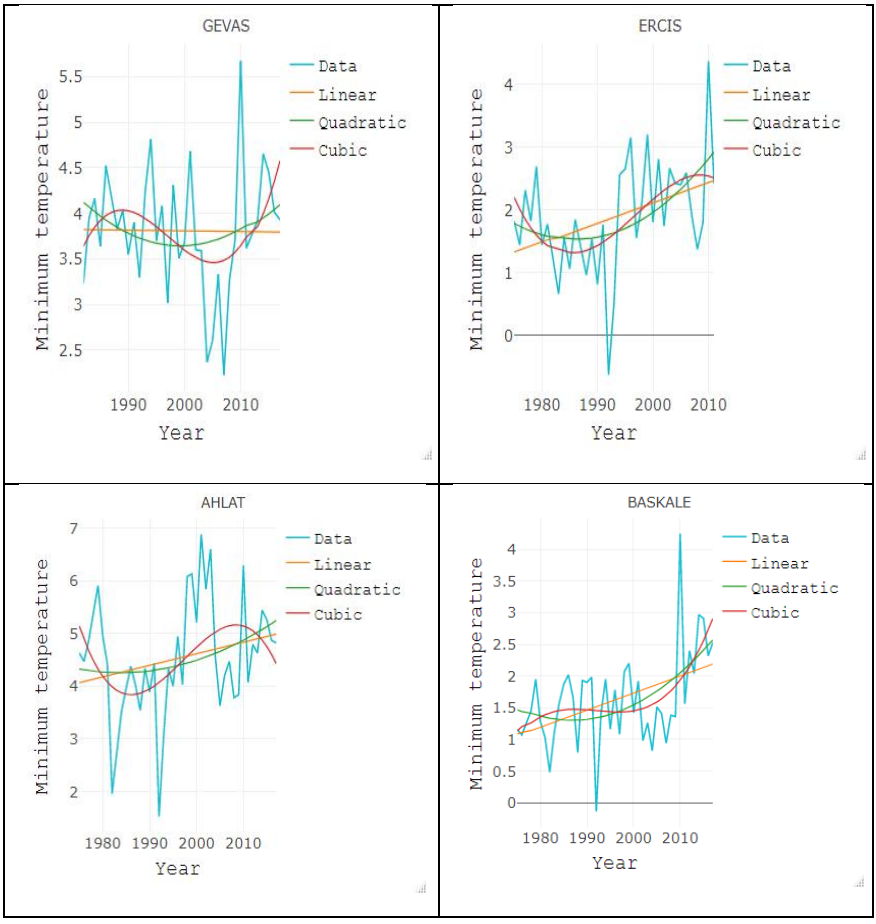

Fig. 2 Visual representation of annual minimum temperature trend of meteorological stations

There is a trend towards an increase in mean annual maximum temperatures at all stations (Fig. 3 and Table 2). Muradiye, Tatvan, Ozalp, Gevas, and Baskale have significant trend according to %99 confidence interval (Table 2). There is an increasing trend in Van with respect to the 95% confidence interval. As with the minimum temperature trend, there is no high increasing trend in Ahlat and Ercis in the maximum temperature values.

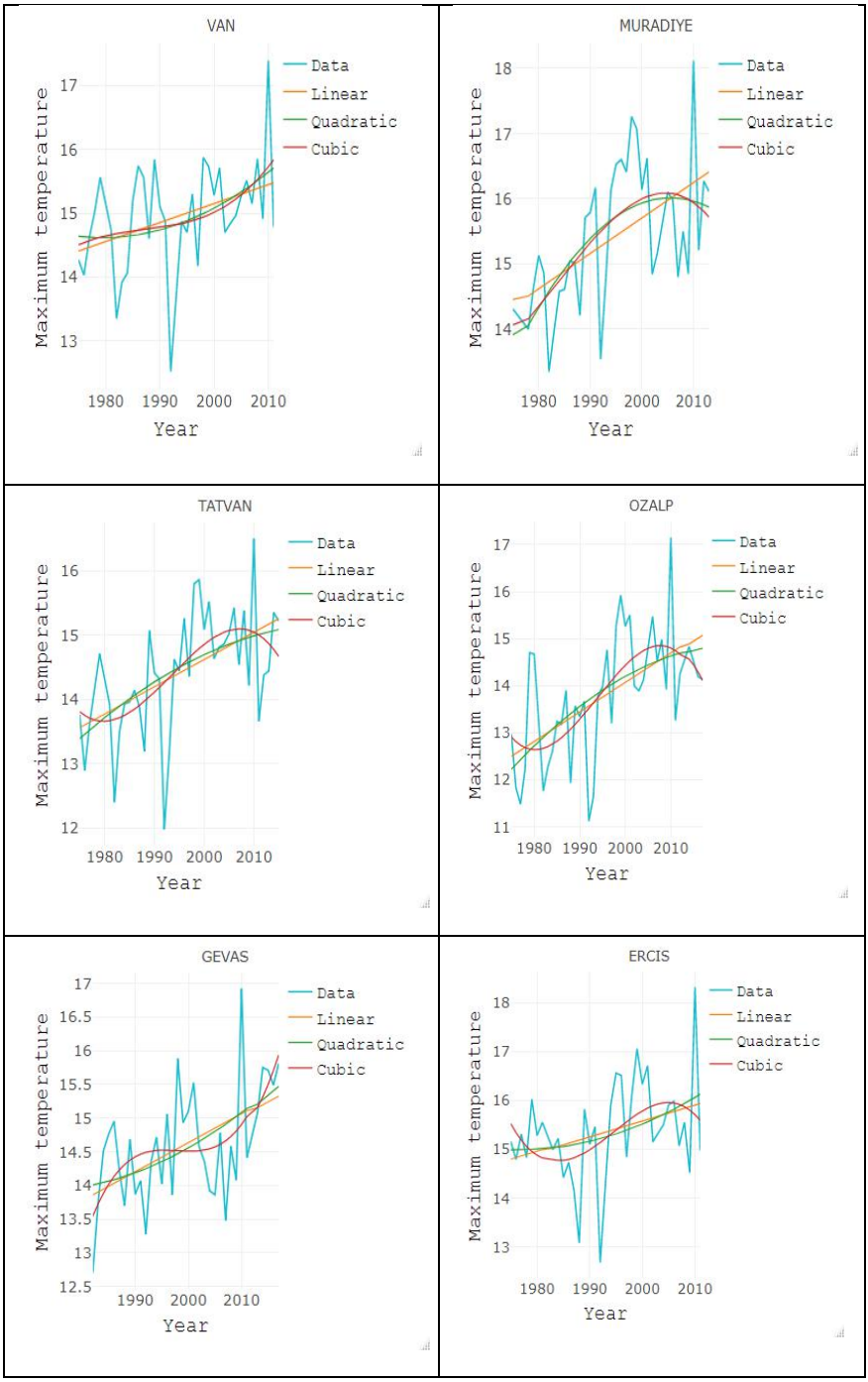
VAN
Maximum temperature
Year
Data
Linear
Quadratic
Cubic
MURADIYE
Maximum temperature
Year
Data
Linear
Quadratic
Cubic
TATVAN
Maximum temperature
Year
Data
Linear
Quadratic
Cubic
OZALP
Maximum temperature
Year
Data
Linear
Quadratic
Cubic
GEVAS
Maximum temperature
Year
Data
Linear
Quadratic
Cubic
ERCIS
Maximum temperature
Year
Data
Linear
Quadratic
Cubic

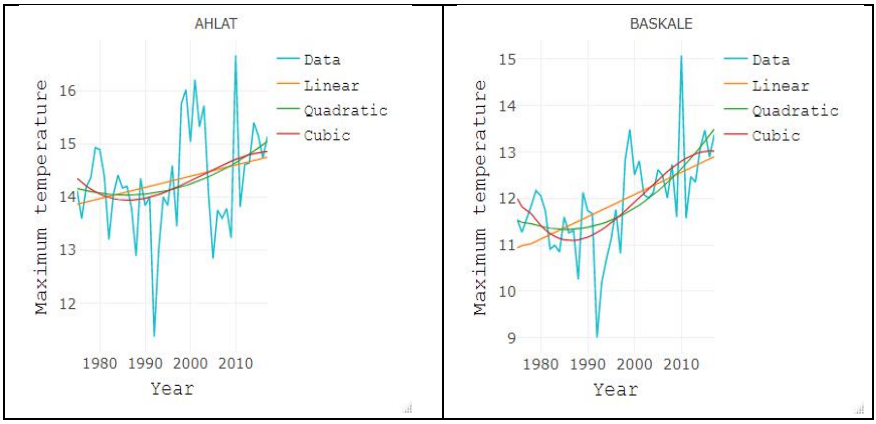

Fig. 3 Visual representation of mean annual maximum temperature trend of meteorological stations

Table 2 MK trend test statistic, Z_{MK} of each meteorological station ('•', '*', and '**' emphasize whether Z_{MK} is statistically significant with respect to 90%, 95%, and 99% confidence intervals respectively)

	Tmin	**Tmax**
Muradiye	4.2**	3.31**
Van	4.04**	2.12*
Tatvan	3.36**	3.76**
Ozalp	1.86•	4.05**
Gevas	-0.18	2.77**
Ercis	1.89•	1.65•
Ahlat	1.51	1.34
Baskale	2.61**	3.67**

3.1. Evaluation of land-cover change

When we look at the two land cover maps (Fig. 4 and 5), the striking point was that the croplands have increased considerably since 2001. While the total croplands on the basin was approximately 122.000 ha (4888 pixel as represented at Table 3) in 2001, this number was around 180.000 ha (7229 pixel as represented at Table 4) in 2019. Most of this change has happened from grasslands to cropland areas.

Urban and built-up areas have increased over the basin with little growth from 2001 to 2019 (Tables 3 and 4). Over the course of 19 years, about 400 hectares of urban growth have taken place over the basin. This growth has largely occurred in city centres and surroundings. Generally, the grassland areas have transformed into urban and built-up areas.

Some of the grasslands observed in 2001 have turned into croplands and urban areas during 19 years.

There has been some reduction in barren spaces. An important part of this area has turned into cropland areas (Fig. 4 and 5).

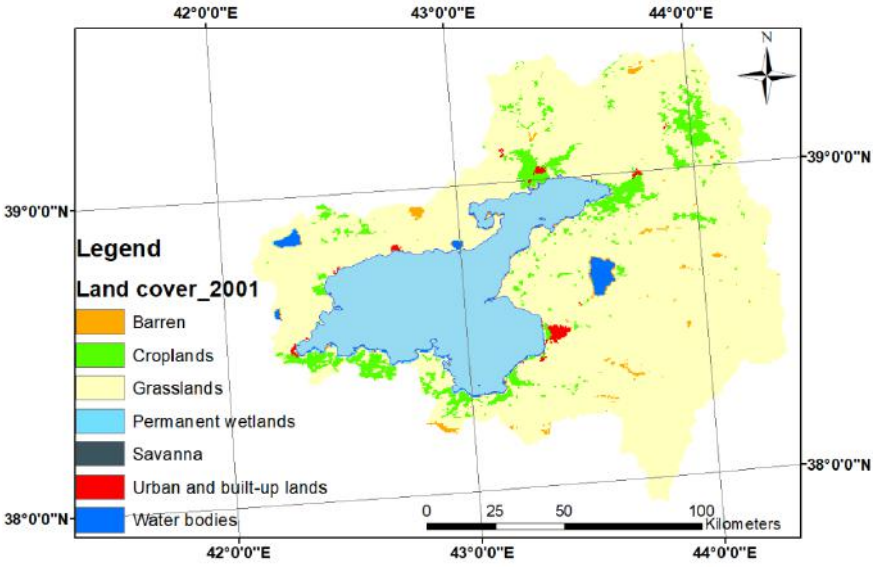

Fig. 4 MODIS land cover dataset belongs to 2001 of Van Lake basin

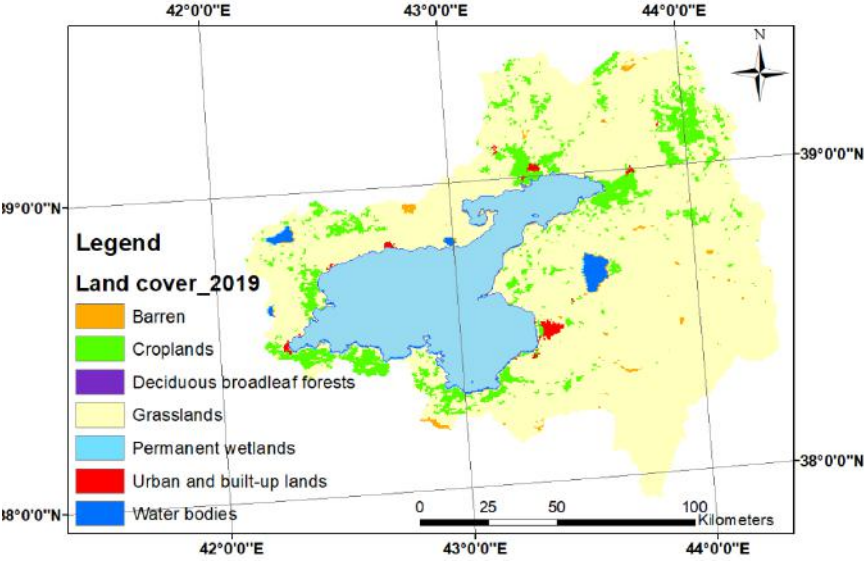

Fig. 5 MODIS land cover dataset belongs to 2019 of Van Lake basin

Table 3 Land cover of Van Lake Basin obtained in 2001

Id	Value	Count	Land cover type
1	9	1	Savannas
2	10	60821	Grasslands
3	11	350	Permanent wetlands
4	12	4888	Croplands
5	13	368	Urban and built-up lands
6	16	993	Barren
7	17	16612	Water bodies

Table 4 Land cover of Van Lake Basin obtained in 2019

Id	Value	Count	Land cover type
1	4	1	Deciduous broadleaf forests
2	10	58582	Grasslands
3	11	493	Permanent wetlands
4	12	7229	Croplands
5	13	384	Urban and built-up lands
6	16	717	Barren
7	17	16627	Water bodies

4. Conclusions

This study investigated the trend existence of minimum and maximum temperature over Van Lake basin during 1975-2015 by visually (Fig. 2 and 3) and MK trend test (Table 2). Increasing minimum temperature trends were observed at six stations, increasing maximum temperature trends were observed at seven stations. None of the stations had a decreasing trend for both variables that could be considered statistically significant.

Van and Tatvan where the high trend were observed, are the places with the highest population density within the basin boundaries. Significant increase in minimum and maximum temperatures in Van and Tatvan may be one of the reasons for rapid urbanization.

Gevas and Ahlat where no significant minimum temperature trend were observed, are two settlements with less urbanization and more natural forest cover. There is also no trend in maximum temperatures in Ahlat, but there is a significant increasing trend in Gevas for maximum temperatures. Agriculture is a high priority activity in Gevas, so being prepared for warmer and drier conditions in the future is of great importance for efficient agricultural activities in this region.

High test statistics values at maximum and minimum temperatures are remarkable in Muradiye and Baskale. In Ozalp, high test statistics values only at maximum temperatures is striking. Although urbanization was not

much in Muradiye, Baskale and Ozalp, forest cover takes up little space. In addition, Muradiye, Baskale and Ozalp were located further away from the Van Lake, so they cannot benefit from the temperate effect of the lake. These may explain the upward trend at Muradiye, Baskale, and Ozalp stations. Since the increase in temperature trend may pose a risk to natural life and resources, these regions should be given importance in future development plans.

References

1. Bostan, P., (2020). Assessing variations in climate extremes over Euphrates Basin, Turkey. Theor Appl Climatol 141, 1461-1473 https://doi.org/10.1007/s00704-020-03238-9.
2. Bostan, P. A., (2013). Analysis and Modelling of Spatially and Temporally Varying Meteorological Parameter: Precipitation over Turkey, A thesis submitted to the Graduate School of Natural and Applied Sciences of Middle East Technical University, Ankara.
3. Cui L, Wang L, Lai Z, Tian Q, Liu W, Li J (2017) Innovative trend analysis of annual and seasonal air temperature and rainfall in the Yangtze River Basin, China during 1960-2015. Journal of Atmospheric and Solar-Terrestrial Physics 164: 48-59.
4. Kendall, M. G., (1970). Rank Correlation Methods, 4th Ed., Griffin, London.
5. Mann HB (1945) Nonparametric tests against trend. Econometrica 13, No. 3, 245-259.
6. Novotny, E.V., Stefan, H.G., (2007). Stream flow in Minnesota: Indicator of Climate Change, Journal of Hydrology 334, 319-333.
7. Yue, S., Pilon, P., Phinney, B., Cavadias, G., (2002). The influence of autocorrelation on the ability to detect trend in hydrological series. Hydrological Processes 16, 1807-1829.

CHAPTER XII

DESIGNING PERFORMANCE MONITORING AND EVALUATION SYSTEM OF A THERMAL POWER PLANT USING PROCESS PARAMETERS[1]

Dr. Mehmet BULUT

Electricity Generation Company Inc., Ankara, Turkey
e-mail: mehmetbulut06@gmail.com, Orcid ID:0000-0003-3998-1785

1. INTRODUCTION

Thermal power plants, which are still widely used for electricity production from hydrocarbon sources, are one of these Electricity generation options. Thermal Power Plants, due to their complex structure, are composed of sections that interact with each other and are called units, and a change in the performance of any unit or equipment affects the operation of the entire plant positively or negatively. Performance monitoring and evaluation systems are designed to support the measurement and monitoring of the performance of staff and equipment and to increase the availability by preparing equipment based maintenance plans according to the maintenance needs of the equipment.

Among the types of energy, electrical energy has become as vital to society as blood flowing in human veins. Although there are many different generation techniques for electricity generation, hydrocarbon-based thermal power plants maintain a high ratio among them. A Thermal Power Plant, which is one of the electricity generation options, consists of many elements that interact with each other and any fluctuations in the performance of any of them affect the whole system positively or negatively. There are a number of parameters that determine the performance of each of these components and which have an impact on its performance and which should be known.

In order to obtain maximum power from the plant, it should monitor the interaction between the plant equipment and their negative impact on each other should be minimized. For example, a problem with the air filters of a combined cycle power plant with natural gas fuel does not only affect the compressor, but also changes in the performance of all elements up to the cooling tower and leads to losses in power generation. Therefore, it is quite problematic for the operator in the plant control room to determine the reason behind the change in the performance of the

[1]Research supported by TUBITAK within the scope of the project titled "Thermal power plant performance monitoring and evaluation system design and implementation" with 110G092 project number.

element and which measures should be taken to eliminate it timeously. In power plants, instantaneous values are taken and transmitted to the control room by data collection systems (SCADA, DCS) for control purposes. However, when we look at the combined cycle power plant, it is seen that there are approximately 2000 parameters that should be followed for even only a single unit. Therefore, by using advanced automation systems, it is tried to reduce the intervention and operational load in the control room.

Automation systems are only geared towards power plant operation and aim to facilitate the operation, especially to reduce the workload of the operator and to minimize the human factor. These systems for the purpose of control and automation collect the necessary data suitable for their purpose and store them temporarily. For this reason, in the plants where the automation system is located, sufficient data and appropriate platforms cannot be provided by the operators to evaluate the deterioration in the performance of the plants and equipment over time. Furthermore, since the deterioration in the performance of the equipment cannot be observed over time, the maintenance need for the components with impaired performance can only be assessed according to the periodic maintenance time situation. Since it is up to the operator to decide whether equipment needs maintenance, the performance of the equipment continues to degrade further.

However, by measuring and monitoring the performance of the plant elements and equipment, it is possible to support the preparation of maintenance programs according to the maintenance needs of the equipment and thus to perform the maintenance on-site and on time and increase the availability. For this purpose, performance monitoring and evaluation systems are designed. These systems continuously monitor and evaluate the data obtained during the operation of the plant, calculate the required performance parameters for the units and equipment and compare them with their actual values. Therefore, the performance monitoring and evaluation system calculates the corrected value of the measured value in the reference environment and operating conditions and compares it with the reference values and determines the degradation in the unit or equipment. In terms of performance monitoring and evaluation, it is very important to regularly store data and evaluate the past and present situations based on this data. Therefore, automation and control systems and performance monitoring and evaluation systems serve different purposes.

There have been several previous studies to analyze the behavior of Thermal Power Plants (TPPs) using optimization techniques Konrad Swirski proposed using statistical data analysis to improve the features of existing performance monitoring systems in their study [1]. Process

performance monitoring and evaluation; It is a process that needs to be done to measure, maintain and improve the thermal efficiency, maintenance planning of the power plant [2]. In the study of Özdemir et al., the performance of the plant was examined in four main parameters as Thermal Efficiency, Pipe Efficiency, Turbine Efficiency and Boiler Efficiency in the light of the data received from the Thermal Power Plant. In the five-year period of a system operating under high temperature and pressure, contamination, wear, fatigue, etc. that occur in the system elements. performance changes due to reasons have been identified [3]. For the variation of each of the operational parameters in a thermal power plant, performance calculations are made to configure the energy variation database. These can then be used as assessment criteria based on detecting deviations from a reference system updated during plant performance tests. Balaram et al, they aimed to identify the operational gaps associated with the operation of operational parameters in the power plant process [4].

It is of great importance to define the operational gaps associated with the operational parameters in the power plant process [5] and calculate key performance indicators for the management of power plants [6]. Blanco in their study, aims to identify and monitor the semi-stable conditions associated with measurements in the time series of the power plant process [7]. The models are then used for performance monitoring by comparing the calculated measured value with the reference value. The data-based migration plant system modeling method ensures that the model, which can provide a higher accuracy in performance monitoring, is constantly updated. By using the real-time operating data of the plant, the system monitoring study can be done by creating the mathematical models of the plant components [8]. The maintenance priorities [9] required for the power plant can be made by performing performance modeling [10] of a thermal power plant or by using the simulation and parametric optimization of thermal power [11]. Similarly, it can be evaluated as a decision support system [12] about the plant as a tool for safer operation in the plant.

In this chapter, it is aimed to continuously monitor the current performances and performance losses of units and equipment in order to determine operational problems of power plant operators and managers, to improve unit performance, to accomplish maintenance plans and to make economical decisions. In order for the developed performance monitoring and evaluation system to be successful and efficient, it should indicate the amount of change in unit and equipment performances and the share of equipment in total performance loss. In this way, power plant operators can estimate the amount, location and economic losses resulting from this loss. In addition to providing an economic enterprise

with continuous monitoring of performance, it will also improve future operational conditions and increase safety via helping to predict future problems.This chapter describes the development and design of the Power Plant Performance Monitoring and Evaluation System based on the parameters affecting the performance of thermal power plants.In order to monitor and evaluate the performance of thermal power plants, the requirements of the system were revealed and the efficiency and performance increases to be achieved by designing and using this system specific to a natural gas power plant were examined.

2. TYPES OF PERFORMANCE MONITORING AND EVALUATION SYSTEMS

2.1 Automation systems

Computer-controlled thermal power plant automation began to develop in the world in the 1960s. Especially in parallel with the development of computer technology it has become widespread rapidly. Computer-controlled thermal power plant automation started in Japan in 1968, SPAC-1 automation software developed by Toshiba was applied to the Hachinohe power plant's 3rd Unit of 250 MW power capacity and turbine automation was provided. Since 1968, the scope and depth of power plant automation have expanded step by step and the 2nd unit of the Hokkaido Power Company Shiriuchi Power Plant is shown as a good example of today's level of automation in power plants. Today's popularity and success of power plant automation are analyzed as follows. These items are regarded as the basic factors of the popularity of today's successful plant automation.

The most important factor, however, is the evolutionary approach of plant automation development. Its scope has been evolved as follows;

1. Turbine run-up control,
2. Boiler start-up control,
3. Auxiliaries start/stop control,
4. Unit shutdown control,
5. Unit normal mode control,
6. Emergency mode control.

All existing thermal power plants have control and automation systems in different structures to control the process. Automation systems currently used in power plants are generally designed for the following purposes:

- To reduce the number of manual operations while the plant is in operation,
- To contribute to the service life extension of the plant elements,
- To ensure that the downtime is as short as possible,
- Performing high reliability generation with field data,

- Minimizing interface problems for power plant operators, manufacturers and automation system designers
- Ensuring mutual control of the elements interacting with each other,
- Commissioning and deactivation of the plant safely and smoothly.

2.2 Performance monitoring systems

Unlike purposes of automation systems, performance monitoring and evaluation systems provide online data extracted from measurement points placed in the system to determine the performance of both the equipment and the plant. By storing this data, a data bank is created on both equipment and power plant scale, thus enabling the monitoring of the performance changes of both power plant elements and power plant. Furthermore, it compares the design performance of the plant with its current situation considering the changing external conditions and thus provides the operator with information on whether the change in performance is due to external conditions, aging of the plant or another reason. Thus, the operator can monitor the change in performance of the plant elements due to aging and also have information about when the improvements should be made.

- The advantages of performance monitoring and evaluation systems can be listed as follows;
- To provide instant information about the operation of the plant via calculating the efficiency and degradation of the plant and its components
- Increasing plant revenue by increasing plant availability
- To monitor the performance of the equipment and thus to identify problems in advance
- To create a data bank on the operating characteristics of equipment and power plant
- To determine the improvement potentials of the power plant and its components
- Improving the availability by providing rapid diagnosis and faster solutions in case of failure
- To create a background for predictive maintenance methods
- To increase the availability by reducing the number and time of start-ups
- To optimize load distribution and operation in power plant groups
- To protect the power plant components and equipment against the

life cycle shortening.

However, none of the performance monitoring systems developed to provide great benefits in terms of electricity supply, production costs, operation of plants and availability are able to provide these benefits. There are many difficulties in determining the most appropriate one from the existing performance monitoring and evaluation systems of which with different aims and abilities, to the needs of the plants. The practices show that these generic software programs do not provide the expected benefits in general. Therefore, designing performance monitoring and evaluation systems according to the structure and needs of the plants will provide many more benefits than using a package program.

Firstly, since a measurement, monitoring and evaluation will be made according to the priorities and needs to be determined in the power plants, the outputs to be obtained from these systems will be able to respond more to the expectations of the plant (plant and equipment performance values, reference performance values, performance losses and indicators, solution suggestions, etc). For example, the average sudden stop time of units is 70 hours for power plants. For a 400 MW power plant, the generation loss resulting from these halts is approximately 28,000MWh. Even if these downtimes can be reduced by 50% thanks to a performance monitoring and evaluation system specific to the power plant, the power plant will be able to generate an additional 14,000,000 kWh of energy. In many of the SCADA or other monitoring systems used in today's power plants, performance analysis either can not be accomplished or intended to. In many of the SCADA or other monitoring systems used in today's power plants, performance analysis either can not be accomplished or evaluated for this task.

Depending on the development of automation and computer systems and the increasing importance of efficiency as much as production with energy crises in the world, it has come to the fore that the operation of the power plants is not sufficient and the performance should be monitored also. Therefore, plant equipment manufacturers have developed plant monitoring systems with or after the plant. For example, GE has developed System 1 (software for optimization and diagnostic) to share and organize power plant information. System 1 includes real-time optimization of the equipment and selected process, condition monitoring and event diagnostics and is widely used in many industries. Thanks to this system, it is possible for the personnel to identify and evaluate the critical situations quickly. Therefore, equipment availability and reliability are increased and maintenance costs are reduced.

Alstom has developed the flexible automation system ALSPA P320, which includes the advanced plant management system (OPTIPLANT).

ABB has developed the OPTIMAX system for power plant monitoring and optimization (maintenance and lifetime power plant management, power optimization, compressor cleaning optimization, etc.). Siemens has developed the SPPA-P3000 system, which includes optimization of different areas such as boiler start-up, optimum design values or combustion. The aforementioned systems improve the efficiency of the plant by monitoring the important operating parameters and assisting the operator. There are also other systems for monitoring and diagnosing power plants. For example, the SOLCEP system installed in a power plant in Indonesia calculates the temperature ratio and compares it with the expected value. The on-line energy efficiency control system installed in the Compostilla coal power plant (Germany) can calculate deviations from the existing plant (reference) values by calculating the efficiency of the element and total efficiency. DADIC is a system for detecting abnormal conditions in a combined cycle power plant. In order to increase capacity and reduce operating costs, real-time on-line performance monitoring and optimization system has been installed in Seoincheon (1800 MW) and Sinincheon (2000 MW) combined cycle power plants in Korea.

When the national and international patents related to the systems and methods developed to perform performance monitoring in thermal power plants are examined, Cheng Xu et al. [13] patent describes the thermal power plant performance monitoring technique; It is based on the application of statistical analyzes (principal component analysis, linear and nonlinear regression analysis) to the collected plant data in order to determine the best plant operating parameters that will increase the primary performance indicators in any situation or operation level of the plant. Stephen L. Fehr et al. on the other hand, stated the ideas that will provide capabilities to the performance monitoring system to calculate the production costs, specific effective heat consumption, capacity and emissions of electricity generation plants based on current operating and atmospheric conditions [14].

In most thermal power plants, there is no performance monitoring system for performance evaluation, but only some parameters (temperature, flow, pressure, etc.) are measured within the control systems for the operation of the plant. These parameters, measured by the control system, can be used to determine the performance of a part of the plant and elements, but do not express the current state. At present, any loss in the performance of the plants is evaluated by the plant personnel. Even if they are very experienced, it is very difficult for the operators to fully evaluate the performance results due to the excess of parameters in the power plant and its elements and the lack of reference performance values in different operational and environmental conditions. The fact

that each plant has a separate design and technology makes it difficult to make human-based assessments healthy. Aside from the personnel knowledge and experience, an additional system that can evaluate the power plant performance is needed [15-44]. Therefore, performance monitoring and evaluation systems that compare the actual value with the reference performance value and determine the economic size of it contribute to achieving healthier results for the power plants.

3. DEVELOPING A PERFORMANCE MONITORING SYSTEM

3.1 Establishing a Data Management System

In today's digital world, an optimally operating power plant needs meaningful and accurate data to ensure reliable operation of equipment and units. Data from control systems, SCADA systems, energy management systems, sensors in the field equipment should be organized for optimization and accessible for evaluation.

In order to establish the infrastructure of the evaluation and monitoring system in Ambarlı Combined Cycle Power Plant, it is planned to establish a PI system to collect data from the plant site. The abbreviation "PI" in English is the abbreviation of "Process (Plant) Information"), used to describe all information (data) produced by a process consisting of electrical or mechanical equipment. Generally, the PI system is used to collect, save and manage data in a process or job.

The PI system is capable of gathering processes and enterprises from multiple points (established in different geographical locations) in one place. In this way, all systems can be observed in one place and all data required for analysis can be collected. The operation of the system is simply as follows: Data received from a data source comes to the PI system via an interface, which can be reported by the user in any desired format.

The information generated by the PI system for an industrial enterprise can be low in availability and large in capacity. For this reason, there are several commercial programs called “PI Management Systems" which are developed to make this information usable and meaningful and to convert it into data that can be saved and stored. The PI system is basically a PC-based system and is capable of communicating with the interfaces (OPC- Open Platform Communications) with other industrial devices that collect sensor data and status messages from intelligent machines, as shown in Figure 1.

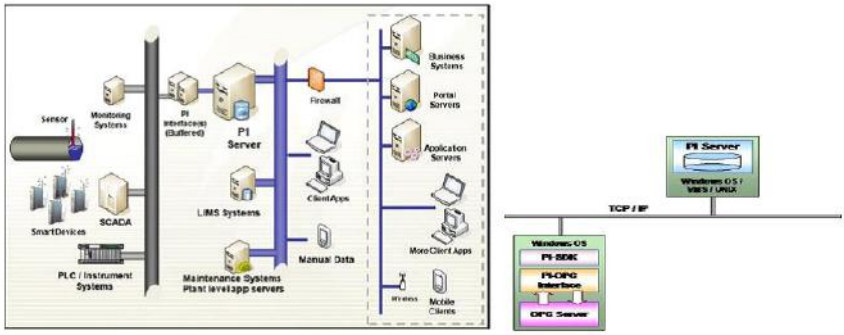

Figure 1. Typical PI system network connection (left) and basic structure (right) (Copyright: OsiSoft)

3.2 Data Processing and Filtering

The PI system is capable of receiving all parameter data from the OPC machine at regular intervals. The raw state of these data may be too bulky for a healthy observation of the process. It is also possible that unnecessary data is saved and stored for years. In order to prevent this, some of the observed data in the PI System can be compressed with the name Exception and archived data with the name Compression. In this way, unnecessary data is not stored and system performance can be kept high, resources can be used more efficiently.

In PI data processing stage; All data from the OPC server connected to the SCADA system is observed and recorded depending on a particular algorithm to be meaningful and give an idea, Figure 2. The collected parameters are stored in archive files, all data between each start and end time.

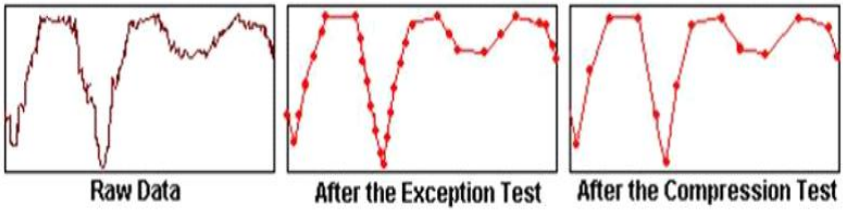

.

Figure 2. Steps of raw data processing and trend formation

3.3 Determination Of Performance Parameters

The purpose of the performance monitoring and evaluation system to identify the operational problems of the plant managers and operators, to improve the unit performance, to make maintenance plans and to monitor the performances and performance losses of the units and equipment in order to make economic decisions. Therefore, a successful performance monitoring system should show the amount of change in unit and equipment performances and the share of equipment in total performance

loss. For this, long-term monitoring of all the values obtained during the operation of a power plant, performance analysis and comparison with past performance values is very important in detecting the degradation of the unit or equipment.

The performance monitoring and evaluation system calculates the corrected value of the measured value in the reference environment and operating conditions and compares it with the reference values and determines the degradation in the unit or equipment. Degradation is defined as performance loss due tomechanical problems in equipment, contamination, aging, wear and the like. As a result, degradations are important because they represent the performance of existing units and equipment and should be continuously monitored by performance monitoring systems. For performance monitoring, it is necessary to calculate the expected and actual (current-measured) performance. The difference between these two performances will give us degradation rate. However, since performance losses due to operating and environmental conditions are not within the scope of degradation, the calculation should not take this into account. In order to make the necessary comparisons in order to evaluate the actual performance, the design and off-design performance values of the unit where the performance monitoring and evaluation system will be installed are needed.

The aim of the study is to design and then realize a plant performance monitoring and evaluation system that will monitor and measure the mechanical, hydraulic and thermodynamic parameters affecting the plant performance on a plant-by-plant basis and thus compare the plant's total performance. With this system to be installed, the operator can be informed about the performance levels of the equipment. In addition, it will be provided the operator with the flexibility of movement to determine the parameters that cause performance failure and to identify and solve the problem, to contribute to the solution of the problem quickly, easily and as independently of the human factor. When monitoring the performance of a unit, the performance degradation of both the unit and the equipment must be determined separately. Total degradation indicates the current state of the unit, while equipment degradation indicates where the total degradation stems from. Once the equipment-based degradations are identified, it is also possible to plan the work required for performance recovery. Therefore, first of all, A CCPP Power Plant was divided into 3 main sections and the parameters and performance indicators affecting the performance of these sections were determined in Table 1.

Table 1 Parameters and performance ındicators affecting the performance of the plant.

Model Name	Parameter Affecting Performance	Performance Outputs
Gas Turbine	Outdoor Temperature Air pressure Relative humidity GT Filter Pressure Loss GT Drop Pressure Loss IGV Angle Fuel AID	Net Power Heat Rate GT Exhaust Flow GT Exhaust Temperature
Heat Recovery Steam Generator - HRSG	GT Exhaust Flow GT Exhaust Temperature	YB Steam Flow YB Steam Temperature AB Steam Flow AB Steam Temperature
Steam Turbine and Water Cycle	YB Steam Flow YB Steam Temperature AB Steam Flow AB Steam Temperature Coolant (Water) Temperature	Net Power Condenser Pressure
All Cycle	Outdoor Temperature Coolant (Water) Temperature	Net Power Heat Rate

Two different methods can be used to evaluate the determined performance parameters by the performance monitoring system.
These are;

1- Curve-based method (correction method)
2- Model-based method

In the curve-based method, the correction factors obtained from the correction curves prepared by the manufacturer or made as a result of the simulations and analyses are used for the parameters affecting the performance. The expected power calculation for the gas turbine made using correction factors is given in (1). Another method is the model-based method. In this method, computer simulation including physical models of the equipment is operated with data measured from the plant and expected performance values are obtained.

$$N_{expected} = N_{measured} \prod_{i=0}^{n} DF_i \quad (1)$$

The curve-based method was used in the application to be made at A CCPP Plant. For this reason, performance curves supplied by the producer at the plant were investigated and correction curves were obtained with the help of the curves found. However, as a result of the evaluations, it was seen that the number of performance curves obtained from the units of the A CCPP Plant was insufficient to calculate many of the performance indicators. For this reason, in order to obtain the required performance curves, the three main sections forming the power plant were simulated with the GateCycle ™ program and performance curves

were obtained. In addition, the simulation model of the whole cycle was created by combining these sections validated with the design values, and the effects of the parameters affecting the whole cycle were examined and the results were presented. Off design simulation models are used to examine the operation of the equipment that is dimensioned according to design values with the design mode under different operating conditions. Thus, with the parametric studies, the effects of various operating values on power plant performance can be seen. It is possible to obtain designs close to the actual design by entering the known design information into the program in the current system. In addition, the effect of equipment-based degradation on the power plant can be examined in the prepared models.

3.4 Designing Of Performance Monitoring System

In the studies, it is determined that some additional measurements are needed besides the measured data in the plant to calculate the performance indicators of A CCPP. In this context, firstly the most suitable locations and measuring devices for additional measuring points were determined. A CCPP performance calculations required for additional measurement devices is listed Table 2 and GT Additional Measuring Points is shown in Figure 3.

Table 2 Performance calculations required for additional measurement devices.

Q	**Measuring point**	**Related equipment/ Measured parameter**	**Range**	**Unit**	**Output Signal**	**Measuring environment**
1	Outdoor environment Conditions	Outdoor Ambient Temperature And Moisture Measuring		C,	mA	
2	Filter inlet-outlet	Differential pressure transmitter	0-300	mbar	mA	Pneumatic
1	Compressor outlet	Pressure transmitter	0-2	mbar	mA	Pneumatic
1	Compressor inlet nozzle	Differential pressure transmitter	0-300	mbar	mA	Pneumatic
4	Combustion chamber entrance - exit.	Differential pressure transmitter	0-300	mbar	mA	Pneumatic, High temperature, 1200 C

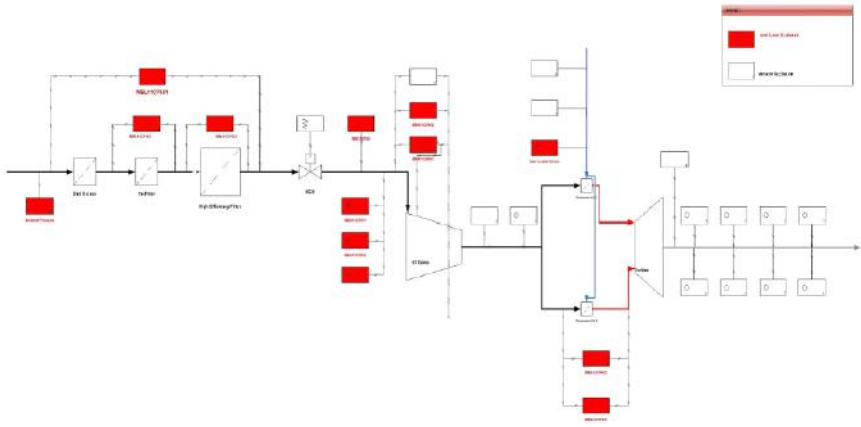

Figure 3. GT Additional Measuring Points

As a result, in order to set up a Performance Monitoring and Evaluation system at A CCPP Plant, in addition to the existing signals measured from the 1st Unit, the equipment selection and the necessary installation works for 59 signals determined by the project team were completed.

As an instrumentation work at A CCPP Plant, PI software developed by OsiSOFT was installed on a server computer in order to receive the signals of the 1st Unit of the plant and additional measurement points. At the same time, this computer is configured as a web server and it is possible to access web-based switchboard data. This system was then upgraded to make it possible to add additional measuring points to the system, as shown in Figure 4.

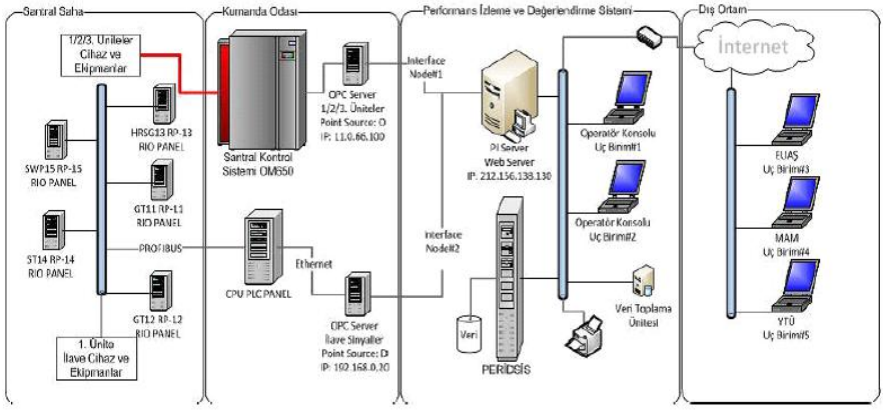

Figure 4. Final status of the system control architecture after additional measuring points

4. THERMAL POWER PLANT PERFORMANCE ANALYSIS

4.1 Performance Indicators and Calculations

In order to calculate the overall unit performance, the effects of the deterioration in the equipment on the overall unit performance should be calculated. As a result, the operator will also be able to assess the relative importance of deterioration in each monitored performance, making it easier to make decisions about the maintenance needs of the equipment. The effects of the equipment on the overall unit performance can be calculated in 3 parts;

- Effect on Unit Power
- Effect on Unit Heat Rate
- Effect on Unit Costs

Performance monitoring system is a system that continuously evaluates the data obtained during the operation of a unit and compares the performance of the unit and the equipment with the required values according to the current operating and environmental conditions. In order to calculate the expected performance values in the curve-based method, performance curves prepared according to the operating and environmental conditions are needed. Using the correction factors obtained with the help of these curves, expected performance values for both the plant and the equipment constituting the plant can be calculated.

As a result of this process, the calculated values can be compared with the actual values and the degradations on the basis of plant and equipment can be calculated. Generally, the performance curves are delivered to the plant by plant and / or equipment manufacturers. However, if these performance curves cannot be found, the necessary curves and performance values can be obtained by analyzing the simulation models of the power plants. While performing the performance analyzes of the A CCPP Plant where the application will be made, some of the required performance curves were obtained from the plant files. The list of curves to be used in the performance monitoring system is given in Table 3.

Table 3. Correction curves required for performance calculation

No	Equipment	Performance curves	Performance indicator
1	Gas turbine	Filter pressure loss	Power
2	Gas turbine	Inlet air pressure	Power
3	Gas turbine	Outlet air pressure	Power
4	Gas turbine	Outdoor temperature	Power

5	Gas turbine	Air relative humidity	Power
6	Gas turbine	Fuel LHV - Net calorific value	Power
7	Gas turbine	Inlet Guide Vane (IGV) Angle	Power
8	Gas turbine	Filter pressure loss	Heat rate
9	Gas turbine	Inlet air pressure	Heat rate
10	Gas turbine	Outlet pressure loss	Heat rate
11	Gas turbine	Outdoor temperature	Heat rate
12	Gas turbine	Air relative humidity	Heat rate
13	Gas turbine	Fuel LHV - Net calorific value	Heat rate
14	Gas turbine	Inlet Guide Vane (IGV) Angle	Heat rate
15	Gas turbine	Filter pressure loss	Exhaust flow
16	Gas turbine	Inlet air pressure	Exhaust flow
17	Gas turbine	Outlet air pressure	Exhaust flow
18	Gas turbine	Outdoor temperature	Exhaust flow
19	Gas turbine	Air relative humidity	Exhaust flow
20	Gas turbine	Fuel LHV - Net calorific value	Exhaust flow
21	Gas turbine	Inlet Guide Vane (IGV) Angle	Exhaust flow
22	Gas turbine	Filter pressure loss	Exhaust temperature
23	Gas turbine	Inlet air pressure	Exhaust temperature
24	Gas turbine	Outlet air pressure	Exhaust temperature
25	Gas turbine	Outdoor temperature	Exhaust temperature
26	Gas turbine	Air relative humidity	Exhaust temperature
27	Gas turbine	Fuel LHV - Net calorific value	Exhaust temperature
28	Gas turbine	Inlet Guide Vane (IGV) Angle	Exhaust temperature
29	Waste Heat Boiler	Exhaust flow	HP Vapor flow change.
30	Waste Heat Boiler	Exhaust flow	LP Vapor flow change.
31	Waste Heat Boiler	Exhaust temperature	HP Vapor flow change.
32	Waste Heat Boiler	Exhaust temperature	LP Vapor flow change.
33	Waste Heat Boiler	Exhaust temperature	HP Vapor flow change.
34	Steam turbine	HP steam flow	Power

35	Steam turbine	LP steam flow	Power
36	Steam turbine	Condenser pressure	Power
37	Steam turbine	HP steam temperature	Power
38	Steam turbine	HP steam flow	Turbine efficiency
39	Steam turbine	LP steam flow	Turbine efficiency
40	Steam turbine	Condenser pressure	Turbine efficiency
41	Steam turbine	HP steam temperature	Turbine efficiency
42	Steam turbine	Cooling water temperature	Condenser pressure

Since the number of curves obtained from the plant is insufficient to calculate most of the performance indicators, the plant is simulated with GateCycle ™ software to obtain the necessary performance curves and the necessary performance curves are obtained. Off-design simulation models are used to examine the operation of the equipment that is dimensioned according to design values with the design mode under different operating conditions. Thus, with the parametric studies, the effects of various operating values on power plant performance can be seen. In addition, the effect of equipment-based degradations on the unit can be examined in the prepared models. While simulating the power plant, 3 main sections are examined and finally, the whole cycle is simulated by combining these 3 main sections and parametric analyses are completed. The three main parts of the Am CCPP Plant cycle are as follows:

- Gas Turbine
- Waste Heat Boiler (WHB)
- Steam Turbine and Water Cycle

The parameters affecting the gas turbine performance are the parameters that affect the compressor inlet air and these weather conditions (pressure, temperature and flow) and fuel properties. According to the changes in these parameters, gas turbine outputs (power, outlet temperature and pressure) and efficiency change. With the simulation model, the effects of the changes in these parameters on the gas turbine outputs can be revealed. When the guaranteed values are compared with the simulation results in design mode, it is seen that the model in design mode (Figure 5) represents the gas turbines used in A CCPP plant and the GT simulation made in GateCycle ™ program is verified.

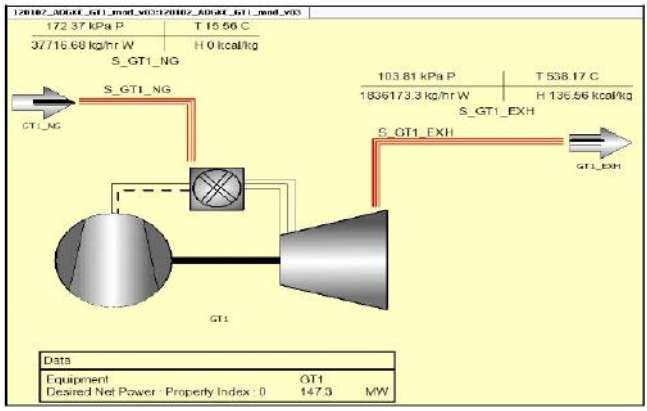

Figure 5. A CCPG GT GateCycle ™ simulation

The following parametric analyzes were performed to verify the off-design simulation model and the results are given in Figures 6, 7, 8, 9, 10, 11 respectively.

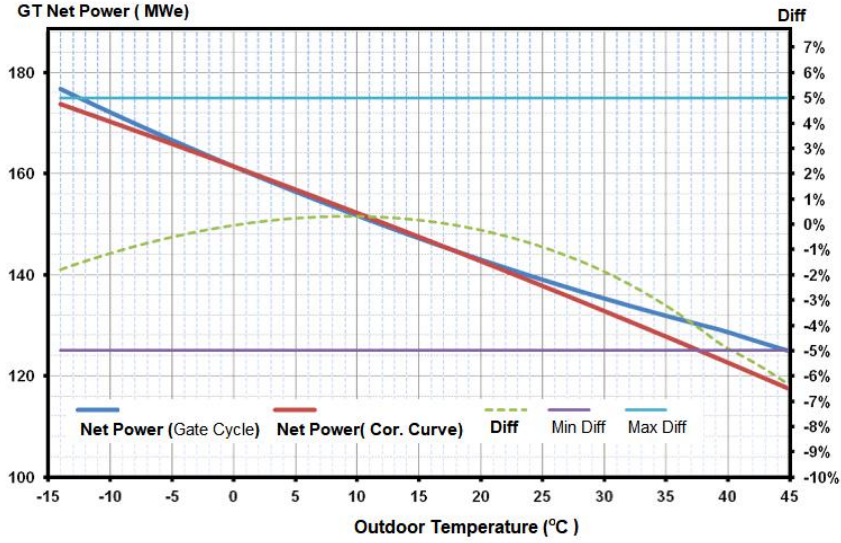

Figure 6. Change in GT net power according to outdoor temperature

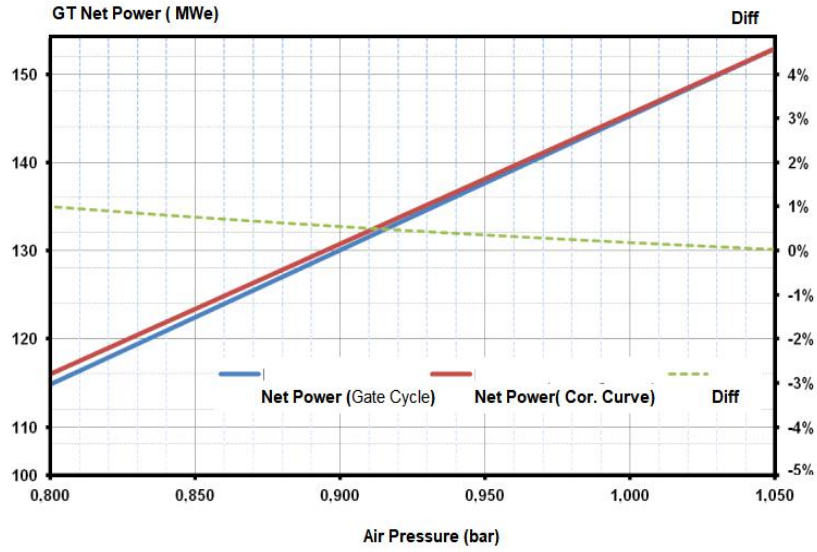

Figure 7. Change in GT net power relative to change in air pressure

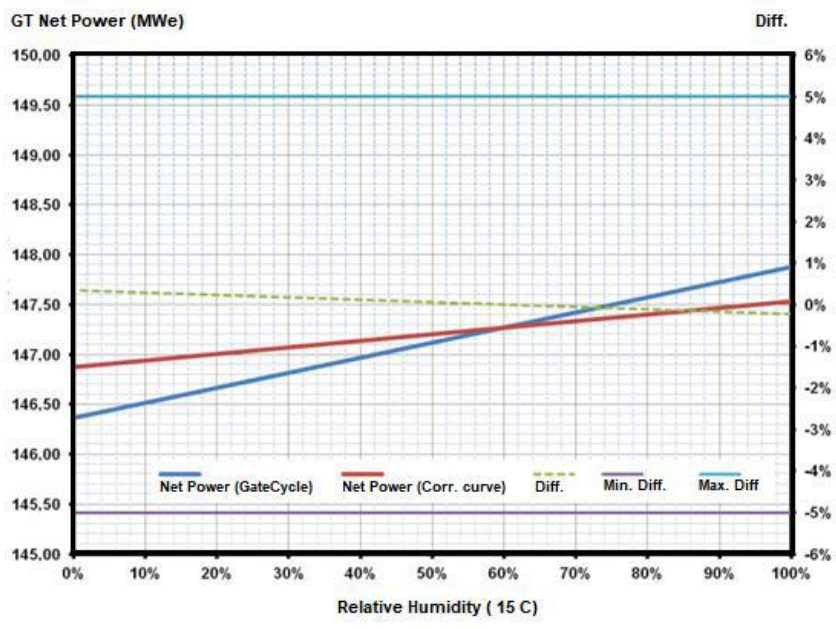

Figure 8. Change in GT net power relative to change in relative humidity (15 ° C)

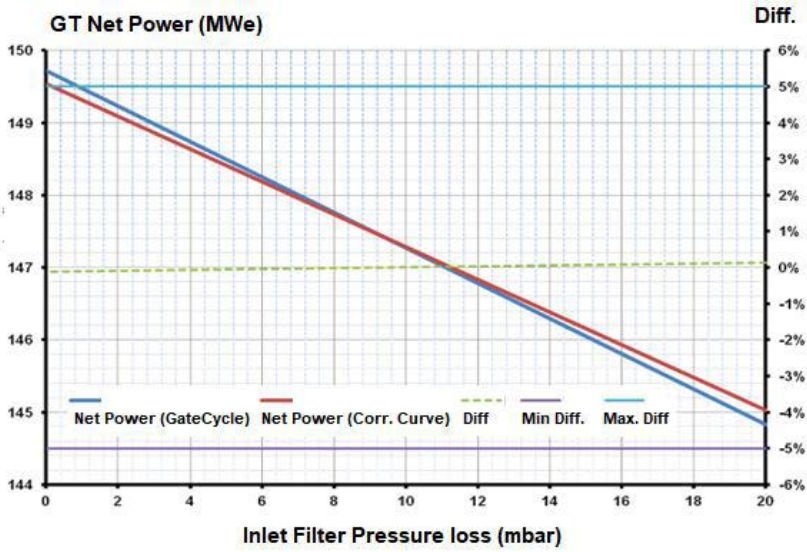

Figure 9. Change in GT net power according to inlet filter pressure loss

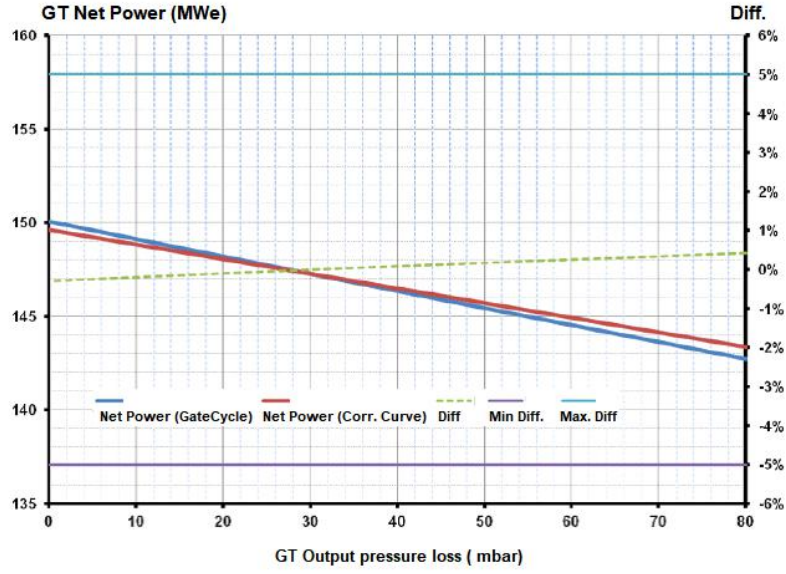

Figure 10. Change of GT net power according to GT output pressure loss

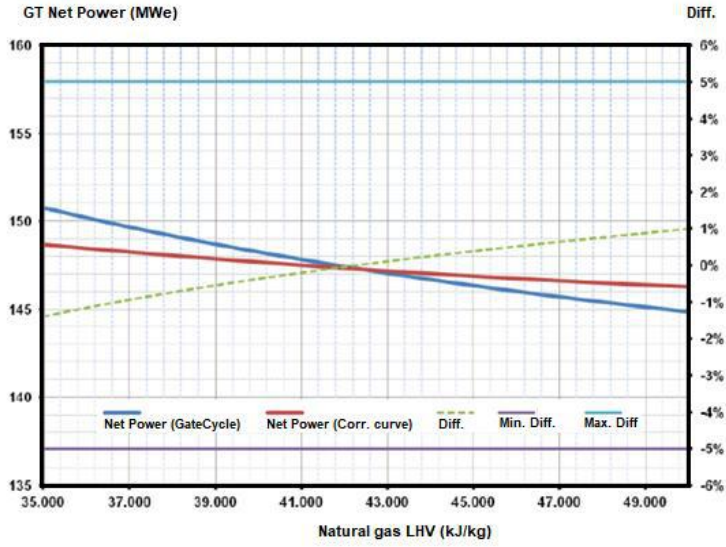

Figure 11. Change in GT net power relative to change in natural gas lower thermal value.

When these graphs are examined, the maximum difference between the power calculated according to the reference correction curves and the GateCycle ™ model is calculated as -6% in the outdoor temperature change curve. This difference occurs in sections where the outdoor temperature is 45 ° C. The difference between -15 ° C and 30 ° C is the highest -2%, which is within acceptable limits for simulation studies. The performance indicators of these main parts were determined and the data to be measured were determined. Among these data, the existing ones at the plant and the data that should be added were determined. The devices to be installed in additional measurement sites were determined and bided and these measurement data were transferred to the PI system. Thus, a data system was created to calculate performance indicators for each part.

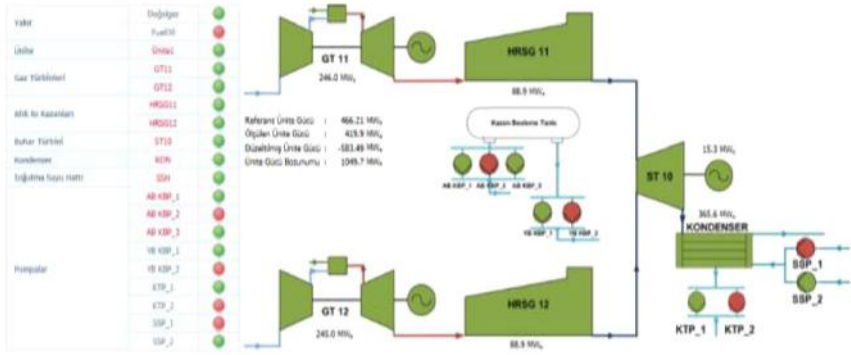

Figure 12. Power plant modeling screenshot

6. RESULTAND EVALUATION

There are many studies on thermal power plant performance monitoring systems applied in the energy world. Thermal power plants should be operated at maximum efficiency and profitability due to their high production income and economic size. In this sense, great importance is given to performance monitoring systems and studies show that these systems increase energy efficiency. Thanks to the data collection system installed in the plant, all physical and mechanical quantities (pressure, flow rate, temperature, power, etc.) that can be monitored from the control room can be monitored from outside with the user-defined user name and password and necessary performance calculations can be made. The necessary measurements and performance parameters of the power plant are determined on the basis of equipment and total power plant in order to perform performance calculation. Additional measurements (pressure, temperature, flow, etc.) required to calculate the defined performance parameters were determined and appropriate measurement points were determined for these measurements at the plant.

Thanks to the designed system, performance parameters on the basis of unit and equipment, degradation, degradation costs and trends in a given time period will be followed and an important historical database will be created for the plant in the future. These data provide input both for the operation of the plant and for the predictive maintenance of the plant.A Natural Gas Combined Cycle Power Plant has been selected as the power plant where the project will be implemented and the PI System, which forms the infrastructure of the evaluation and monitoring system, has been established. Thus, all systems can be observed in one place and all data required for analysis can be collected. Then, the necessary measurements and performance parameters of the plant for performance calculation are determined on the basis of equipment and total plant. After that, the actual working situation is simulated in the computer environment and the design working conditions are verified and correction curves are obtained for the equipment (pump, gas turbine, waste heat boiler, etc.).

Using the correction factors obtained from these correction curves, the total unit and equipment (pump, gas turbine, waste heat boiler, steam turbine, etc.) performance parameters, degradations, the share of equipment in total degradation, hourly cost of equipment degradations and the necessary algorithms including impact and solution analysis were developed and a special program was developed for A Natural Gas Combined Cycle Power Plant.With this program, performance parameters on the basis of unit and equipment, degradations, degradation costs and trends in a certain time period can be followed and an important historical

database for the plant can be created in the future. In addition, these data will help the plant team both in the operation of the plant and predictive maintenance of the plant. Thus, the status of the units and equipment in the power plant can be evaluated more healthily and possible performance losses will be minimized.

REFERENCES

[1] Konrad Swirski, Power Plant Performance Monitoring Using Statistical Methodology Approach, Journal of Power Technologies 91 (2) (2011) 63–76

[2] Liping Li, Process Performance Monitoring and Degradation Analysis, Thermal Power Plants, Mohammad Rasul, IntechOpen, (2012). DOI: 10.5772/27335

[3] Özdemir M. B., Menlik T., Variyenli H. İ. ve Sevin L., "Bir termik santralin performans analizi ve rehabilitasyon metotları", Politeknik Dergisi, 20(4): 971-978, (2017).

[4] Balaram Saha, V. Patel and K. Chaterjee, "Assessment of process parameter to improving power plant performance," 2014 Innovative Applications of Computational Intelligence on Power, Energy and Controls with their impact on Humanity (CIPECH), Ghaziabad, 2014, pp. 441-446, doi: 10.1109/CIPECH.2014.7019125.

[5] T. Sudhakar1, Dr.B. Anjaneya Prasad, Dr. K. Prahlada Rao, Analysis of Process Parameters to Improve Power Plant Efficiency, Journal of Mechanical and Civil Engineering (IOSR-JMCE), Volume 14, Issue 1 Ver. II (Jan. - Feb. 2017), PP 57-64

[6] Simona Vasilica Oprea and Adela Bâra (July 13th 2017). Key Technical Performance Indicators for Power Plants, Recent Improvements of Power Plants Management and Technology, Aleksandar B. Nikolic and Zarko S. Janda, IntechOpen, DOI: 10.5772/67858.

[7] Blanco, Jesús M. & Vazquez, L. & Peña, F., 2012. "Investigation on a new methodology for thermal power plant assessment through live diagnosis monitoring of selected process parameters; application to a case study," Energy, Elsevier, vol. 42(1), pages 170-180.

[8] Guo Z., Guo S., Liu P., Li Z., 2017, Operation data based modelling and performance monitoring of steam turbine regenerative system under full working conditions, Chemical Engineering Transactions, 61, 127-132 DOI:10.3303/CET1761019

[9] Malik S., Tewari P.C. Performance modeling and maintenance priorities decision for the water flow system of a coal-based thermal

power plant, Int. J. Qual. Reliab. Manage., 35 (4) (2018), pp. 996-1010, 10.1108/IJQRM-03-2017-0037

[10] Kumar R., Sharma A.K., Tewari P.C. Performance modeling of furnace draft air cycle in a thermal power plant, Int. J. Eng. Sci. Technol., 3 (8) (2011), pp. 6792-6798

[11] Kumar P.R., Raju V.R., Kumar N.R. Simulation and parametric optimization of thermal power plant cycles, Perspect. Sci., 8 (2016), pp. 304-306, 10.1016/j.pisc.2016.04.060

[12] Kumar R., Performance evaluation and decision support system of the water circulation system of a steam thermal power plant, Elixir Mech. Eng., 44 (2012), pp. 7551-7557

[13] Cheng, Xu et al., Use of statistical analysis in power plant performance monitoring, United States Patent 8200369, Publication Date: 06/12/2012

[14] Stephen L. Fehr, Linda A. Hutchinson, Systems and methods for calculating and predicting near term production cost, incremental heat rate, capacity and emissions of electric generation power plants based on current operating and, optionally, atmospheric conditions, United States, US7489990B2, Publication Date: 2009-02-10

[15] K.Kawai, Y.Takizawa, S. Watanabe, Advanced Automation for Power-Generation Plants - Past, Present and Future, IFAC Proceedings, Vol. 31, Issue 26, September 1998, Pages 209-214

[16] K. Kawai, Y. Takizawa, S. Watanabe, Advanced automation for power-generation plant s - past, present and future, Control Engineering Practice 7 (1999) 1405}1411

[17] Sergio Usón, Antonio Valero, Luis Correas, Energy efficiency assessment and improvement in energy intensive systems through thermoeconomic diagnosis of the operation Applied Energy 87 (2010) 1989–1995

[18] Si-Moon Kim, Yong-Jin Joo, Implementation of on-line performance monitoring system at Seoincheon and Sinincheon combined cycle power plant, Energy 30 (2005) 2383–2401

[19] Sergio Usón, Antonio Valero, Thermoeconomic diagnosis for improving the operation of energy intensive systems: Comparison of methods, Applied Energy 88 (2011) 699–711

[20] Performance Monıtorıng of Gas Turbıne Saves Two Compressor Washes Per Year, Rovsing Dynamics, September 2007.

[21] Tsuyoshi Lijima et.al, Hitachi's Latest Supervisory and Control System for Advanced Combined Cycle Power Plants, Hitachi Review Vol. 51 (2002), No. 5

[22] S. Cafaro, L. Napoli, A. Traverso, A.F. Massardo, Monitoring of the thermoeconomic performance in an actual combined cycle power plant bottoming cycle, Energy 35 (2010) 902–910

[23] Jiejin Cai, Xiaoqian Ma, Qiong Li, On-line monitoring the performance of coal-fired power unit: A method based on support vector machine, Applied Thermal Engineering 29 (2009) 2308–2319

[24] Si-Moon Kim, Yong-Jin Joo, Implementation of on-line performance monitoring system at Seoincheon and Sinincheon combined cycle power plant, Energy 30 (2005) 2383–2401

[25] Prasad, E. Swidenbank, B. W. Hogg, A novel performance monitoring strategy for economical thermal power plant operation, IEEE Transactions on Energy Conversion, Vol. 14, No. 3, September 1999

[26] Robert Holzworth, Walter Walejeski, Integrated performance monıtorıng for asset optımızatıon, POWER2009-81212, Proceedings of POWER 2009, ASME Power 2009, July 21-23, 2009, Albuquerque, New Mexico, USA

[27] Xianchang Cao, Chunfa Zhang, Anzhong Jiang. "A new method of energy degradation on-line analysis for coal-fired unit-expansion line Approximating method", Applied Thermal Engineering 22(2002) 339-348

[28] Yongping Yang, Kun Yang, etc. "The potentiality of energy-conserving and diagnostic theory of in coal fired power plants", Journal of Electrical Engineering in China, 1998,18(2):13l-134.

[29] Valero A, Verda V, Serra L. The effects of the control system on the thermoeconomic diagnosis of a power plant. Energy 2004; 29:331–59.

[30] Torres C, Valero A, Serra L, Royo J. Structural theory and thermoeconomic diagnosis. Part I: on malfunction and dysfunction analysis. Energy Convers Manage 2002; 43:1503–18.

[31] Torres C, Valero A, Serra L, Royo J. Structural theory and thermoeconomic diagnosis. Part II: application to an actual power plant. Energy Convers Manage 2002; 43:1519–35.

[32] Valero A, Lozano MA, Bartolome JL. On-line monitoring of power-plant performance, using exergetic cost techniques. Appl Therm Eng 1996; 16:933–48

[33] Yang SK., A condition-based preventive maintenance arrangement for thermal power plants, Electric Power Systems Research 2004, Vol 72, pp. 49-62.

[34] Kawai K., Takizawa Y., Watanabe S., , Advanced automation for power generation plants: past, present and future. Control Engineering Practice, 1999 Vol 7 pp.1405-1411.

[35] Fast M., Palme T., Application of artificial neural networks to the condition monitoring and diagnosis of a combined heat and power plant, Energy 2009. doi: 10.1016/j.energy.2009.06.005.

[36] Usón S., Valero A., Correas L., Energy efficiency assessment and improvement in energy intensive systems through thermoeconomic diagnosis of the operation, Applied Energy 2009 doi: 10.1016/j.apenergy.2009.12.004

[37] Verda V., Borchiellini R, Exergy method for the diagnosis of energy systems using measured data, Energy, 2007 Vol.32, pp.490-498.

[38] Cafaro S., Napoli L., Traverso A., Massardo AF., Monitoring of the thermoeconomic performance in an actual combined cycle power plant bottoming cycle, Energy 2009, doi: 10.1016/j.energy.2009.07.016.

[39] Cai J., Ma X., Li Q., Online monitoring the performance of coal-fired power unit: A method based on support vector machine, Applied Thermal Engineering, 2009 Vol.29, pp.2308-2319.

[40] Rui, Xie; Yihong, Wang, Monitoring and Warning System for Power Plant Based on Virtual Instrument Technology, Electronic Measurement and Instruments, 2007. ICEMI apos;07. 8th International Conference on Volume, Issue, Aug. 16 2007-July 18 2007 Page(s):3-131 - 3- 135 Digital Object Identifier (doi) 10.1109/ICEMI.2007.4350871

[41] Li Pan; Flynn, D.; Cregan, M., Statistical model for power plant performance monitoring and analysis, Universities Power Engineering Conference, 2007. UPEC 2007. Volume, Issue, 4-6 Sept. 2007 Page(s):121 – 126

[42] Kamei T., Tomura T., Kato Y., Latest Power Plant Control System, Hitachi Review, 2003 Vol.52 No:2, pp.101-105.

[43] Maruyama Y., Suzuki H., Miyakawa J., Kitagawa K., Yamada T., Global Standart Power Plant Monitoring and Control System, Hitachi Review, Vol.58 No:5, pp.194-197.

[44] Report, Thermal power plant performance monitoring and evaluation system design and implementation, TUBITAK Project No. 110G092.

CHAPTER XIII

AN INTEGRATED AHP AND PROMETHEE APPROACH TO SELECT THE MOST SUITABLE AUTOMOBILE FOR CONSUMERS

Asst. Prof. Dr. Fatih ÖZTÜRK

Istanbul Medeniyet University, Istanbul, Turkey
e-mail: fatih.ozturk@medeniyet.edu.tr, Orcid ID: 0000-0003-4113-055X

1. Introduction

In all processes, decisions are made to select, evaluate and progress. Multi-Criteria Decision-Making (MCDM) methods have been used in several industries to make reliable decisions under multiple conflicting criteria. In the automotive industry, MCDM methods have predominantly been used in supplier selection problems. This study uses the Analytical Hierarchy Process (AHP) and the Preference Ranking Organisation Method for Enrichment Evaluation (PROMETHEE) methods for selecting the most suitable automobile for consumers. AHP was used to attribute weights for each criterion. Three subject matter experts were involved in the study to evaluate the importance of each criterion. PROMETHEE was used to rank seven alternatives under nine criteria. This study provides an insight into the use of MCDM methods in the selection of an automobile.

In the automotive industry, manufacturers aim to develop the best business strategies in both manufacturing and marketing to be able to stand in the competitive market [1], [2]. As part of their strategy, manufacturers follow the most updated technology in their production lines by aiming to minimise their costs, meet regulatory requirements and improve the quality of their products. In addition, manufacturers analyse customer behaviours to design products that respond to their needs and preferences [3], [4]. The automotive manufacturer companies might only target wealthy consumers, or they might target a broader range of consumers by providing a more extensive range of products [5] – [7].

As many manufacturers available in the market, consumers have numerous alternatives to purchase a car. They make purchasing decisions under several criteria, including price, fuel economy, performance, brand perception, service quality, exterior and comfort [1], [5], [6], [8], [9]. More specifically, customers desire to purchase the best quality of the car with the lowest price. However, these criteria might be conflicting as in price and quality. Quality comes with a price. At this point, Multi-Criteria Decision-Making (MCDM) methods can be used in several industries to deal with the complexity in the decision-making process [10], [11].

In the automotive industry, MCDM methods have been predominantly used to support decision-making in supplier [4], [12]–[16], and design concept selection problems [17]. A few studies, however, used MCDM methods in car selection problems. Apak et al. [5] used the Analytical Hierarchy Process (AHP) method in a luxury car selection problem. Similarly, Byun [1] used AHP to support decisions made in a car selection problem. Sakthivel et al. [6] used a hybrid MCDM approach for evaluating cars. Raut et al. [18] applied Analytical Quality Fuzzy (AQF) to determine the best automobile among the alternatives. Singh et al. [19] used fuzzy AHP and TOPSIS methods to select a sedan car from the Indian car market. Despite the potential value of each MCDM method, researchers suggested integrating different MCDM methods to make more reliable decisions [20].

This study used an integrated AHP and Preference Ranking Organisation Method for Enrichment Evaluation (PROMETHEE) approach for selecting the most suitable automobile. The study used AHP to attribute weights to the selection criteria and PROMETHEE to rank alternatives considering nine criteria.

2. Study design

This study applied an integrated AHP and PROMETHEE approach to select the most suitable car among seven alternatives under nine selection criteria. The design of this study involves three stages: data collection, AHP application and PROMETHEE application (see Figure 1).

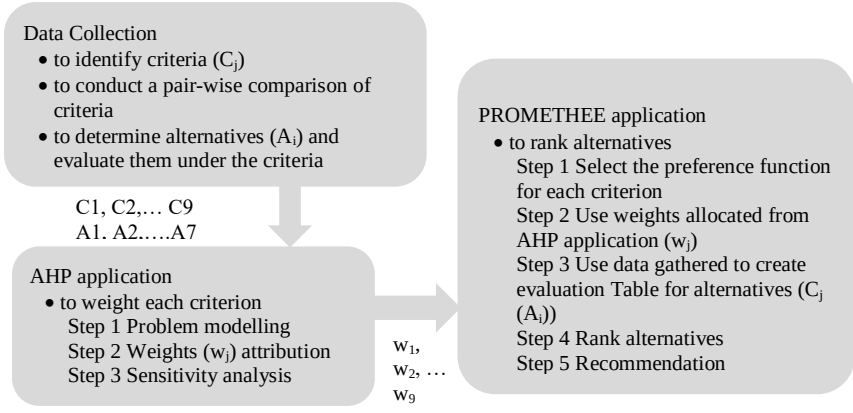

Figure 1: Study Design for the Selection of the most Suitable Car

In the data collection stage, authors first identified the selection criteria by reviewing literature [1], [5], [6], [8], [9] and automobile-related web sites [21]. Second, the authors designed a questionnaire to compare the

importance of each criterion (Cj). A paired comparison analysis was undertaken by using a 1 to 9 scale. Three subject-matter experts (SMEs) were involved in the questionnaire. The geometric mean of the responses from three SMEs was calculated to attribute weights in the AHP analysis. Third, the authors determined alternatives (Ai) and evaluated them under the criteria identified (Cj(Ai)) by browsing a UK based car review website. On this website, experts assign a score from 1 to 100 to evaluate cars under multiple criteria [21]. These scores were used in PROMETHEE analysis to evaluate alternatives.

AHP application, which was developed by Saaty [22], was undertaken in three main steps. First, the problem is modelled in a hierarchical structure by including the overall objective and criteria (n=1, 2,..j). Second, a pair-wise comparison matrix was created to attribute weights (wj) of relative importance to the criteria. Third, a sensitivity analysis was undertaken for consistency checking [22]. In this study, all calculations were made by using MS Excel.

The PROMETHEE method, which was developed by Brans [23], was applied by following six main steps. First, a preference function was selected for each criterion. Brans proposes six possible types of preference functions (i.e. usual, u-shape, v-shape, level, linear and gaussian) to the decision-makers [24]. This study selected the preference function of linear as it fits well with quantitative data. Furthermore, the objective of each criterion in terms of being maximisation or minimisation was stated. Second, relative importance to the criteria was assigned through the weights calculated in the AHP application. Third, evaluation Table that represents the value (Cj(Ai)) of the alternative i (Ai) under criteria j (Cj) was constructed. Fourth, alternatives were ranked through PROMETHEE I and PROMETHEE II. Fifth, the most suitable option was determined based on the ranking orders. This study used Visual PROMETHEE software to apply the method.

3. Results

In this study, nine criteria were identified: performance (C_1), handling (C_2), comfort (C_3), space (C_4), styling (C_5), build (C_6), equipment (C_7), fuel consumption (C_8) and price (C_9). Table 1 provides a description of each criterion and the weights attributed.

Table 1: The Description of Each Criterion

Criteria	Description	Weight
Performance	The consideration of torque, horsepower, engine volume, fuel type, etc.	0.13
Handling	The ability of a car to respond to the inputs of a driver	0.19
Comfort	The consideration of temperature, noise, vibration, air quality, light and ergonomics	0.05
Space	Space for occupants and luggage capacity	0.06
Styling	The style of the interior and exterior parts and accessories	0.04
Build	The body and chassis of a car	0.07
Equipment	Equipment and systems in a car (e.g. full-LED front lights and airbags and touch screen system)	0.04
Fuel consumption	Calculated by the litres used to get 100 km distance	0.21
Price	The price of a brand-new car	0.21

Seven alternatives were selected among the car brands having a good reputation in the market: Mercedes S-Class (A1), BMW 5 Series-Touring (A2), Skoda SuperB-MK3 (A3), Range Rover-MK4 (A4), Citroen C3 Aircross (A5), Peugeot 3008 (A6) and Honda Civic Type-R (A7). Figure 2 models the problem in a hierarchical structure. The first level represents the objective of the study: selecting the most suitable car. The second level shows the criteria, and the third level shows the alternatives.

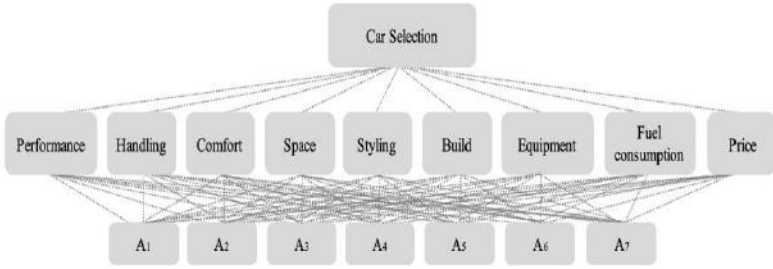

Figure 1: Problem Modelling

The relative importance of each criterion was calculated by using the dataset obtained by SMEs, and, in turn, weights (wj) attributed to each criterion (j) as demonstrated in Table 1. Fuel consumption (w8= 0.21) and price (w9= 0.21) appears to be the most important criteria when selecting a car.

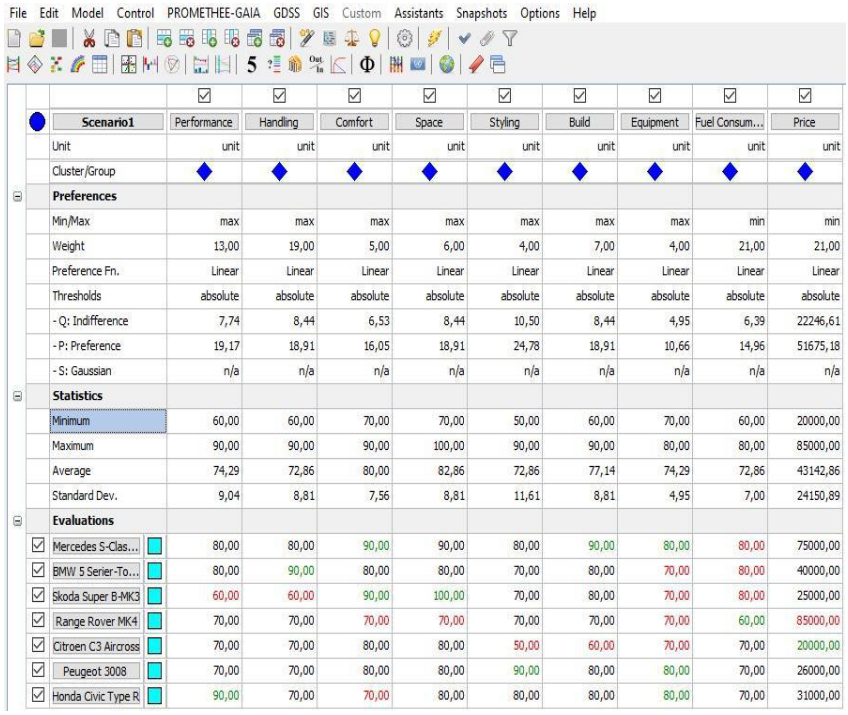

Scenario1	Performance	Handling	Comfort	Space	Styling	Build	Equipment	Fuel Consum...	Price
Unit	unit	unit	unit	unit	unit	unit	unit	unit	unit
Cluster/Group									
Preferences									
Min/Max	max	max	max	max	max	max	max	min	min
Weight	13,00	19,00	5,00	6,00	4,00	7,00	4,00	21,00	21,00
Preference Fn.	Linear	Linear	Linear	Linear	Linear	Linear	Linear	Linear	Linear
Thresholds	absolute	absolute	absolute	absolute	absolute	absolute	absolute	absolute	absolute
- Q: Indifference	7,74	8,44	6,53	8,44	10,50	8,44	4,95	6,39	22246,61
- P: Preference	19,17	18,91	16,05	18,91	24,78	18,91	10,66	14,96	51675,18
- S: Gaussian	n/a	n/a	n/a	n/a	n/a	n/a	n/a	n/a	n/a
Statistics									
Minimum	60,00	60,00	70,00	70,00	50,00	60,00	70,00	60,00	20000,00
Maximum	90,00	90,00	90,00	100,00	90,00	90,00	80,00	80,00	85000,00
Average	74,29	72,86	80,00	82,86	72,86	77,14	74,29	72,86	43142,86
Standard Dev.	9,04	8,81	7,56	8,81	11,61	8,81	4,95	7,00	24150,89
Evaluations									
Mercedes S-Clas...	80,00	80,00	90,00	90,00	80,00	90,00	80,00	80,00	75000,00
BMW 5 Serier-To...	80,00	90,00	80,00	80,00	70,00	80,00	70,00	80,00	40000,00
Skoda Super B-MK3	60,00	60,00	90,00	100,00	70,00	80,00	70,00	80,00	25000,00
Range Rover MK4	70,00	70,00	70,00	70,00	70,00	70,00	70,00	60,00	85000,00
Citroen C3 Aircross	70,00	70,00	80,00	80,00	50,00	60,00	70,00	70,00	20000,00
Peugeot 3008	70,00	70,00	80,00	80,00	90,00	80,00	80,00	70,00	26000,00
Honda Civic Type R	90,00	70,00	70,00	80,00	80,00	80,00	80,00	70,00	31000,00

Figure 2: Visual PROMETHEE Input Screen

The Visual PROMETHEE software was used to rank the alternatives. Figure 3 demonstrates the input screen of the software. First, the criteria and options were entered. Next, the details of the criteria to be minimised or maximised, and the weights of each criterion were entered. Then, the evaluation Table was filled based on the data obtained from a car review website [21]. After that, the preference functions and thresholds values for each criterion were selected to run the analysis.

The Visual PROMETHEE software calculated the positive (Phi+) and negative (Phi-) flow values for the PROMETHEE I partial ranking results, and the net (Phi) flow value for the PROMETHEE-II complete ranking (see Figure 4).

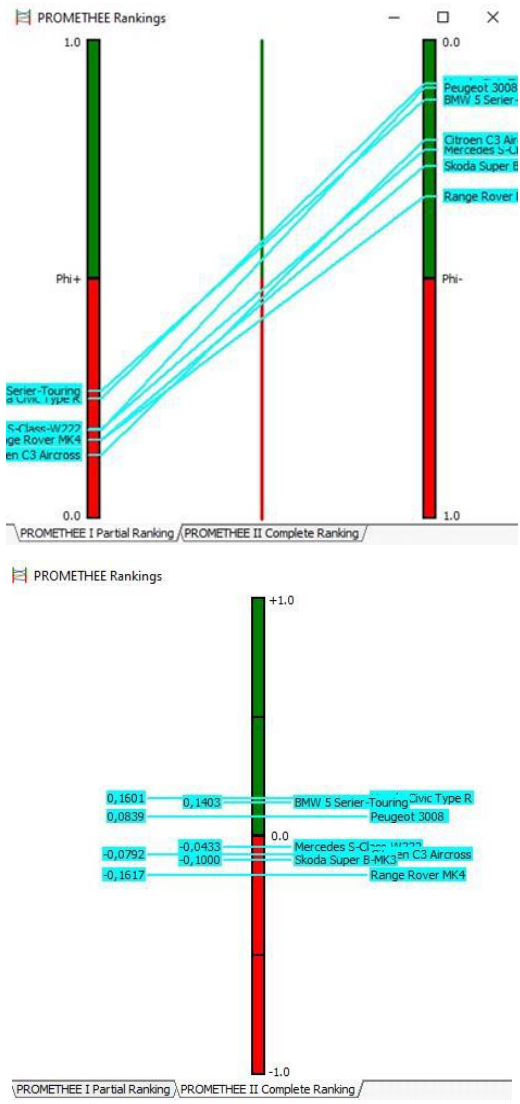

Figure 3: PROMETHEE-I and PROMETHEE-II Scores

Table 2 lists the Phi, Phi^{+} and Phi^{-} scores and provides a ranking order for the alternatives. The application of PROMETHEE suggests the selection of Honda Civic Type R under given nine criteria. However, it must be noted that the weight attribution to each criterion plays a significant role in the ranking. In this study, SMEs gave priority on technical features of the cars when selecting a car. However, others, for

instance, might prefer comfort over performance, or might not have any preference in terms of price.

Table 1: PROMETHEE Phi, Phi+ and Phi- Scores and alternative Ranking

Alternative	Rank	Phi	Phi^+	Phi^-
Honda Civic Type R	1	0.1601	0.2502	0.0901
BMW 5 Series-Touring	2	0.1403	0.2652	0.1249
Peugeot 3008	3	0.0839	0.1846	0.1007
Mercedes S-Class	4	-0.0433	0.1873	0.2306
Citroen C3 Aircross	5	-0.0792	0.1308	0.2100
Skoda SuperB-MK3	6	-0.1000	0.1631	0.2631
Range Rover MK4	7	-0.1617	0.1644	0.3261

4. Conclusions

This study used an integrated approach to AHP and PROMETHEE to select the most suitable car among the seven alternatives under nine criteria. AHP was used to attribute weights to each criterion, and PROMETHEE was used to rank alternatives. The integration of two methods enables making a more reliable evaluation.

Once several criteria and alternatives are involved in the decisions making process, it can be challenging for decision-makers to reach to a conclusion. In such circumstances, MCDM methods are useful to support decisions made by considering the importance of each criterion. Although each consumer might have different preferences, the selection findings can be quickly revised based on their preferences [25].

In the automotive industry, MCDM methods have mostly been used by manufacturers to select suppliers. This study provided an example of its different use by focusing on consumers' preferences on the selection of the car. All stakeholders can use MCDM methods because almost all processes involve making decisions. For instance, MCDM methods could have been applied by dealers to better respond to consumers' preferences. Dealers might develop a web-based programme by using MCDM methods to customise consumers' search results in line with their preferences.

References

[1] D. H. Byun, "The AHP approach for selecting an automobile purchase model," *Inf. Manag.*, vol. 38, no. 5, pp. 289–297, 2001.

[2] A. (Pazirandeh) Arvidsson and L. Melander, "The multiple levels of trust when selecting suppliers – Insights from an automobile manufacturer," *Ind. Mark. Manag.*, pp. 1–12, 2020.

[3] A. Giampieri, J. Ling-Chin, W. Taylor, A. Smallbone, and A. P.

Roskilly, “Moving towards low-carbon manufacturing in the UK automotive industry,” *Energy Procedia*, vol. 158, pp. 3381–3386, 2019.

[4] M. R. Galankashi, S. A. Helmi, and P. Hashemzahi, “Supplier selection in automobile industry: A mixed balanced scorecard-fuzzy AHP approa ch,” *Alexandria Eng. J.*, vol. 55, no. 1, pp. 93–100, 2016.

[5] S. Apak, G. G. Göğüş, and İ. S. Karakadılar, “An Analytic Hierarchy Process Approach with a Novel Framework for Luxury Car Selection,” *Procedia - Soc. Behav. Sci.*, vol. 58, pp. 1301–1308, 2012.

[6] G. Sakthivel, M. Ilangkumaran, G. Nagarajan, A. Raja, P. M. Ragunadhan, and J. Prakash, “A hybrid MCDM approach for evaluating an automobile purchase model,” *Int. J. Inf. Decis. Sci.*, vol. 5, no. 1, pp. 50–85, 2013.

[7] B. Bartikowski, F. Fastoso, and H. Gierl, “Luxury cars Made-in-China: Consequences for brand positioning,” *J. Bus. Res.*, vol. 102, pp. 288–297, 2019.

[8] S. Weber, “Consumers’ preferences on the Swiss car market: A revealed preference approach,” *Transp. Policy*, vol. 75, no. December 2018, pp. 109–118, 2019.

[9] I. Galarraga, S. Kallbekken, and A. Silvestri, “Consumer purchases of energy-efficient cars: How different labelling schemes could affect consumer response to price changes,” *Energy Policy*, vol. 137, p. 111181, 2020.

[10] F. Ozturk and G. K. Kaya, “Personnel selection with fuzzy VIKOR: an application in automotive supply industry,” *Gazi Univ. Sci. J. Part C Des. Technol.*, vol. 8, no. 1, pp. 94–108, 2020.

[11] A. O. Kuşakçı, B. Ayvaz, F. Öztürk, and F. Sofu, “Bulanik Multimoora İle Personel Seçimi: Havacilik Sektöründe Bir Uygulama,” *Ömer Halisdemir Üniversitesi Mühendislik Bilim. Derg.*, vol. 8, no. 1, pp. 96–110, 2019.

[12] N. Jamil, R. Besar, and H. K. Sim, “A Study of Multicriteria Decision Making for Supplier Selection in Automotive Industry,” *J. Ind. Eng.*, vol. 2013, pp. 1–22, 2013.

[13] L. Turcksin, A. Bernardini, and C. Macharis, “A combined AHP-PROMETHEE approach for selecting the most appropriate policy scenario to stimulate a clean vehicle fleet,” *Procedia - Soc. Behav. Sci.*, vol. 20, pp. 954–965, 2011.

[14] F. Dweiri, S. Kumar, S. A. Khan, and V. Jain, “Designing an

integrated AHP based decision support system for supplier selection in automotive industry," *Expert Syst. Appl.*, vol. 62, pp. 273–283, 2016.

[15] A. Manello and G. Calabrese, "The influence of reputation on supplier selection: An empirical study of the European automotive industry," *J. Purch. Supply Manag.*, vol. 25, no. 1, pp. 69–77, 2019.

[16] M. Alkahtani, A. Al-Ahmari, H. Kaid, and M. Sonboa, "Comparison and evaluation of multi-criteria supplier selection approaches: A case study," *Adv. Mech. Eng.*, vol. 11, no. 2, pp. 1–19, 2019.

[17] C. Renzi, F. Leali, and L. Di Angelo, "A review on decision-making methods in engineering design for the automotive industry," *J. Eng. Des.*, vol. 28, no. 2, pp. 118–143, 2017.

[18] R. D. Raut, H. V. Bhasin, and S. S. Kamble, "Multi-criteria decision-making for automobile purchase using an integrated analytical quality fuzzy (AQF) technique," *Int. J. Serv. Oper. Manag.*, vol. 10, no. 2, pp. 136–167, 2011.

[19] R. Singh, Rashmi, and S. Avikal, "A MCDM-based approach for selection of a sedan car from Indian car market," in *Harmony Search and Nature Inspired Optimization Algorithms*, Springer Singapore, 2019, pp. 569–578.

[20] S. Vinodh, A. Patil, T. S. Sai Balagi, and P. Sundara Natarajan, "AHP-PROMETHEE integrated approach for agile concept selection," *Int. J. Serv. Oper. Manag.*, vol. 18, no. 4, pp. 449–467, 2014.

[21] RAC, "Car reviews," *RAC*, 2020. [Online]. Available: https://www.rac.co.uk/drive/car-reviews/. [Accessed: 10-Jun-2020].

[22] R. W. Saaty, "The analytic hierarchy process-what it is and how it is used," *Math. Model.*, vol. 9, no. 3–5, pp. 161–176, 1987.

[23] J. P. Brans and B. Mareschal, "PROMETHEE methods," in *International Series in Operations Research and Management Science*, vol. 78, New York: Springer, 2005, pp. 187–219.

[24] J. P. Brans, P. Vincke, and B. Mareschal, "How to select and how to rank projects: the PROMETHEE method", *Eur. J. Oper. Res.*, vol. 24, pp. 228–238, 1986.

[25] F. Öztürk, "Qualität, Effizienzsteigerung und integrierte Managementsystemen im türkischen Eisenbahnsektor'', *Social and Natural Sciences Journal*, Volume 8, ISSUE 2, pp.14-19, 2014.

CHAPTER XIV

MODERNIZATION AND CHANGE OF HOUSING IN TURKEY

Assoc. Prof. Deniz DEMIRARSLAN*&Lecturer Oğuz DEMIRARSLAN**

*Kocaeli University, Kocaeli, Turkey
e-mail: demirarslandeniz@gmail.com, Orcid ID: 0000-0002-7817-5893

** Maltepe University, Istanbul, Turkey
e-mail: oguzdemirarslan@maltepe.edu.tr, Orcid ID: 0000-0001-9512-5022

1.Introduction

Modernization which is defined as a thought system that has started in Europe in the 17th century and which has influenced the whole world afterward as marking on communal life and organization forms comprises various transformations in social life. Modernization is perceived as the struggle of accepting the features of highly developed societies by less developed societies (Giddens, 2004: 19). In modernization processes, generally, dualities such as culture/civilization, new/old are observed. In the Ottoman community, concepts of Modernization and Westernization have been used synonymously. In the 19th century, modernizing generations ranging from reformist bureaucrats to the leaders of the new Republic, have tried to reach the level of western civilization and to progress by importing institutions, forms, and techniques. At the beginning of the 19th century, during the period when the Ottoman economy opened up to the capitalist global economy, The English Commercial Agreement of 1838 has constituted an important turning point. European commodities such as furniture, building materials, and costumes being produced after this agreement, have begun to come to the Empire (Goffman and Masters, 1999:199). With the Reorganization Reforms (1839), modernization has become a rule in each area of the community. The continuous contact had with European products and traditions has created a change in the living style. This situation was first felt in the palace life and then, it was felt in the housings of segments being noble and having high incomes (Berkes, 1975:30). Ottoman community has adopted the Western lifestyle with culture, traditions, fashion, dining, and culinary culture and they have preferred the Western style of furniture and decoration in their homes. Item usage and in-house lifestyle habits from nomadic life have been replaced by a new lifestyle called “Alafranga” (European Style). Since the Reforms Period, furniture, kitchen tools, heating and lighting equipment, or their imitations that were brought from the West have been used. This situation has changed home life and house planning by influencing various actions such as eating, drinking, sitting, and sleeping. Modernizing life has disrupted the cultural balance of life and has caused a confusion to be experienced between the old and the new. The transformation of home and

lifestyle has caused a new architecture to arise and apartment life was adopted as being the most suitable one. Housing architecture has always been an effective reform and change tool besides being a powerful symbol due to its nature (Tanyeli, 1996: 284-298).

Changes occurring at housing spaces reveal important information about the transformation of lifestyles of communities and daily applications of individuals. The transformation of the house cannot only be considered as physical changes as per functional requirements. This is a cultural change occurring at the same time. With regard to housing, cultural change means a physical change that occurs as per the housing settlements and changing identities of habitants. Lifestyles of people living in a defined environment can reshape their identities with the impact of their cultural changes. Structure, order, style, decoration, and furniture of housing make it become a place different than others where it can define itself. According to the saying of Rapoport (1981); housing is a process, an identity, a personal value, and a venue where status is being defined. Furniture, objects, and their placement in the venue give certain messages. All of them are defined as cultural change and cultural change can be summarized as a complete alteration of society or as a partial transformation taking place in certain segments of the community. Socio-cultural and economic developments, the effects of Western civilization, reforms, women-human rights, changing roles in family members, nuclear family type have influenced lifestyles and changing housing plan orders in Turkey in the modernization period starting from the 19th century until today. In this article, the impacts of the modernization movement that has started within the institution of the Ottoman State from the beginning of the 19th century, on the housing changes, housing typology, and housing designs from the period of starting till nowadays have been examined.

2.Housing During Modernization Process in Turkey

In Turkey, the modernization process has emerged starting from the beginning of 19th century and it is continuing. However, the major change in housings is observed starting from the second half of the 19th century.

2.1. Change in Housing in the Second Half of 19th Century and at the Beginning of 20th Century

Turks were living for years in Middle Asia and after immigrating to Anatolia in the form of a nomadic community in the tents named as “Yurt”. Turks who began to live in permanent settlement in time, have established “Turkish House” in which they have used fixtures beings shaped with their own cultures, traditions, and needs. Due to the structure of Turkish-Islamic thought style based on the principle that “less is more”, in Turkish houses very few objects were used for years (Kuçukerman, 1985: 32; Gunay, 1999: 214). Items such as couch and cupboard in the interior are mostly

fixed items attached to the structure. Room which is the main component of Turkish house is a multi-functional living unit. In the housings where traditional Turkish family in the form of wide family lived, each room was organized to meet the needs of a nuclear family. In each room it is possible to sit, rest, eat meals, cook meals, and even to have a bath. Planning of Turkish house was established with the organization of rooms around a hall named as "sofa". Sofa is a multi-functional central space and circulation area where other rooms opened to. Spatial relationship of sofa and the rooms constitute housing typology: Such as houses with exterior sofa, interior sofa, middle sofa, and houses without sofa. Houses generally had two floors. Upper floor is the living area (Eldem, 1984: 14-15). The kitchen, bathroom, and toilet are usually in the garden outside. Housing features are similar for each segment in the community and richness was only reflected on number of rooms and decoration. Housing rooms and privacy are among the most important characteristics of these housings (Fig.1).

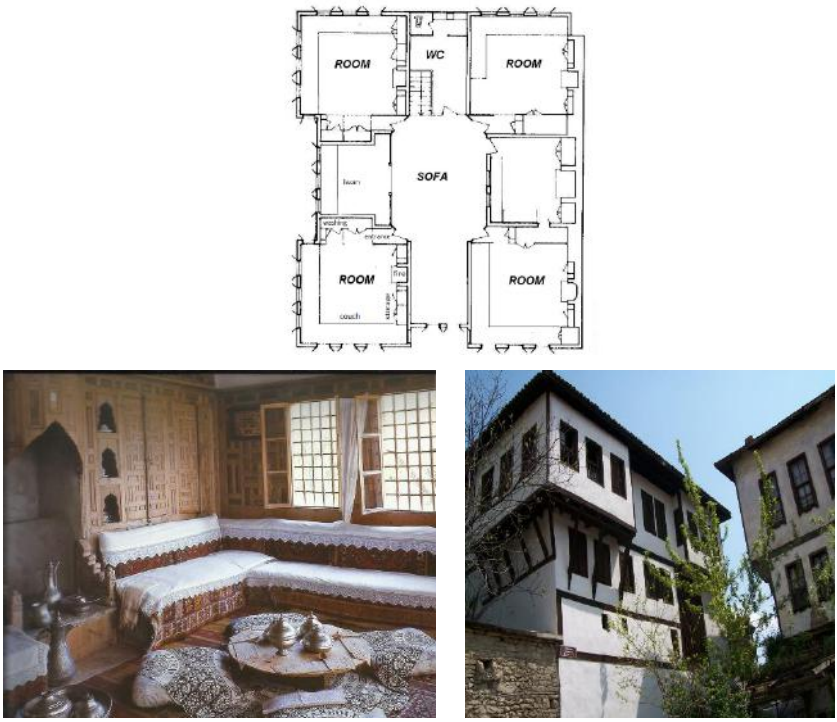

Fig.1. Traditional Turkish House Plan Type (Gunay, 1999: 214), Traditional Turkish House Room (Gunay, 1999: 171) and General Appearance of Traditional Turkish House.

The traditional house of the Ottoman period has begun to transform during the Modernization period. At the end of the 19th century, modernization efforts of the Ottoman period had impacts on urban spaces, housing typologies, architectural styles, and decoration. As a result of increasing population and usage of European commodity household goods, row houses have come out as a new housing typology. Row houses took the place of houses that were previously built in the gardens. Row houses were built for medium-income merchants, artisans, and bureaucrats in certain regions in Istanbul. The primary factor that differentiated a row house from a traditional house was related to the floor plan (Batur et all, 1978: 60-65). An introverted type of plan relating to traditional houses was developed as facing the street in this type of housing. The lower floor of housing was constituted of store and living area and the upper floor was constituted of the bedroom floor (Fig.2). Gorgulu (2016: 167) has defined row houses by stating: "With the emergence of medium classes for the first time in the 1880s, row houses and apartments began to be built. The medium class was constituted of non-Muslim merchants realizing trade with Europe. Hence, apartment blocks and row house type of structuring examples have come out in non-Muslim quarters."

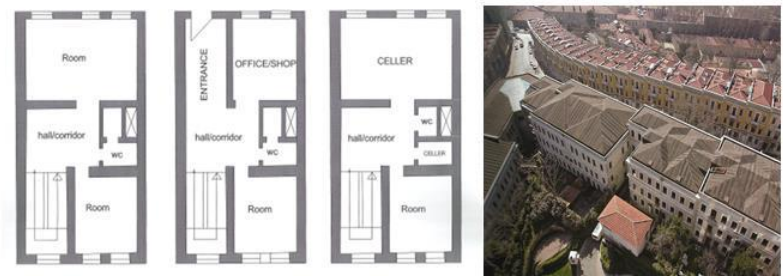

Fig.2. Row House Plan Type- Akaretler (Kızıl, 1981: 36) and View of Istanbul Row Houses - Akaretler (Kuban, 2007: 655).

Another new typology was related to apartment blocks that were constructed in the Pera region of Istanbul as being the centre of modernization due to lack of land. When a Muslim Ottoman family chose to settle in Pera where Westernization movements were seen for the first time, they were deemed as having made a choice that determined a modern lifestyle. For this reason, people began to live in apartments having European type of corridor plan in Pera instead of a traditional Turkish house with sofa. Using Western-style furniture in these housings was accepted as being an expression of change relating to cultural and social status. According to Rapoport (1981: 12-13) personal identity is more at the forefront in modern Western culture and in this regard, housing is an element with which the individual symbolized himself. The same situation was lived through in the Ottoman period and housings have reflected the

status and richness of individuals in the community. These apartment blocks were designed by important European architects of that period. Western-type of housings that reached our time such as Decugis (1895- Architect Vallaury), Botter (1900- Architect d'Aranco), Doğan (1894), Kamondo, Mısır (1905-1910, Architect Hovsep Aznavuryan), Frej (1905-1906, Architect Khyrikiadis), Tayyare Apartments (1918, Architect Kemaleddin) have provided an appropriate housing solution for the bourgeoisie as they were located close to finance region of Istanbul (Figue-3). In contrast to various apartments that were built in Neoclassical, New Baroque, Art Nouveau, Eclectic styles, Tayyare Apartments were built in national architectural style (Kuban, 2007: 654). It constitutes the first structuring group being realized with a reinforced concrete skeleton system in Istanbul and the first mass housing work in Turkey. Plan solutions of Tayyare Apartments resemble plan solutions of multi-floor social housing structures aiming to meet the sheltering requirements of the urban population that rapidly increased after the Industrial Revolution in Western European cities (Fig.3,4) (Yavuz, 1993: 24). As a result, in cities, vertical and high-density buildings started to be built. These houses were generally constructed on narrow parcels in various regions of the city. The typical floor plan of this type of house is composed of a living room facing the street, rooms being connected with a corridor, and service spaces. Each one of the rooms has a different function (Fig.4). During this period, family structure has changed towards a nuclear family. For this reason, in the housings being built during the modernization period, separation of men and women which was the case in traditional houses was eliminated. Buildings are composed of four or six floors.

Fig.3. View of Mısır and Tayyare Apartments (Kuban, 2007: 656).

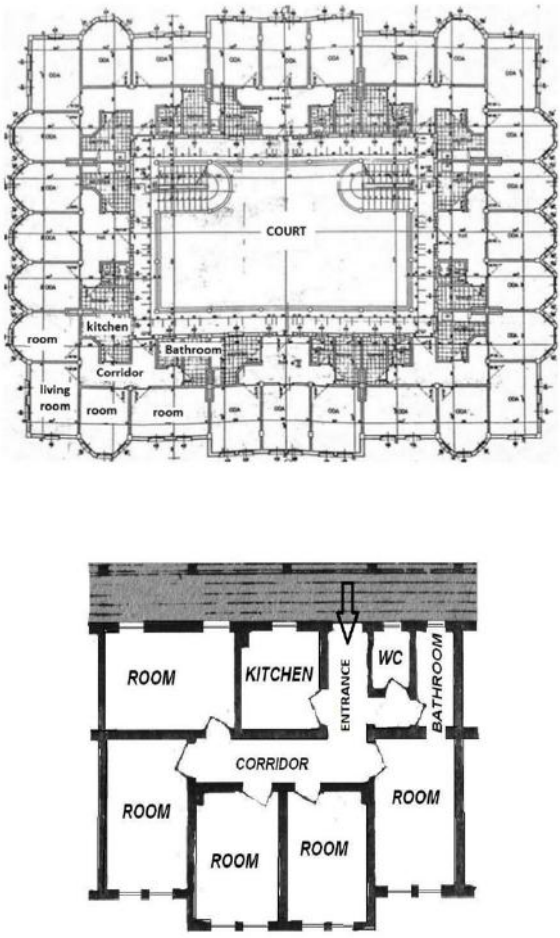

Fig.4. Floor plan of Tayyare Apartments (Kuban, 2007: 656), Typical Apartment Flat Plan of The Period (Kızıl, 1981: 36).

2.2. Change in Housing During the Republican Period

These relations between modernization and housing and mutual effects have also continued during the Republican period. The new state that was established in the year 1923 and the reforms that were realized have constituted an effective factor regarding these relations. In the early Republican period, housing policy was established around the logic of nationality instead of the requirements of capitalist urbanization. With the planning of Ankara as the capital of the new Republic, government staff and public officers came to the agenda (Keles, 2002: 147-148). Surely, in the first decades of the Republic, workers were considered among those needing sheltering on a systematic basis (Bozdoğan, 2001: 239-241). In the 1930s, housings designed in reinforced concrete skeleton system as being

applied in the Modernization movement, began to be constructed. Housing designs of foreign architects such as Ernst Egli, Clemens Holzmeister, Bruno Taut have also influenced the designs of Turkish architects during the early Republican period (Kopuz, 2018: 363- 373). On the other hand, life in traditional Turkish house was not in harmonization with the new life of developing urban bourgeoisie of the Republican period. Until the 1940s, housing typology was influenced by the tension between official ideology and practical reality. When multi-floor housing production forms in the early Republican period are generally reviewed, it is seen that urban bourgeois that was tried to be newly established have built apartment blocks with their accumulations. These apartment blocks were mainly built to obtain a certain revenue and they were leased out. For this reason, housings that were built in the 1930s-1940s being privately owned were named "rental houses". In connection with radiator usage, plan schemes were designed as rooms opening to a central hall or being lined up in the corridor (Gorgulu, 2016: 170) (Fig.5).

Fig.5. Flat Plan of Ankara Rental Houses (Arkitekt Magazine, 1937, Istanbul).

The years following the Second World War have been determinant in solving the housing problem from various aspects in Turkey. The economic and social dynamics leading to urbanization tendencies, the establishment of housing policies, and the emergence of a Turkish-style slum (gecekondu) house are observed in this period. Characteristics of the period are related to the rapid economization, industrialization, and the increase of irregular settlements in the city centres occurring with the changing economic policy. Starting from 1950 onward, illegal/legal housing structures have increased. Increasing migration and insufficiency of housing stock have enabled for small and medium scale enterprises to come out. Housing standards were established and published by the government in March 1964. Accordingly, the maximum base area of a

housing unit is determined as 63 m² (Public Housing Standards, 1964: 8). These standards have dissuaded luxurious constructions and it was passed on to mass housing production. During the rapid apartment block construction process, acceleration of the transformation of traditional housings and independent houses into apartment blocks, and lack of complementary municipality and construction legislation have caused irregular urbanization to take place. Property Ownership Law (1965), has constituted a turning point for the popularization of "apartment" type of housings as being dominant middle-class home typology and for them to become a standard. These buildings, the quality of which was low but the exchange value of which was relatively high were mainly built only for their usage values. They don't represent an architectural style and they all look similar to one another. When it was reached to the 1980s, urban areas were covered with apartment blocks and slums. As being different from the architectural structuring of the early Republican period representing the "ideal house" phenomenon of nationality, modernization, and national bourgeoisie, the housing sector between the 1950s and 1980s, has become an experience where instant interests and needs of urban middle classes and urban poverty class were met spatially. In the year 1981, Social Housing Law has been reviewed and the government motivated private construction companies. However, settlement projects continued to be undertaken basically by local administrations in a significant way. In the last fifty years period, the urban population in Turkey increased dramatically. The difference between requirements and official housing supply, caused uncontrolled growth to take place and for the emergence of environmental problems that threatened the residents of big cities. With Mass Housing Law which became effective in year the 1984, the number of housings increased, and big scale housing areas have been developed outside the city to meet housing requirements. On the other hand, in recent years increasing number of luxurious housing developments are being observed.

2.2.1. Basic Housing Typologies of the Republican Period

The main housing typologies of the Republican period are in the form of apartment blocks, slums (gecekondu), mass housings, and luxurious housings. Furthermore, these types of housings are structures being formed with modernist discourse for the urban population with the features being unique to them.

2.2.1.1. Apartment Blocks

The increasing population density in cities has caused for housings to develop as horizontally and vertically. Flat is a prototype that combines living areas both side by side and on top of one another. Production types of these units are observed in two major groups: Build-sell (Contractor)

production type and mass housing production. The build-sell type of housing production method is a production based on private sector (Gorgulu, 2003: 50). The owner of housing gives his old housing to a contractor making this type of production, he causes the housing to be demolished, and he becomes the owner of a flat in return for a certain ratio. Mass housings are built by building cooperatives or official institutions. Regardless of production form, the purpose of rapid development of apartments as dominant housing typology in big urban centres as being based on socio-cultural and economic context starting from the 1950s, is related with the imposition of the "ideal house" opinion on the urban middle class as it has started in the 19th century. Following the 1999 Marmara Earthquake, the urban transformation has started in big cities and new apartment blocks began to be constructed by demolishing old and worn buildings. Especially starting from the 2000s, apartment block structures with very high floors have taken their place in the housing sector under the name of "residence". Being the owner of a flat in these high floor buildings has been accepted as a feature determining high status in the society. These housings which attract attention with their planning fitting to a consumption focused lifestyle, have become quite foreign to the Turkish housing order. Apartment flats that were designed for a nuclear family during the modernization process were reduced in terms of area and studio type of flats (open kitchen, 1 room, 1 hall) began to be built.

Shortly, starting from the 1950s onward, modern flat has become a dominant structure establishing environment with the urban structure and social life with its scale, typology, production processes, and social aspects. As the most common residential unit, the apartment block is also equated with the concept of housing. Multilevel processes such as population growth, economic and cultural change, technological transformations, legal regulations, and a general change in the urban population's enjoyment and lifestyles have interacted in this expansion of apartments as the dominant urban housing layer. Moving to an apartment flat, establishing interior spaces having modern taste and styles, making changes relating to role models within the house constitute the dynamics of this differentiation. In the design of the apartments, the corridor has replaced the sofa in the traditional residence. The corridor turns into a line and separates the rooms facing the street from the service areas facing the backside. Generally, housing plans consist of a living space and 2-3 rooms. The number of flats on each floor changes between three to six and elevator is only mandatory in buildings having more than five floors (Fig.6). These prototypes do not belong to Anatolia. They are seen everywhere where modernization has touched. In interior space, people have met with their sitting rooms for the first time and the rooms have been defined as bedrooms, dining, and sitting rooms for the first time. Rooms in these flats nearly had equal sizes as per the Housing Standards of 1964.

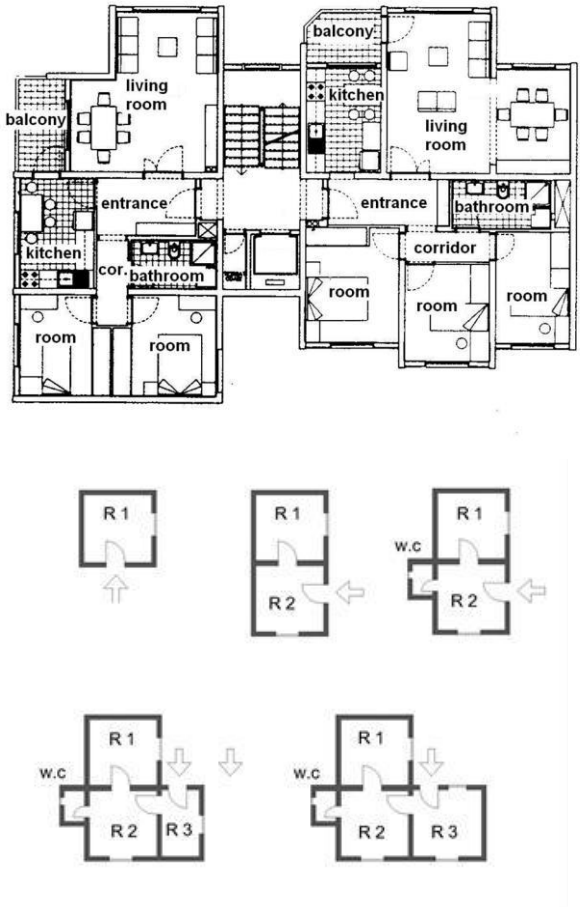

Fig.6. A Typical Apartment Flat Plan and Space Organization in the First Examples of Slum Scheme of Space Variations for Slums in the Application for the Aga Khan Awards (The Aga Khan Award for *Architecture, 1980).*

2.2.1.2. Slum (Gecekondu)

When people began to migrate from villages to cities as a result of industrialization at the end of the1940s, cities were introduced with the concept of slum (gecekondu). Slums are defined as "gecekondu" in Turkey. Growing industrialization and developing transportation networks in the 1950s attracted villagers to the cities. As can be imagined, the housing stock of cities remained far behind the housing requirements of those coming. For this reason, at the end of the 1940s and the beginning of the 1950s, people from the worker's classes have built slums, preferably close to the works that were provided for them (Cakır, 2012: 212). During this period, slum quarters have turned into slum villages surrounding the

city. In the first examples of slums, a housing unit contains a single venue that accommodates all types of activities, as in traditional housing. The number of rooms increased as income and needs increasing. For this reason, at the first stage of squatting, simple spatial organizations were generally used (Saglamer, 1993: 207-220; Turgut, 2001: 17-25). They had low-quality construction standards. Its residents still maintained their rural lifestyles and rituals, a high level of privacy, and regionalism. With the privileges given by the government, these housings have attained legal form at certain times. By benefiting from this situation, these housings were given to the build-sell sector and they were transformed from simple shelters into apartment blocks (Fig.6).

2.2.1.3. Mass Housings

Although Mass Housing Law came out in 1984 in Turkey, the starting of mass housing production is based on much more passed years. As it was also mentioned above, the first mass housing application in Turkey is accepted as being Tayyare Apartments. This building production system starting with apartment blocks was observed as row houses in the early Republican period, as independent houses in the 1950s, and as new apartment blocks in the 1970s. Saracoglu Housings that were built for staff as Ankara became the capital city (Paul Bonatz, 1945) was constituted of row houses and in this project where typical German housing settlement and Bauhaus principles were applied as settlement order, building fronts were bearing traces from traditional Turkish architecture (Bilgin, 1999: 482) (Fig.7).

While modern lines were seen in mass housings in apartment form that were produced by cooperatives after 1950, especially as it was the case in the example of Istanbul Levent Housings, independent houses with gardens have also been built in the form of mass housing. It is seen that housings of 90-100 m2 were built in the majority of plans applied in the 1970s during when important housing examples such as Atakoy housings were produced and having the perception that the placement of smaller flats would reduce the costs and enable for a greater number of families to have shelter, has affected the projects (Fig.8). With the establishment of the Collective Housing Administration in 1984, many mass housing projects were realized in the big cities with the partnership of government banks. In the 1990s, besides apartment blocks, independent houses for high-income groups were also built as part of mass housing production. Features of almost all of these housings are that flat plans are generally constituted of corridor/ hall, living room, 2 rooms, kitchen, and bathroom.

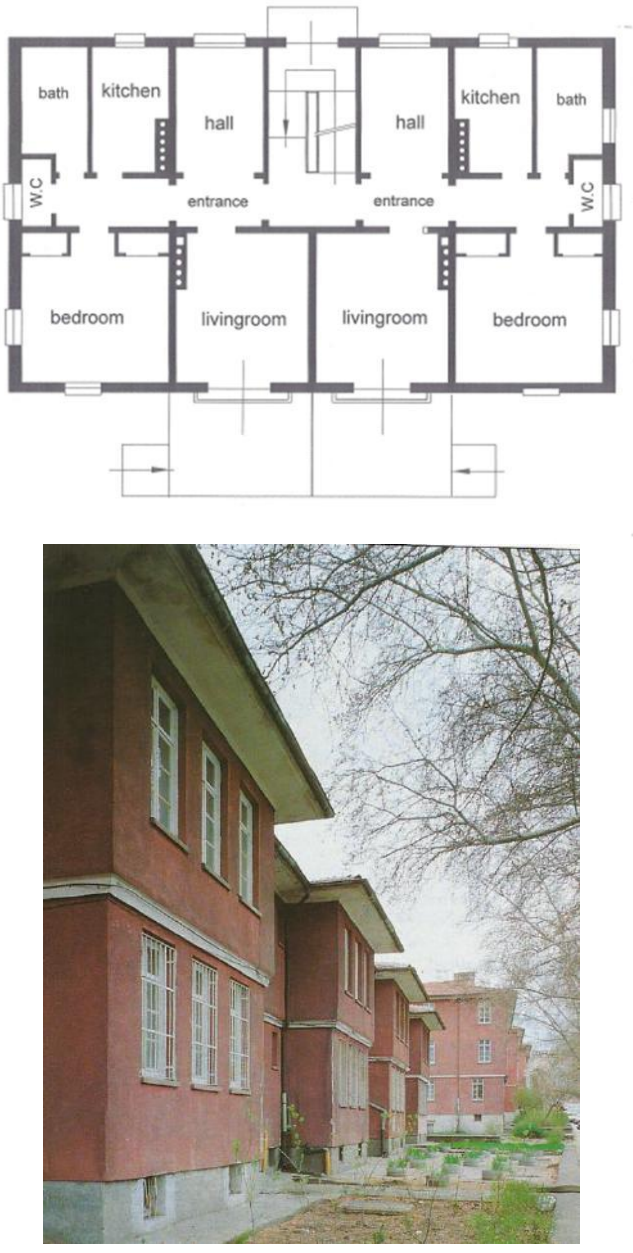

Fig.7. Saraçoğlu Houses Flat Plan Type – Ankara, Saracoglu Houses-Ankara (Bilgin, 1999: 482).

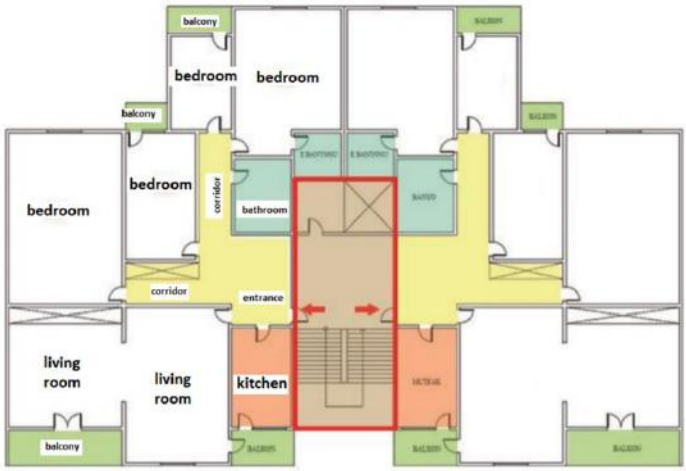

Fig.8. Mass Housings Flat Plan Scheme- Atakoy, Istanbul.

2.2.1.4. Luxurious housings

In recent years, increasing numbers of luxurious housing settlements have been observed inside and around the cities throughout Turkey. These settlements were especially preferred by high- income families. Luxurious housings are observed in two forms: Residences and gated communities. In recent years, residences being multi-floor housing blocks have been established near business centres, including various services of a five-star hotel. These developments in the urban centre attract high-income groups. These high residences being constructed as a live fashion, have disseminated throughout Turkey starting from Istanbul. Residences being built as multi-floor buildings where modernizing life is presented as a new sheltering form creates a living alternative near the centre for the urban citizen not wishing to reside away from the city centre. Besides having the function of sheltering, it also bears many structure groups such as shopping, entertainment, sports centre, office structures within its body. This social richness is at such a dimension that many mass housing settlements bear the quality of sub-cities. In these housings, all services including cleaning and dining services are met by professional building operators, and provision of a controlled and secure environment to the user comes to the agenda. Due to the transmitted life conditions, it is required for the housings to be designed in the form of studio type but their sizes vary between 70 m2 to 532 m2 (Fig.9) (Gorgulu, 2016: 175). Before the 1980s, luxurious housings in Turkey belonged to the elite segment living in housings with a private design having gardens. Concurrently with the rise of the giant high-rise buildings, there was an interest in reviving the local character of the old cities and gated communities began to be widespread. Enterprises were selling these housings in the form of villa or

apartment as a neighbourhood relationship. Advertisements were introducing luxurious apartment flats being constructed with imported building materials and reflecting “modern lifestyle” and the big villas that were built as per international standards. Advertisement slogans were in the form of “high security” and “ultra-luxurious”. The most important feature of these new housing complexes being surrounded with security walls and being away from centres of many cities, urban complexity, and noise, was that they were seen as the symbol of modernization and status rise.

Fig.9 Example of A Residence Flat Plan and Residences, Apartments and City Texture, Istanbul.

3.Conclusion

Housing is a formation that reveals the protection needs of individuals and cultural, social, and economic aspects of communal life and which is an indicator of civilization. Sheltering is a widely seen problem in Turkey and developing countries. This problem does not have a qualitative or a quantitative aspect. Modernization efforts, migration, and irregular urbanization based on economic issues make it harder for the problem to be resolved. As a result of the modernization movement which effected the shaping of housings in the Ottoman State Period, starting from the second half of the 19th century, the traditional house model in plan type having sofa where the room constituted the core area of the house, as fitting to Turkish family structure, has transformed first into row house and then into apartment type of housing. In the first years following the establishment of Turkish Republic, this transformation was observed. The passage from multi-functional room to spaces with a single function, has generally revealed a standard plan type being comprised of 2-3 rooms and living space. In time starting from the 1950s Turkish population has undergone a dense urbanization process (Table-1). Rapid urbanization has inevitably caused for slums to appear around the city areas. The solution to problems relating to harmonization with urban living and a new lifestyle was seen to be rapid and cheap production of housings and hence, mass housing units have been built. Apartment blocks have been internalized with modernist discourse. Starting from the 2000s onward, luxurious housings were seen as the symbol of modern lifestyle.

Table 1. Modernization and Change of Housing Form in Turkey

Period	Housing types	Plan form
Ottoman Period from the ending of 19th century to the ending of 20th century	Traditional Housing Type	With sofa
	Row Houses	Hall / Corridor
	Apartment Blocks	Corridor
Republican period (20th century-nowadays)	Row houses	Hall/corridor
	Apartment Blocks	Corridor
	Slum	Simple spatial organization
	Collective Housing (Apartment Blocks and garden housing)	Corridor
	Luxury Houses (Residence, Garden Housing	Corridor

The modernization phenomenon has planned modernizing housing and city. The modernization phenomenon has caused foreign housing structures to emerge as being away from traditional living and being foreign to the requirements of the Turkish family structure. The quarter has turned into a place of collective housing or gated communities. Under these conditions, the housing environment has constituted major housing typologies of the modernization period in Turkey in the form of row houses, apartments, slums, collective housings, and luxurious housings. However, the housing type that was adopted by low, middle, and high-income groups of the community during this process was mainly related with apartments. Apartment blocks have been adopted by society as the expression of modernization. Even the slums have been transformed into apartments in time. While mass housings were built in the form of apartment blocks, especially the high-income segment of the community have begun to prefer closed housing settlements resembling traditional settlement form, again. As a conclusion, the housing phenomenon in Turkey concerning modernization is a status-identity symbol having passage from sofa to the corridor, from multi-functional room to single function room, and from low floor housings to multi-floor/luxurious housings, both with regards to spatial and perceptual aspects (Table-1).

References

---, (1937), *Arkitekt Dergisi*, Istanbul, Turkey.

---, (1964), *Halk Konutları Standartları*, Imar ve Iskan Bakanlıgı Press, Ankara, Turkey.

----, (1980), Gecekondus: Various Cities in Turkey, The Aga Khan Award for Architecture.

Batur A., Fersan N., Yucel A. (1978). "Reuse of 19th Century Rowhouses in Istanbul", Conservation as Cultural Survival, The Aga Khan Award for Architecture, Istanbul, Turkey.

Berkes N. (1975), *Türk Düşününde Batı Sorunu*, Bilgi Press, Istanbul, Turkey.

Bilgin I. (1996), "Housing and Settlement in Anatolia in the Process of Modernization, *Housing and Settlements in Anatolia: A Historical Perspective*, Habitat II, Tarih Vakfı Press, Istanbul, Turkey, pp. 472-490.

Bozdoğan S. (2001), *Modernizm And Nation Building*, Metis Pub., Istanbul, Turkey.

Cakır, S. (2012), "Türkiye'de Göç, Kentleşme/Gecekondu Sorunu ve Üretilen Politikalar", *SDU Faculty of Arts and Sciences Journal of Social Sciences*, May 2011, No:23, pp.209-222.

Eldem S. H. (1984), *Turk Evi: Osmanlı Dönemi I, Türkiye Anıt Cevre Turizm Degerlerini Koruma Vakfi Press*, Istanbul, Turkey.

Giddens, A. (2004). *Modernliğin Sonuçları*. Ayrıntı Press, Istanbul, Turkey.

Goffman E, Masters D. (1999), "Istanbul: From Imperial to Peripheralized Capital", *The Ottoman City between East and West Aleppo, Izmir and Istanbul*, Ed. Edhem Eldem, Cambridge University Press, Cambridge, United Kingdom, pp.194-196.

Gorgulu T. (2003), "İstanbul'da Çeşitlenen Konut Üretim Biçimleri ve Değişen Konut Alışkanlıkları",*Mimarist,* 2003/7, pp.50-60.

Gorgulu T. (2016), "Apartman Tipolojisinde Gecmisten Bugune; Kira Apartmanından Rezidansa Gecis", *TUBA-KED* 14/2016, pp.165-178.

Gunay R. (1999), *Safranbolu Evleri*, Yem Press, Istanbul, Turkey.

Keles R. (2002), *Kentleşme Politikası*, İmge Press, Ankara, Turkey.

Kızıl, F. (1981), Toplumsal Geleneklerin Konut İci Mekan Tasarımlamasına Etkisi Ve Toplumsal Geleneklerimizi Daha İyi Karsılayacak Konut İci Fiziksel Cevre Kosullarının Belirlenmesi, IDGSA Press, Istanbul, Turkey.

Kopuz A.D. (2018), "Türkiye'de Erken Cumhuriyet Dönemi Yabancı Mimarların İzleri, Franz Hillinger Örneği", *Megaron* 13/3, pp. 363-373.

Kuban D. (2007), *Osmanlı Mimarisi*, Yem Press, Istanbul, Turkey.

Kucukerman O. (1985), *Turkish House*, Turing Press, Istanbul, turkey.

Rapaport, A. (1981), Identity and Environment: A Cross-cultural Perspective, in *Duncan, Housing and Identity: Cross-cultural Perspective*, Croom Helm Press, London, United Kingdom.

Rapoport, A. (1998). "Using Culture in Housing Design", *Housing and Society*, 25, pp.1-20.

Saglamer, G. (1993), "Continuation of Vernacular in Squatter Settlements", Marjorie Bulos, Necdet Teymur (Edit.), *Housing: Design, Research*, Education, Avebury, pp.207-220.

Tanyeli U. (1996), "Osmanlı Barınma Kültüründe Batılılaşma-Modernleşme: Yeni Bir Simgeler Dizgesinin Oluşumu", *Tarihten Günümüze Anadolu'da Konut ve Yerleşme*, Habitat 2, YEM Press,İstanbul, Turkey, pp. 284-298.

Turgut, H. (2001), "Culture, Continuity and Change: Structural Analysis of the Housing Pattern in Squatter Settlement", *GBER* Vol. 1 No. 1 2001 pp 17-25.

Yavuz Y. (1993), “Siteler”, *Istanbul Ansiklopedisi*, Kultur Bakanlıgı Tarih Vakfı Press, Istanbul, Turkey.

Yürekli, H., Yürekli, F., (2005), *The Turkish House*. The Building Information Centre Publication, İstanbul.

The figures that are not mentioned in the references are belonged to the author.

CHAPTER XV

THE POTENTIAL USE OF FIBROUS WEBS ELECTROSPUN FROM POLYLACTIC ACID / POLY Ɛ-CAPROLACTONE BLENDS IN TISSUE ENGINEERING APPLICATIONS

Janset OZTEMUR* & Assist. Prof. Dr. Ipek YALCIN-ENIS**

*Istanbul Technical University, Textile Technologies and Design Faculty, Department of Textile Engineering, e-mail: oztemurj@itu.edu.tr
Orcid ID: 0000-0002-7727-9172

**Istanbul Technical University, Textile Technologies and Design Faculty, Department of Textile Engineering, e-mail: ipekyalcin@itu.edu.tr
Orcid ID: 0000-0002-7215-3546

1. Introduction

Tissue engineering (TE) is an interdisciplinary field that allows the production of functional tissues and organs by imitating natural biological materials. Currently, tissue engineering applications attract great interest by researchers due to important reasons such as donor failure, tissue/organ incompatibility, unsuccessful tissue/organ transplantation (Chandra, Soker, and Atala, 2020).

There are many fabricating techniques to produce a fibrous scaffold surface like self-assembling (Yu, Bao, Shi, Yang, & Yang, 2017), freeze-drying (Norouzi and Shamloo, 2019), phase separation (Biswas, Tran, Tallon, & O'Connor, 2017), solvent casting (Mao et al., 2018) and 3D printing (Jammalamadaka and Tappa, 2018). Although these methods achieve success in many criteria such as cell viability, cell adhesion, and proliferation as well as scaffold permeability, they have some limitations in terms of pore architecture and fiber diameter controllability (Rogina, 2014). Electrospinning is a highly preferred, effective, and simple method that offers advanced and adjustable morphological properties (Bhardwaj and Kundu, 2010). Thus, it is obvious that this technique meets the desired features of the biomedical areas, especially in tissue engineering applications.

On the other hand, biomaterial selection has a crucial role in the design and production of medical applications since the long and short term mechanical properties, cell-cell and cell-matrix interactions, biocompatibility, biodegradability, toxicity, manufacturability, and the form of the final scaffold are related with the biomaterial used in fibrous web fabrication (Chesterman, Zhang, Ortiz, Goyal and Joachim, 2020; Suwantong, 2016). Biomaterials can be divided into two groups; natural polymers (collagen, fibrin, hyaluronan, chitosan, gelatin, elastin, keratin, silk, etc.) and synthetic polymers (poly (vinyl alcohol) (PVA),

polyglycolide (PGA), polylactide (PLA), polycaprolactone (PCL), polydioxanone (PDS), polyurethanes (PU), etc.) (Chesterman et al., 2020; Khang et al. 2006). Even though natural polymers have highly desirable biocompatibility, they suffer from limited mechanical properties. PLA and PCL are food and drug administration (FDA) approved polymers that are mostly preferred in biomedical applications due to their biocompatibility and biodegradability (Herrero-Herrero, Gómez-Tejedor, and Vallés-Lluch 2018). To highlight the strengths of both polymers, the PLA/PCL blend has been one of the prominent biomaterials in recent years.

The properties of fibrous webs can be customized along with the production method and the material selections. Therefore, this review highlights the properties of PLA and PCL biopolymers, electrospinning theory, current studies on electrospinning of PLA/PCL blends, and potential applications, particularly in tissue engineering.

2. Tissue-engineered scaffolds

The purpose of tissue engineering is to create new tissues instead of damaged tissue by mimicking natural tissue/organ in many aspects such as structural, mechanical, and biological features. Moreover, tissue engineering is an interdisciplinary concept that combines the engineering principles and life sciences like biology and chemistry for the development of biological substitutes that rebuild, regenerate, and enhance the function of tissue (Langer and Vacanti, 1993; Parenteau, Sullivan and Brockbank, 2008).

Scaffold and cell are the main components of tissue engineering that are interconnected with each other. Extracellular matrix (ECM), which is one of the most essential components in the cell microenvironment that provides mechanical reinforcement to preserve tissue/organ structure, and affects cell behaviour in many aspects such as cell viability, migration, proliferation, and differentiation (Barthes et al., 2014; Yi, Ding, Gong and Gu, 2017). Therefore, a tissue-engineered scaffold should be a convenient structure that imitates the regulatory role of the natural ECM and leads the way in tissue regeneration (Luo, 2020). On the other hand, there are morphological features that a scaffold should possess, such as high surface to volume ratio (Adhikari, Tucker, and Thomas, 2019), adequate pore architecture and porosity (Loh and Choong, 2013), optimum fiber diameter at nano/micro scale and desired fiber orientation (Li et al., 2018). Also, pore size and fiber diameter have a proportional relationship; pore size increases as the fiber diameter increases (Han et al., 2019). Pore size is an essential parameter as it affects mass transfer such as water and nutrient diffusion into the scaffold, also assists cell behaviours like cell impregnation, viability, and proliferation (Luo, 2020). In addition to the importance of the biological and morphological properties of tissue-

engineered scaffolds, the mechanical features of the scaffolds are also undeniably important. While numerous tissues, including the cardiac muscle, heart valves, and blood vessels have distinctly elastomeric properties, tensile modulus and strength are of vital significance for tendons and ligaments (Ma, 2008). Moreover, there are many application areas which are developing day by day such as breast (Donnely, Griffin, and Butler, 2020), blood vessels (Yalcin et al., 2016), heart valves (Hasan et al., 2018), artificial liver (Semnani et al., 2017), bone and cartilage reconstruction (Hassanajili, Karami-Pour, Oryan and Talaei-Khozani, 2019; Nava, Draghi, Giordano and Pietrabissa, 2016), nervous system (Haddad et al., 2016), corneal degeneration (Ghezzi, Rnjak-Kovacina, and Kaplan, 2015), dental applications (Mohandesnezhad et al., 2020), urinary bladder (Ajalloueian, Lemon, Hilborn, Chronakis and Fossum, 2018), and skin regeneration (Chua et al., 2016).

3. Overview of PLA and PCL polymers

3.1. Polylactic acid (PLA)

PLA is an aliphatic polyester that is biocompatible, bioabsorbable, and biodegradable biomaterial (Lasprilla, Martinez, Lunelli, Jardini and Maciel, 2012). Although ultimate safety in PLA-based scaffolds depends on the solvent system to be created for surface formation, PLA is degraded by hydrolysis of ester bonds, and there is no toxicity during degradation. On the other hand, PLA has good mechanical strength, but it is a highly brittle polymer due to its low elongation at break. Despite it is very attractive for tissue engineering applications owing to its superior biocompatibility, biodegradability, non-toxicity, and sufficient mechanical features, the stiffness of the polymer limits its utilization (Murariu and Dubois, 2016; Pawar, Tekale, Shisodia, Totre and Domb, 2014). As a result, PLA is frequently blended with other polymers to improve the thermomechanical properties of both itself and the polymer it is used with. (Saini, Arora and Kumar, 2016). The physicochemical properties of PLA can be seen in Table 1 (Nampoothiri, Nair, and John, 2010, Table 2; Saini et al., 2016, Table 1).

Table 1 Physicochemical properties of PLA

Physiochemical Properties of PLA	
Chemical Formula	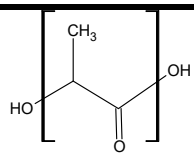
Solubility	Soluble in chloroform, methylene chloride, dioxane, acetonitrile, 1,1,2-trichloroethane,

	dichloroacetic acid, toluene, acetone, ethylbenzene at room temperature, and soluble in tetrahydrofuran (THF) only when heated to boiling point. Insoluble in water but it can dissolve in selective alcohols and alkanes.
Crystallinity	Semicrystalline (PDLA); 0-37% (PLLA); Amorphous (PDLLA)
Density	1.25 g/cm^3
Glass Transition Temperature, T_g	50-64 °C
Melting Point, T_m	145-186 °C
Tensile Strength	28-50 MPa
Young's Modulus	1.2-3 GPa
Elongation at Break	2-6%

3.2. Poly (Ɛ-caprolactone) (PCL)

PCL is an aliphatic, non-toxic, biocompatible, and biodegradable hydrophobic polyester, also it is convenient for recellularization thanks to its slow-degradation rate (Valderrama-Treviño et al., 2019; Yalcin et al., 2016). Depending on the structural properties such as crystallinity level and molecular weight, it can take months to years for PCL to degrade. While this is suitable for some tissue engineering applications, it imposes limitations for applications such as bone tissue regeneration (Mondal, Griffith, and Venkatraman, 2016). For this reason, PCL can be used alone or blended with different polymers in some applications. On the other hand, such features like excellent biocompatibility, mechanical strength and stability, non-cytotoxicity, and flexibility make PCL attractive biomaterial to be used in several tissue engineering applications (Siddiqui, Asawa, Birru, Baadhe, & Rao, 2018). The physicochemical properties of PCL can be seen in Table 2 (Mondal et al., 2016, Table 1).

Table 2 Physiochemical properties of PCL

Physiochemical Properties of PCL	
Chemical Formula	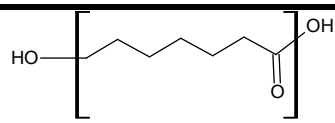
Solubility	Highly soluble in benzene, chloroform, DCM, and toluene at room temperature. Slightly soluble in acetone, 2-butanone, DMF and acetonitrile. Insoluble in water, alcohol, diethyl ether.
Density	1.1 g/cm^3
Crystallinity	67%

Glass Transition Temperature, T_g	-65 to -60 °C
Melting Point, T_m	65°C
Tensile Strength	14 MPa
Young's Modulus	190 MPa
Elongation at Break	>500%

4. Electrospinning method

4.1. The working principle

Electrospinning is an efficient method that encourages the innovation for manufacturing uniform and advanced fibers by using electric force. The main components of the electrospinning system are the feed pump, high voltage power supply, collector, and syringe (needle tip) as shown in Figure 1. The working principle of the electrospinning method is based on the theory of exceeding the surface tension of the polymer solution and creating a jet by applying high voltage. The electric field generated between the tip and the collector causes the viscoelastic polymer solution transforming from spherical to conical shape (Taylor cone) to be repelled with a certain surface charge. When the electrostatic repulsive forces in the polymer solution exceed the surface tension of the polymer, the charged jet begins to detach from the Taylor cone and moves uniaxially from the electric field towards the grounded collector. Simultaneously, with the rapid spread of the jet, the solvents in the polymer solution evaporate and fibers in nano/micrometre sizes begin to form. These formed fibers are collected on the collecting surface and provide surface formation (Asmatulu and Khan, 2018).

The electrospinning technique is generally governed by parameters such as solution, production, and ambient factors. Each of these parameters significantly affects the morphology of the fiber obtained, and the desired fiber morphology can be achieved by adjusting these parameters properly (Long et al., 2018)

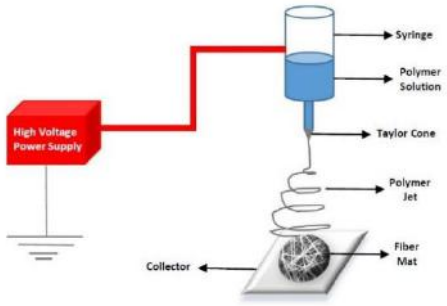

Fig. 1 Components of electrospinning unit (The image is created by the authors)

4.2. Electrospinning parameters

4.2.1 Solution Parameters

Solution properties such as concentration, molecular weight, viscosity, surface tension, and conductivity are the main parameters affecting fiber morphology.

Concentration

A minimum concentration of the solution is needed in the electrospinning enabling fiber formation to proceed. This solution concentration should be adjusted to an optimum value according to the properties of the materials used; otherwise, proper conditions will not be achieved and fiber formation cannot be obtained according to the desired properties (Bhardwaj and Kundu, 2010). Studies in the literature show that very low solution concentration causes bead formation instead of fiber formation, whereas very high solution concentration prevents continuous fiber formation by causing difficulty in polymer flow from the nozzle (Ahmed, Lalia, and Hashaikeh, 2015). Moreover, concentration and fiber diameter are directly proportional, and the fiber diameter decreases as concentration decreases (Costa, Bretas, and Gregorio, 2010).

Molecular Weight and Viscosity

Molecular weight is one of the aspects that play an important role in the production of high strength and high fiber orientation while having a significant impact on rheological and electrical properties such as viscosity, surface tension, conductivity, and dielectric strength. Increased molecular weight can effectively reduce the defects in the molecular chain ends and enhance molecular strength. Moreover, the molecular weight of the polymer represents the number of entangled polymer chains in a solution, and hence the viscosity of the solution (Bhardwaj and Kundu, 2010; Gupta and Kothari, 1997). Viscosity plays an important role in the determination of fiber diameter and morphology during the electrospinning process. The effect of viscosity occurs in the same way as concentration; while low viscosity causes droplet formation, with increasing viscosity, uniform and beadless fibers can be obtained. On the other hand, in cases where the viscosity is too high, the polymer solution dries at the needle tip before the jet formation starts and fiber formation cannot be achieved (Pham, Sharma, and Mikos, 2006).

Surface Tension

To produce a fibrous web with an electrospinning technique, the polymer solution loaded with the effect of the electric field in the first place is expected to exceed the surface tension and form a jet, so surface tension

is an important parameter. A solution with a very high surface tension cannot form fibers. However, the surface tension can be adjusted by changing the material used or adding surfactants to the solution (Rogina, 2014).

Conductivity (Surface charge density)

Since the electrospinning process is a system working with the effect of the electric field, the electrical conductivity of the solution that will provide the fiber formation has an important effect on the stable operation of the system. As experimental studies in the literature show, it is possible to obtain uniform and thin fibers with increased electrical conductivity (Tan, Inai, Kotaki and Ramakrishna, 2005; Uyar and Besenbacher, 2008).

4.2.2 Production parameters

In addition to the solution parameters, production parameters mainly as voltage, feed rate, and tip to collector distance significantly affect the structure of the final fibrous web.

Voltage

The electric charge that triggers fiber formation from the polymer solution is directly related to the applied voltage. For this reason, adjusting the voltage is an important parameter that directly affects fiber production (Khajavi and Abbasipour, 2017). The increasing voltage will increase electrical efficiency, resulting in polymer build-up at the nozzle; depending on the viscosity and feed rate of the polymer, this may cause an advantage or disadvantage. For this reason, the voltage setting should be considered together with these parameters (Subbiah, Bhat, Tock, Parameswaran and Ramkumar, 2005). Further, applied voltage affects fiber diameter. In some studies, due to the increasing potential difference, the solution comes to the collector with increasing acceleration and causes a larger fiber diameter (Bakar, Fonk, Eleyas and Nazeri, 2018; Deitzel, Kleinmeyer, Harris and Tan, 2001).

Feed Rate

Voltage and feed rate are interrelated production parameters, and as the voltage, the feed rate is a parameter that must be adjusted according to the components of the solution. However, the slow feed rate is generally a preferred option to allow the polymer solution to evaporate and form a jet (Bhardwaj and Kundu, 2010). At very fast feed rates, the solution will reach the collector without evaporation and production will result in pilling, wet fiber, or thick fiber formation (Khan and Kafiaha 2016; Rasouli, Pirsalami, and Zebarjad, 2019).

Tip to Collector Distance

The tip to collector distance can be optimized considering the voltage and feed rate parameters. A minimum distance from the tip to the collector is required to give the fibers sufficient time to dry before reaching the collector, otherwise, fiber irregularity or thicker fibers may occur at very close or far distances (Angel, Guo, Yan, Wang and Kong, 2020; Khan and Kafiaha, 2016).

4.2.3 Ambient parameters

Environmental factors affecting fiber morphology can be determined mainly as ambient temperature and humidity. The effects of these factors on different polymer solutions differ, so although it is known that they affect fiber morphology, it is not correct to make a definite judgment (Haider A., Haider S., and Kang, 2018). Current studies have shown that relative humidity especially defines the structural porosity. According to the outcomes of these studies, the pores in the fiber structure appear with increasing moisture due to the breath figure mechanism (Medeiros, Mattoso, Offeman, Wood and Orts, 2008; Megelski, Stephen, Chase and Rabolt, 2002). In many studies in the literature, it is seen that porous fibers are produced by electrospinning many polymers such as PLA in a humid environment with the effect of the breath figure mechanism (Huang and Thomas, 2018). On the other hand, higher temperature allows a higher rate of vaporization of the solvent and decreases the viscosity of the polymer solution; hence, thinner fibers can be obtained (İçoğlu and Oğulata, 2017).

4.3. Current studies on electrospinning of PLA/PCL blends

Studies using PLA (Abudula et al., 2019; Grémare et al., 2018; Haddad et al., 2016; Leyva-Verduzco et al., 2019) or PCL (Enis, Vojtech, and Sadikoglu, 2017; Ko, Choi, Jung and Kim, 2015; Metwally et al., 2019; Sharif et al., 2018; Wu et al., 2018) polymers alone are quite common in the literature, but the number of articles on blends of these polymers is limited. On the other hand, the use of PLA/PCL blends as raw materials in tissue engineering applications has gained the attention of researchers in recent years. In this context, researchers have started to work on the production and solution parameters of PLA/PCL blends based on their use in tissue engineering applications. Under this title, studies in which PLA/PCL blends are used have been reviewed in detail.

In a study of Lu et al. (2016), fibrous webs electrospun from PLA/PCL blends were produced and optimized for potential tissue engineering applications. The solutions at 8, 10, and 12% concentrations for electrospinning application are prepared using dimethylformamide:dichloromethane (DMF:DCM) solvent systems at 90:10, 80:20, 70:30 & 60:40 ratios, and PLA/PCL at 90/10, 80/20, 70/30,

60/40 & 50/50 blend ratios. According to the results, the optimum solvent ratio is 80:20 (DMF:DCM); polymer blend ratio is 70/30 (PLA/PCL) and polymer concentration is 8%. Besides, optimum production parameters are defined as 12 kV voltage, 15 cm needle-collector tip distance, and 0.6 ml/h feed rate. Morphological and mechanical test results indicate that PLA/PCL blend membranes have lower fiber diameter, lower crystallinity, and reduced contact angle compared to pure PLA and PCL polymers which improve biocompatibility and cell activities. In light of these findings, it is concluded that the PLA/PCL membrane can be a potential material for tissue engineering applications. Haroosh et al. (2010) studied the effect of PLA/PCL ratio and solvent type on the electrospinnability of PLA/PCL blends. 15% PCL and 8% PLA are dissolved in various solvent systems that are DCM:DMF (3:1), chloroform:methanol (2:1), and chloroform:acetone (2:1). Moreover, PLA/PCL blend ratios are 1/0, 3/1, and 1/1. The production parameters are adjusted as 25-28 kV voltage, 2 ml/h feed rate, and 13-15 cm distance between needle and collector. In the results, it is observed that the solution viscosity decreases with increasing PCL in the solution. This may be due to the lower molecular weight of PCL than PLA. Besides, when DCM:DMF is used as a solvent system for PLA/PCL (1/0), smooth and homogeneously distributed fibers with a diameter of 450nm is achieved, and this value increases to 490 nm for PLA/PCL (3/1). Although fibers with a diameter of 250 nm are obtained for PLA/PCL (1/1), bead formations are observed. This means that the fiber diameter can be decreased by lowering the solution viscosity but this may result in nonhomogeneous fiber distribution leading undesired bead formations. Moreover, as the PCL content increases, the fiber diameter decreases, but smooth fibers cannot be seen in the structure and beaded structures are observed in cases where chloroform:methanol (510±25 nm for 1/0 ratio, and 325±40 nm for 3/1 ratio) and chloroform:acetone (570±30 nm for 1/0 ratio, and 375±45 nm for 3/1 ratio) solvent systems are used. Also, no fiber formation is obtained for PLA/PCL (1/1). DCM:DMF has been determined as the most effective solvent system since it increases the solution conductivity compared to other solvent systems and allows the production of thinner fibers. Similarly, Herrero et. al. (2018) produced electrospun PLA, PCL, and PLA/PCL webs and examined the influences of main electrospinning parameters on the final structure. 50% w/w PLA/PCL blend is dissolved in chloroform:methanol and DCM:DMF solvent systems at different ratios (66:33% to 80:20% v/v) and the polymer concentration varies between 5-23% w/v. The production parameters are set to 20-25 kV voltage, 2ml/h feed rate, and 13-15 cm tip to collector distance. It is determined by the SEM analysis that the polymer concentration for each sample (5-8% for PLA, 8-10% for PCL, and 10-15% for PLA/ PCL) is the most effective electrospinning parameter on fiber morphology. As the polymer concentration increases, the fiber

diameter increases since beady structures appear at low polymer concentrations. On the other hand, the effect of solvent type is also noticeable. Using DCM:DMF solvent system results in beady structure while continuous fibers are produced when chloroform:methanol solvent system for PLA/PCL at 8% concentration. On the other hand, while using 12% polymer concentration and DCM:DMF (75:25) solvent system (at 2 ml/h feed rate, 15cm type-collector distance, and 25 kV voltage) under-micron level fibers are obtained; when the polymer concentration is increased to 20% and the voltage is decreased to 20 kV above-micron level fibers are produced. Thus, it can be said that in addition to the polymer concentration and solvent type, the voltage also affects the fiber diameter. Yao et al. (2017) designed a suitable PCL/PLA (at 4:1 mass ratio) electrospun fibrous scaffold for in-vitro osteogenetic differentiation and in-vivo bone formation. They also produced neat PCL fibrous webs (at 8% concentration based on the preliminary study) to compare them with PLA/PCL webs. To produce electrospun webs PLA/PCL solutions are prepared at 7, 8, 9, and 10% concentrations. The beaded fibers are obtained at 7% concentration, and the fiber diameters range is 120-900 nm. Unlike surfaces at 7% concentration, bead-free structures are produced at 8, 9, and 10% concentrations, and fiber diameters are measured as 250nm-1μm, 400 nm-1.5 μm, and 500 nm-2 μm, respectively, since the concentration increases and the fiber diameter increases. The solution concentration at 8% is determined as the most optimal one, and this concentration is preferred for the production of PLA/PCL blend nanofiber. The feed rate and applied voltage are set to 3 ml/h and 13 kV for PCL solution, respectively; whereas 1.5 ml/h and 15 kV are used for PCL/PLA blend solution. When PCL 3D scaffolds are compared with PCL/PLA 3D scaffolds it is observed that PCL/PLA 3D scaffolds have higher mechanical features with enhanced biological properties that enable mechanical support to cell growth, encourage cell activities, hMSCs osteogenic differentiation in-vitro, cranial bone formation in-vivo.

Besides optimization of the main electrospinning parameters for PCL/PLA blends and studying the effects of these parameters on fiber morphology, some studies mostly focus on the blend ratio of PCL/PLA blends and its effects on the morphological, structural, biological and mechanical properties of the final fibrous webs. For instance, Xu et al. (2018) conducted a study on the electrospinning of PCL/PLA blends and the parameters that affect the osteogenetic differentiation of human mesenchymal stem cells (hMSCs). In this study, PCL/PLA blends (100/0, 60/40, and 20/80 wt.) with polymer concentrations of 8%, 12%, and 14%, respectively, dissolved in DCM:DMF (2:1 w/w) solvent system. The voltage (13 kV) and the feed rate (2-3 ml/h) are kept constant for all samples. Porous structures are obtained with interconnected and

hierarchically ordered pores that range from sub-microns to 300 μm in size. This pore size diversity is a desirable property in terms of cell activities, for instance, large pores provide structural stability, cell proliferation, ECM deposition, and tissue formation, while small pores provide activities such as seeding and gene expression. Due to the highest porosity (99.0%) thus lowest density (12.6 mg/cm^3), the PCL/PLA (20/80) sample has the highest absorption capacity among the three sample types. Moreover, it can be said that the bending strength of all three scaffolds is suitable, thanks to the hierarchical pore arrangement and nanofiber connections. Moreover, as the PLA in the structure increases, the modulus/stiffness ratio increases, and 40% PLA is defined as the minimum value. Alkaline phosphatase (ALP) activity, calcium content, and gene expression level increase too, possibly due to greater stiffness and bioactivity of PLA. Consequently, considering all the properties and cell activities, it is concluded that PCL/PLA (20/80) is the most suitable nanofibrous web for osteogenic differentiation of hMSCs. Sharma et al. (2019) investigated the performance of PLA/PCL fibrous webs with different polymer compositions that designated PLAF (100/0), PPF-50 (50/50), PPF-60 (60/40), PPF-70 (70/30), PPF-80 (80/20), PPF-90 (90/10) and PCLF (0/100). The PLA/PCL blends are prepared in chloroform:DMF (4:1, v/v) solution system at 10% polymer concentration. The electrospinning parameters (tip-collector distance is 15cm, the feed rate is 1ml/h and the voltage is 20 kV) are kept constant for all surfaces. The average fiber diameter increases with the increase in PLA content (PPF-70, PPF-80, and PPF-90) owing to the high molecular weight and modulus of PLA. Similarly, the crystallinity ratio increases from 16.1% to 21.5% with the increase of PLA content in the structure. Moreover, the mechanical analysis shows that the tensile strength increases between PPF-50 and PPF-80 but a decrease is observed for PPF-90. This can be explained by the reduced ductility of increased PLA content. On the other hand, although all samples are hydrophobic, it can be said that the PLA in the web content reduces the contact surface angle and thus hydrophobicity. Sankaran et al. (2014) conducted a study indicating the development of 3D tubular nanofibrous scaffolds produced from PLA/PCL blends at two different blend weight ratios; 75/25 and 25/75. 15% of polymer concentration is used and chloroform:DMF (7:3) solvent system is preferred. 0.003ml/min feed rate and 10cm type collector distance are kept constant as production parameters while voltage is varied due to the blend ratio (14 kV for 25/75 and 16 kV for 75/25). The PLA/PCL (75/25) and PLA/PCL (25/75) fiber diameters are measured as 380±95 nm and 429±98 nm, respectively. Physicochemical analyses results show that the samples have hydrophobic structures, which is a limitation for cell adhesion, and the relative contact angles for 75:25 and 25:75 blend ratios are 97±1.5° and 87±2°, respectively. While PLA/PCL (75/25) has 23.72±2.51 μm pore size and

19.4±4.19% porosity, PLA/PCL (25/75) has 9.71±3.37μm pore size and 20.8±4.4% porosity in the structure. Also, the PLA/PCL (75/25) scaffold shows superior cell viability compared to tissue culture polystyrene (TCPS), but after day 7, when human umbilical vascular endothelial cells proliferated, it is slightly lower than PLA/PCL (25/75). This can be explained by the improved flexibility of the PLA/PCL (25/75) scaffold due to its PCL content. In summary, the PLA/PCL (25/75) based scaffold is thought to be a potential vascular graft for cardiovascular applications. Although PCL and PLA are polymers preferred stand-alone in many studies, their blended usage has become favoured due to their superior tensile strength, high pore size, biocompatibility, and biodegradability properties. As can be deduced from the studies detailed above, there are advantages to using at least 25% and even more than 40% PLA in PLA/PCL blends. The PLA/PCL blend ratio should be adjusted according to the properties expected from the end-use.

Some studies also highlight the advantages of using electrospun PLA/PCL webs for tissue-engineered scaffolds in heart valves, dental applications, tendons, muscles, skins, nerves, and vascular grafts. In a study of Hasan et al. (2018), a potential tri-leaflet heart valve structure was produced via the electrospinning method using PCL/PLLA blends. In the preliminary part of this study, the different PCL/PLLA ratios (0/100, 10/90, 30/70, 50/50, 70/30, 90/30, 100/0) are used, and results indicate that the cell viability tends to increase up to 70% PLA content but afterward, it falls. Therefore, a polymer ratio of 30/70 is preferred for later analysis. The experiment is carried out using a 10% polymer concentration for PCL:PLLA (30/70) solution at 15 kV voltage, 6ml/h feed rate, and 20 cm needle tip and collector distance. Humidity and temperature are kept constant at 30% and 23°C, respectively. As a result, fibers with 2.3 ± 0.21 μm diameter, 0.25-2.5 MPa elastic modulus, 20-110 MPa tensile strength, and 40-110% strain values are obtained. No toxic effects are observed and cell activity and proliferation occur efficiently. As a result, it has been observed that the PCL/PLLA heart valve preserves the mechanical properties of PCL and the biological properties of PLA and constitutes an alternative to bioprosthetic and mechanical heart valves. In a study of Mohandesnezhad et al. (2020) to produce a scaffold for dental tissue engineering applications, PLA/PCL polymers (at 1/4 molar ratio) are dissolved in DCM/Methanol (4/1 v/v ratio) solvent system, and solutions are prepared with 15% polymer concentration. Hydroxyapatite (HA) and zeolite are added to the solutions one by one or together, and fibrous scaffolds are produced by the electrospinning method. During electrospinning, 20-25 kV voltage, 15 cm tip-collector distance, 2 ml/h feed rate are set as production parameters, and the ambient temperature is kept constant at 25°C. According to the Fourier Transform Infrared Spectra

(FTIR) analysis, the characteristic peaks of the PLA, PCL, nHA, and Zeolite can be seen in the FTIR spectra of PCL/PLA/nHA/Zeolite so, it can be said that homogenous chemical structure is formed. When the contact angle analysis is examined, it can be seen that the PLA/PCL blend has the highest contact angle (125.5°) thus shows the highest hydrophobicity. However, it can be said that the contact angle is slightly reduced with the addition of nHA and Zeolite (108°) which results in an improvement in cell viability. Dong et al. (2019) designed a three dimensional PLA/PCL anisotropic scaffold which composed of oriented microfibers and randomly distributed nanofibers, also a randomly distributed nanofibrous scaffold is produced by common electrospinning method to compare with the nano/micro hybrid structure. The solution is prepared with PLA/PCL (1/1) blend and DCM:DMF (v/v, 7:3) solvent system at 10% polymer concentration. The applied voltage is 20 kV and the feed rate is 0.8 ml/h. The anisotropic hybrid structure consists of 40.83±15.40 μm diameter microfibers and 871±177nm diameter nanofibers together, while the randomly distributed nanoweb consists of 869±90 nm diameter nanofibers. Moreover, the average pore size and porosity which are essential for the cell proliferation of hybrid structure (907.67±315.64 μm^2, 91.89±3.48%) are higher than the nanofibrous scaffold structure (263.42±89.51 μm^2, 83.4±1.79%). As a result of the mechanical analysis, it is concluded that the hybrid structure is more resistant to loads in different directions and its tensile strength is higher due to its anisotropic structure. On the other hand, the elongation at break values of the two structures are similar. These results show that the PLA/PCL nano/micro hybrid structure can be a suitable scaffold structure for anisotropic tissues such as tendons, muscles, skins, and nerves. Liu et al. (2017) designed a bio-inspired high strength three-layer nanofibrous vascular graft (3LVG) from electrospun PLA/PCL blends. The inner layer is produced from PLA/PCL blend (3/7 w/w) nanofibers for enhanced cell compatibility thus fast endothelization. The middle layer consists of PU/PCL (3/1 w/w) nanofibers to support adequate strength and elasticity. The outer layer is again produced from PLA/PCL (3/7 w/w) blend but with radially aligned nanofibers which allow the growth of smooth muscle cells circumferentially. SEM analysis images in the research show that a securely attached three-layer structure is achieved without delamination problem. Using different cell types, the cell attachment and proliferation analyses are realized and results indicate that both inner and outer layers have good cell proliferation at the end of the 7 days. Also, the 3LVG has sufficient mechanical properties like 63.40 MPa and an elongation at break of 266.78% in the longitudinal direction, and 52.34 MPa, and 319.72% in the lateral direction. With the promising mechanical properties and good cell viability in each layer, the 3LVG can be a potential vascular graft.

5. Conclusion

Thanks to the unique and controllable features of the electrospun fibrous webs including nano/micro-scaled fibers, high surface area, adjustable pore shape and size, and high porosity, they have been used in various tissue engineering applications. In addition to the advanced singular properties of PLA and PCL biopolymers, it is seen in many studies that the PLA/PCL blend combines the superior properties of these two polymers. While PLA has low elongation at break and low toughness at fracture causing high stiffness and brittleness in the structure, the blend of PLA with PCL is more developed in terms of these properties. Moreover, PLA has a fast degradation rate while PCL has a slow degradation rate of up to 3 years. PLA/PCL blend offers adjustability in degradation rate according to the end-use area. On the other hand, in addition to the superior biocompatibility and biodegradability of both polymers, the blending of PLA and PCL in the same solvents, as seen in the literature, provides convenience in terms of manufacturability. This indicates that the PLA/PCL blend can be a potential material in tissue engineering applications.

REFERENCES

Abudula, T., Saeed, U., Memic, A., Gauthaman, K., Hussain, M. A., & Al-Turaif, H. (2019). Electrospun cellulose Nano fibril reinforced PLA/PBS composite scaffold for vascular tissue engineering. Journal of Polymer Research, 26(5). https://doi.org/10.1007/s10965-019-1772-y

Adhikari, K. R., Tucker, B. S., & Thomas, V. (2019). Tissue engineering of small-diameter vascular grafts. *Biointegration of Medical Implant Materials, 1957*, 79–100. https://doi.org/10.1016/B978-0-08-102680-9.00004-4

Ahmed, F. E., Lalia, B. S., & Hashaikeh, R. (2015). A review on electrospinning for membrane fabrication: Challenges and applications. *Desalination*, *356*, 15–30. https://doi.org/10.1016/j.desal.2014.09.033

Ajalloueian, F., Lemon, G., Hilborn, J., Chronakis, I. S., & Fossum, M. (2018). Bladder biomechanics and the use of scaffolds for regenerative medicine in the urinary bladder. *Nature Reviews Urology*, *15*(3), 155–174. https://doi.org/10.1038/nrurol.2018.5

Angel, N., Guo, L., Yan, F., Wang, H., & Kong, L. (2020). Effect of processing parameters on the electrospinning of cellulose acetate studied by response surface methodology. *Journal of Agriculture and Food Research*, *2*(November 2019), 100015. https://doi.org/10.1016/j.jafr.2019.100015

Asmatulu, R., & Khan, W. S. (Eds.). (2018). *Synthesis and Applications of Electrospun Nanofibers*. Elsevier. https://doi.org/10.1016/b978-0-12-813914-1.00014-6

Bakar, S. S. S., Fong, K. C., Eleyas, A., & Nazeri, M. F. M. (2018). Effect of Voltage and Flow Rate Electrospinning Parameters on Polyacrylonitrile Electrospun Fibers. *IOP Conference Series: Materials Science and Engineering*, *318*(1). https://doi.org/10.1088/1757-899X/318/1/012076

Barthes, J., Özçelik, H., Hindié, M., Ndreu-Halili, A., Hasan, A., & Vrana, N. E. (2014). Cell Microenvironment Engineering and Monitoring for Tissue Engineering and Regenerative Medicine: The Recent Advances. *BioMed Research International*, *2014*(i). https://doi.org/10.1155/2014/921905

Bhardwaj, N., & Kundu, S. C. (2010). Electrospinning: A fascinating fiber fabrication technique. *Biotechnology Advances*, *28*(3), 325–347. https://doi.org/10.1016/j.biotechadv.2010.01.004

Biswas, D. P., Tran, P. A., Tallon, C., & O'Connor, A. J. (2017). Combining mechanical foaming and thermally induced phase separation to generate chitosan scaffolds for soft tissue engineering. *Journal of Biomaterials Science, Polymer Edition*, *28*(2), 207–226. https://doi.org/10.1080/09205063.2016.1262164

Chandra, P. K., Soker, S., & Atala, A. (2020). Tissue engineering: current status and future perspectives. In *Principles of Tissue Engineering*. INC. https://doi.org/10.1016/b978-0-12-818422-6.00004-6

Chesterman, J., Zhang, Z., Ortiz, O., Goyal, R., & Kohn, J. (2020). Biodegradable polymers. In *Supramolecular Design for Biological Applications*. INC. https://doi.org/https://doi.org/10.1016/B978-0-12-818422-6.00019-8

Chua, A. W. C., Khoo, Y. C., Tan, B. K., Tan, K. C., Foo, C. L., & Chong, S. J. (2016). Skin tissue engineering advances in severe burns: review and therapeutic applications. *Burns & Trauma*, *4*, 1–14. https://doi.org/10.1186/s41038-016-0027-y

Costa, L. M. M., Bretas, R. E. S., & Gregorio, R. (2010). Effect of Solution Concentration on the Electrospray/Electrospinning Transition and on the Crystalline Phase of PVDF. *Materials Sciences and Applications*, *01*(04), 247–252. https://doi.org/10.4236/msa.2010.14036

Deitzel, J. M., Kleinmeyer, J., Harris, D., & Beck Tan, N. C. (2001). The effect of processing variables on the morphology of electrospun. *Polymer*, *42*, 261–272.

Dong, X., Zhang, J., Pang, L., Chen, J., Qi, M., You, S., & Ren, N. (2019). An anisotropic three-dimensional electrospun micro/nanofibrous hybrid PLA/PCL scaffold. *RSC Advances*, *9*(17), 9838–9844. https://doi.org/10.1039/C9RA00846B

Donnely, E., Griffin, M., & Butler, P. E. (2020). Breast Reconstruction with a Tissue Engineering and Regenerative Medicine Approach (Systematic Review). *Annals of Biomedical Engineering*, *48*(1), 9–25. https://doi.org/10.1007/s10439-019-02373-3

Enis, I. Y., Vojtech, J., & Sadikoglu, T. G. (2017). Alternative solvent systems for polycaprolactone nanowebs via electrospinning. *Journal of Industrial Textiles*, *47*(1), 57–70. https://doi.org/10.1177/1528083716634032

Ghezzi, C. E., Rnjak-Kovacina, J., & Kaplan, D. L. (2015). Corneal Tissue Engineering: Recent Advances and Future Perspectives. *Tissue Engineering - Part B: Reviews*, *21*(3), 278–287. https://doi.org/10.1089/ten.teb.2014.0397

Grémare, A., Guduric, V., Bareille, R., Heroguez, V., Latour, S., L'heureux, N., … Le Nihouannen, D. (2018). Characterization of printed PLA scaffolds for bone tissue engineering. *Journal of Biomedical Materials Research - Part A*, *106*(4), 887–894. https://doi.org/10.1002/jbm.a.36289

Gupta, V. B., & Kothari, V. K. (1997). Manufactured Fibre Technology. In *Manufactured Fibre Technology*. https://doi.org/10.1007/978-94-011-5854-1

Haddad, T., Noel, S., Liberelle, B., El Ayoubi, R., Ajji, A., & De Crescenzo, G. (2016). Fabrication and surface modification of poly lactic acid (PLA) scaffolds with epidermal growth factor for neural tissue engineering. *Biomatter*, *6*(1), e1231276. https://doi.org/10.1080/21592535.2016.1231276

Haider, A., Haider, S., & Kang, I. K. (2018). A comprehensive review summarizing the effect of electrospinning parameters and potential applications of nanofibers in biomedical and biotechnology. *Arabian Journal of Chemistry*, *11*(8), 1165–1188. https://doi.org/10.1016/j.arabjc.2015.11.015

Han, D. G., Ahn, C. B., Lee, J. H., Hwang, Y., Kim, J. H., Park, K. Y., … Son, K. H. (2019). Optimization of electrospun poly(caprolactone) fiber diameter for vascular scaffolds to maximize smooth muscle cell infiltration and phenotype modulation. *Polymers*, *11*(4). https://doi.org/10.3390/polym11040643

Haroosh, H. J., Chaudhary, D. S., & Dong, Y. (2010). Electrospun

PLA/PCL Fibers with Tubular Nanoclay: Morphological and Structural Analysis. *Journal of Applied Polymer Science*, *116*(5), 3930–3939. https://doi.org/0.1002/app.35448

Hasan, A., Soliman, S., El Hajj, F., Tseng, Y. T., Yalcin, H. C., & Marei, H. E. (2018). Fabrication and in Vitro Characterization of a Tissue Engineered PCL-PLLA Heart Valve. *Scientific Reports*, *8*(1), 1–13. https://doi.org/10.1038/s41598-018-26452-y

Hassanajili, S., Karami-Pour, A., Oryan, A., & Talaei-Khozani, T. (2019). Preparation and characterization of PLA/PCL/HA composite scaffolds using indirect 3D printing for bone tissue engineering. *Materials Science and Engineering C*, *104*(March), 109960. https://doi.org/10.1016/j.msec.2019.109960

Herrero-Herrero, M., Gómez-Tejedor, J. A., & Vallés-Lluch, A. (2018). PLA/PCL electrospun membranes of tailored fibres diameter as drug delivery systems. *European Polymer Journal*, *99*(December 2017), 445–455. https://doi.org/10.1016/j.eurpolymj.2017.12.045

Huang, C., & Thomas, N. L. (2018). Fabricating porous poly(lactic acid) fibres via electrospinning. *European Polymer Journal*, *99*(September 2017), 464–476. https://doi.org/10.1016/j.eurpolymj.2017.12.025

İçoğlu, H. İ., & Oğulata, R. T. (2017). Effect of Ambient Parameters On Morphology Of Electrospun Poly (trimethylene terephthalate (PTT) Fibers. *Tekstil ve Konfeksiyon*. 215–223.

Jammalamadaka, U., & Tappa, K. (2018). Recent advances in biomaterials for 3D printing and tissue engineering. *Journal of Functional Biomaterials*, *9*(1). https://doi.org/10.3390/jfb9010022

Khajavi, R., & Abbasipour, M. (2017). Controlling nanofiber morphology by the electrospinning process. In *Electrospun Nanofibers*. Elsevier Ltd. https://doi.org/10.1016/B978-0-08-100907-9.00005-2

Khan, Z., & Kafiaha, F. M. (2016). Preparation of polysulfone electrospun nanofibers : effect of electrospinning and solution parameters. *Membrane Technology for Water and Wastewater Treatment, Energy and Environment*, *2013*(Mst), 309–318. https://doi.org/10.13140/RG.2.1.4289.9681

Khang, G., Lee, S. J., Kim, M. S., & Lee, H. B. (2006). *BIOMATERIALS : TISSUE-ENGINEERING AND SCAFFOLDS*. John G. Webster, *Encyclopedia of Medical Devices and Instrumentation* (366–383) John Wiley & Sons, Inc.

Ko, Y. M., Choi, D. Y., Jung, S. C., & Kim, B. H. (2015). Characteristics of plasma treated electrospun polycaprolactone (PCL) nanofiber

scaffold for bone tissue engineering. *Journal of Nanoscience and Nanotechnology*, *15*(1), 192–195. https://doi.org/10.1166/jnn.2015.8372

Langer, R., & Vacanti, J. (1993). Tissue Engineering. *Science*, *260*(5110), 920–926. https://doi.org/10.1126/science.8493529

Lasprilla, A. J. R., Martinez, G. A. R., Lunelli, B. H., Jardini, A. L., & Maciel, R. (2012). Poly-lactic acid synthesis for application in biomedical devices — A review. *Biotechnology Advances*, *30*(1), 321–328. https://doi.org/10.1016/j.biotechadv.2011.06.019

Leyva-Verduzco, A. A., Castillo-Ortega, M. M., Chan-Chan, L. H., Silva-Campa, E., Galaz-Méndez, R., Vera-Graziano, R., … Santos-Sauceda, I. (2019). Electrospun tubes based on PLA, gelatin and genipin in different arrangements for blood vessel tissue engineering. *Polymer Bulletin*, (0123456789). https://doi.org/10.1007/s00289-019-03057-7

Li, X., Wang, X., Yao, D., Jiang, J., Guo, X., Gao, Y., … Shen, C. (2018). Effects of aligned and random fibers with different diameter on cell behaviors. *Colloids and Surfaces B: Biointerfaces*, *171*(June), 461–467. https://doi.org/10.1016/j.colsurfb.2018.07.045

Liu, K., Wang, N., Wang, W., Shi, L., Li, H., Guo, F., … Zhao, Y. (2017). A bio-inspired high strength three-layer nanofiber vascular graft with structure guided cell growth. *Journal of Materials Chemistry B*, *5*(20), 3758–3764. https://doi.org/10.1039/c7tb00465f

Loh, Q. L., & Choong, C. (2013). Three-dimensional scaffolds for tissue engineering applications: Role of porosity and pore size. *Tissue Engineering - Part B: Reviews*, *19*(6), 485–502. https://doi.org/10.1089/ten.teb.2012.0437

Long, Y. Z., Yan, X., Wang, X. X., Zhang, J., & Yu, M. (2018). Electrospinning: The Setup and Procedure. In *Electrospinning: Nanofabrication and Applications* (pp. 21–52). Elsevier Inc. https://doi.org/10.1016/B978-0-323-51270-1.00002-9

Lu, Y., Chen, Y., & Zhang, P. (2016). *Preparation and Characterisation of Polylactic Acid (PLA)/ Polycaprolactone (PCL) Composite Microfibre Membranes*. *3*(117), 17–25. https://doi.org/10.5604/12303666.1196607

Luo, Y. (2020). Three-dimensional scaffolds. R. Lanza, R. Langer, J.P. Vacanti, A. Atala. *In Principles of Tissue Engineering* (s. 343-360) Elsevier Inc. https://doi.org/10.1016/b978-0-12-818422-6.00020-4

Ma, P. X. (2008). Biomimetic materials for tissue engineering. *Advanced*

Drug Delivery Reviews, *60*(2), 184–198. https://doi.org/10.1016/j.addr.2007.08.041

Mahapatro, A., & Singh, D. K. (2011). Biodegradable nanoparticles are excellent vehicle for site directed in-vivo delivery of drugs and vaccines. *Journal of Nanobiotechnology*, *9*(1), 55. https://doi.org/10.1186/1477-3155-9-55

Mao, D., Li, Q., Li, D., Chen, Y., Chen, X., & Xu, X. (2018). Fabrication of 3D porous poly(lactic acid)-based composite scaffolds with tunable biodegradation for bone tissue engineering. *Materials and Design*, *142*, 1–10. https://doi.org/10.1016/j.matdes.2018.01.016

Medeiros, E. S., Mattoso, L. H. C., Offeman, R. D., Wood, D. F., & Orts, W. J. (2008). Effect of relative humidity on the morphology of electrospun polymer fibers. *Canadian Journal of Chemistry*, *86*(6), 590–599. https://doi.org/10.1139/V08-029

Megelski, S., Stephens, J. S., Chase, D. B., & Rabolt, J. F. (2002). *Micro- and Nanostructured Surface Morphology on Electrospun Polymer Fibers*. 8456–8466. https://doi.org/10.1021/ma020444a

Metwally, S., Karbowniczek, J. E., Szewczyk, P. K., Marzec, M. M., Gruszczyński, A., Bernasik, A., & Stachewicz, U. (2019). Single-Step Approach to Tailor Surface Chemistry and Potential on Electrospun PCL Fibers for Tissue Engineering Application. *Advanced Materials Interfaces*, *6*(2), 1–12. https://doi.org/10.1002/admi.201801211

Mohandesnezhad, S., Pilehvar-Soltanahmadi, Y., Alizadeh, E., Goodarzi, A., Davaran, S., Khatamian, M., Akbarzadeh, A. (2020). In vitro evaluation of Zeolite-nHA blended PCL/PLA nanofibers for dental tissue engineering. *Materials Chemistry and Physics*, *252*(January), 123152. https://doi.org/10.1016/j.matchemphys.2020.123152

Mondal, D., Griffith, M., & Venkatraman, S. S. (2016). International Journal of Polymeric Materials and Polycaprolactone-based biomaterials for tissue engineering and drug delivery : Current scenario and challenges. *GPOM*, *65*(5), 255–265. https://doi.org/10.1080/00914037.2015.1103241

Murariu, M., & Dubois, P. (2016). PLA composites : From production to properties ☆. *Advanced Drug Delivery Reviews*, *107*, 17–46. https://doi.org/10.1016/j.addr.2016.04.003

Nampoothiri, K. M., Nair, N. R., & John, R. P. (2010). An overview of the recent developments in polylactide (PLA) research. *Bioresource Technology*, *101*(22), 8493–8501. https://doi.org/10.1016/j.biortech.2010.05.092

Nava, M. M., Draghi, L., Giordano, C., & Pietrabissa, R. (2016). The effect of scaffold pore size in cartilage tissue engineering. *Journal of Applied Biomaterials and Functional Materials*, *14*(3), e223–e229. https://doi.org/10.5301/jabfm.5000302

Norouzi, S. K., & Shamloo, A. (2019). Bilayered heparinized vascular graft fabricated by combining electrospinning and freeze drying methods. *Materials Science and Engineering C*, *94*, 1067–1076. https://doi.org/10.1016/j.msec.2018.10.016

Parenteau, N. L., Sullivan, S. J., Brockbank, K. G. M., & Young, J. H. (2008). Biotechnology Sector. In Julia Polak (Ed.), *Advances in Tissue Engineering* (pp. 469–490).

Pawar, R. P., Tekale, S. U., Shisodia, S. U., Totre, J. T., & Domb, A. J. (2014). *Biomedical Applications of Poly (Lactic Acid)*. 40–51.

Pham, Q. P., Sharma, U., & Mikos, A. G. (2006). Electrospinning of Polymeric Nanofibers for Tissue Engineering Applications: A Review. *Tissue Engineering*, *12*(5), 1197–1211.

Rasouli, M., Pirsalami, S., & Zebarjad, S. M. (2019). Optimizing the electrospinning conditions of polysulfone membranes for water microfiltration applications. *Polymer International*, *68*(9), 1610–1617. https://doi.org/10.1002/pi.5858

Rogina, A. (2014). Electrospinning process: Versatile preparation method for biodegradable and natural polymers and biocomposite systems applied in tissue engineering and drug delivery. *Applied Surface Science*, *296*, 221–230. https://doi.org/10.1016/j.apsusc.2014.01.098

Saini, P., Arora, M., & Kumar, M. N. V. R. (2016). Poly(lactic acid) blends in biomedical applications. *Advanced Drug Delivery Reviews*, *107*, 47–59. https://doi.org/10.1016/j.addr.2016.06.014

Sankaran, K. K., Krishnan, U. M., & Sethuraman, S. (2014). Axially aligned 3D nanofibrous grafts of PLA-PCL for small diameter cardiovascular applications. *Journal of Biomaterials Science, Polymer Edition*, *25*(16), 1791–1812. https://doi.org/10.1080/09205063.2014.950505

Semnani, D., Naghashzargar, E., Hadjianfar, M., Dehghan Manshadi, F., Mohammadi, S., Karbasi, S., & Effaty, F. (2017). Evaluation of PCL/chitosan electrospun nanofibers for liver tissue engineering. *International Journal of Polymeric Materials and Polymeric Biomaterials*, *66*(3), 149–157. https://doi.org/10.1080/00914037.2016.1190931

Sharif, S., Ai, J., Azami, M., Verdi, J., Atlasi, M. A., Shirian, S., &

Samadikuchaksaraei, A. (2018). Collagen-coated nano-electrospun PCL seeded with human endometrial stem cells for skin tissue engineering applications. *Journal of Biomedical Materials Research - Part B Applied Biomaterials*, *106*(4), 1578–1586. https://doi.org/10.1002/jbm.b.33966

Sharma, D., & Satapathy, B. K. (2019). Performance evaluation of electrospun nanofibrous mats of polylactic acid (PLA)/poly (e-caprolactone) (PCL) blends. *Materials Today: Proceedings*, *19*, 188–195. https://doi.org/10.1016/j.matpr.2019.06.698

Siddiqui, N., Asawa, S., Birru, B., Baadhe, R., & Rao, S. (2018). PCL - Based Composite Scaffold Matrices for Tissue Engineering Applications. *Molecular Biotechnology*, *60*(7), 506–532. https://doi.org/10.1007/s12033-018-0084-5

Subbiah, T., Bhat, G. S., Tock, R. W., Parameswaran, S., & Ramkumar, S. S. (2005). Electrospinning of nanofibers. *Journal of Applied Polymer Science*, *96*(2), 557–569. https://doi.org/10.1002/app.21481

Suwantong, O. (2016). Biomedical applications of electrospun polycaprolactone fiber mats. *Polymers for Advanced Technologies*, *27*(10), 1264–1273. https://doi.org/10.1002/pat.3876

Tan, S. H., Inai, R., Kotaki, M., & Ramakrishna, S. (2005). Systematic parameter study for ultra-fine fiber fabrication via electrospinning process. *Polymer*, *46*(16), 6128–6134. https://doi.org/10.1016/j.polymer.2005.05.068

Uyar, T., & Besenbacher, F. (2008). Electrospinning of uniform polystyrene fibers: The effect of solvent conductivity. *Polymer*, *49*(24), 5336–5343. https://doi.org/10.1016/j.polymer.2008.09.025

Valderrama-Treviño, A. I., Uriarte-Ruiz, K., Romero, J. J. G., Castell Rodriguez, A. E., Maciel-Cerda, A., Banegaz-Ruiz, R., & Barrera-Mera, B. (2019). Tubular electrospun scaffolds tested in vivo for tissue engineering. *International Journal of Research in Medical Sciences*, *7*(2), 635. https://doi.org/10.18203/2320-6012.ijrms20190373

Wu, Y., Qin, Y., Wang, Z., Wang, J., Zhang, C., Li, C., & Kong, D. (2018). The regeneration of macro-porous electrospun poly(ε-caprolactone) vascular graft during long-term in situ implantation. *Journal of Biomedical Materials Research - Part B Applied Biomaterials*, *106*(4), 1618–1627. https://doi.org/10.1002/jbm.b.33967

Xu, T., Yao, Q., Miszuk, J. M., Sanyour, H. J., Hong, Z., Sun, H., & Fong, H. (2018). Tailoring weight ratio of PCL/PLA in electrospun three-dimensional nanofibrous scaffolds and the effect on osteogenic differentiation of stem cells. *Colloids and Surfaces B: Biointerfaces*,

171(July), 31–39. https://doi.org/10.1016/j.colsurfb.2018.07.004

Yalcin, I., Horakova, J., Mikes, P., Sadikoglu, T. G., Domin, R., & Lukas, D. (2016). Design of Polycaprolactone Vascular Grafts. *Journal of Industrial Textiles*, *45*(5), 813–833. https://doi.org/10.1177/1528083714540701

Yao, Q., Cosme, J. G. L., Xu, T., Miszuk, J. M., Picciani, P. H. S., Fong, H., & Sun, H. (2017). Three dimensional electrospun PCL/PLA blend nanofibrous scaffolds with significantly improved stem cells osteogenic differentiation and cranial bone formation. *Biomaterials*, *115*, 115–127. https://doi.org/10.1016/j.biomaterials.2016.11.018

Yi, S., Ding, F., Gong, L., & Gu, X. (2017). Extracellular Matrix Scaffolds for Tissue Engineering and Regenerative Medicine. *Current Stem Cell Research & Therapy*, *12*(3), 233–246. https://doi.org/10.2174/1574888X11666160905092

Yu, P., Bao, R. Y., Shi, X. J., Yang, W., & Yang, M. B. (2017). Self-assembled high-strength hydroxyapatite/graphene oxide/chitosan composite hydrogel for bone tissue engineering. *Carbohydrate Polymers*, *155*, 507–515. https://doi.org/10.1016/j.carbpol.2016.09.001